BINDER-GRADE BUMPING AND HIGH BINDER CONTENT TO IMPROVE PERFORMANCE OF RAP-RAS MIXTURES

Final Report

SPR 797

Oregon Department of Transportation

BINDER-GRADE BUMPING AND HIGH BINDER CONTENT TO IMPROVE PERFORMANCE OF RAP-RAS MIXTURES
Final Report

SPR 797

by

Erdem Coleri, PhD
Sogol Sadat Haddadi; Shashwath Sreedhar; Sunny Lewis; Yuqi Zhang; Blaine Wruck

School of Civil and Construction Engineering
Oregon State University
101 Kearney Hall
Corvallis, OR 97331

for

Oregon Department of Transportation
Research Section
555 13th Street NE, Suite 1
Salem OR 97301

and

Federal Highway Administration
400 Seventh Street, SW
Washington, DC 20590-0003

January 2018

Technical Report Documentation Page

1. Report No. FHWA-OR-RD-18-05	2. Government Accession No.	3. Recipient's Catalog No.
4. Title and Subtitle Binder-Grade Bumping and High Binder Content to Improve Performance of RAP-RAS Mixtures		5. Report Date January 2018 6. Performing Organization Code
7. Author(s) Erdem Coleri, PhD; Sogol Sadat Haddadi; Shashwath Sreedhar; Sunny Lewis; Yuqi Zhang; Blaine Wruck		8. Performing Organization Report No. SPR 797
9. Performing Organization Name and Address School of Civil and Construction Engineering Oregon State University 101 Kearney Hall, Corvallis, OR 97331		10. Work Unit No. (TRAIS) 11. Contract or Grant No.
12. Sponsoring Agency Name and Address Oregon Dept. of Transportation Research Section and Federal Highway Admin. 555 13th Street NE, Suite 1 400 Seventh Street, SW Salem, OR 97301 Washington, DC 20590-0003		13. Type of Report and Period Covered Draft Report 14. Sponsoring Agency Code

15. Supplementary Notes

1.0 Abstract

General reduction in pavement program funding levels over the past decade and the possible consequent increase in pavement road roughness within the next couple years created a need for low cost yet effective alternative ways to rehabilitate, preserve and maintain roadway network in Oregon. Recycling highway construction materials and minimizing the use of virgin materials can reduce the pavement life cycle costs, improve highway network condition, conserve natural resources, and protect the environment. Although using recycled asphalt pavements (RAP) and recycled asphalt shingles (RAS) is beneficial in many aspects, asphalt pavements with high RAP and RAS contents are more susceptible to cracking. Aged binder in RAP and RAS makes asphalt pavements more brittle and creates long-term durability problems. Using softer virgin binder grade (binder-grade bumping) and higher virgin binder content improve cracking performance of pavements with high amounts of RAP and RAS. However, careful considerations are required in designing asphalt pavements with high RAP and RAS. Softer virgin binder grade and higher binder content make pavements more resistant to cracking, but more susceptible to permanent deformation. Hence, a balance of the combination of RAP and RAS content, binder content, and binder grade should be considered in the mix design.

In this study, the performance and cost benefits of using binder-grade bumping and increased binder content strategies in RAP and RAS mixture production in Oregon are quantified. To be able to provide recommendations for asphalt mixture design procedures, blending of binder around RAP is also quantified by using an innovative procedure developed in this study. Laboratory test results were used to develop mechanistic-empirical (ME) pavement models for asphalt mixtures with different RAP and RAS contents. Using the predicted performance from ME models and cost calculations for different combinations of RAP content, binder content, and binder type, life-cycle cost analysis (LCCA) were conducted to determine the performance and cost benefits of using binder-grade bumping and high binder content in Oregon asphalt mixtures. Binder-grade bumping and high binder content strategies recommended in this study are expected to increase the RAP and RAS content in asphalt mixtures, reduce the life-cycle cost, improve the cracking performance, and encourage the widespread use of high RAP/RAS asphalt mixtures in Oregon.

17. Key Words Recycled asphalt pavements, Recycled asphalt shingles, binder-grade bumping, mechanistic empirical modeling, semi-circular bend test; blending, life-cycle cost, life-cycle assessment.	18. Distribution Statement Copies available from NTIS, and online at: http://www.oregon.gov/ODOT/Programs/Pages/Research-Publications.aspx

19. Security Classification (of this report) Unclassified	16. Security Classification (of this page) Unclassified	21. No. of Pages 208	22. Price

SI* (MODERN METRIC) CONVERSION FACTORS

APPROXIMATE CONVERSIONS TO SI UNITS

Symbol	When You Know	Multiply By	To Find	Symbol
		LENGTH		
in	inches	25.4	millimeters	mm
ft	feet	0.305	meters	m
yd	yards	0.914	meters	m
mi	miles	1.61	kilometers	km
		AREA		
in^2	square inches	645.2	millimeters squared	mm^2
ft^2	square feet	0.093	meters squared	m^2
yd^2	square yards	0.836	meters squared	m^2
ac	acres	0.405	hectares	ha
mi^2	square miles	2.59	kilometers squared	km^2
		VOLUME		
fl oz	fluid ounces	29.57	milliliters	ml
gal	gallons	3.785	liters	L
ft^3	cubic feet	0.028	meters cubed	m^3
yd^3	cubic yards	0.765	meters cubed	m^3
NOTE: Volumes greater than 1000 L shall be shown in m^3.				
		MASS		
oz	ounces	28.35	grams	g
lb	pounds	0.454	kilograms	kg
T	short tons (2000 lb)	0.907	megagrams	Mg
		TEMPERATURE (exact)		
°F	Fahrenheit	(F-32)/1.8	Celsius	°C

APPROXIMATE CONVERSIONS FROM SI UNITS

Symbol	When You Know	Multiply By	To Find	Symbol
		LENGTH		
mm	millimeters	0.039	inches	in
m	meters	3.28	feet	ft
m	meters	1.09	yards	yd
km	kilometers	0.621	miles	mi
		AREA		
mm^2	millimeters squared	0.0016	square inches	in^2
m^2	meters squared	10.764	square feet	ft^2
m^2	meters squared	1.196	square yards	yd^2
ha	hectares	2.47	acres	ac
km^2	kilometers squared	0.386	square miles	mi^2
		VOLUME		
ml	milliliters	0.034	fluid ounces	fl oz
L	liters	0.264	gallons	gal
m^3	meters cubed	35.315	cubic feet	ft^3
m^3	meters cubed	1.308	cubic yards	yd^3
		MASS		
g	grams	0.035	ounces	oz
kg	kilograms	2.205	pounds	lb
Mg	megagrams	1.102	short tons (2000 lb)	T
		TEMPERATURE (exact)		
°C	Celsius	1.8C+32	Fahrenheit	°F

*SI is the symbol for the International System of Measurement

ACKNOWLEDGEMENTS

The authors would like to thank the Oregon Department of Transportation (ODOT) for providing funding for this research. The authors thank the members of the ODOT Project Technical Advisory Committee and ODOT research for their advice and assistance in the preparation of this report. In particular, Norris Shippen, Larry Ilg, Justin Moderie, Cole Mullis, and Anthony Boesen participated on the TAC. The authors would like to thank Tim Flowerday, Nicholas Kolstad, John Paul Morton, Andrew Johnson, Mostafa Estaji, Ihsan Obaid, Natasha Anisimova, Matthew Haynes, and Jawad Qassem for their help with sieving, batching, and measuring theoretical maximum specific gravity of prepared samples, as well as James Batti for his help in the laboratory. Also, a special thank you to Terri Zahler from McCall Oil for providing asphalt binders, and to Mike Miller from Oldcastle Materials for providing aggregates and RAP materials used in this study.

DISCLAIMER

TABLE OF CONTENTS

LIST OF FIGURES

LIST OF TABLES

1.0 INTRODUCTION

General reduction in pavement program funding levels over the past decade and the possible consequent increase in pavement road roughness within coming years created a need for alternative low-cost and effective ways to rehabilitate, preserve and maintain the roadway network in Oregon (ODOT, 2013). Recycling highway construction materials and minimizing the use of virgin materials can reduce the pavement life cycle costs, improve highway network condition, conserve natural resources and protect the environment. Although the use of recycled materials in asphalt pavements is beneficial in most cases by reducing the need for virgin materials and lowering construction costs, asphalt pavements with high recycled asphalt pavement (RAP) and recycled asphalt shingle (RAS) contents should be carefully designed to avoid premature cracking (West et al., 2012).

A benefit of conserving raw binder and aggregates is to create economic savings. Reducing the amount of virgin asphalt binder and aggregates used in HMA mixes has direct cost-saving potential. Willis et al. (2012) suggested that supplementing 50% RAP/RAS into HMA mixes can save agencies up to 35% on the cost of raw materials in asphalt paving projects. In 2014, the use of RAP/RAS on U.S. roads displaced 20M barrels of oil and 68M tons of aggregate (Hansen and Copeland 2014). This resulted in a savings of $2.8B based on binder cost of $550/ton and aggregate cost of $9.50/ton, according to a study by National Asphalt Pavement Association (NAPA) (Hansen and Copeland 2014). This evidence is testament to the ability of RAP/RAS use to provide economic benefits to federal and state transportation agencies. Reducing asphalt mixture costs by using higher percentages of RAP will allow agencies to maintain and rehabilitate more roadway sections and reduce network-level pavement roughness. Consequently, vehicle operating costs will decrease and road user comfort will increase by maintaining pavements at higher levels of service.

Although using RAP is beneficial in many aspects, asphalt pavements with high RAP contents are more susceptible to cracking. Aged binder in RAP makes asphalt pavements more brittle and creates long-term durability problems (Bennert et al. 2014). Using a softer virgin binder grade (binder-grade bumping) and a higher virgin binder content improves cracking performance of pavements with high amounts of RAP (Bennert et al. 2014; Aurangzeb et al. 2012; Li et al. 2008; West et al. 2009). However, careful considerations are required in designing asphalt pavements with high RAP contents. A softer virgin binder grade and higher binder content make pavements more resistant to cracking, but more susceptible to permanent deformation. Hence, a balance of the combination of RAP content, binder content and binder grade should be considered in the mix design.

In this study, the performance and cost benefits of using binder-grade bumping and increased binder content strategies in RAP/RAS mixture production in Oregon were quantified. To be able to provide recommendations for asphalt mixture design procedures, blending of binder around RAP was also quantified by using an innovative procedure developed in this study. While the use of binder-grade bumping and high virgin binder content strategies generally increase the cost of

virgin binder used in the asphalt mixture, increased RAP/RAS content and improved RAP/RAS performance may reduce the overall life-cycle cost of recycled asphalt concrete material used in construction. In this study, laboratory test results were used to develop mechanistic-empirical (ME) pavement models for different RAP/RAS mixtures. Using the predicted performance from ME models and cost calculations for different combinations of RAP content, binder content and binder type, life-cycle cost analyses (LCCA) were conducted to investigate the performance and cost benefits of using binder-grade bumping and high binder content in Oregon RAP/RAS mixes. Binder-grade bumping and high binder content strategies recommended in this study are expected to increase the RAP/RAS content in asphalt mixtures, reduce the life-cycle cost, improve the cracking performance and encourage the widespread use of high RAP/RAS asphalt mixtures in Oregon.

1.1 KEY OBJECTIVES OF THIS STUDY

The main objectives of this study are to:

- Identify the effects of binder-grade bumping and higher binder content on RAP/RAS performance;
- Determine the impact of these alternatives on increasing RAP/RAS contents without sacrificing performance;
- Suggest asphalt mixture design strategies to produce high RAP/RAS asphalt mixtures with high cracking and rutting performance.
- Quantify the percentage of binder around RAP aggregates blending into asphalt mixtures and the effects of blending on mixture performance;
- Predict the impact of RAP/RAS content, virgin binder grade and binder content on in-situ cracking and rutting performance using mechanistic-empirical (ME) modeling; and
- Quantify the cost benefits of increasing RAP/RAS content in asphalt mixtures using ME modeling and life cycle cost analysis (LCCA).

1.2 MAJOR RESEARCH PRODUCTS DEVELOPED IN THIS STUDY

The major research products developed in this study are given as follows:

- Recommended RAP and binder contents for mixtures with different virgin binder types to meet rutting and cracking performance requirements;
- Recommended binder contents for RAP/RAS mixtures with different virgin binder types;

- Regression models to predict rutting and cracking performance of high (25 to 45% RAP) and low (0 to 25% RAP) RAP mixtures using binder content, RAP content and binder type as independent variables;

- An innovative process for RAP binder blending measurement;

- Blending percentages for different RAP sources and suggestions for mix design processes to account for reduced blending;

- A cost calculation spreadsheet to compare unit cost of asphalt mixtures with different RAP/RAS contents, binder contents and binder types;

- A software to analyze the data produced by the semi-circular bend (SCB) test; and

- A software to analyze the data produced by the Flow Number test.

1.3 ORGANIZATION OF THE REPORT

This report is organized as follows: This introductory chapter is followed by the literature review. Strategies developed to improve performance of RAP and RAS mixtures are discussed in Chapter 3. Chapter 4 presents the measured blending of virgin binder with the binder around RAP aggregates and provides recommendations for mixture design. Chapter 5 presents the results of the mechanistic-empirical pavement design guide (MEPDG) simulations and life cycle cost analysis conducted to determine the cost and performance effectiveness of asphalt mixtures tested in Chapter 3. Finally, Chapter 6 presents the conclusions, summary of the work and recommendations.

2 LITERATURE REVIEW

2.1 INTRODUCTION

Reclaimed Asphalt Pavement (RAP) and Reclaimed Asphalt Shingles (RAS) have inherent value as recycled construction materials. Using RAP and RAS as a supplement for virgin aggregate and binder in Hot Mix Asphalt (HMA) has significant merit for conserving raw materials, reducing mixture costs, and reaching sustainability goals. The major goal of this study is to investigate methods of increasing the RAP/RAS content in HMA mixtures beyond the current threshold in order to displace a maximum amount of virgin materials while still preserving the long-term durability of the finished asphalt concrete.

The use of RAP/RAS in the United States became widespread after the 1970s oil embargo that drove up the cost of petroleum products, although asphalt recycling existed to some degree prior to this event. Following the oil embargo, many state DOTs permanently adopted the use of RAP/RAS in their mix designs. Although a sharp reduction in oil prices has recently been observed, depletion of readily available oil reserves is expected to increase the cost of oil and petroleum products in the long run. More strict regulations for new rock mines are also expected to increase the cost of aggregates (Willis et al. 2012). These phenomena necessitate a more proactive approach to increase the recycled content used in HMA paving.

Looking forward, the use of high RAP/RAS mixtures will help the asphalt pavement industry to become more energy independent, more sustainable, and more profitable while promoting environmental stewardship within all pavement agencies. Even as oil prices rise and fall, efforts to increase the use of RAP/RAS should not be discontinued. This practice can help to establish a notion of sustainability in pavement engineering.

A benefit of conserving raw binder and aggregates is creating economic savings. Reducing the amount of virgin asphalt binder and aggregates used in HMA mixes has direct cost-saving potential. Willis et al. (2012) suggested that supplementing 50% RAP/RAS into HMA mixes can save agencies up to 35% on the cost of raw materials in asphalt paving projects. In 2014, the use of RAP/RAS on U.S. roads displaced 20M barrels of oil and 68M tons of aggregate (Hansen and Copeland 2014). This resulted in a savings of $2.8B based on binder cost of $550/ton and aggregate cost of $9.50/ton, according to a study by National Asphalt Pavement Association (NAPA) (Hansen and Copeland 2014). This evidence is testament to the ability of RAP/RAS use to provide economic benefits to federal and state transportation agencies.

Saving money by using more recycled content also means that agencies will have more money to allocate toward pavement improvement projects. This means that more roads can be maintained at higher levels of service. This is conducive to user comfort and vehicle operating cost (VOC) savings (mostly fuel consumption), as pavement roughness is a major factor in VOCs.

The primary concern when using high RAP/RAS mixes lies in the altered long-term durability properties of HMA mixtures. The dilemma is finding a way to use higher RAP contents in HMA without compromising any long-term durability. Aged binder in RAP is less ductile than virgin binder and gives rise to failure under repeated high axle loads and thermal effects. The placed high-RAP asphalt concrete mix becomes very brittle and is highly susceptible to fatigue cracking. Ideally, a high RAP content HMA mix should exhibit comparable or better strength and durability as compared to conventional non-RAP mixtures.

Another concern on the percentage of RAP that can be used stems from the variability of this material. When RAP is milled off an old surface, it might be mixed in with original pavement materials, as well as maintenance treatments such as patches and chip seals. Due to this variability, agencies tend to limit the percentage RAP that can be used in new mixtures. The way RAP materials are stockpiled can also have ramifications; i.e. when a stockpile includes more homogeneous RAP, a higher percentage is allowed compared to stockpiles with RAP containing more maintenance treatment materials (Copeland 2011).

According to the NAPA (Hansen and Copeland 2014), asphalt pavement is the most recycled material in the U.S. On average, a RAP content of 19.6% by weight was reported for U.S. state DOT HMA mixes with only 0.1M tons landfilled (Hansen and Copeland 2014) while the current upper bound on recycled content in HMA mixes for several state DOTs was reported to be around 30%, although proportions range from state to state. In states where virgin aggregate is scarcer, a higher RAP content might be used. Climate also dictates the limit of recycled content to some degree since thermal cracking is a major concern for mixes with high RAP content.

Abroad, RAP is being utilized in a similar manner. Japan has delved into the use of RAP and have reported the successful use of mixes containing up to 51% RAP without any compromise on durability (Hansen and Copeland 2014). However, it should be noted that truck weights and axle loads in Japan are significantly lower than the U.S., which prevents any direct performance comparisons. European countries also make use of RAP to achieve sustainability targets, but use far less recycled content as compared to the U.S. (World Highways 2013).

With the many variables and potential consequences associated with using high RAP/RAS contents in HMA, there is a need for a way to evaluate changes in the lifespan and sustainability of the pavement. Life Cycle Assessment (LCA) is a useful tool in identifying economic and environmental benefits of using RAP/RAS in large-scale projects. LCA considers each component of a project in terms of functional units. Having a unit cost analysis helps to identify where the majority of a project's resources are utilized and provides a measure of their effectiveness. Analyzing HMA mix design in this way will allow engineers to pinpoint areas where significant savings are opportune. LCA takes into account the environmental impacts of all components of a project to yield a comprehensive analysis of the project's environmental footprint. These types of analyses can be useful to identify factors that are critical to achieve organizational sustainability goals.

2.2 STRATEGIES TO INCREASE RAP/RAS CONTENT

Due to ever growing demand of asphalt pavement materials and limited supply of aggregate and asphalt binder, using RAP in HMA mixtures started to create significant benefits. For this reason, agencies are interested in finding ways to increase the RAP content of HMA mixtures. Prior to the introduction of the Superpave® method, RAP was frequently used by different state DOTs. Superpave® did not really provide a thorough method for using RAP in HMA mixtures (Copeland 2011) while it encouraged agencies to use RAP in asphalt mixtures. Moreover, due to high content of fines in RAP stockpiles and high variability in RAP, most DOTs refused to implement higher RAP percentages in their paving operations. As a result, the RAP content threshold was capped at 15 percent in the past. But in the late 2000s, a notable increase in binder costs brought about major interest in using higher percentage of RAP as a more cost-effective option in HMA paving. Therefore, a basis for allowing pavement designers to use a higher percentage of RAP was needed, as state DOTs were requesting more structured guidelines for using higher RAP contents. As can be seen in Figure 2.1 and Figure 2.2, there is a growing interest of using higher RAP content in the U.S. Figure 2.1 shows the increased RAP use in the U.S. by comparing the amount of RAP used prior to and after 2007. Figure 2.2 shows the current use of RAP contents of 25 percent and above for all U.S. states.

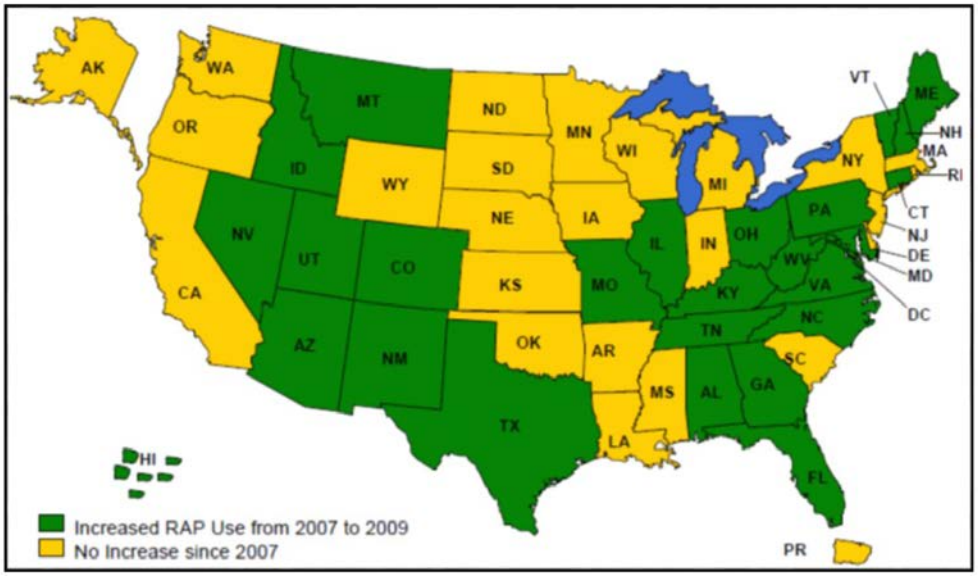

Figure 2.1: Map of U.S. states with increased RAP use since 2007 (Copeland 2011).

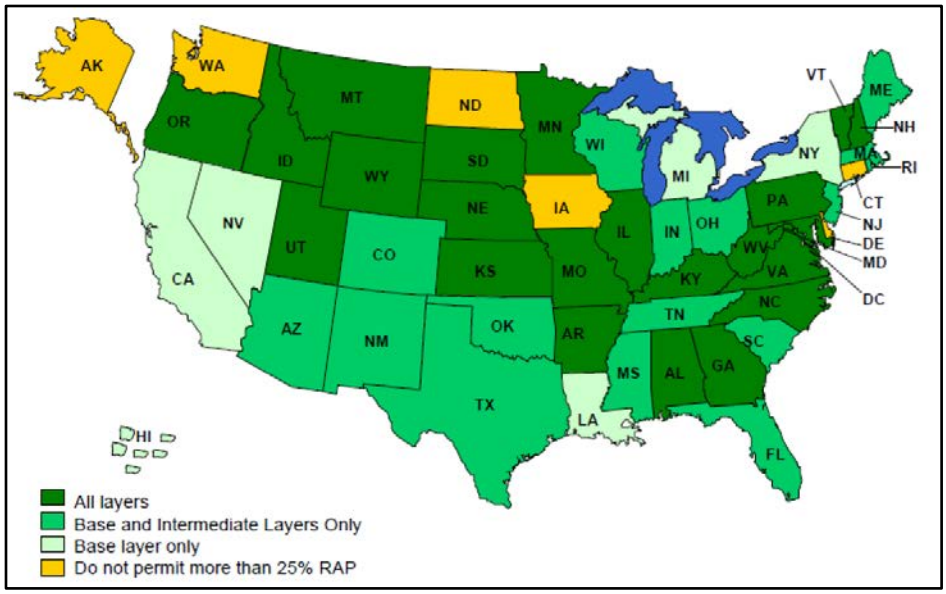

Figure 2.2: Map of U.S. states using RAP contents of 25% or greater in various HMA layers (Copeland 2011).

The primary concern when using high RAP/RAS mixes lies in the altered long-term durability properties of HMA mixtures. The dilemma is finding a way to use higher RAP contents in HMA without compromising any long-term durability. Major concerns result from higher cracking susceptibility due to stiffer RAP mix. Regarding these concerns, the following strategies were generally suggested in the literature to increase the RAP content without compromising the cracking resistance (Bennert et al. 2014):

1. Softer virgin binder grade (binder-grade bumping)
2. Increased binder content
3. Recycling agents
4. Polymer and rubber modifiers
5. Warm mix asphalt

2.2.1 Binder-Grade Bumping

With the increasing global awareness to achieve sustainable practices in pavement construction, the necessity to use higher percentages of RAP in asphalt mixtures is gaining more attention. One of the strategies identified to be effective in increasing RAP/RAS content is binder grade bumping. Binder grade bumping refers to decreasing high binder PG grade by one or two grades while double-bumped grade means decreasing high and low binder grades by one grade.

Aurangzeb et al. (2012) carried out a study with an objective to quantify the impact of binder-grade bumping on the performance of high RAP asphalt mixtures. The virgin aggregates and RAP were obtained from two districts of Illinois Department of Transportation. In order to assess the effect of binder grade bumping on the performance of RAP mixtures, PG 58-22 and PG 58-28 binders were used. Eight asphalt mixtures were prepared, four for each of the two districts.

The four mixtures for each district consisted of a control mix (no RAP), a mix with 30% RAP, a mix with 40% RAP, and a mix with 50% RAP. Wheel-tracking and beam fatigue tests were carried out on these asphalt mixtures. The findings from this study are as follows:

- Although there was a viscoelastic softening effect of binder grade bumping on mixtures, the mixtures with the softest binder had a smaller rut depth than the control mixture as show in the Figure 2.3. It was also observed that the addition of RAP improved the rutting resistance of asphalt mixtures.

- In general, single grade bumping improved the fatigue behavior of asphalt mixtures. However, double-grade bumping did not show any significant improvement as compared to single-grade bumping.

Li et al. (2008) investigated the effect of binder grade on RAP performance by conducting dynamic modulus and semi-circular bend (SCB) fracture tests. Two different RAP sources, three RAP contents (0%, 20%, and 40%), and two different asphalt binder grades (PG 58-28 and PG 58-34) were used for specimen preparation. Based on the dynamic modulus tests, it was concluded that softer binder (PG 58-34) provides higher fracture resistance and increases fatigue life. West et al. (2012) investigated the performance of four sections with surface layers containing 45% RAP and different virgin binder grades (PG 52-28, PG 67-22 and PG 76-22). After a total of 20 million ESALs, mixes with softer binders showed better cracking performance than the mixes with stiffer binders. This result suggested that using binder-grade bumping can be an effective strategy to improve cracking performance of high RAP mixes. The NCAT laboratory study conducted by Willis et al. (2012) concluded that binder-grade bumping along with a 0.3% increase in binder content significantly improved the cracking performance of 50% RAP mixes.

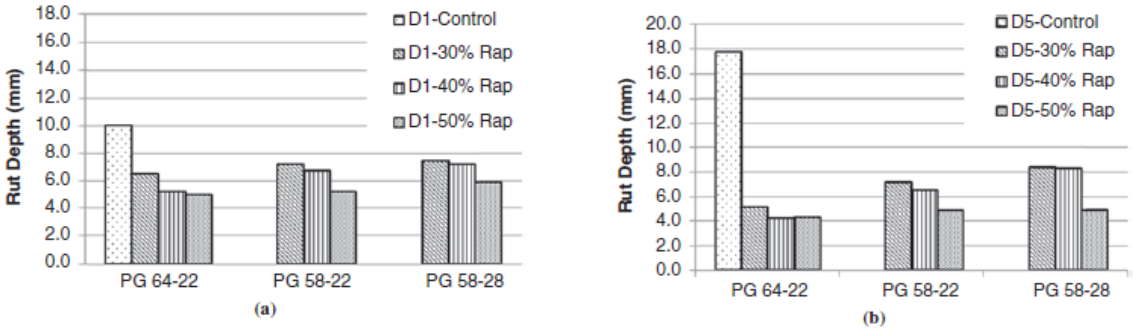

Figure 2.3: Wheel-tracking test results: (a) District 1 (b) District 5 (Aurangzeb et al. 2012).

2.2.2 High Binder Content

One of the major drawbacks of using higher RAP content is the increased stiffness of the mixture which in turn reduces the fatigue performance. This problem can potentially be overcome by increasing the ductility of the mix by increasing the binder content. A study conducted by West et al. (2009) investigated the performance of two sections with 20% RAP, four sections with

45% RAP, and one control section with no RAP at the National Center for Asphalt Technology (NCAT) test track. RAP sections were constructed with 50 mm thick overlays in 2006. Sections with 20% RAP had asphalt mixes with 5.6% binder content with PG 76-22 and PG 67-22 binders. The binder content for the sections with 45% RAP was 5.0% with PG 52-28, PG 67-22, PG 76-22, and PG 76-22 plus 1.5% Sasobit binders. The control section consisted of 5.8% asphalt binder with the PG 67-22.

After 24 months (9.4 million ESALs), rutting was measured with scanning laser rut-bar, cracking was measured by weekly visual inspections, and roughness was measured by using inertial profiler technology (AASHTO R 43-07). International Roughness Index (IRI) was almost equal for all segments except for the control section and the section with 20% RAP and PG 67-22 binder, which had higher IRI levels. Moreover, rut depths were the greatest for the section with 20% RAP and PG 67-22 followed by the section with virgin binder. Minor cracks with low severity were observed at 45% RAP section with PG 76-22 plus Sasobit (reflection cracks) and 20% RAP section with PG 76-22 (top-down cracks). Other segments did not show any cracking. According to Asphalt Pavement Analyzer (APA) rutting test results, mixes with softer asphalt binders and higher VFA showed higher rutting. Furthermore, results from dynamic modulus tests illustrated that mixtures with stiffer binder and higher percentage of RAP had higher dynamic moduli.

The beam fatigue test was also conducted (AASHTO T 321-07) on long-term aged samples. Results are shown in Figure 2.4. Sections with 45% RAP asphalt mixes exhibited significantly lower fatigue resistance than the 20% RAP sections and the sections without RAP due to the lower effective binder content. The design binder content for the 45% RAP mixes was 5% while the effective binder content for the final mix was expected to be higher as a result of the blending of virgin binder with the RAP binder. However, significantly lower fatigue resistance for the 45% RAP mixes suggested that RAP and virgin binders were not completely blended. Although the 45% RAP mixes with softer binders (PG 52-28 and PG 67-22) have higher fatigue resistance than the stiffer ones (PG 76-22 and PG 76-22 with Sasobit), the effect of binder grade on the fatigue test results was not significant when compared with the effect of effective binder content. It was concluded that the effect of binder-grade bumping becomes less influential as RAP content of the mix increases.

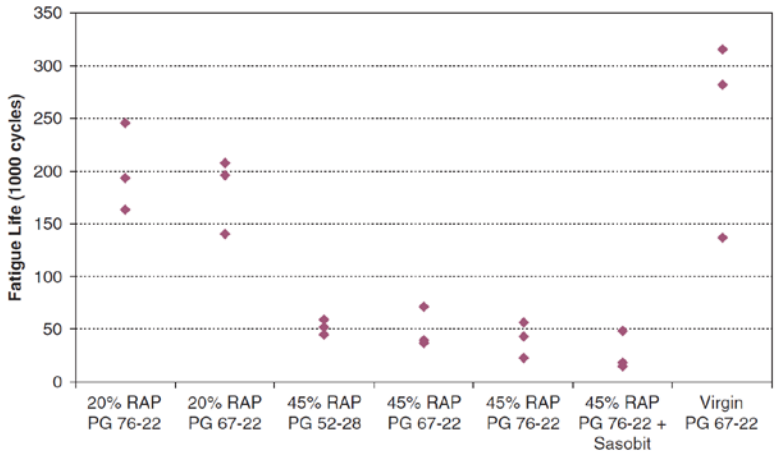

Figure 2.4: Plot of beam fatigue test results for RAP experimental sections

(West et al. 2009).

2.2.3 Recycling Agent

For mixtures with higher percentage of RAP and RAS, one of the strategies for improving the resistance to cracking is using recycling agents such as rejuvenators and softening agents. While softening agents, such as slurry oil and lube stock, can reduce binder viscosity, rejuvenators are used to create chemical reactions in the binder phase to improve its physical properties. The conventional method for softening the hardened aged binder in RAP is using virgin binder. In addition, rejuvenators can be used to reduce the viscosity of RAP mixtures (Tran et al. 2012; Zaumanis et al. 2013). Since adding rejuvenator to the mixture containing RAP has some uncertainties, including inadequate blending between rejuvenator and recycled binder and the required reaction time, it is not widely used. However, selecting a proper amount of rejuvenator, ensuring appropriate mixing, and allowing the required reaction time to occur offset these uncertainties and improve the crack resistance of mixtures (Tran et al. 2012).

Rejuvenators restore the physical and chemical properties of aged binder and reduce the viscosity of the mix (Roberts et al. 1996). They encompass high amounts of maltene components (napthenic and polar aromatic fractions) that can be used to replace the maltenes lost due to binder aging during the construction and use phases. Maltenes incorporated into the RAP mix are expected to reduce the viscosity of the aged and hardened recycled binder (Terrel and Epps 1989). Diffusion of rejuvenators into recycled binder is crucial and consists of four main steps: 1) RAP aggregates are covered with rejuvenator; 2) rejuvenator penetrates to the aged binder layer around the aggregates and softens the binder (at this step the amount of raw rejuvenator decreases); 3) the rejuvenator penetrates further into the inner layer of the binder which softens the inner layer of the binder while viscosity of binder in outer layer gradually increases; 4) the equilibrium of viscosity is reached in the layers of the recycled binder. The rejuvenator diffuses further into the layer of aged binder during mixing, construction, and use phases of the pavement life cycle (Carpenter and Wolosick 1980).

Tran et al. (2012) evaluated the effect of rejuvenators on HMA mixtures containing high percentages of RAP and RAS. In this study, a mix with no RAP or RAS (control mix), two 50% RAP mixtures with and without rejuvenator, and two 20% RAP plus 5% RAS mixtures with and without rejuvenator were prepared using Cyclogen L rejuvenator and virgin binder with PG 67-22. Dynamic shear rheometer (DSR) and bending beam rheometer (BBR) tests were conducted on extracted RAP binder with different percentages of rejuvenators to determine the optimum amount of rejuvenator required to reach the performance properties of mix with PG 67-22 binder. In the first stage, the optimum amount of rejuvenator was determined to be around 12% of the total recycled binder. In the second stage, mixtures were blended with optimum percentage of rejuvenator and tested to determine Tensile Strength Ratio (TSR) to evaluate moisture susceptibility, dynamic modulus test for mixture stiffness, energy ratio test (resilient modulus, creep compliance, and indirect tensile tests) for resistance to top-down cracking, indirect tensile test (IDT) for resistance to low temperature cracking, modified Overlay Tester (OT) for resistance to reflective cracking, and Asphalt Pavement Analyzer (APA) for rutting resistance. Results illustrated that rejuvenator decreased the mixture stiffness, improved all four fracture properties from the energy ratio test, improved low temperature performance of mixture, and increased resistance to rutting (the improvement against rutting was not significant). It was concluded that using rejuvenator for high amount of recycled binder could be an effective method for enhancing the binder properties.

Shen et al. (2007) compared properties of mixtures containing RAP and rejuvenator against mixtures with a softer binder instead of a rejuvenator. Amounts of rejuvenators for mixtures were determined by blending charts of RAP binders with rejuvenators which were established through dynamic shear rheometer and bending beam rheometer tests (considering the properties of binder with PG 64-22). Ten mixtures with RAP (five with rejuvenator and five without rejuvenator) and two mixtures without RAP (control mixtures) were designed and tested to evaluate the impact of rejuvenators and softer binders on mix performance. Several asphalt specimens with RAP contents up to 48 percent, one oil type rejuvenator, and virgin binders with PG 64-22 and PG 52-28 were prepared. Indirect tensile strength and APA tests were conducted for evaluating the moisture susceptibility and rutting properties of mixtures. This study showed that the RAP content could be increased by up to 10% more in mixtures using rejuvenators with PG 64-22 virgin binder as compared to mixtures containing the softer PG 52-28 binder. It was concluded that blending charts were proper tools to estimate the rejuvenator contents. Furthermore, mixtures with rejuvenators illustrated better mechanical and rutting properties than mixtures containing softer binder.

A study by Oliveira et al. (2013) used motor oil as a rejuvenator to evaluate the properties of mixtures containing 100% RAP. Using penetration grade, softening point, and dynamic viscosity tests, the optimum amount of rejuvenator required to increase penetration grade from 10/20 to 20/30 was estimated to be around 5%. Conventional control HMA mixtures were produced with 5.1% binder content and a binder classified as 35/50 penetration grade. Water sensitivity (by conducting indirect tensile strength tests with dry and wet specimens), permanent deformation (using wheel tracking test), stiffness modulus (using four-point bending beam test), and fatigue cracking tests were conducted on control HMA and 100% RAP mixtures to assess their properties. Test results showed that 100% RAP mixtures are more resistant to moisture than the control mix. Fatigue cracking and rut resistance of 100% RAP mixes were also higher than the

control mix. It was concluded that high performance 100% RAP mixes can be produced by providing appropriate storing and production conditions.

2.2.4 Combining RAP/RAS with Warm Mix Asphalt (WMA)

The workability and compactibility of HMA with high RAP content have always been a challenge to control (Petersen 1984). Aged, stiffened RAP binder can cause problems during mixing and construction. Using Warm-Mix Additives (WMA) is a strategy to mitigate problems brought on by using high percentages of RAP in asphalt pavements. Below are summaries of studies looking at the effects of WMA on RAP mixes.

Tao and Mallick (2009) evaluated the impact of using two types of WMA (Sasobit H8 and Advera zeolite) on the workability, density, seismic modulus (tested at 0°C, 26.7°C, and 50°C) and strength (by conducting indirect tensile strength) of 100% RAP mixes. One RAP source with 6% asphalt binder content was used in this study. Sasobit H8 (1.5%, 2.0%, and 5.0% by weight of total asphalt binder) and Advera zeolite (0.3%, 0.5%, and 0.7% by weight of total mix) were mixed with RAP and compacted with a standard gyratory compactor (SGC) at 125°C. Mixes with Sasobit H8 additives exhibited higher bulk specific gravity (BSG) after compaction as compared to the control mix with 100% RAP and no additives. The mix with 0.3% Advera zeolite also had a higher BSG than the control mix. This trend resulted from increased compactibility due to added WMA. However, the mixes with 0.5% and 0.7% of Advera zeolite had lower BSG than the control. It was indicated that lower BSG is a result of excessive volume expansion at higher additive contents created by water vapor. The workability of the mixes were tested by using a torque tester after adding 2.0% Sasobit H8 and 0.5% Advera zeolite to the mixes. The mixes showed greater workability than the control mix at 110°C and less workability at 80°C. This study showed that both WMAs had a stiffening effect on the mix at low temperatures. Moreover, mixes with WMA had a higher seismic modulus than the control mix at all temperatures.

A study carried out by Mallick et al. (2008) investigated the feasibility of preparing 75% RAP mixtures with WMA (Sasobit H8) to determine whether these mixes met standard specifications.

Table 2.1 summarizes the properties of the mixtures prepared in this study. Samples were tested for BSG, indirect tensile strength at -10 °C, rutting resistance (using the asphalt paver analyzer test), and seismic modulus at 0 °C, 25 °C, and 40 °C. This study showed that Sasobit H8 increased compactibility and enhanced workability of the mix. It was concluded that preparing mixtures with 75% RAP with air void contents similar to mixtures without RAP was possible. The control mix had the highest indirect tensile strength, whereas the mixture with WMA and PG 42-42 asphalt binder showed the lowest indirect tensile strength. Adding Sasobit H8 to the mixtures resulted in a tensile strength increase for the same binder performance grade. Rut depths were least for the mixture without WMA and PG 52-28 binder and greatest for the mixture with WMA and PG 42-42 binder. All rut depths were less than 4 mm due to stiffness brought on by the high RAP content in the mixtures. The seismic modulus test showed that stiffness of the RAP mixes with the softest binder and Sasobit H8 were close to the control mixture at all the test temperatures. Mallick et al. (2008) stated that it is possible to prepare 75% RAP mixes with the same air void content as mixes without RAP at lower temperatures.

Table 2.1: Mixture Properties

	Control mix	Mix 1	Mix 2	Mix 3	Mix 4
RAP content	0%	75%	75%	75%	75%
WMA type	NA	NA	Sasobit H8	Sasobit H8	NA
WMA content (by weight of total asphalt binder)	0%	0%	1.5%	1.5%	0%
Virgin binder grade	PG 64-28	PG 52-28	PG 52-28	PG 42-42	PG 42-42
Virgin binder content	4.7%	1.5%	1.5%	1.5%	1.5%
Compaction temperature	150 ^{o}C	135 ^{o}C	125 ^{o}C	125 ^{o}C	125 ^{o}C
Number of prepared samples	18	18	18	18	2

In a study conducted by Zhao et al. (2012), rutting resistance, fatigue resistance, and moisture susceptibility of WMA and HMA mixes containing different amounts of RAP were evaluated. The WMA mixtures were produced with a foaming technology at 0%, 30%, 40%, and 50% RAP contents. Standard HMA mixtures, as control mixes, contained 0% and 30% RAP. Rutting resistance was tested with the asphalt pavement analyzer (APA) rutting test and Hamburg wheel-tracking test. Results illustrated that rutting resistance was improved by adding more RAP to the mixtures. This improvement was more significant for WMA-RAP mixtures than HMA-RAP mixtures. Moisture susceptibility was tested with the tensile strength ratio (TSR) test. Mixtures containing RAP showed less moisture susceptibility than mixtures without RAP. This trend was observed in both WMA and HMA mixtures. However, WMA mixtures had lower TSR than HMA mixtures, indicating that moisture susceptibility is a concern for WMA mixtures. Fatigue performance was tested with Superpave IDT (including resilient modulus, creep, and indirect tensile strength tests) and beam fatigue tests. According to beam fatigue test results, adding more RAP to the WMA samples increased fatigue cracking performance. On the other hand, for mixes without WMA, increased RAP content reduced fatigue life. It is worth noting that increasing the RAP content in WMA mixtures increased the energy ratio (ER) values and fracture resistance of the WMA mixtures, leading to longer fatigue life.

2.2.5 Modification of RAP/RAS Mixtures

Modification of RAP/RAS mixes with crumb rubber and polymer improves the mechanical characteristics of HMAs and allows the use of higher RAP/RAS contents. Although polymer and rubber modification increase the cost of asphalt mixes, increased RAP content can offset the high cost of modified binders. Below are studies that investigated the effects of modification on mixes with high RAP contents.

Hajj et al. (2009) investigated the impact of three sources of RAP in three contents (0%, 15%, and 30%) on the mechanical characteristics of the mixtures. Two different types of binders (PG

64-22 and PG 64-28NV[1] polymer-modified) were used for preparing laboratory mixtures. Fatigue beam tests were conducted at different strain levels to evaluate the cracking resistance of prepared mixes. This study showed that polymer-modified mixtures had greater fatigue performance than unmodified mixtures regardless of RAP content. While polymer-modified mixtures containing RAP had lower fatigue resistance than polymer-modified mixtures without RAP, they showed higher fatigue resistance than unmodified mixtures without RAP. This study concluded that using RAP with polymer modification could enhance the fatigue performance of mixtures and offset the increased costs of using these modifications when life cycle cost analysis (LCCA) is used to evaluate the cost effectiveness for the design period.

A study conducted by West et al. (2009) investigated the performance of two sections with 20% RAP with PG 76-22 and PG 67-22 asphalt binders, four sections with 45% RAP with PG 52-28, PG 67-22, PG 76-22, and PG 76-22 binder with 1.5% Sasobit warm-mix additive, and one control section with PG 67-22 asphalt binder and no RAP at the National Center for Asphalt Technology (NCAT) test track. The field study showed that the 45% RAP sections with softer binders were compacted easier than the sections with polymer-modified binders. It was also observed that adding Sasobit to modified binders did not improve compactibility. Moreover, conducting indirect tensile tests (IDT) to estimate creep compliance, fracture energy, and resilient modulus showed that polymer modification was effective in increasing the energy ratio and reducing the potential for top-down cracking.

Xiao et al. (2007) assessed the rutting performance of crumb rubber-modified RAP mixtures. Two rubber types (Ambient and Cryogenic), four rubber contents (0%, 5%, 10%, and 15% by weight of virgin binder), and three rubber sizes were selected for preparing RAP mixtures from two RAP sources with different contents (0%, 15%, 25%, and 30% for one RAP source and 0%, 15%, and 38% for the other). Wet and dry Indirect Tensile Strength (ITS) tests and Asphalt Pavement Analyzer (APA) rutting tests were conducted with the prepared specimens. This study concluded that higher percentages of RAP reduced the rut depth and increased the ITS and stiffness values. On the other hand, increasing the rubber content decreased the ITS value and creep stiffness. Moreover, this study showed that the effect of rubber size on rutting performance was insignificant. In general, crumb rubber reduced air voids and improved rutting performance.

Influence of crumb rubber size and type on RAP mixture properties were investigated in the study carried out by Xiao et al. (2009). This study used three rubber sizes and two rubber types (ambient and cryogenic) in the specimens with 25% RAP and virgin binder with PG 64-22. Indirect tensile strength tests (ITS) for moisture susceptibility, resilient modulus tests, and the flexural bending beam fatigue tests were conducted to evaluate the performance of asphalt mixes. It was concluded that using crumb rubber as a modifier in RAP mixtures could reduce the need for adding virgin binder and increase the moisture resistance by increasing the Tensile Strength Ratio (TSR). In general, using RAP and crumb rubber increased the resilient modulus at different temperatures. However, as the size of crumb rubber increased, resilient modulus decreased regardless of rubber types. Addition of crumb rubber improved the fatigue performance of mixtures as the rubber size increased. However, it should be noted that increased rubber size can create compaction problems during construction.

[1] NV indicated that the binder grading showed additional toughness and ductility for virgin and RTFO aged binder at 40^{o}F besides the standard Superpave binder testing requirements.

Mohammad et al. (2011) conducted a study on evaluating the crumb rubber effect on high RAP content mixtures. Six different mixtures were prepared: 1) HMA mixture with PG 64-22 binder; 2) HMA mixture with SBS polymer-modified asphalt binder classified as PG 70-22M[2]; 3) HMA mixture with SBS polymer-modified asphalt binder classified as PG 76-22M; 4) HMA mixture with crumb rubber modified binder (wet process) graded as PG 76-22; 5) mixture with 15% RAP and SBS polymer-modified asphalt binder classified as PG 76-22M; and 6) mixture with dry blending 40% RAP, crumb rubber additives, and PG 64-22 binder. Moisture resistance, rutting performance, and cracking resistance were evaluated using a modified Lottman test, loaded - wheel tracking test, flow number test, dynamic modulus test, semi-circular bending test, and dissipated creep strain energy test. The results of this study showed that adding crumb rubber additives led to softening the blended asphalt binder. Moreover, rubber modified mixture with high RAP content showed adequate moisture resistance. However, the mixture with no RAP content and rubber modified binder failed in moisture resistance test. SBS modified mixture with PG 76-22M binder and rubber modified mixture with high RAP content ranked first and last in fracture energy, respectively, whereas they both showed adequate performance in permanent deformation. It was concluded that these results could be due to the properties of asphalt binder with PG 64-22 and the high RAP content.

In summary, polymer-modification was observed to improve fatigue cracking resistance of high RAP mixes. For this reason, polymer modification can be an effective strategy to increase RAP content of asphalt mixes. However, life cycle cost analyses and performance modeling should be used to evaluate the cost effectiveness of using polymer modification in RAP mixes. It is prudent to note that the studies focusing on the use of rubber modification to improve cracking performance of RAP mixtures did not suggest any significant improvement in performance created by the use of crumb rubber.

2.3 METHODS TO CHARACTERIZE AND DESIGN ASPHALT MIXTURES WITH RAP/RAS

2.3.1 Binder Extraction and Recovery

In order to incorporate high RAP content in new mix designs, it is necessary to know the asphalt binder content present in the RAP, the physical properties of the asphalt binder such as complex modulus and phase angle, and the physical properties of RAP aggregates such as gradation and angularity. It is therefore essential to extract the asphalt binder and aggregates from the RAP mixture. There are various techniques to extract the binder for testing such as centrifuge, vacuum, and reflux methods. Some of these techniques are described in the subsequent sections.

[2] M: Modified

2.3.1.1 Extraction and Recovery of Asphalt from Solution by Abson Method

This procedure follows ASTM D2172/D2172–11 and ASTM D1856–09 standards. The procedure is as follows:

- About 650 to 2500 g of RAP mixture is placed into a container and a solvent such as trichloroethylene, normal Propyl Bromide, or methylene chloride is added. This container is then placed into a centrifuge extraction apparatus.

- The centrifuge is revolved gradually up to a speed of 3600 revolutions per minute.

- The above procedure is subsequently repeated by adding 200 ml of solvent each time until the extract is of light straw color. The extract is then collected.

- The collected extract is centrifuged for approximately 30 min at 770 times the gravitational acceleration in centrifuge tubes.

- The above solution is concentrated by distillation to about 200 ml and the residue is transferred into a 250 ml distillation flask.

- The distillation is continued until the temperature reaches 135 °C. Once this temperature is reached, carbon dioxide is injected at a rate of 100 ml/min. When the temperature reaches 160 °C, the rate of carbon dioxide injection is increased to 900 ml/min. The temperature and carbon dioxide gas flow rate is maintained until the dripping of condensed solvent ceases.

The recovered asphalt is re-liquefied by heating for use in the determination of physical properties. The extraction and recovery apparatus used in this method is as shown in Figure 2.5.

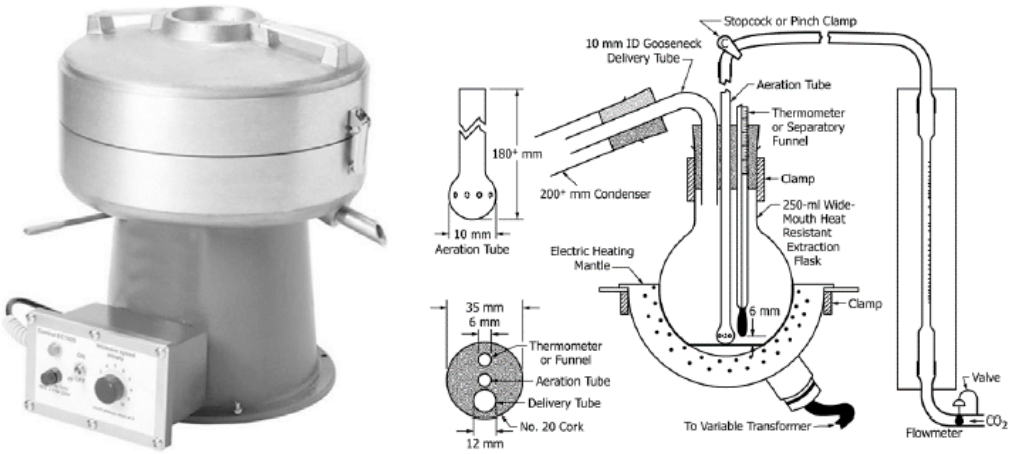

Figure 2.5: Extraction and recovery apparatus

(ASTM D2172/D2172–11 and ASTM D1856 – 09).

2.3.1.2 The Modified Strategic Highway Research Program (SHRP) Extraction and Recovery Technique

This method (AASHTO TP2 1996) is the most preferred procedure for binder extraction. The binder extracted from this technique results in minimal change to the binder properties. A brief procedure is described as follows:

- In order to obtain approximately 50 to 60 g of recovered asphalt, a sample of 1000 to 1100 g of RAP mixture needs to be prepared.
- This RAP mixture is then oven dried at approximately 110 °C.
- This method uses an extraction cylinder that is rotated axially for approximately 5 min to blend the solvent and the RAP mixture. Approximately 600 ml of solvent, such as n-propyl bromide or toluene, is added to the cylinder and then nitrogen gas is injected into the vessel at the rate of 1000 ml/min.
- The effluent is then vacuumed at a pressure of 700 mm Hg into the Rotavapor recovery flask where the primary distillation is carried out at a vacuum pressure of 700 mm Hg in an oil bath at approx. 100 °C.
- The above steps are repeated using 400 ml solvent and 30 minute rotation time until the extract achieves a light straw color.
- The effluents are transferred into centrifuge bottles and centrifuged for 25 min at 3600 rpm. The centrifuged effluents are then poured back into the distillation

flask and distilled at approximately 175 °C until the condensation rate is less than 1 drip every 30 s.

The recovered asphalt binder is harvested from the distillation flask for further determination of physical properties. The extraction and recovery apparatus used in this method is as shown in the Figure 2.6.

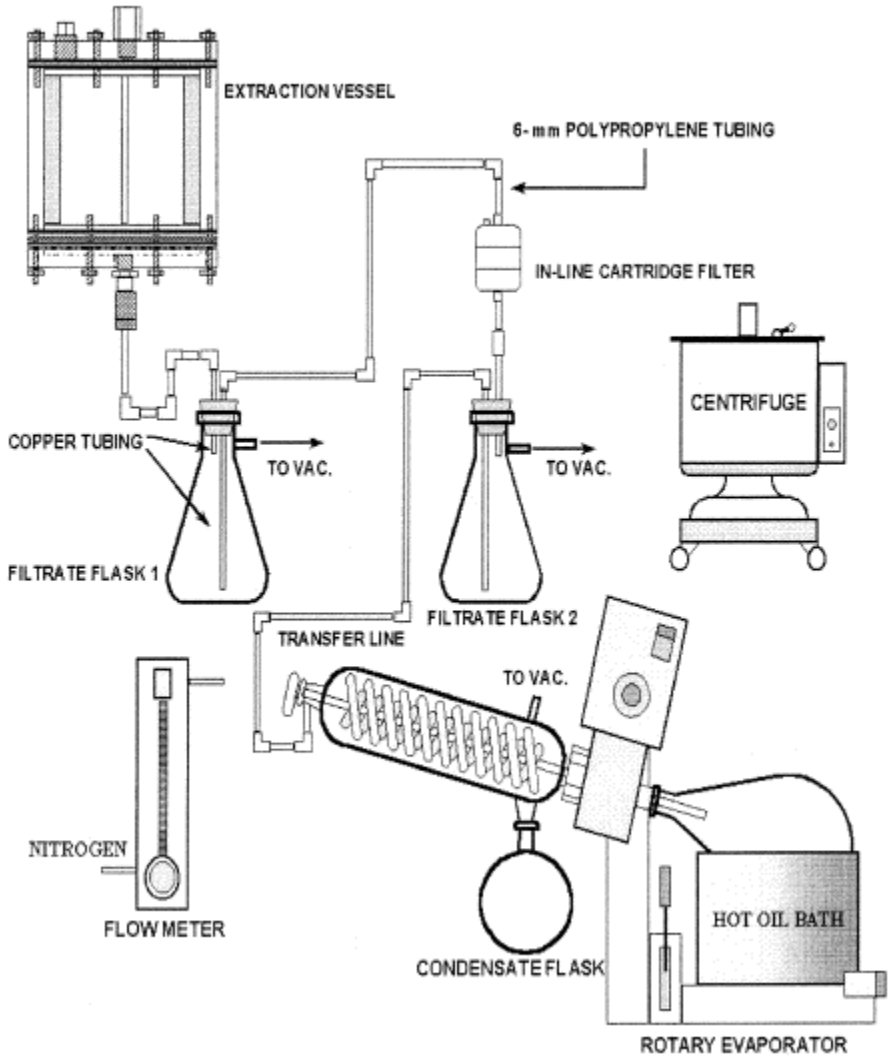

Figure 2.6: SHRP extraction and recovery apparatus (AASHTO TP2 1996).

2.3.2 Recovered Aggregates and Binder Experiments

As mentioned in the previous section, it is important to determine the physical properties of the aggregates and binder extracted from RAP. The aggregate that is saved after binder extraction is analyzed for gradation in accordance with AASHTO T30. Also, the bulk specific gravity of the aggregates is determined in order to calculate voids in mineral aggregates (VMA) and to estimate

the binder content of the mixture. Apart from this, the properties of the RAP aggregates along with virgin aggregates are analyzed for adequacy for use in the Superior Performing Asphalt Pavements (Superpave®) method. The properties determined are coarse aggregate angularity (ASTM D5821), fine aggregate angularity (AASHTO T304 Method A), percentage of flat and elongated particles (ASTM D4791), and percentage of fine clay particles contained in the fine aggregate (AASHTO T176).

Recovered RAP binder is classified according to AASHTO MP1 by testing unaged, rolling thin film oven (RTFO) aged, and pressure aging vessel (PAV) aged binders with the dynamic shear rheometer (DSR) and the bending beam rheometer (BBR). After determining the physical properties and critical temperatures of the recovered RAP binder, blending charts are used to determine the performance grade of the virgin binder that is required to achieve a specific final performance grade.

2.3.3 Blending Charts

Under NCHRP 9-12 (McDaniel and Anderson 2001) recommended guidelines, there are three tiers of RAP usage. The first tier is for lower RAP contents and gives an estimate about the RAP content that can be used in the mix without changing the PG grade of the virgin binder. The second tier is for intermediate RAP content and establishes the amount of RAP that can be used in the mix when the virgin binder grade is decreased by one PG grade. The third tier is for higher RAP contents and for this tier it is necessary to know the properties of the RAP binder and requires blending charts to determine the amount of RAP to be used in the mix.

In order to construct blending charts, it is essential to know the physical properties of the recovered RAP binder and the desired final grade. Apart from these, either the physical properties of virgin binder or the percentage of the RAP in the mixture are required. Depending upon the unknown parameter, there are two blending methods that are briefly explained in the next section.

2.3.3.1 Method A – Blending at a Known RAP Content (Unknown Virgin Binder Grade)

In situations where the amount of RAP to be used in the mix is predetermined, this blending method is used. If the final blended binder grade, RAP content, and the physical properties of the recovered RAP are known, then using this blending chart allows an appropriate virgin binder grade to be determined. The following Equation (2.1) is proposed in NCHRP 9-12 (McDaniel and Anderson 2001) to calculate the critical temperature of the virgin binder.

$$T_{virgin} = \frac{T_{blend} - (\%RAP \times T_{RAP})}{1 - \%RAP} \quad (2.1)$$

Where,

T_{virgin} = critical temperature of the virgin asphalt binder,

T_{blend} = critical temperature of the blended asphalt binder,

%RAP = percentage of RAP expressed as decimal, and

T_{RAP} = critical temperature of recovered RAP binder.

Figure 2.7 shows an example of blending chart prepared using method A.

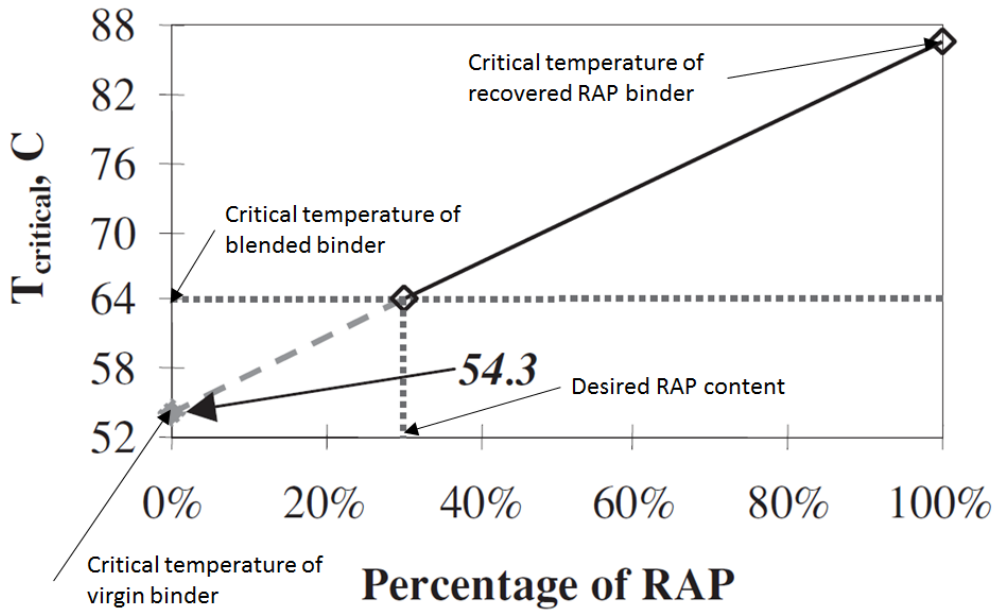

Figure 2.7: Blending chart for Method A (McDaniel and Anderson 2001).

2.3.3.2 Method B – Blending with a Known Virgin Binder Grade (Unknown RAP Content)

In cases where the grade of the virgin binder to be used in the RAP mixture is fixed, the required RAP content needs to be determined. In this case, method B for blending is used. The percent of RAP can be determined if the final blended binder grade, virgin asphalt binder grade, and the physical properties of the recovered RAP binder are known. The following Equation (2.2) is used to determine the percentage of RAP (McDaniel and Anderson 2001).

$$\%RAP = \frac{T_{blend} - T_{virgin}}{T_{RAP} - T_{virgin}} \quad \textbf{(2.2)}$$

Where,

T_{virgin} = critical temperature of the virgin asphalt binder,

T_{blend} = critical temperature of the blended asphalt binder,

%RAP = percentage of RAP expressed as decimal, and

T_{RAP} = critical temperature of recovered RAP binder.

Figure 2.8 shows an example of blending chart prepared using method B.

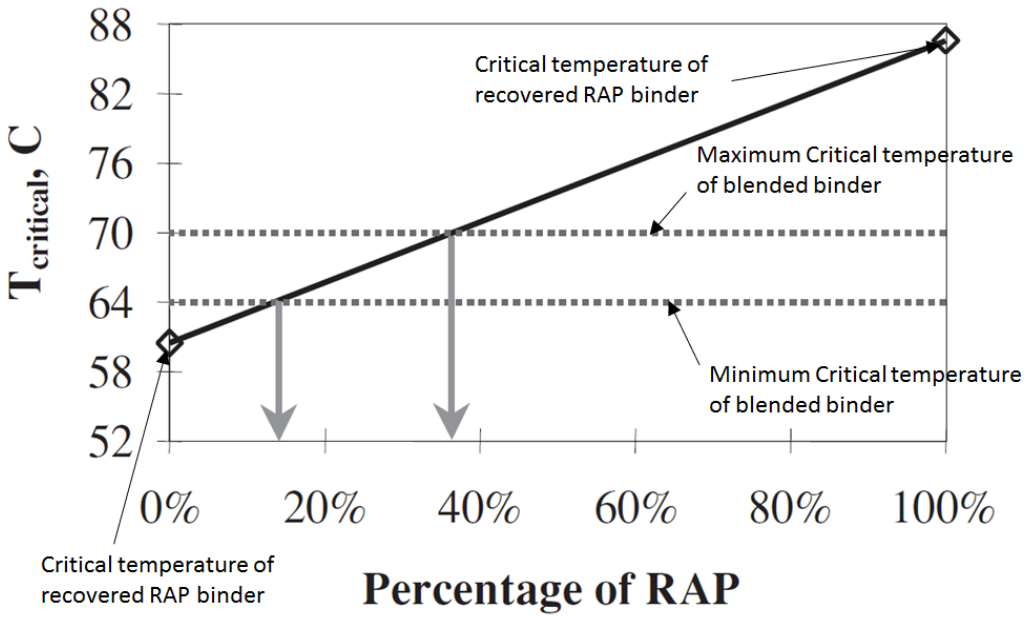

Figure 2.8: Blending chart for Method B (McDaniel and Anderson 2001).

2.3.4 Mix Design Procedure

The mix design procedures involving RAP mixtures are similar to that of conventional asphalt mixtures. However, the RAP materials should meet the typical aggregate gradation and quality specifications in order to be mixed with the virgin materials. After separating aggregate and binder in the RAP, the aggregates are tested for gradation and quality. McDaniel and Anderson (2001) suggest that the PG binder grade can remain the same when less than 15% RAP is used in HMA. It is suggested to lower the PG binder grade by one grade when 15-25% RAP is used in the mixture. When using more than 25% of RAP, it is suggested to use the blending chart to determine the amount of RAP and PG binder grade that should be used in the mixture. The mix design process is summarized in Figure 2.9.

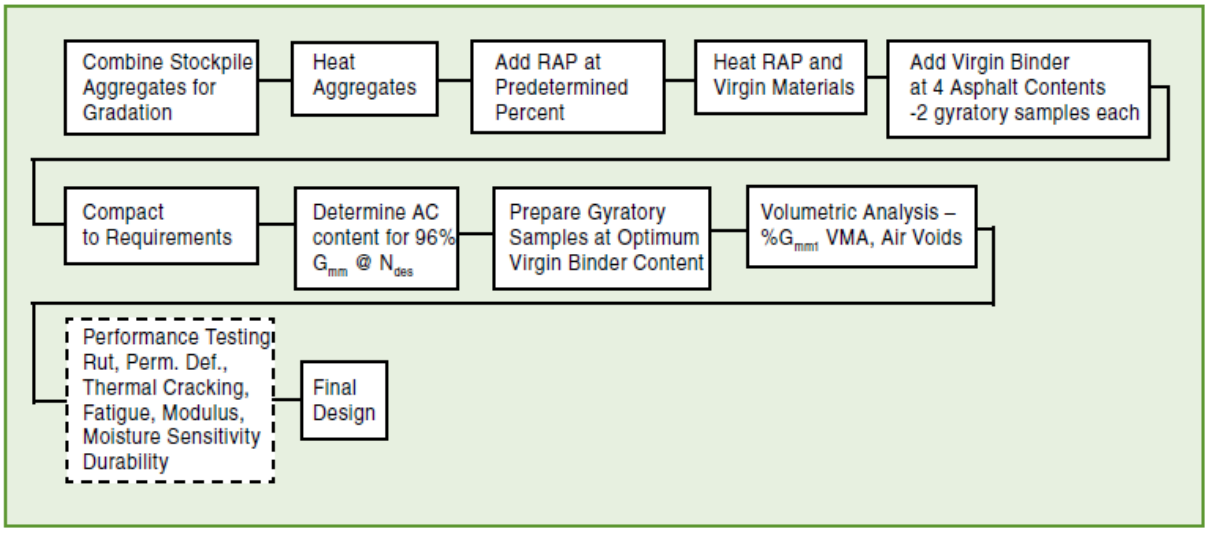

Figure 2.9: Mix design process involving RAP (Newcomb et al. 2007).

2.4 BLENDING OF RAP AND VIRGIN BINDER

In designing RAP mixtures, it is important to know the extent that virgin and RAP binders blend with each other. This could be the basis for estimating the amount and type of the virgin binder to add to RAP mixtures to reach desirable binder performance. This section summarizes some influential studies done in this area.

McDaniel et al. (2001) investigated how aged RAP binder affected the virgin binder grade and to what extent the RAP binder was blended with the virgin binder. In this study, three RAP mixes (with low, medium, and high stiffness), two virgin binders (PG 52-34 and PG 64-22), two RAP contents (10% and 40%), and one aggregate type were used. All mixtures had the same gradation with the same binder content. Three types of mixtures were prepared. In the first mixture, Black Rock (BR), the RAP materials were considered as aggregate with no blending between virgin binder and RAP binder. For this mixture, the RAP binder was extracted, and the recovered RAP aggregate was mixed with virgin binder. The second mixture, Actual Practice (AP), RAP (with the binder film intact) was blended with virgin aggregate and binder. The third mixture, Total Blending (TB), RAP binder was extracted and blended with the virgin binder separately. Then, blended binder was mixed with the recovered RAP aggregate. In order to evaluate the impact of blending on mix properties, Frequency Sweep (FS), Simple Shear (SS), and Repeated Shear at Constant Height (RSCH) tests were conducted at intermediate and high temperatures. Indirect Tensile Creep (ITC) and Indirect Tensile Strength (ITS) tests were conducted at low temperatures. The results showed that there were no significant differences in stiffness and deformation between the three mixtures with 10% RAP content. However, the BR mixture with 40% RAP had lower stiffness and higher deformation. AP and TB mixtures illustrated similar responses that showed that blending of virgin and recycled binder occurred to some extent, and considering RAP materials as black rock is a false assumption. Using five different RAP

contents (0%, 10%, 20%, 40%, and 100%), it was concluded that blending charts could be an effective guide for selecting proper RAP and binder properties.

Study conducted by Huang et al. (2005) investigated the level of blending of RAP binder with the virgin binder under typical mixing conditions. At first, aggregates with three RAP contents (10%, 20%, and 30%) were passed through the No.4 sieve and mixed with coarse virgin aggregates retained on the No.4 sieve. Virgin and RAP aggregates were mixed at 190^{o}C for 3 minutes in order to estimate the amount of RAP binder removed from the RAP particles and transferred onto the virgin aggregates. After mechanical blending, RAP aggregates were separated from virgin aggregates, and asphalt contents for both mixtures were measured using the ignition oven. Results indicated that only 11% of the RAP binder was transferred to the virgin aggregate after pure mechanical blending. At the second stage, the 20% RAP mixture was mixed with virgin aggregate and binder (PG 64-22) at 190 ^{o}C for 3 minutes to simulate asphalt plant mixing. Staged extraction and recovery was used by soaking the RAP mixtures in trichloroethylene to determine the level of blending between the virgin binder and the binder-coated RAP aggregates. The results showed that a large portion of RAP binder created a stiff layer around the RAP aggregates causing them to act as composite black rocks (BR) and only a small amount of RAP binder was blended in this process.

A study carried out by Bonaquist (2007) suggested a method to assess adequate mixing between virgin and RAP materials. Stiffness of the mixtures containing RAP was measured by dynamic modulus testing to develop master curves for the mixtures. Effective shear modulus of the binder was then estimated using the Hirsch model, an equation deriving mixture dynamic modulus from the volumetric properties of the mixture and the binder shear modulus. The mixture binder was then extracted and recovered for deriving the binder modulus master curve using the dynamic shear rheometer (DSR) test. This study indicated that if the binder shear modulus master curves from the Hirsch model and from the extracted binder overlap, then the virgin and RAP binders in the RAP mixture are verified to be completely blended. Figure 2.10 and Figure 2.11 shows the optimal blending (mixture with 45 percent RAP, virgin binder with PG 64-22, and the total binder content 4.5% with 44% of the total binder provided by RAP) and poor blending (mixture with 5% RAS, virgin binder with PG 64-22, and the total binder content 6.4% with 20% of the total binder provided by RAS), respectively. Figure 2.11 shows that the G* backcalculated from the mix is lower than the recovered G*, indicating that blending between the RAP binder and the virgin binder is not significant. McDaniel et al. (2012) used the same procedure suggested by Bonaquist to assess the extent of blending between RAP and virgin binder on 25 plant mixes (15 to 40% RAP content) from four Indiana contractors and one Michigan contractor. It was stated that variability in asphalt plant production affected the blending between RAP and virgin binder to a considerable extent.

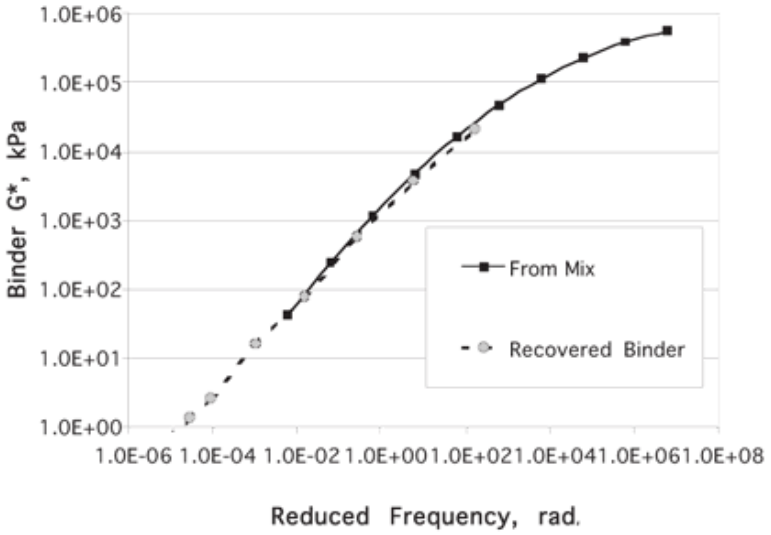

Figure 2.10: Example of good blending (Bonaquist 2007).

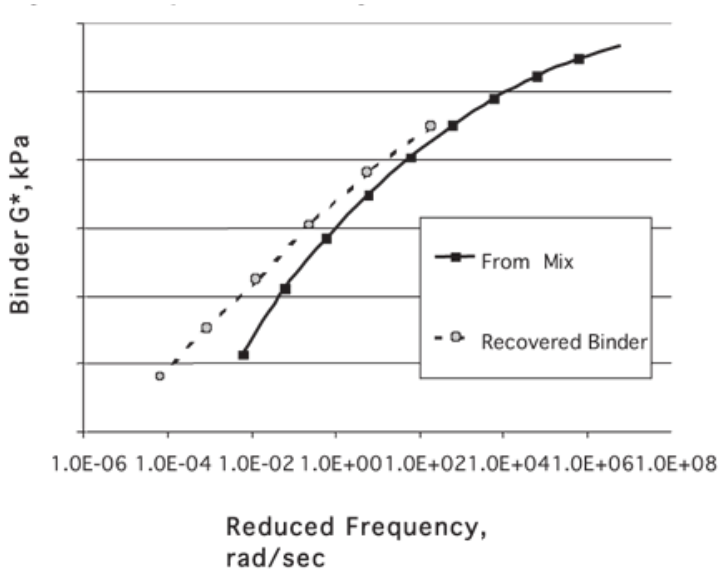

Figure 2.11: Example of poor blending (Bonaquist 2007).

Zofka et al. (2004) carried out a study focusing on creating blending charts for selecting proper amounts of RAP in asphalt mixtures and adopting simple tests for evaluating the asphalt binder properties. Three different RAP contents (0%, 20 %, and 40%), two RAP types, and two different asphalt binders (PG 58-28 and PG 58-34) were selected for this study. Bending beam rheometer tests (BBR) were conducted to estimate the creep compliance and stiffness of the mixtures containing RAP. The Hirsch model was then used for back-calculating the binder properties. Using the Hirsch model eliminated need for binder extraction from mixtures

containing RAP for determining the binder properties. As a result of these tests, a blending chart was developed. It was suggested that blending charts should only be used for evaluating low temperature properties due to the significant impact of RAP materials on the low temperature PG value. Moreover, they concluded that further investigation was required for improving the Hirsch model to minimize the under-prediction of binder stiffness.

Michael (2011) assessed the mix tests and prediction models for determining the RAP binder properties. A new method was proposed as an alternative to using the blending charts (considering 100% blending between RAP and virgin binder) and testing the extracted blended binder in mixtures containing RAP. Using dynamic modulus testing and with known volumetric properties of the mixture, this study used the Hirsch and Christensen-Anderson models for characterizing the RAP binder. At the first stage, two mixes without RAP (limestone aggregate mixed with PG 67-22 and PG 76-22) and six 100% RAP mixes from different sources were evaluated to investigate the differences and similarities between the binder stiffnesses obtained by the Hirsch and Christensen-Anderson methods and testing of the extracted binder. Dynamic modulus and relaxation modulus tests were conducted for estimating E^* and E(t), which are the inputs in the Hirsch model. It was concluded that the Hirsch model could appropriately predict the critical temperature of RAP. At the second stage, three RAP percentages (20%, 35%, and 50%) from three RAP sources and three binders (PG 58-28, PG 67-22, and PG 76-22) were used for preparing 27 mixes with similar gradation and binder contents for testing the sensitivity of the Hirsh model to changes in the binder properties and RAP percentages. The results showed that the measured dynamic modulus and back-calculation stiffnesses were insensitive to binder grades and RAP percentages. It was concluded that the back-calculation procedure may not be a reliable method and more investigation is required before using it to develop blending charts. It was further suggested that the Hirsch and Christensen-Anderson models should be calibrated to improve the predictions.

2.5 FIELD PERFORMANCE OF RAP-RAS MIXTURES

As a result of using aged recycled material from different sources, there are uncertainties associated with the fatigue and rutting performance of reclaimed asphalt pavements. Although laboratory experiments show acceptable performance for RAP and RAS mixtures when compared with conventional HMA mixes, field performance should be taken into account to evaluate the short and long term performance of mixtures containing RAP and RAS. Studies evaluating the field performance of RAP and RAS mixtures are summarized below.

The Louisiana Department of Transportation (Paul 1996) constructed five roadway sections with RAP mixes between the years 1978-1981. The purpose was to compare the performance of these sections with and without RAP (in 5 sites) over a five-year period. RAP mixes and control mixes (without RAP) had identical properties including gradation, binder content, and compaction. The analysis included evaluation of pavement condition ratings, serviceability, structural properties and mixture and binder properties. Serviceability of the pavements was measured using pavement condition ratings based on the Mays Ride Meter (MRM). The Dynamic Deflection Determination System (Dynaflect) was used to evaluate the structural properties of the pavements. Cores were taken from each site to determine binder content and gradation. The results of this study showed that there were no significant differences in pavement condition

ratings, recovered asphalt binder characteristics or structural properties of the pavements with RAP contents ranging from 20 to 50 percent and the conventional HMA mixtures. However, sections with RAP experienced slightly more cracking than the control pavements.

Eighteen states in the U.S. conducted overlay rehabilitation, known as the Specific Pavement Study 5 (SPS-5), between 1989 and 1998 for the purpose of comparing long-term performance of mixes without RAP to mixes containing 30% RAP. Each project consisted of eight test sections: a control section without an asphalt overlay and 7 other sections with overlay thicknesses ranging from 50 to 125 mm, both milled and not milled, and with and without RAP pavements. West et al. (2011) measured the International Roughness Index (IRI), rutting, fatigue cracking, longitudinal cracking, transverse cracking, block cracking, and raveling of these sections to evaluate the performance of mixes with and without RAP. The results showed that performance of pavements with RAP was very close to the in-situ performance of pavements constructed without any RAP. However, RAP mixtures showed slightly more longitudinal and transverse cracking.

Carvalho et al. (2010) collected performance data from 18 SPS-5 sites 8 to 17 years after rehabilitation. The purpose of the study was to evaluate the short-term and long-term in-situ performances of RAP mixes by considering the effects of overlay thickness, environmental factors, and surface conditions. In general, there were no statistically significant differences in overall performance of overlays with or without RAP. Only 22% of the pavements without RAP showed greater performance in fatigue cracking while the remaining 78% had fatigue cracking performance equal to the mixes containing RAP. Moreover, pavements without RAP showed slightly better performance when thinner overlays were used. As the thickness increased, overlays with and without RAP exhibited no discernable difference in cracking performance. Results from falling-weight deflectometer (FWD) tests also pointed out equal structural performance for HMA overlays with and without RAP.

Williams and Shaidur (2015) investigated the causes of early cracking by evaluating the cracking performance of 10 sections (6 with top-down cracking and 4 without top-down cracks) within the state of Oregon highway system. These sections had RAP contents ranging from 0% to 30%. FWD tests and dynamic core penetrometer (DCP) tests were conducted to evaluate the structural performance. Cores from cracked and uncracked sections were taken for laboratory investigations. Dynamic modulus tests and indirect tensile (IDT) tests were performed at different frequencies on the samples extracted from the field. Binders were extracted from the cores and tested by dynamic shear rheometer (DSR) tests and bending beam rheometer (BBR) tests to indicate their performance properties. Cracked sections exhibited a higher dynamic modulus, stiffer binder (with higher complex shear modulus) and lower indirect tensile strength. In general, cracked sections showed higher variability in measured indirect tensile strength, air void contents, and mix densities. It can be concluded that variability is a major cause of top-down cracking and decreased fatigue cracking resistance. Since the RAP mixtures are more prone to variability due to use of RAP from different sources and problems associated with blending the RAP and virgin materials, it is expected that RAP mixtures are more susceptible to top-down fatigue cracking.

Based on the aforementioned studies, cracking is the most critical distress in RAP mixtures during the design life. Since distresses (top-down cracking and rutting) are generally confined to

the upper layers for well-constructed thick asphalt pavement structures, removal of top one or two layers and replacing them with thin asphalt overlays (thinlays) was determined to be a cost-effective strategy to preserve and/or improve highway network condition (Newcomb 2009). Therefore, using thin overlays and chip seals on top of the reclaimed asphalt pavements could increase the long-term durability of RAP sections and reduce the aging rate of pavement surface.

2.6 ECONOMIC AND ENVIRONMENTAL BENEFITS OF USING RAP/RAS MIXTURES

Analyzing the benefits and drawbacks of using high RAP mixes should be done by considering economic, societal and environmental factors and quantifying them in terms of monetary costs and environmental impacts. Life Cycle Assessment (LCA) procedures are fast becoming the best way to accomplish this for pavements. An agency that uses LCA can select specific performance indicators to focus in their project that will help reduce the cost and environmental impact of asphalt paving with high RAP/RAS mixes. The key components of LCA for pavements consider material production, construction, maintenance and rehabilitation, vehicle operating costs (VOC) during the use phase and recycling.

One aspect of LCA more specific to economic costs and benefits is Life Cycle Cost Analysis (LCCA). LCCA can be used to deal specifically with changes in asphalt mix costs that result from the use of high RAP mixes, which could include reduced virgin binder use or increased maintenance frequency. LCCA is most crucial for large projects where significant savings can be made.

Construction energy use is a portion of the LCA that allows the analyst to study the effects of resource and labor-oriented energy use and emissions on the environmental cost of the project. Since pavement maintenance frequency ultimately controls the level of service of the roadway and directly impacts vehicle operating costs, the cost of deferred maintenance reflects directly in the analysis. It is worth noting, however, that more data needs to be obtained from asphalt mixing plants concerning the difference in energy use and emissions in procurement of mixes using high RAP contents versus conventional HMA mixes. Costs associated with roughness related excess fuel consumption from vehicles over the lifespan of the pavement can be considered, but may require data acquisition from pavement and tire experts in order to formulate an analysis subcategory (UC 2014). Economic savings brought on by using RAP will allow DOTs to maintain roads more often and reduce network level pavement roughness which will translate to lower user costs.

An example of using LCA for evaluating RAP comes in a recent study by Aurangzeb et al. (2013), where a 50% RAP mix was used to investigate environmental and cost savings as compared to a standard HMA mix. This study focused on the binder course only and considered impacts based on greenhouse gas (GHG) emissions and energy use. The study used a hybrid LCA, meaning that it encompassed environmental impact factors from traditional LCAs as well as cost-based factors from typical life cycle costs analysis (LCCA). Societal impacts were not considered here, but if they were of importance, they ought to be considered early on in the analysis so that any areas that need improvement can be changed before the project is too far along. In the study by Aurangzeb et al. (2013), it was found that using 50% RAP in a HMA mix can reduce the feedstock energy, or embodied energy of asphalt binder, by as much as 40%. The

construction phase turns out to be a very small portion of the embodied energy or global warming potential of a high RAP paving project, with only 6-8% of global warming potential attributed to this phase (Aurangzeb et al. 2013). Overall, it was found that the material procurement phase yielded the most energy savings and GHG emission reduction of all phases considered in this LCA, based on data obtained from an asphalt plant who participated in the study (Aurangzeb et al. 2013). In the study by Aurangzeb et al. (2013), it was realized that the LCA did not accurately quantify the conservation of resources brought on by using a high RAP mix. There needs to be more attention paid to this area by pavement engineers in charge of creating the LCA.

A study from the University of Texas at Austin asserts that using RAP may not be equally viable in all cases, and can sometimes incur more costs due to decreased maintenance intervals. The objective of the study by Aguiar-Moya et al. (2011) was to examine the long term cost effectiveness of using RAP mixtures according to service life, as well as cracking susceptibility and rate. An additional goal was to show that LCCA is the best way to analyze these factors. Aguiar-Moya et al. (2011) asserts that RAP usage should be decided on a case-by-case basis, as the effective use of RAP could vary between regions or for different RAP contents. Augiar-Moya et al. (2011) suggested to develop regional deterioration models for RAP mixes in different lift thicknesses and RAP contents in order to have an index of RAP durability. The Aguiar-Moya et al. (2011) study utilized data from the FHWA LTPP SPS-5 experiment in Texas to quantify benefits and drawbacks of RAP use. However, it is worth noting that this experiment is outdated in comparison to the recent evolution of RAP use in state DOTs, so more long-term RAP mix durability data needs to be obtained. In general, the finding of this study was that although RAP helps to mitigate rutting failure, it does give rise to a higher degree of cracking failure that occurs in a shorter amount of time. Aguiar-Moya et al. (2011) suggested using lower PG grade virgin binder to help to combat cracking and preserve the durability of the finished pavement. Aguiar-Moya et al. (2011) also suggested that more research be put into studying high RAP mixes that utilize fractioned RAP as well as RAS.

Andreen et al. (2011) investigated the cost effectiveness of using RAP in HMA paving, as base rock, and as a dust suppression method on gravel roads. Andreen et al. (2011) used a “means equal comparison”, basing savings per ton of RAP utilized, to analyze the cost effectiveness of RAP in these three applications. In HMA paving, materials transport and virgin materials displaced were selected as LCA impact categories. Andreen et al. (2011) found that a saving of $40.87 per ton was realized when using RAP in HMA, with most of these savings coming from reducing energy consumption at the HMA plant. This was the most significant of all savings between RAP use on gravel roads, as base rock, and in HMA paving. Andreen et al. (2011) indicated that calculated savings will increase with increasing RAP content. Andreen et al. (2011) also mentioned that normalizing the savings on a per ton of RAP basis was the key to simplifying the analysis.

A study by the National Taiwan University examined the environmental benefits of using RAP in HMA mixes. Lee et al. (2011) used the PaLATE LCA tool in conjunction with energy use and CO_2 emission data obtained from HMA plants and binder manufacturers to investigate the potential for RAP to reduce CO_2 production and energy consumption in HMA paving. The study was based on a comparison to a conventional HMA mix cradle-to-grave analysis. Using CO_2 emissions and energy use as the performance indicators in the LCA, Lee et al. (2011) found that

by using a mix with 30% RAP, approximately 84% less CO_2 is emitted and 80% less energy is used based on a cradle-to-grave analysis of the RAP mix and its components, with most of these savings attributed to the re-use of asphalt and the displaced virgin materials that would otherwise comprise the mix. Lee et al. (2011) suggests that the environmental impact can further be reduced if energy saving measures and odor control devices are implemented at the HMA plants. Lee et al. (2011) indicated that RAP HMA mixes are indeed cost effective to use if the RAP mix can achieve 80-90% of the service pavement life of conventional HMA mix. Lee et al. (2011) further indicated that the performance and durability of RAP mixes can be increased if recycling agents or additives are used to mitigate cracking failure.

A National Center for Asphalt Technology (NCAT) study investigated the sustainability of using RAP HMA mixes using the Roadprint LCA software tool. Using the NCAT test track in Alabama as a case, this study by Willis (2015) quantified the benefits of using RAP using a triple bottom-line methodology, focusing on environmental, economic and societal benefits. Willis (2015) used a basis of CO_2 equivalents to analyze the emissions reduction of RAP use and chose to focus on two phases of pavement life in the LCA: materials and construction/production. Willis (2015) chose to study using RAP on its own, using RAP in conjunction with Warm Mix Asphalt (WMA), and using RAP combined with locally sourced materials to conduct the analysis. Willis (2015) found that utilizing recycled asphalt resulted in a 9-26% energy savings and a 5-29% reduction in CO_2 emissions when using RAP alone. A 19-42% energy savings and a 6-39% reduction in CO_2 emissions were realized when using RAP along with locally sourced materials. Finally, focusing on impact reduction at the asphalt plant, Willis (2015) found that 12-17% less energy was used and 6-9% less CO_2 was emitted when using RAP along with the WMA technique. In general, Willis (2015) found that it is most sustainable to use RAP in conjunction with locally sourced materials in order to reduce embodied energy brought on by materials transport. Willis (2015) did not obtain economic or societal results, as a LCCA is most useful for those aspects.

LCA is a powerful impact estimation tool, but it still has a few caveats and can become quite complicated for broad projects that encompass many different road types or performance indicators. In order for it to be useful in pavement engineering, it is important to keep industry professionals and decision makers in the loop on how LCA works and how it can help firms and agencies analyze costs and environmental impacts accurately. Additionally, if this tool is to be used on an international scale, then significant standardization must be implemented to make the LCA relevant to all regions of the world. This will require collaboration from pavement agencies internationally to create a LCA tool that encompasses a wide enough perspective to account for regional needs.

2.7 SUMMARY

A review of literature indicated that significant economic and environmental benefits can be achieved by using RAP/RAS in asphalt mixes. In the study by Aurangzeb et al. (2013), it was found that using 50% RAP in a HMA mix can reduce the feedstock energy, or embodied energy of asphalt binder, by as much as 40%. Andreen et al. (2011) found that a saving of $40.87 per ton was realized when using RAP in HMA, with most of these savings coming from reducing energy consumption at the HMA plant. Lee et al. (2011) found that by using a mix with 30%

RAP, approximately 84% less CO_2 is emitted and 80% less energy is used while Willis (2015) found that utilizing recycled asphalt resulted in a 9-26% energy savings and a 5-29% reduction in CO_2 emissions. Lee et al. (2011) also indicated that RAP HMA mixes are indeed cost effective to use if the RAP mix can achieve 80-90% of the service pavement life of conventional HMA mix. Findings of these research studies emphasize the importance of increasing RAP/RAS contents in asphalt mixes.

Several studies in the literature focused on developing strategies to increase the RAP content without compromising the cracking resistance. Aurangzeb et al. (2012) carried out a study with an objective to quantify the impact of binder-grade bumping on the performance of high RAP asphalt mixtures. Results of the study showed that in general, single grade bumping improved the fatigue behavior of asphalt mixtures. However, double-grade bumping did not show any significant improvement as compared to single-grade bumping. West et al. (2009) investigated the impact of binder-grade bumping and increased binder content on cracking performance of high RAP mixes. It was concluded that the effect of binder grade on the fatigue test results was not significant when compared with the effect of effective binder content. Thus, West et al. (2009) suggested the use of increased binder content as a strategy to improve cracking resistance of RAP/RAS mixtures. The NCAT laboratory study conducted by Willis et al. (2012) concluded that binder-grade bumping along with a 0.3% increase in binder content significantly improved the cracking performance of 50% RAP mixes.

One of the strategies for improving the resistance to cracking is using recycling agents such as rejuvenators and softening agents. Tran et al. (2012) evaluated the effect of rejuvenators on HMA mixtures containing high percentages of RAP and RAS. It was concluded that using rejuvenator for high amount of recycled binder could be an effective method for enhancing the binder properties. Shen et al. (2007) compared properties of mixtures containing RAP and rejuvenator against mixtures with a softer binder instead of a rejuvenator. Ten mixtures with RAP (five with rejuvenator and five without rejuvenator) and two mixtures without RAP (control mixtures) were designed and tested to evaluate the impact of rejuvenators and softer binders on mix performance. It was concluded that mixtures with rejuvenators illustrated better mechanical and rutting properties than mixtures containing softer binder.

The workability and compactibility of HMA with high RAP content has always been a challenge to control (Petersen 1984). Aged, stiffened RAP binder can cause problems during mixing and construction. Using WMA is a strategy to mitigate problems brought on by using high percentages of RAP in asphalt pavements. In a study conducted by Zhao et al. (2012), rutting resistance, fatigue resistance, and moisture susceptibility of WMA and HMA mixes containing different amounts of RAP were evaluated. Mixtures containing RAP showed less moisture susceptibility than mixtures without RAP. This trend was observed in both WMA and HMA mixtures. However, WMA mixtures had lower TSR than HMA mixtures, indicating that moisture susceptibility is a concern for WMA mixtures. According to beam fatigue test results, adding more RAP to the WMA samples increased fatigue cracking performance. On the other hand, for mixes without WMA, increased RAP content reduced fatigue life.

Modification of RAP/RAS mixes with crumb rubber and polymer improves the mechanical characteristics of HMAs and allows the use of higher RAP/RAS contents. Several studies in the literature investigated the effects of modification on mixes with high RAP contents. In summary,

polymer-modification was observed to improve fatigue cracking resistance of high RAP mixes. For this reason, polymer modification can be an effective strategy to increase RAP content of asphalt mixes. However, life cycle cost analyses and performance modeling should be used to evaluate the cost effectiveness of using polymer modification in RAP mixes. It should be noted that the studies focusing on the use of rubber modification to improve cracking performance of RAP mixtures did not suggest any significant improvement in performance created by the use of crumb rubber.

In designing RAP mixtures, it is important to know the extent that virgin and RAP binders blend with each other. This could be the basis for estimating the amount and type of the virgin binder to add to RAP mixtures to reach desirable binder performance. Several studies in the literature focused on the quantification of blending. McDaniel et al. (2001) investigated how aged RAP binder affected the virgin binder grade and to what extent the RAP binder was blended with the virgin binder. It was concluded that blending of virgin and recycled binder occurred to some extent, and considering RAP materials as black rock is a false assumption. In addition, blending charts were determined to be an effective guide for selecting proper RAP and binder properties. On the other hand, study conducted by Huang et al. (2005) showed that a large portion of RAP binder created a stiff layer around the RAP aggregates causing them to act as composite black rocks (BR) and only a small amount of RAP binder was blended in this process. Zofka et al. (2004) suggested that blending charts should only be used for evaluating low temperature properties due to the significant impact of RAP materials on the low temperature PG value.

In this study, the performance and cost benefits of using binder-grade bumping and increased binder content strategies in RAP/RAS mixture production in Oregon were quantified. To be able to provide recommendations for asphalt mixture design procedures, blending of binder around RAP was also quantified by using an innovative procedure developed in this study. While the use of binder-grade bumping and high virgin binder content strategies generally increase the cost of virgin binder used in the asphalt mixture, increased RAP/RAS content and improved RAP/RAS performance may reduce the overall life-cycle cost of recycled asphalt concrete material used in construction. In this study, laboratory test results were used to develop mechanistic-empirical (ME) pavement models for different RAP/RAS mixtures. Using the predicted performance from ME models and cost calculations for different combinations of RAP content, binder content and binder type, life-cycle cost analyses (LCCA) were conducted to investigate the performance and cost benefits of using binder-grade bumping and high binder content in Oregon RAP/RAS mixes. Binder-grade bumping and high binder content strategies recommended in this study are expected to increase the RAP/RAS content in asphalt mixtures, reduce the life-cycle cost, improve the cracking performance and encourage the widespread use of high RAP/RAS asphalt mixtures in Oregon.

3 DEVELOPMENT OF STRATEGIES TO IMPROVE PERFORMANCE OF RAP/RAS MIXTURES

3.1 INTRODUCTION

Due to ever growing demand of asphalt pavement materials and limited supply of aggregate and asphalt binder, using RAP in HMA mixtures creates significant benefits. For this reason, agencies are interested in finding ways to increase the RAP content of HMA mixtures. The primary concern when using high RAP/RAS mixes lies in the altered long-term durability properties of HMA mixtures. The dilemma is finding a way to use higher RAP/RAS contents in HMA without compromising long-term durability. Major concerns over higher cracking susceptibility stem from increased stiffness of RAP/RAS mixes. Regarding these concerns, the following strategies were generally suggested in the literature to increase the RAP content without compromising the cracking resistance (Bennert et al. 2014):

1. Softer virgin binder grade (binder-grade bumping);
2. Increased binder content;
3. Recycling agents;
4. Polymer and rubber modifiers; and
5. Warm mix asphalt

This study evaluates the effects of binder-grade bumping and high virgin binder content on cracking performance of asphalt mixtures. These two strategies were determined to be effective in improving cracking performance. SCB, DM and FN tests were conducted on laboratory prepared samples with high (30% and 40%) and low (0% and 15%) RAP contents and RAP&RAS. Three binder contents (6%, 6.4%, and 6.8%), and three binder grades (PG 58-34, PG 64-22, and PG 76-22) were used to prepare high RAP mixtures to assess the impact of these variables on cracking and rutting performance. Two binder contents (6% and 6.8%), and two binder grades (PG 64-22 and PG 76-22) were used to prepare low RAP and RAP&RAS mixtures. Linear regression models correlating FI and FN (dependent variables) with RAP content, binder content and binder grade (independent variables) were also developed. Possible combinations of these three independent variables (RAP content, binder type and binder content) to produce asphalt mixtures with acceptable cracking and rutting performance were determined by using the developed regression models.

3.2 MATERIALS

This section provides information about virgin binders, virgin aggregates and RAP aggregates used in this study. All the materials were obtained from local sources.

3.2.1 Aggregates

This study intends to evaluate the effects of binder content, RAP content and binder grade on cracking performance of asphalt mixtures. Therefore, to determine the effects of these variables on performance, gradation was kept constant for all the samples. Virgin aggregates were donated

by Old Castle Materials from the River Bend Sand and Gravel Company in Salem, Oregon. The virgin aggregates were delivered in three gradations, namely coarse (1/2" to #4), medium (#4 to #8), and fine (#8 to zero). To determine the gradation of each stockpiled aggregate, wet-sieve and dry-sieve analyses were performed on multiple samples of each stockpile following AASHTO T 27-11. Aggregate gradations are presented in Section 3.3.1.

3.2.2 Recycled Asphalt Pavement (RAP) and Recycled Asphalt Shingles (RAS)

RAP and RAS materials were also provided by Old Castle Materials from the River Bend Sand and Gravel Company in Salem, Oregon. Gradation, binder content and theoretical maximum specific gravity (G_{mm}) of RAP and RAS materials were provided by Old Castle. AASHTO T 308-10 was followed for binder extraction and RAP and RAS binder content measurements. The quantity of binder in RAP materials was determined as 6.22% while the RAS binder content was determined to be 19.54%. AASHTO T 30-10 was followed to determine the gradation of extracted RAP and RAS aggregates. For five samples of RAP and RAS materials, RAP and RAS aggregates were extracted and their gradations were determined, as shown in Table 3.1 and Table 3.2, respectively. Then, to get the final RAP and RAS aggregate gradation, the percent passing #200 sieve is reduced by 1 percent. This correction is applied due to the aggregate breakdown in the ignition oven test (AASHTO T 30-10). Results from each sieve analysis and the final average gradation for RAP and RAS aggregates are presented in

Figure 3.1 and Figure 3.2, respectively. Detailed information about the RAP and RAS gradations, binder contents and theoretical specific gravities are given in APPENDIX A:.

Table 3.1. RAP Aggregate Gradations

Stockpile	Sample 1	Sample 2	Sample 3	Sample 4	Sample 5	Average	Final Gradation
Sieve Size	Percentage Passing						
3/4"	100.0	100.0	100.0	100.0	100.0	100.0	100.0
1/2"	98.0	97.6	98.8	98.5	98.5	98.3	98.3
3/8"	88.3	87.5	87.7	90.8	87.1	88.3	88.3
1/4"	70.8	69.0	73.0	75.2	68.5	71.3	71.4
#4	61.3	60.2	63.9	65.6	58.4	61.9	62.0
#8	44.1	42.5	46.7	47.3	40.1	44.1	44.1
#16	31.1	30.1	33.6	33.6	27.3	31.1	31.1
#30	23.4	22.2	25.7	24.7	20.5	23.3	23.3
#50	17.1	16.5	18.7	18.2	15.2	17.1	17.1
#100	12.9	12.4	13.9	13.5	11.7	12.9	12.9
#200	9.6	9.2	10.2	9.6	8.6	9.4	8.4

Table 3.2. RAS Aggregate Gradations

Stockpile	Sample 1	Sample 2	Sample 3	Sample 4	Sample 5	Average	Final Gradation
Sieve Size	Percentage Passing						
3/4"	100.0	100.0	100.0	100.0	100.0	100.0	100.0
1/2"	100.0	100.0	100.0	100.0	100.0	100.0	100.0
3/8"	100.0	100.0	100.0	100.0	100.0	100.0	100.0
1/4"	96.3	97.7	97.3	98.0	95.6	97.0	97.0
#4	88.0	91.3	89.5	92.2	89.9	90.2	90.2
#8	82.4	86.0	82.3	86.5	84.6	84.4	84.4
#16	61.9	64.4	60.1	65.5	62.7	62.9	62.9
#30	40.7	41.6	39.1	42.4	40.2	40.8	40.8
#50	32.9	33.3	33.3	33.3	33.3	33.2	33.2
#100	27.5	27.8	28.5	27.4	28.1	27.9	27.9
#200	21.8	21.9	22.9	21.8	22.4	22.2	21.2

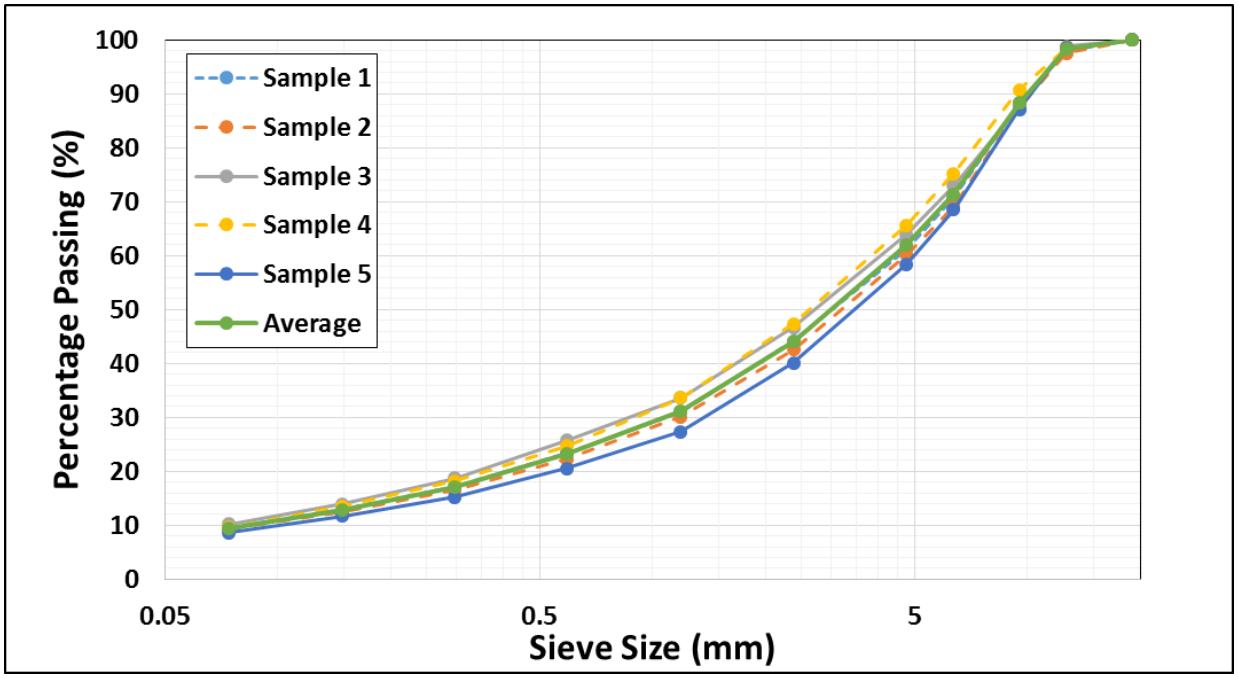

Figure 3.1. RAP Aggregate gradations

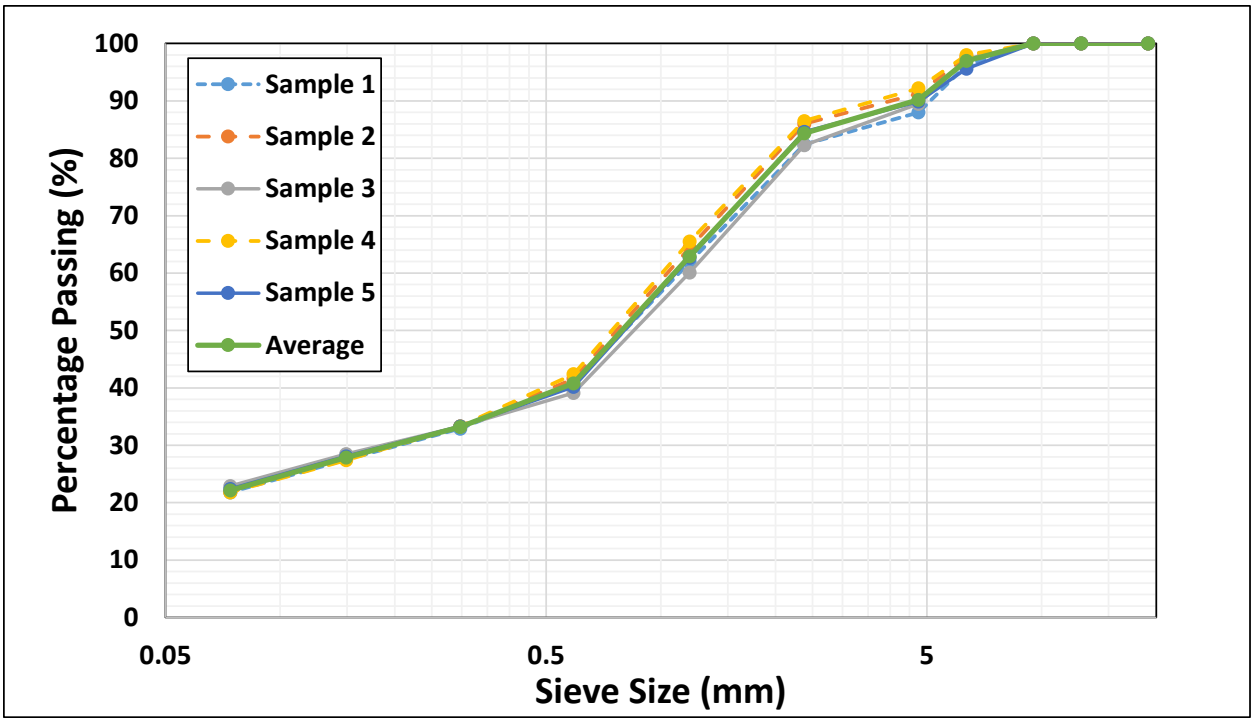

Figure 3.2. RAS aggregate gradations

3.2.3 Binders

McCall Oil and Chemical Corporation in Portland, Oregon (McCall) provided the virgin binders with different binder grades (PG 58-34, PG 64-22 and PG76-22) for this study. Temperature curves, mixing temperatures and compaction temperatures were provided by McCall as well. 7APPENDIX B: shows the temperature curves and binder properties for each binder grade. Laboratory mixing and compaction temperatures were estimated by using the viscosity-temperature lines given in 7APPENDIX B:. An example of the viscosity-temperature line for binder grade of PG 58-34 is presented in

Figure 3.3. The Asphalt Institute (2016) suggested that mixing and compaction temperatures can be determined where the viscosity is within the range of 0.17 ± 0.02 Pa-s and 0.28 ± 0.03 Pa-s, respectively. To create the viscosity-temperature line, rotational viscosity should be measured at 135 ^{o}C and 165 ^{o}C following the procedure described in AASHTO T 316-11.

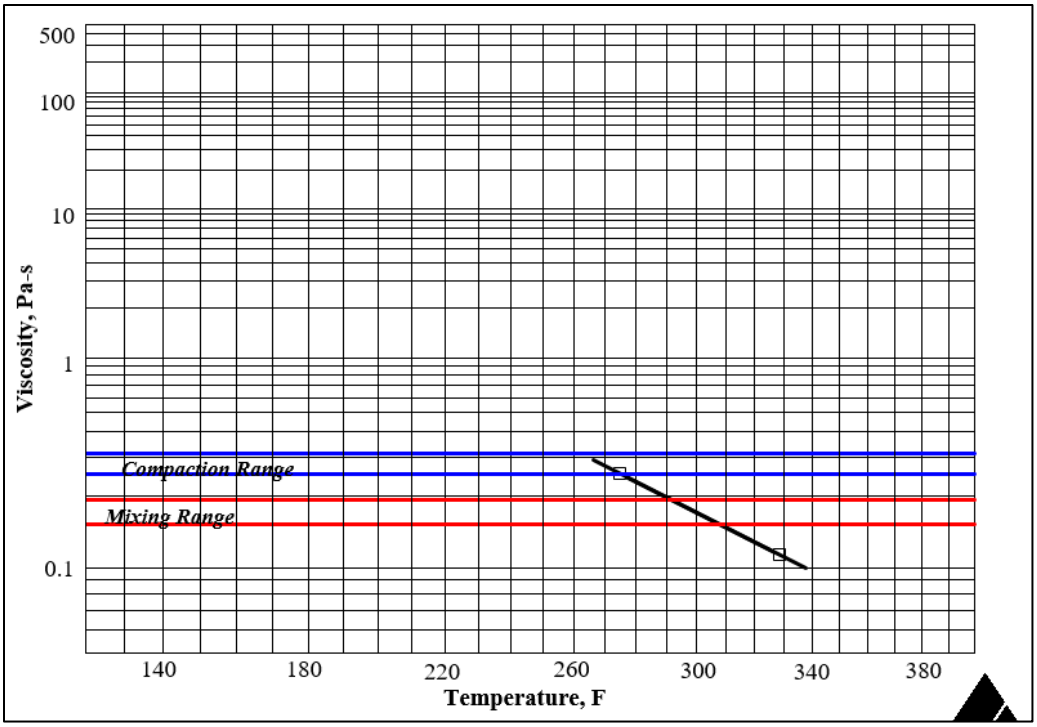

Figure 3.3. Viscosity-temperature line for binder grade of PG 58-34

Asphalt mixtures were prepared with three binder contents (6%, 6.4% and 6.8%) in this study. These binder contents are the percentage of the total binder by the weight of the mix, which includes the recycled binder from RAP/RAS materials. In this study, it was assumed that all the RAP binder was completely blended with the virgin binder (100 % blending).

3.3 SAMPLING AND SPECIMEN PREPARATION

The following process was followed to prepare specimens for testing:

1. Material sampling: 8 barrels of coarse, 7 barrels of medium and 7 barrels of fine aggregates were sampled for this study. Wet-sieve and dry-sieve analysis were performed on one sample from each barrel to determine the gradation of each stockpiled aggregate.
2. The ignition oven test (AASHTO T 30-10) was conducted on the sampled RAP and RAS materials to find the binder content and aggregate gradations;
3. Theoretical maximum specific gravity (G_{mm}) of each combination of RAP and RAS content, binder content and binder grade was measured;
4. Batching sheets were developed and specimens were batched to achieve 7% air content, target gradation and the corresponding measured G_{mm};
5. Specimens were mixed, short-term aged and compacted in the laboratory;
6. The air contents were measured for all the specimens after compaction; and
7. Prepared samples were cut for SCB, DM and FN testing.

3.3.1 Target Gradations

Target gradation was obtained from an ODOT (ODOT TM 319) Level 4 dense-graded mix design. All mixes were designed to reach the target gradation. Target gradation and the gradations of virgin aggregates and extracted RAP and RAS aggregates are presented in Table 3.3 and Figure 3.4.

Table 3.3. Target, Extracted RAP, and Stockpiled Aggregate Gradations

Sieve Size	Percentage Passing					
Stockpile	Coarse	Medium	Fine	RAP	RAS	Target Gradation
3/4"	100.0	100.0	100.0	100.0	100.0	100
1/2"	95.8	100.0	100.0	98.3	100.0	98
3/8"	53.1	98.2	100.0	88.3	100.0	83
1/4"	21.9	64.9	100.0	71.3	97.0	59
#4	13.2	38.0	99.9	61.9	90.2	49
#8	2.3	3.3	83.3	44.1	84.4	31
#16	1.3	1.3	55.1	31.1	62.9	22
#30	1.2	1.2	35.8	23.3	40.8	16
#50	1.1	1.1	23.7	17.1	33.2	11
#100	1.1	1.1	15.6	12.9	27.9	8
#200	0.9	1.0	10.7	8.4	21.2	6.3

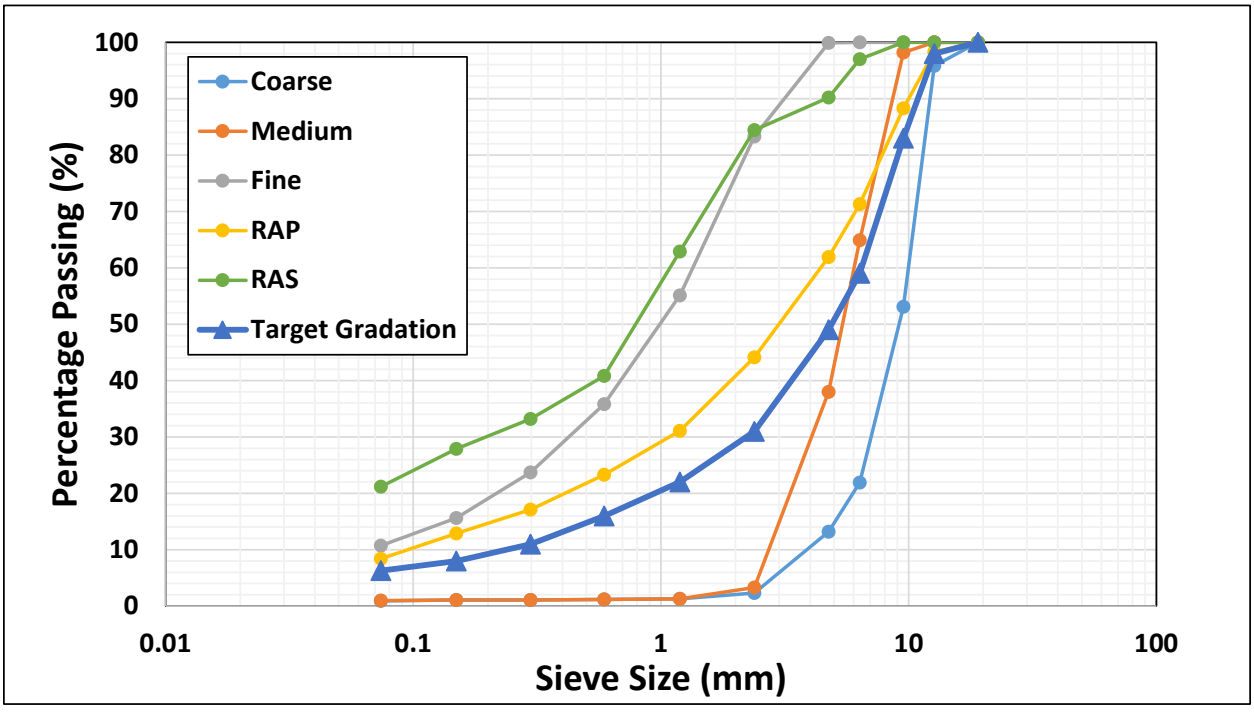

Figure 3.4. Target, extracted RAP, and stockpiled aggregate gradations

3.3.2 Batching

After measuring the gradations of virgin and RAP aggregates, three replicates of each combination of RAP content, binder content and binder grade were mixed according to AASHTO T 312-12 and their G_{mm} were measured following the procedure described in AASHTO T 209-12. All the measured theoretical maximum specific gravities are presented in 7APPENDIX C:. Then, aggregates were batched to meet the final gradation to reach 7% air content. To find the percentage of coarse, medium, fine, RAP and RAS aggregates needed for the target gradation, optimization was conducted with Excel Solver 2013. Having G_{mm}, the bulk specific gravity (G_{mb}) required to reach 7% air-void content of each sample were calculated using Equation (3.1. G_{mb} is the density of asphalt mixture divided by the density of water at 23 ^{o}C (Pavement Interactive 2017) (Equation (3.2). The total volume of the samples was calculated by the known dimensions of the laboratory compacted sample. Then, the total mass of samples was calculated using Equation (3.3. Mass of aggregates and binders were determined afterwards, and samples were batched for mixing and compaction. An example of batching calculation is shown in APPENDIX D:.

$$\text{air voids } (\%) = \frac{G_{mm} - G_{mb}}{G_{mm}} * 100 \quad \textbf{(3.1)}$$

$$G_{mb} = \frac{\text{mass per unit volume of asphalt mixture}}{\text{density of water}} \quad \textbf{(3.2)}$$

$$\text{total mass of sample} = \text{density of water} * G_{mb} * \text{volume of sample} \quad \textbf{(3.3)}$$

3.3.3 Mixing and Compaction

Batched samples were mixed and compacted using AASHTO T 312-12 procedure. Before mixing, aggregates were kept in the oven at 10 ^{o}C higher than the mixing temperature, RAP materials were kept at 110 ^{o}C (Mcdaniel and Anderson 2001), and binder was kept at the mixing temperature for 2 hours. After mixing, prepared loose mixtures were kept in the oven for 4 hours at 135 ^{o}C (AASHTO R 30-10) to simulate short-term aging. The goal of short-term aging is to simulate the aging and binder absorption that occurs during mixing phase of the production process. Then the aged loose asphalt mixtures were kept in the oven for 2 more hours at the compaction temperature prior to compaction.

3.3.4 Air-Void Content

All the samples were prepared for the target 7% air-void content. Air-void contents were measured for all the samples after compaction. To find the air contents, the G_{mb} of the samples were measured after compaction by following AASHTO T 166-12. Air void content for each sample was then determined by using Equation (3.1. Air-void contents for all specimens were required to be within 7%±1% (Newcomb et al. 2015). In this study, all the samples met the requirement for air content while majority of the specimens had air-void contents within 7%±0.5%.

3.4 TEST METHODS

Test methods followed in this study (for SCB, DM and FN tests) to evaluate cracking and rutting performance of prepared asphalt mixtures with different RAP contents, binder contents and binder grades are presented in this Section.

3.4.1 Semi-Circular Bend (SCB) Test

SCB tests were conducted in this study to determine cracking performance of asphalt mixtures. The test method for evaluating cracking performance of asphalt concrete at intermediate temperatures developed by Wu et al. (2005) was followed.

3.4.1.1 Sample Preparation

130 mm tall samples were compacted in the laboratory according to AASHTO T 312-12. Two samples with the thicknesses of 57 ± 2 mm were cut from each gyratory compacted sample using a high-accuracy saw (Figure 3.5a). Then the circular samples (cores) were cut into two identical halves (Figure 3.5b) using a special jig designed and developed at Oregon State University (OSU).

Wu et al. (2005) suggested testing samples with different notch depths (25.4 mm, 31.8 mm, and 38.0 mm). However, Ozer et al. (2016) and Nsengiyumva (2015) showed that reducing the notch depth reduces the variability. For this reason, in this study, a 15 mm notch depth is selected for sample preparation. A notch along the axis of symmetry of each half was created with the table saw using another special cutting jig developed at OSU (Figure 3.5c). Notches were 15 ± 0.5- mm in length and 3 mm wide.

(a) (b)

(c) (d)

Figure 3.5. Cutting and notching procedure for SCB sample preparation.

3.4.1.2 Testing

Tests were conducted at 25 ^{o}C with a displacement rate of 0.5 mm/min (AASHTO TP 105-13). Samples were kept in the chamber at the testing temperature for conditioning the day before being tested. The flat side of semi-circular samples was placed on two rollers (Figure 3.6). As vertical load with constant displacement rate is applied on the samples, applied load is measured (AASHTO TP 105-13). The test stops when the load drops below 0.5 kN. Fracture energy (G_f), fracture toughness (K_{IC}), secant stiffness (S), and flexibility index (FI) are the testing parameters obtained from this test. Procedures followed to calculate these test parameters are given in the next section.

Figure 3.6. SCB loading set up and test

3.4.1.3 Parameters Obtained from SCB Test Results

This section describes the parameters obtained from SCB test results (displacement vs. load curves) including fracture energy (G_f), fracture toughness (K_{IC}), secant stiffness (S) and flexibility index (FI). The most effective parameter to identify the effects of RAP content, binder content and binder type (PG grade) on cracking resistance was also determined. Moreover, a MATLAB (2016) code and a stand-alone software were developed. The developed software takes the raw test data, processes it and calculates all these parameters.

- **Fracture Energy (G_f)**

  Fracture energy (G_f) is obtained by dividing the work of fracture (W_f) by the ligament area (A_{lig} in Equation (**3.4**). As the G_f increases, the work required for crack initiation and propagation increases. Therefore, asphalt mixtures with higher G_f values are expected to show higher resistance to cracking (Ozer et al. 2016). Work of fracture is the area under load versus displacement (P-u) curve (Figure 3.7). The test stops when the load drops below 0.5 kN. The remainder of the curve is extrapolated to estimate the area under the tail part of the P-u curve. W_f is the sum of the area under the curve obtained from the test (W) and the extrapolated tail part (W_{tail}) as it is shown in Figure 3.7.

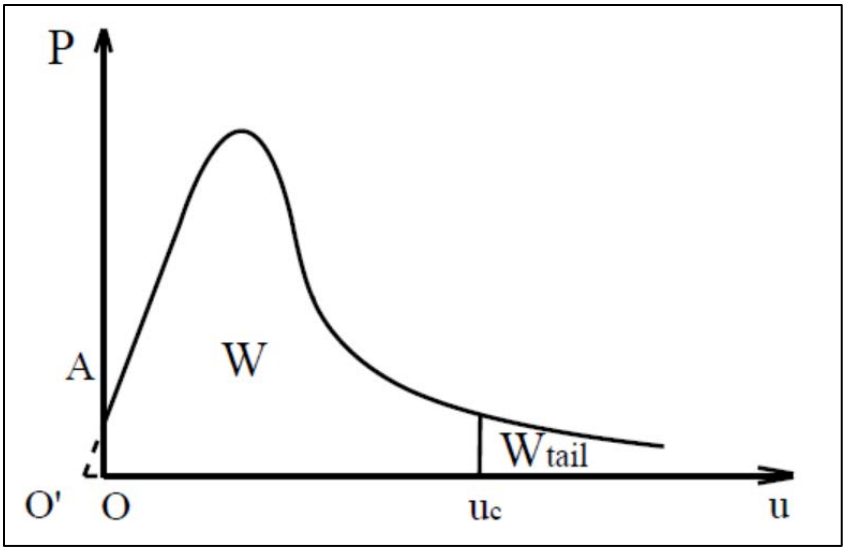

Figure 3.7. Load versus displacement (P-u) curve (AASHTO TP 105-13)

W_f is calculated as follows (AASHTO TP 105-13):

$$G_f = \frac{W_f}{A_{lig}} \quad \textbf{(3.4)}$$

$$W_f = \int P\, du \quad \textbf{(3.5)}$$

$$A_{lig} = (r-a)*t \quad \textbf{(3.6)}$$

Where:

G_f = fracture energy (kJ/m^2),

W_f = work of fracture (kJ),

P = applied load (kN),

u = load line displacement (m),

A_{lig} = ligament area (m^2),

r = sample radius (m),

a = notch length (m), and

t = sample thickness (m).

The quadrangle rule is used to calculate the area under the curve obtained from the test (W) using Equation (**3.7** (AASHTO TP 105-13):

$$W=\sum_{i=1}^{n}(u_{i+1}-u_i)*(P_i)+\frac{1}{2}*(u_{i+1}-u_i)*(P_{i+1}-P_i) \quad \textbf{(3.7)}$$

Where:

P_i = applied load (kN) at the i load step application,

P_{i+1} = applied load (kN) at the i+1 load step application,

u_i = load line displacement (m) at the i step, and

u_{i+1} = load line displacement (m) at the i+1 step.

A power function with a coefficient of -2 is used to fit the post-peak part of the P-u curve starting from the point at which the P value is lower than the 60% of the peak load. After fitting the curve, the coefficient c is obtained using Equation (**3.8** (AASHTO TP 105-13). Then the area under the extrapolated tail part (W_{tail}) is estimated using Equation (**3.9** (AASHTO TP 105-13).

$$P=\frac{c}{u^2} \quad \textbf{(3.8)}$$

$$W_{tail}=\int_{u_c}^{\infty} P\,du=\int_{u_c}^{\infty}\frac{c}{u^2}\,du=\frac{c}{u_c} \quad \textbf{(3.9)}$$

Where:

u = integration variable equal to load line displacement (m), and

u_c = load line displacement value at which the test is stopped (m).

Consequently, total area under the curve (W_f) is obtained as follows (AASHTO TP 105-13):

$$W_f=W+W_{tail} \quad \textbf{(3.10)}$$

- **Fracture Toughness (K_{IC})**

  Fracture toughness (K_{IC}) is the stress intensity factor at peak load. It shows how much energy is required for crack formation. Higher K_{IC} indicates higher brittleness of mixtures. The following equation is used to compute K_{IC} (AASHTO TP 105-13):

$$\frac{K_{IC}}{\sigma_0\sqrt{\pi a}} = Y_{I(0.8)} \quad \textbf{(3.11)}$$

$$\sigma_0 = \frac{P_{peak}}{2rt} \quad \textbf{(3.12)}$$

$$Y_{I(0.8)} = 4.782 + 1.219\left(\frac{a}{r}\right) + 0.063 * \exp\left(7.045\left(\frac{a}{r}\right)\right) \quad \textbf{(3.13)}$$

Where:

P_{peak} = peak load (MN),

r = sample radius (m),

t = sample thickness (m),

a = notch length (m), and

$Y_{I(0.8)}$ = the normalized stress intensity factor (dimensionless).

- **Secant Stiffness (S)**

  Secant stiffness (S) is the ratio of the peak load to the vertical deformation required to reach the peak deformation. Higher values for S indicate higher resistance to crack initiation and higher brittleness (Harvey et al. 2015).

$$S\ (KN/mm) = \frac{\Delta y}{\Delta x} = \frac{\text{peak load}}{\text{vertical deformation at peak load}} \quad \textbf{(3.14)}$$

- **Flexibility Index (FI)**

  Flexibility index (FI) is the ratio of the fracture energy (G_f) to the slope of the line at the post-peak inflection point of the load-displacement curve (

  Figure 3.8). FI correlates with brittleness, and it was developed for asphalt materials by Ozer et al. (2016). Lower FI values show that the asphalt mixtures are more brittle with higher crack growth rate (Ozer et al. 2016).

$$FI = A * \frac{G_f}{abs(m)} \quad \textbf{(3.15)}$$

  Where:

  G_f = fracture energy (KJ/m^2),

  abs(m) = absolute value of the slope at inflection point of post-peak load-displacement curve,

  A = unit conversion factor and scaling coefficient.

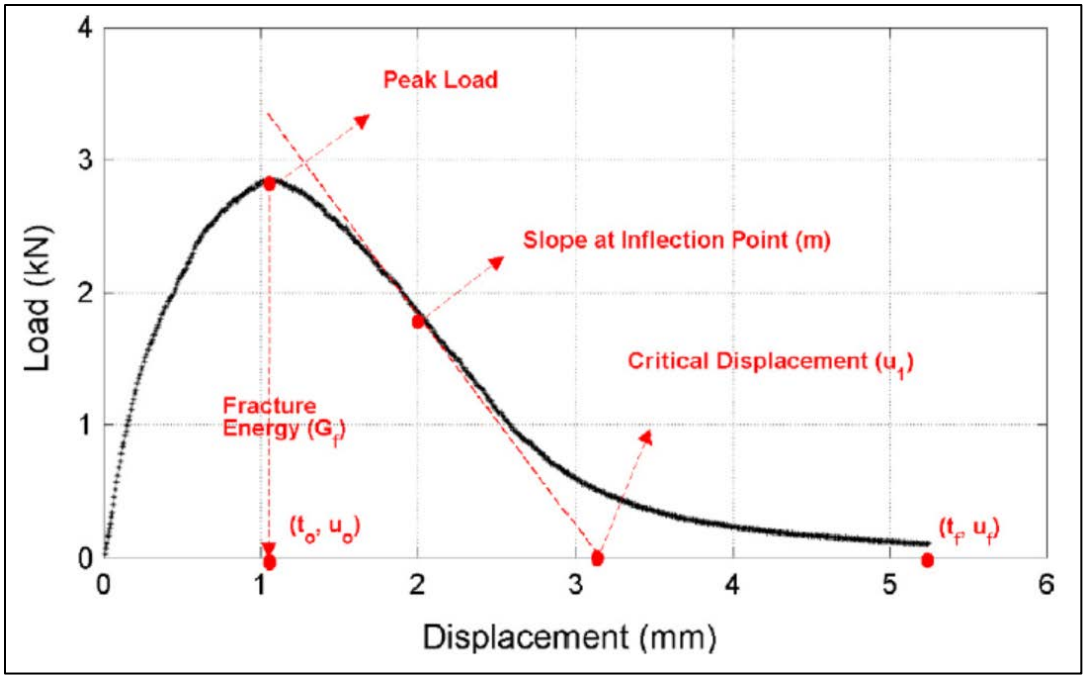

Figure 3.8. Illustration of load-displacement curve and slope at inflection point (m)

(Ozer et al. 2016)

3.4.1.4 Comparison of Fracture Energy (G_f) to Flexibility Index (FI)

Brittle mixtures require higher energy for crack initiation, but once the crack starts, it propagates rapidly. Conversely, ductile mixtures need less energy for crack initiation, but cracks propagate more slowly. Load-displacement curves of ductile and brittle mixtures are shown in Figure 3.9. The area under the load-displacement curve is higher for the brittle mixture compared to the ductile mixture. Thus, the brittle mixture seems to have higher G_f value. On the contrary, since the slope at the inflection point is also higher for the brittle mixture, the FI value decreases. The ductile mixture has a smaller area under the curve and smaller slope at the inflection point and it has higher FI than the brittle mixture. It can be concluded that FI is a better performance indicator than G_f since it properly describes crack initiation and propagation stages of the load-displacement curve (Ozer et al. 2016). Results of this study also show that FI is able to identify the effects of binder content, PG grade and RAP content on cracking resistance (See Section 3.5.2.1).

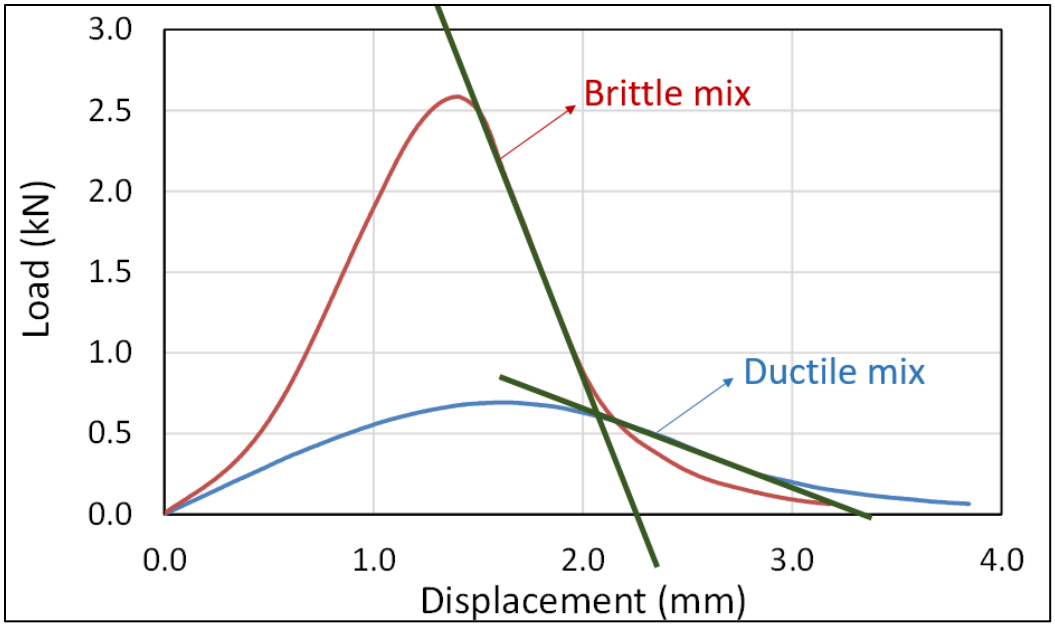

Figure 3.9. Illustration of load-displacement curve of ductile and brittle mixtures

3.4.2 Dynamic Modulus Test

Asphalt concrete mixtures are viscoelastic materials that show both viscous and elastic behavior. At lower temperatures and higher loading frequencies, elastic behavior becomes more dominant while viscous components are more apparent at higher temperatures and lower loading frequencies. DM tests are conducted to characterize the elastic modulus of asphalt concrete mixtures at different loading frequencies and temperatures. DM tests are performed at low strain levels (about 100με) to determine the elastic modulus in the linear viscoelastic range. The effects of loading time and temperature on elastic modulus is modeled and presented in the form of master curves (Norouzi et al. 2015).

The DM test can be used to evaluate rutting and cracking performance of asphalt pavements (Zhou et al. 2015) if the asphalt mixtures do not have special additives such as fibers, polymers or rubber. In this study, DM tests were conducted on prepared samples with different RAP contents (0%, 15%, 30% and 40%) and RAP/RAS, binder contents (6%, 6.4% and 6.8%) and binder grades (PG 58-34, PG 64-22 and PG 76-22) (See Table 3.5 and Table 3.11). The procedure described in AASHTO TP 79-13 for unconfined testing is followed in this study. DM test samples were required to be 150 ± 2.5 mm tall and 100 ± 2.5 mm in diameter. Temperatures of 4 ^{o}C, 20 ^{o}C and 40 ^{o}C, and frequencies of 0.1 Hz, 0.5 Hz, 1 Hz, 5 Hz and 10 Hz were used for this study. The frequency of 0.01 Hz was also used only for tests conducted at 40^{o}C. These loading frequencies simulate different traffic speeds. Higher frequencies represent higher vehicle speeds.

The DM test is a strong indicator of asphalt mixture performance. Dynamic modulus and phase angle are two performance variables obtained from DM tests. Dynamic modulus shows how stiff an asphalt mixture is. A higher dynamic modulus value represents higher stiffness. The time

delay between the time point at which peak stress is applied and the time point at which peak strain is observed is used to calculate phase angle. The phase angle represents viscoelastic characteristics of asphalt mixtures. A higher phase angle indicates that the samples are more viscous, more susceptible to rutting and more resistant to cracking (Darnell and Bell 2015).

In this study, 170 mm tall samples were prepared by using gyratory compaction according to AASHTO PP 60-14. Then, samples were cored in 100 mm diameter and their edges were cut off to get 150 mm tall samples. Samples were kept in a conditioning chamber at the testing temperatures the day before being tested.

After conducting the tests, master curves were developed for dynamic modulus and phase angle following the AASHTO PP 61-13 procedure. Master curves display phase angle and dynamic modulus with respect to loading frequencies. Master curves are presented in 7APPENDIX D:show one example of the data generated by the test equipment for the DM test, along with the procedure of developing the master curves.

3.4.3 Flow Number Test

The flow number (FN) test is a performance test for evaluating rutting resistance of asphalt concrete mixtures (Bonaquist et al. 2003). In this test, while constant deviator stress is applied at each load cycle on the test sample, permanent strain at each cycle is measured (Figure 3.10). Permanent deformation of asphalt pavements has three stages: 1) primary or initial consolidation, 2) secondary and 3) tertiary or shear deformation (Biligiri et al. 2007). Figure 3.10 shows three stages of permanent deformation. FN is the loading cycle at which the tertiary stage starts after the secondary stage.

In this study, testing conditions and criteria for FN testing described in AASHTO TP 79-13 for unconfined tests were followed. The recommended test temperature, determined by LTPPBind Version 3.1 software, is the average design high pavement temperature at 50% reliability for cities in Oregon with high populations and at a depth of 20 mm (0.79 in) for surface courses (Rodezno et al. 2015). Tests were conducted at a temperature of 54.7^{o}C with average deviator stress of 600 kPa and minimum (contact) axial stress of 30 kPa. For conditioning, samples were kept in a conditioning chamber at the testing temperature a day prior to being tested. To calculate FN in this study, the Francken model was used. This model is discussed in Section 3.4.3.1.

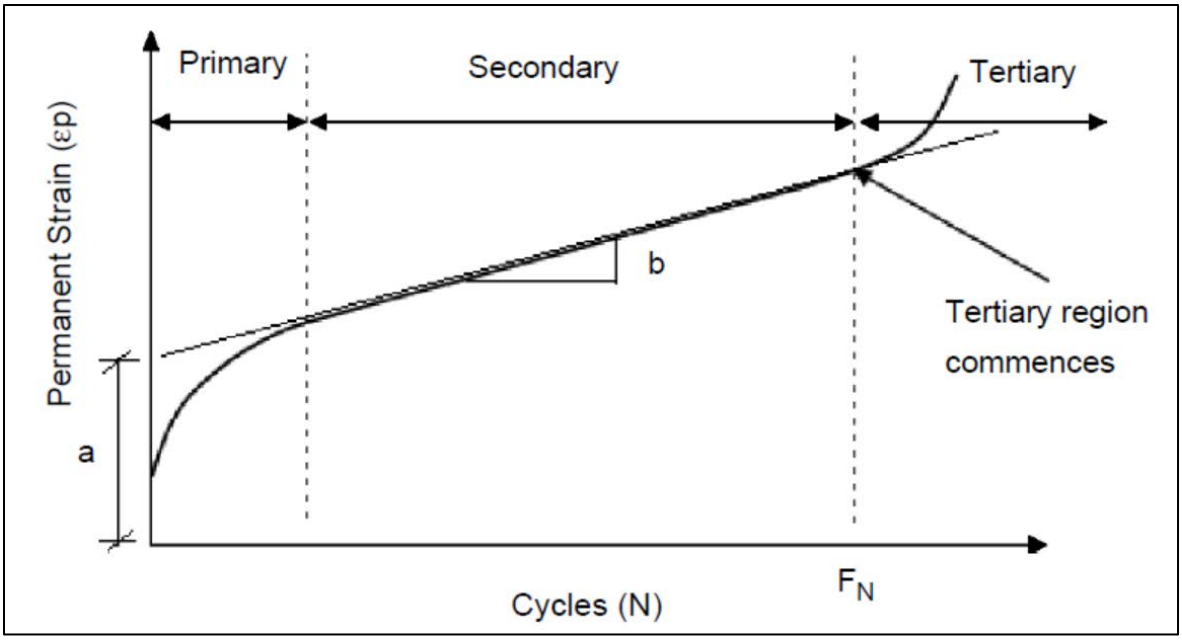

Figure 3.10. Relationship between permanent strain and load cycles in FN test

(Biligiri et al. 2007)

Minimum FN values (calculated by using the Francken model) for different traffic levels recommended by AASHTO TP 79-13 are given in Table 3.4 (Rodezno et al. 2015). All high RAP mixes recommended in this study had FN values higher than the 740 limit.

Table 3.4. Minimum Average FN Requirement for Different Traffic Levels (AASHTO TP 79-13)

Traffic (million ESALs)	Minimum Average FN Requirement
<3	NA
3 to <10	50
10 to <30	190
≥30	740

Note: NA= not applicable.

3.4.3.1 Francken Model

The Francken Model was developed for triaxial and uniaxial repeated-load tests for different temperatures and stress levels (Francken 1977). A study carried out by Biligiri et al. (2007) showed that this model calculates FN more accurately compared to other mathematical models. This model can also represent all three stages of deformation (1.primary or the initial consolidation of the mix, 2. secondary, and 3. tertiary or shear deformation) more properly. Moreover, Dongre et al. (2009) confirmed the robustness of Francken model by fitting FN data obtained from field projects. The model is given as follows:

$$\epsilon_p(N)=AN^B+C(e^{DN}-1) \quad \textbf{(3.16)}$$

Where:

$\epsilon_p(N)$ = permanent deformation or permanent strain from F_n test,

N = number of loading cycles, and

A, B, C, D = regression constants.

The rate of change of the slope of the permanent strain is obtained by taking the second derivative of the Francken model (Equation (**3.17**). The inflection point, at which the sign of the rate of change of slope changes is considered as the FN and indicates when the tertiary stage begins. FN is the number of cycles at which the second derivative of the Francken model is zero. The second derivative of the model is as follows (Dongre et al. 2009):

$$\frac{\partial^2\epsilon_p}{\partial N^2}=A*B*(B-1)*N^{B-2}+(C*D*e^{D*N}) \quad \textbf{(3.17)}$$

The model shown in Equation (**3.16** is fitted to the permanent strain versus the number of cycles for each sample. After estimating the regression constants (A, B, C, and D), to find the number of load cycles at the inflection point, FN is computed at which (3.17 (second derivative of Francken model) is equal to zero. In this study, a code was developed using MATLAB (2016) to analyze the data and calculate regression constants (A, B, C, and D) of the Francken model to find the FN for each test.

3.5 ASPHALT MIXTURES WITH HIGH RAP CONTENTS – PHASE I

This section presents the results of SCB tests to evaluate cracking performance of high RAP (30% and 40%) asphalt mixtures used in this study. FN tests were used to quantify the rutting performance of asphalt mixtures. DM test results were used to quantify the viscous and elastic behavior of all mixes. Regression equations were developed and Monte Carlo simulations were performed using the developed equations to determine the required binder content, binder grade and RAP content of asphalt mixtures to meet rutting and cracking resistance requirements.

3.5.1 Experimental Plan

This section summarizes the experimental plan followed for asphalt mixtures with high RAP contents (30% and 40%). The goal is to find the effects of changing binder content, RAP content and binder grade on cracking and rutting performance of asphalt mixtures with high RAP contents. Therefore, samples with different binder content, binder grade and RAP content were prepared while other variables including air-void content, gradation and sample dimensions were kept the same for all the samples. The mix properties and experimental plan are given as follows:

SCB, DM and FN tests were conducted on samples with two RAP contents (30% and 40%), three binder contents (6%, 6.4% and 6.8%), and three binder grades (PG58-34, PG64-22 and PG76-22). Since the DM test is a non-destructive test (low strain level), the same samples prepared for DM tests were used for FN tests to compare the rutting resistance of HMA mixtures. Table 3.5 shows the experimental plan followed in this study.

Table 3.5. Experimental Plan

Test type	Binder content	RAP content	Binder grade	Temp.[2]	Air-void content	Repl.[3]	Total tests
SCB	6.0% 6.4% 6.8%	30% 40%	PG 58-34 PG 64-22 PG 76-22	25 ^{o}C	7%	4	72
Dynamic Modulus	6.0% 6.4% 6.8%	30% 40%	PG 58-34 PG 64-22 PG 76-22	1 run[1]	7%	2	36
Flow Number	6.0% 6.4% 6.8%	30% 40%	PG 58-34 PG 64-22 PG 76-22	54.7 ^{o}C	7%	2	36

Note: [1]Samples were tested at temperatures of 4 ^{o}C, 20 ^{o}C, and 40 ^{o}C and the loading frequencies of 0.1, 0.5, 1, 5, and 10 Hz. A loading frequency of 0.01 Hz was also used for 40 ^{o}C tests.
[2]Temp. = Temperature.
[3]Repl. = Replicate.

3.5.2 Results and Discussion

3.5.2.1 Semi-Circular Bend Test

SCB tests were conducted at 25 oC in this study to evaluate cracking performance of asphalt mixtures. A full factorial experimental plan with two RAP contents (30% and 40%), three different binder contents (6%, 6.4% and 6.8%) and three binder grades (PG 58-34, PG 64-22 and PG 76-22) is followed in this study (See Table 3.5). Four replicates were tested for each combination. In total, 72 tests were conducted. Applied peak load (P_{peak}), fracture energy (G_f), fracture toughness (K_{IC}), secant stiffness (S) and flexibility index (FI) are the testing parameters obtained from the test results. The results of SCB tests are presented in Figure 3.11 to Figure 3.14.

As is shown in Figure 3.11, FI increases as the binder content increases for mixtures with the same RAP contents. Asphalt mixtures with lower binder contents are more brittle and more susceptible to cracking. Results of this study show that asphalt mixtures with 30% RAP have higher FI than the asphalt mixtures with 40% RAP. Higher RAP contents result in more brittle mixes and less cracking resistance. Moreover, using softer binders increases FI. As was expected, the mixture with the softest binder grade (PG 58-34), the highest binder content (6.8%) and the lowest RAP content has the greatest FI. Conversely, the mixture with PG 76-22 binder grade, 6% binder content and 40% RAP content shows the lowest FI value. Al-Qadi et al. (2015) defined a threshold for FI

representing the cracking performance of asphalt mixtures. Mixtures with FI higher than 10 were considered to have high cracking performance (Al-qadi and Ozer 2015). Also, some samples of production mixes were collected from the plant and compacted in the laboratory in the ODOT SPR785 project (Coleri 2017). The average FI for a non-polymer mix used for construction on a major highway in Oregon was around 9, and the mix with the best cracking resistance (a polymer modified mix) had an FI of 14. Therefore, this study considered 9 to 14 as a possible range of FI values of mixtures with acceptable cracking performance and used an FI of 10 as a limit for acceptance. In this study, five mixtures met the threshold: 1) BC3 6.4%, RAP 30%, PG 58-34, 2) BC 6.8%, RAP 30%, PG 58-34, 3) BC 6.8%, RAP 30%, PG 64-22, 4) BC 6.8%, RAP 40%, PG 58-34, and 5) BC 6.8%, RAP 40%, PG 64-22. It can be concluded that FI is a good performance indicator since it can differentiate the cracking performance of asphalt mixtures with different RAP contents, binder contents and binder grades.

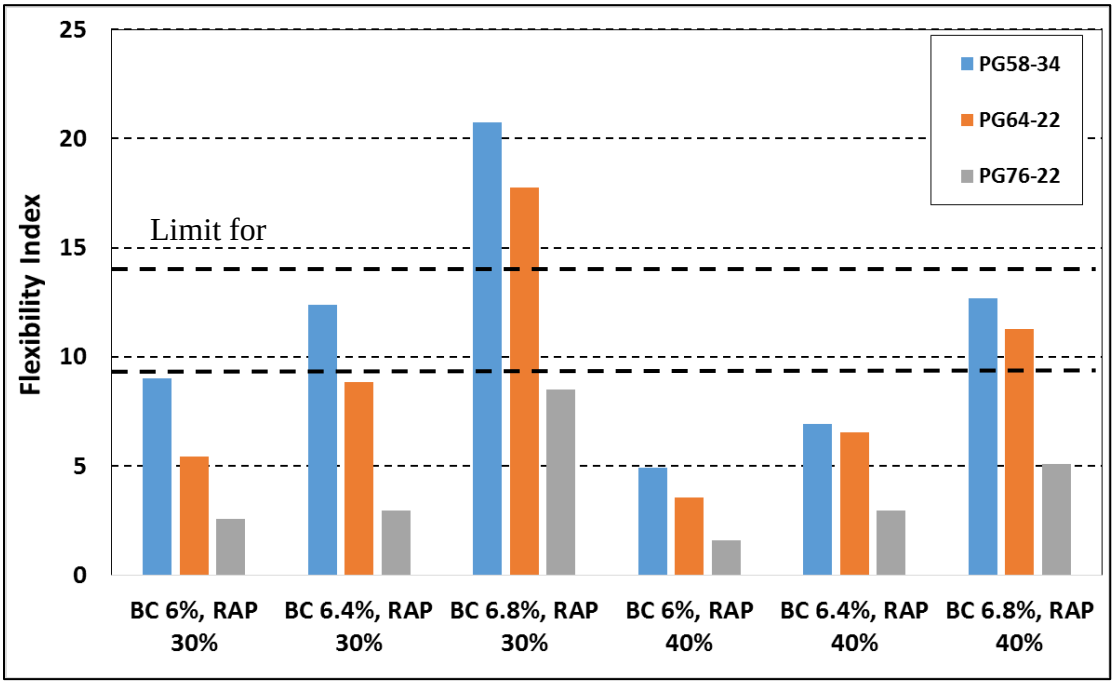

Figure 3.11. Flexibility index for mixtures with different RAP contents (30% and 40%), binder grades (PG 58-34, PG 64-22, and PG 76-22), and binder contents (6%, 6.4%, and 6.8%)

As fracture energy (G_f) increases, the work required for crack formation and propagation increases. Therefore, asphalt mixtures with higher G_f values are expected to show higher resistance to cracking (Ozer et al. 2016). Results of this study show that there is not a strong correlation between the properties of asphalt mixtures and G_f. This is evident especially for mixtures with PG 64-22 binder. As binder content increases, an increase in G_f was not observed (Figure 3.12). Moreover, G_f changed slightly for the mixtures with

[3] Binder content

PG 58-34 and PG 76-22 for different binder contents. Also, G_f could not differentiate the cracking performance of the mixtures with different RAP contents. These results suggest that G_f, the most common parameter that has been used to characterize cracking resistance of asphalt mixtures in several research studies, is not an effective parameter to use for cracking performance evaluation.

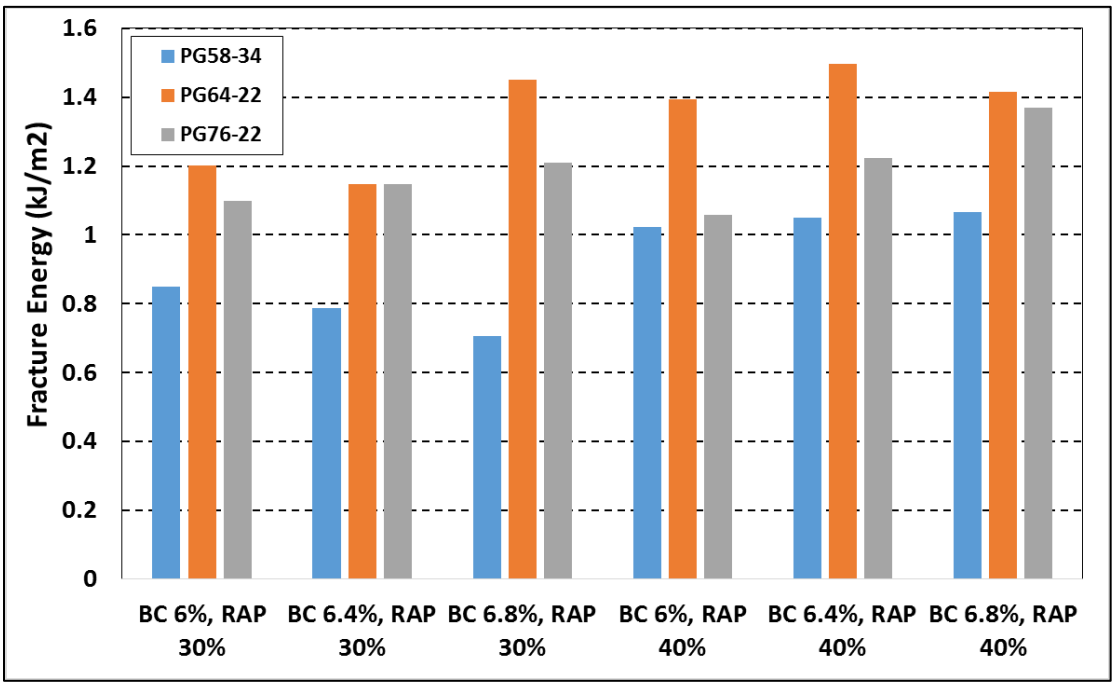

Figure 3.12. Fracture energy for mixtures with different RAP contents (30% and 40%), binder grades (PG 58-34, PG 64-22, and PG 76-22), and binder contents (6%, 6.4%, and 6.8%)

K_{IC} and S correlate well with cracking resistance and brittleness. Higher values for these two variables indicate higher resistance to crack formation and higher brittleness. Figure 3.13 and Figure 3.14 show that mixtures with BC 6.8%, RAP 30%, PG 58-34 and BC 6%, RAP 40%, PG 76-22 have the lowest and the highest S and K_{IC}, respectively. Asphalt mixtures with lower K_{IC} and S values and higher FI require less energy for crack initiation, but since they are more ductile, they have higher crack propagation resistance. In this study, although the mixture with 40% RAP, 6% binder content and PG 76-22 binder has the highest K_{IC} and S values, it has the lowest FI value. This means that it requires higher energy for crack initiation, but once the crack starts, it propagates rapidly. All possible combinations of RAP content, binder content and binder grade to achieve acceptable cracking and rutting performance are determined using regression modeling and suggested strategies are provided in Section 3.5.2.5.

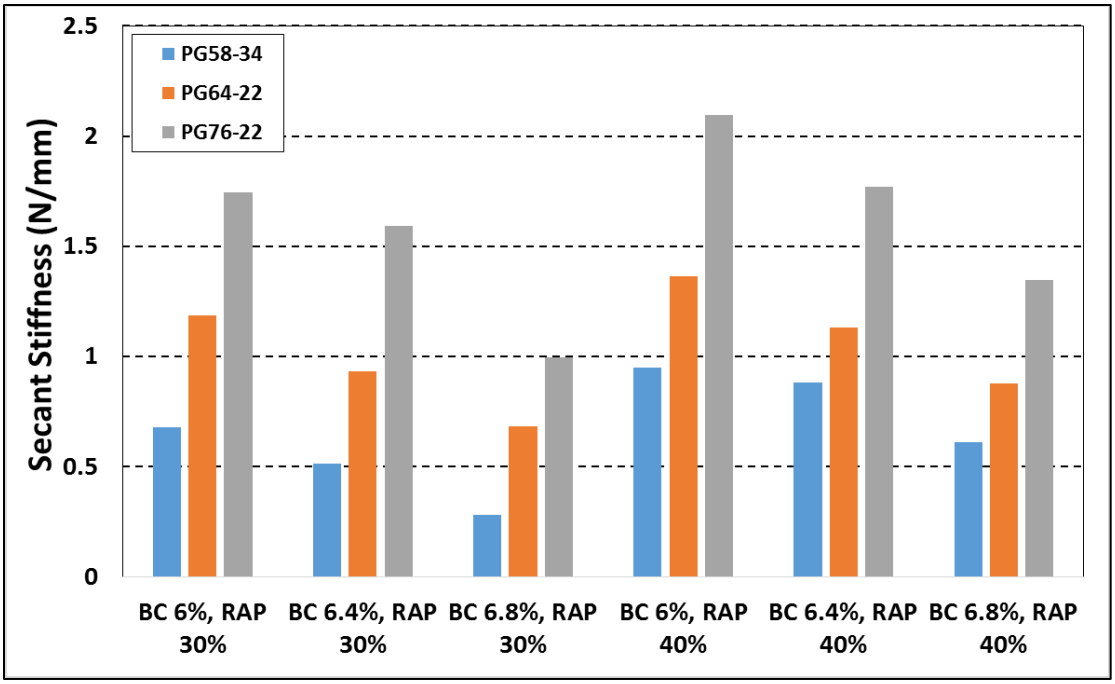

Figure 3.13. Secant stiffness for mixtures with different RAP contents (30% and 40%), binder grades (PG 58-34, PG 64-22, and PG 76-22), and binder contents (6%, 6.4%, and 6.8%)

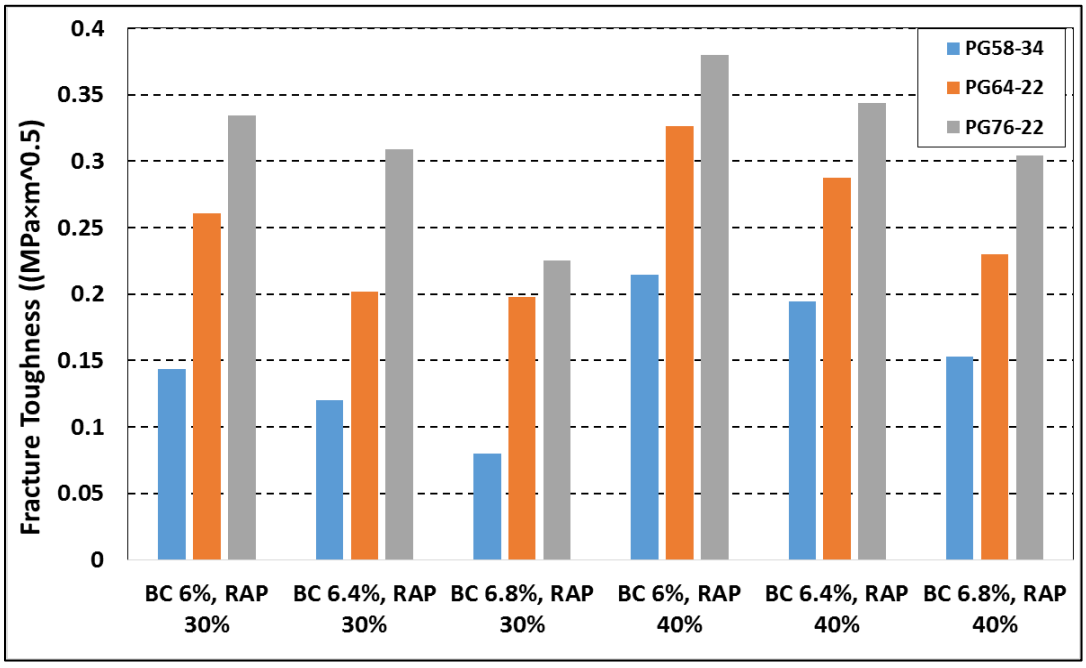

Figure 3.14. Fracture toughness for mixtures with different RAP contents (30% and 40%), binder grades (PG 58-34, PG 64-22, and PG 76-22), and binder contents (6%, 6.4%, and 6.8%)

3.5.2.2 Flow Number Test

The flow number (FN) test is a simple performance test for evaluating rutting performance of asphalt concrete mixtures (Bonaquist et al. 2003). High FN values indicate that asphalt mixtures have high rutting resistance. Figure 3.15 to Figure 3.17 summarize the FN values for all tested asphalt mixtures.

Minimum required FNs suggested by AASHTO TP 79-13 for different traffic levels are presented in Table 3.4. The suggested FN for the traffic level of 10 million to 30 million ESALs is specified as 190 while the FN limit for roadways with ESALs more than 30 million were specified as 740. In Figure 3.15 to Figure 3.17, the dashed red line and the solid red line show the recommended FN for the traffic levels of 10 to <30 million and ≥30 million ESALs, respectively. FN values for all the asphalt mixtures were greater than 50, which is the recommended FN for the traffic level of 3 million to 10 million ESALs. All the asphalt mixtures with PG 64-22 and PG 76-22 binders had FN values higher than 740, except for the mixture with BC 6.8%, RAP 30% and PG 64-22 binder. Mixtures with PG 58-34 binder had acceptable rutting resistance for the traffic level of 10 to <30 million ESALs (with FN greater than 190) except for the mixture with BC 6.8%, RAP 30% and PG 58-34 binder (FN=171). Only two mixtures (BC 6%-RAP 40%-PG 58-34 and BC 6.4%-RAP 40%-PG 58-34) had FN values greater than 740, meaning that they show acceptable rutting performance for a traffic level of ≥30 million ESALs. FN values for all tested asphalt mixtures are presented in Figure 3.18.

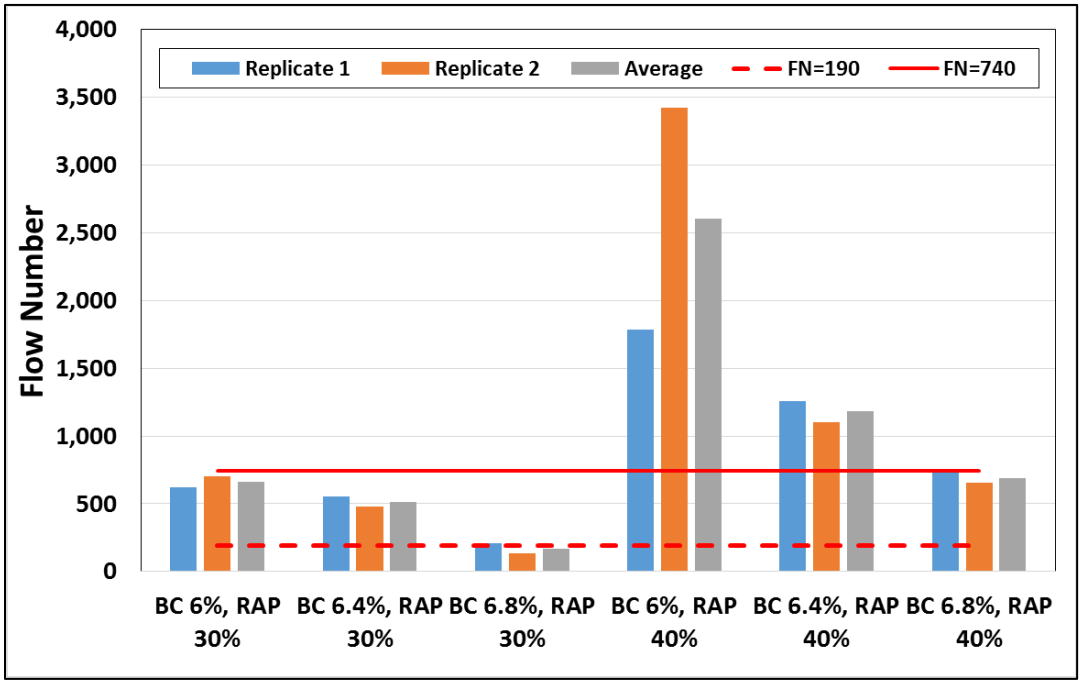

Figure 3.15. Flow number of the mixtures with different RAP contents (30% and 40%), binder grade of PG 58-34, and different binder contents (6%, 6.4%, and 6.8%)

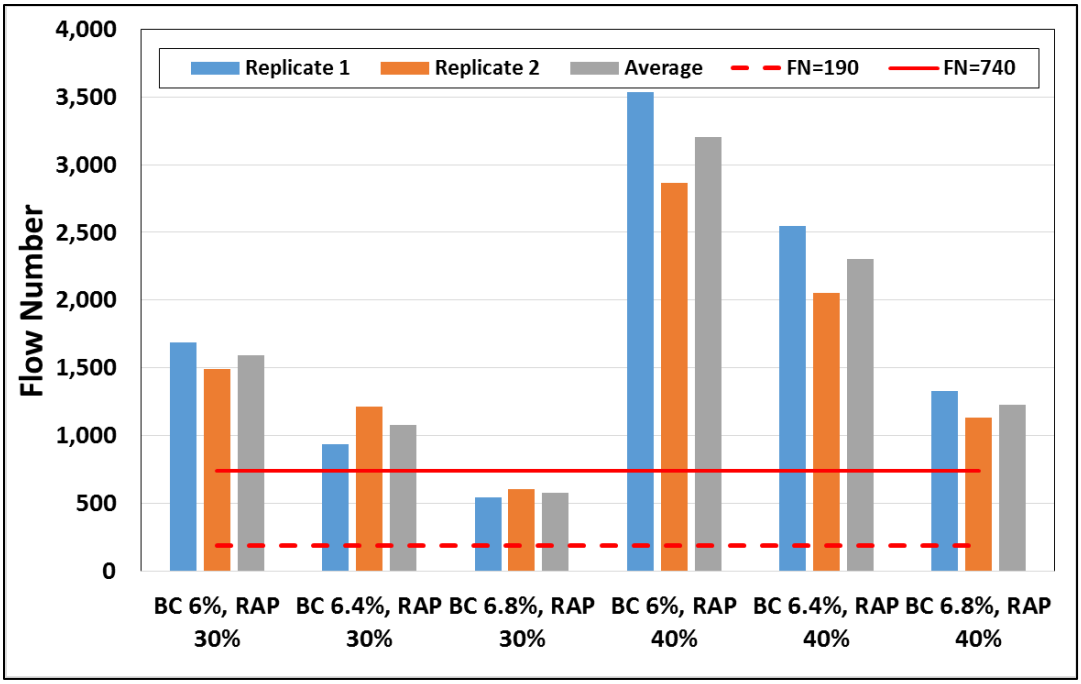

Figure 3.16. Flow number of the mixtures with different RAP contents (30% and 40%), binder grade of PG 64-22, and different binder contents (6%, 6.4%, and 6.8%)

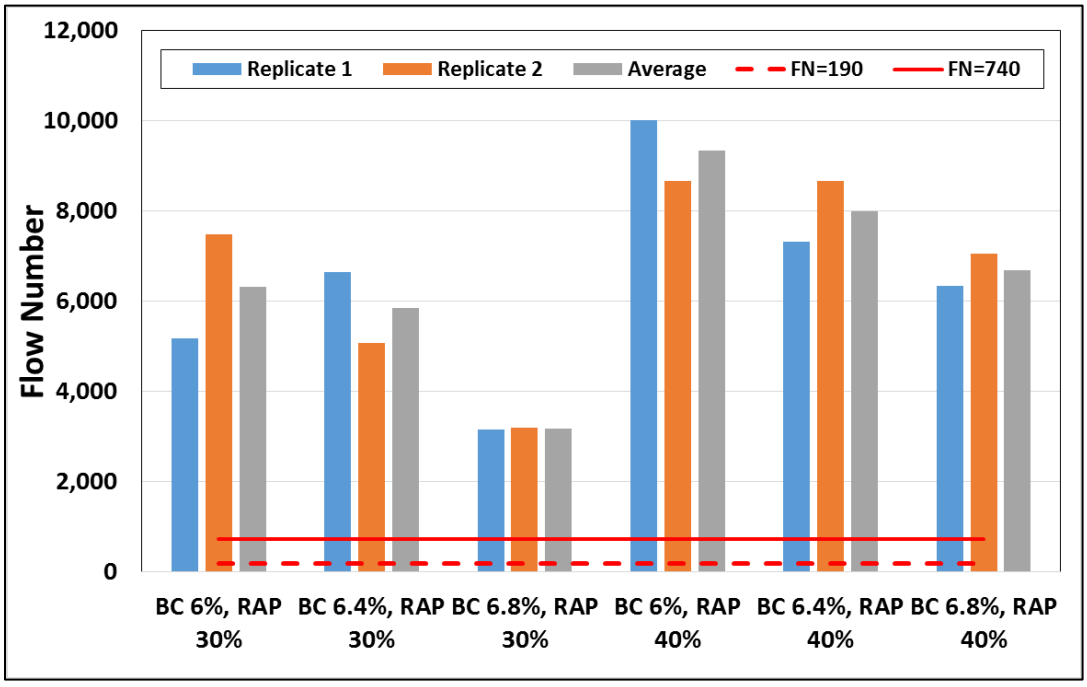

Figure 3.17. Flow number of the mixtures with different RAP contents (30% and 40%), binder grade of PG 76-22, and different binder contents (6%, 6.4%, and 6.8%)

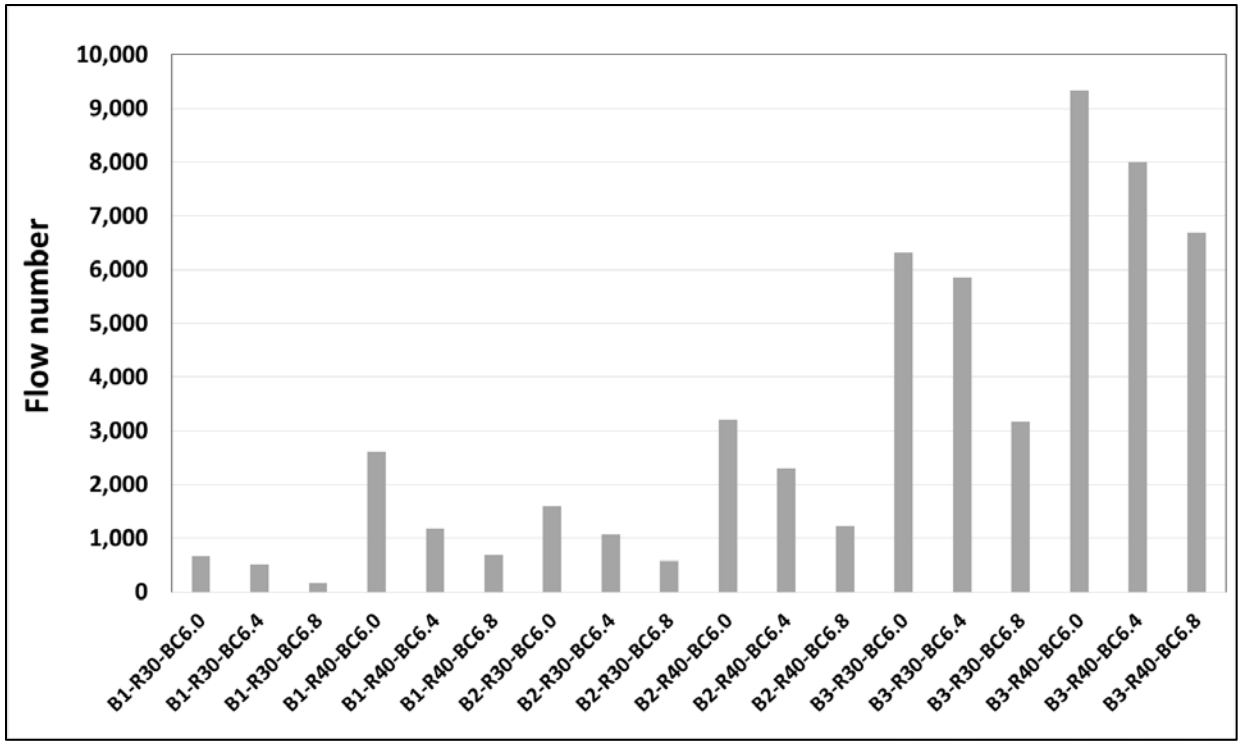

Figure 3.18. Average flow number of the mixtures for all the combinations of RAP contents, binder contents, and binder grades

Note: B1= PG 58-34, B2= PG 64-22, and B3 = PG 76-22.
R30 = 30% RAP, and R40 = 40% RAP.
BC6= 6% binder content, BC6.4 =6.4 % binder content, and BC6.8 = 6.8% binder content.

3.5.2.3 Dynamic Modulus Test

In this study, DM tests were conducted on prepared asphalt samples with different RAP contents (30% and 40%), binder contents (6%, 6.4% and 6.8%), and binder grades (PG 58-34, PG 64-22 and PG 76-22). Two replicate experiments were conducted for each combination of the variables of interest. Therefore, 36 samples in total were tested at the testing frequencies and temperatures given in Section 3.4.2. The testing procedure described in AASHTO TP 79-13 for unconfined mixtures was followed. Dynamic modulus and phase angle master curves are presented and discussed in the following sections.

3.5.2.3.1 Master Curves for Dynamic Modulus

This section represents the dynamic modulus master curves for asphalt mixtures. Average of test results for two replicate mixtures were used to develop each master curve as recommended by AASHTO TP 79-13.

Master curves of dynamic modulus for the mixtures with different RAP contents (30% and 40%), different binder contents (6%, 6.4% and 6.8%), and different binder grades

(PG 58-34, PG 64-22 and PG 76-22) are presented in Figure 3.19 to Figure 3.20. The reference temperature for all the master curves is 20°C.

In general, higher RAP content and lower binder content resulted in a higher dynamic modulus. RAP content plays a significant role in the cracking resistance of the mixtures. For the same binder grade, the mixtures with 40% RAP had higher dynamic moduli than the mixtures with 30% RAP for all binder contents. These master curves were used in Chapter 5 to perform mechanistic-empirical pavement design simulations.

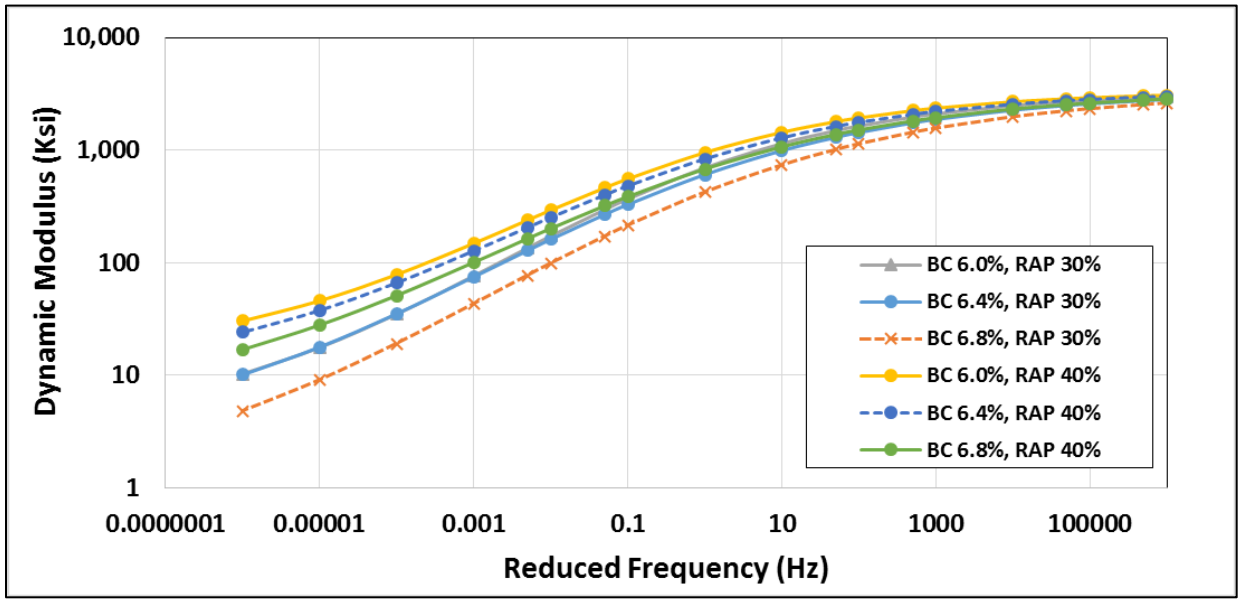

Figure 3.19. Master curves of dynamic modulus for the mixtures with different RAP contents (30% and 40%), binder grade of PG 58-34, and different binder contents (6%, 6.4%, and 6.8%)

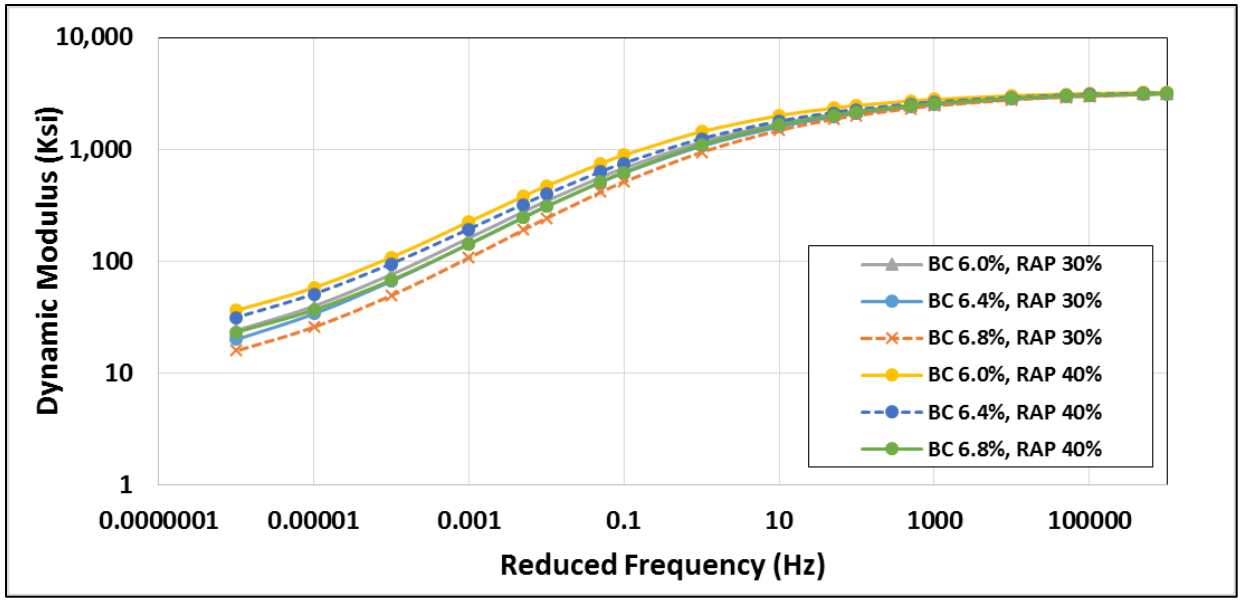

Figure 3.20. Master curves of dynamic modulus for the mixtures with different RAP contents (30% and 40%), binder grade of PG 64-22, and different binder contents (6%, 6.4%, and 6.8%)

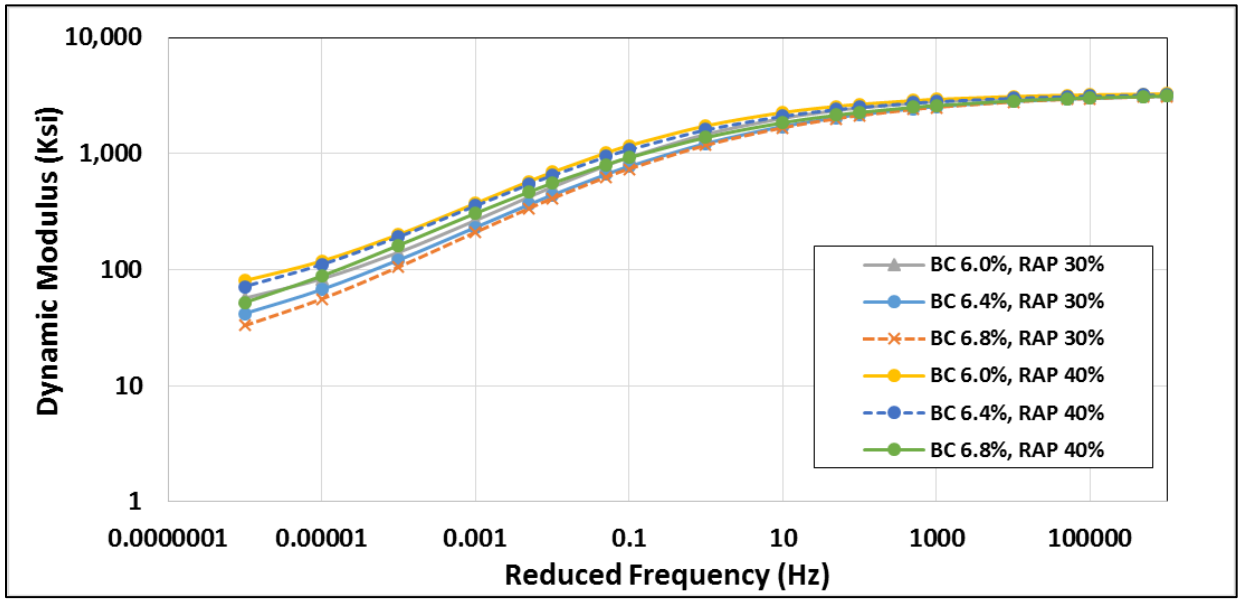

Figure 3.21. Master curves of dynamic modulus for the mixtures with different RAP contents (30% and 40%), binder grade of PG 76-22, and different binder contents (6%, 6.4%, and 6.8%)

To see the effect of binder grade on dynamic modulus, Figure 3.22 to Figure 3.24 were created. It can be seen in these figures that binder grade had a significant effect on the stiffness of the mixtures. The mixtures with softer binder had lower dynamic moduli compared to the mixtures with stiffer binder regardless of their RAP contents. Moreover, dynamic modulus decreased with a higher rate with respect to the load frequency for the

softer binder, especially at low frequency levels. Moreover, the mixture with BC 6%, RAP 30% and PG 64-22 had almost the same dynamic modulus as the mixture with BC 6%, RAP 40% and PG 58-34 for all the frequencies. These two mixtures also had similar FI values in SCB tests. This result proves that FI in SCB tests can describe mixture properties properly. The mixture with BC 6%, RAP 40% and PG 64-22 binder seems to have almost the same master curve as the mixture with BC 6%, RAP 30% and PG 76-22 binder at higher frequencies (higher vehicle speed condition). However, the mixture with BC 6%, RAP 40% and PG 64-22 binder had a lower dynamic modulus at lower frequency levels (lower vehicle speed condition), meaning that it has lower rutting resistance.

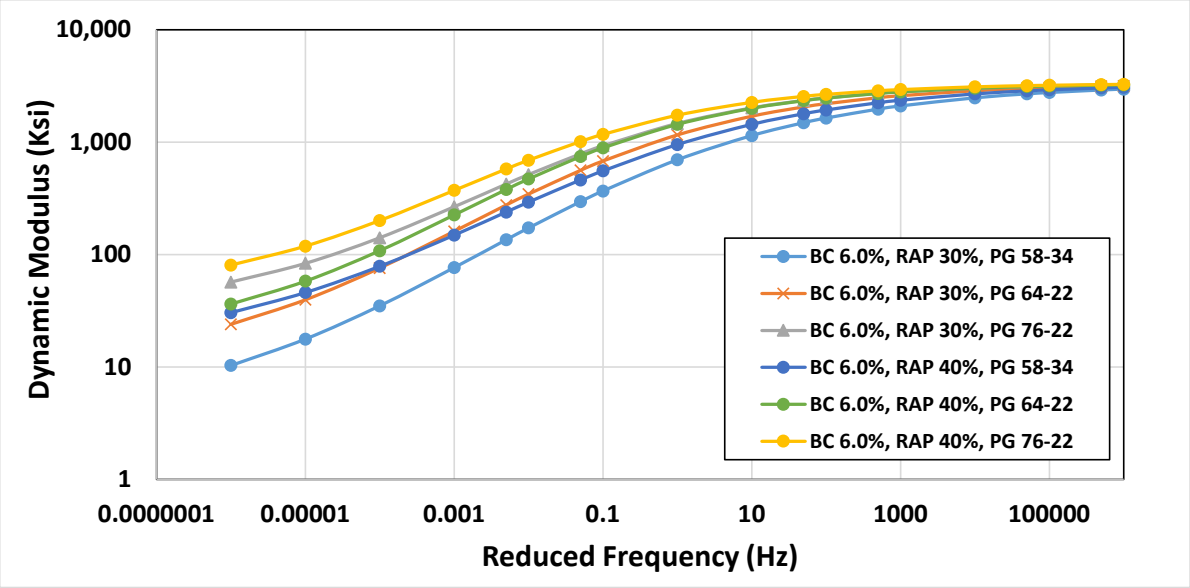

Figure 3.22. Master curves of dynamic modulus for the mixtures with different RAP contents (30% and 40%), different binder grades (PG 58-34, PG 64-22, and PG 76-22), and 6% binder content

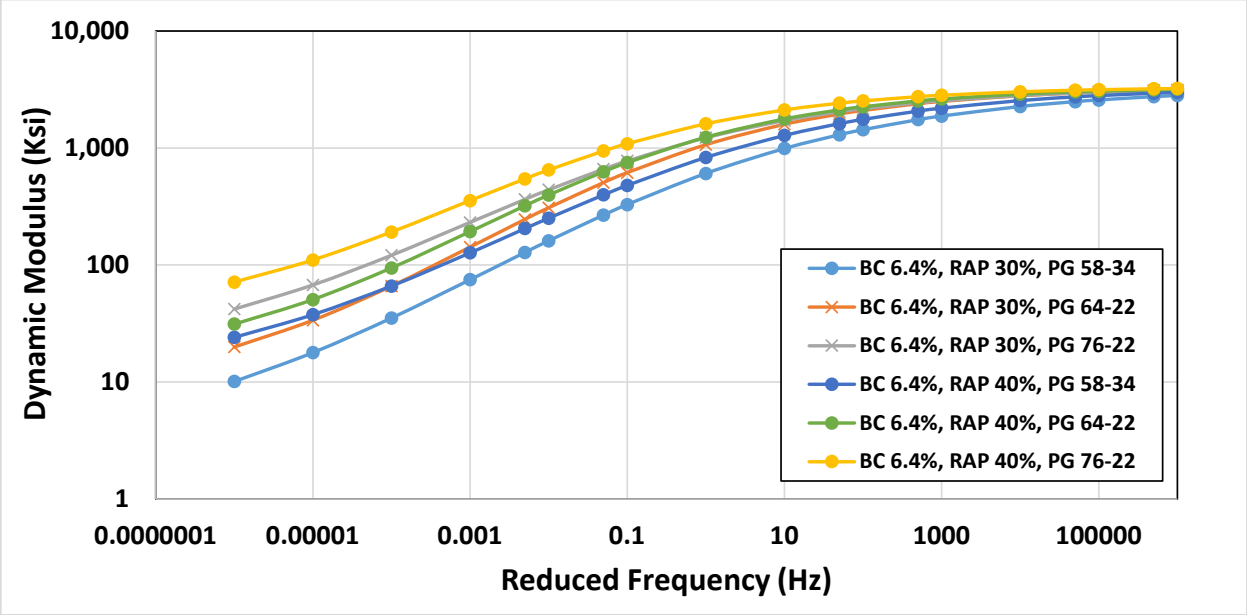

Figure 3.23. Master curves of dynamic modulus for the mixtures with different RAP contents (30% and 40%), different binder grades (PG 58-34, PG 64-22, and PG 76-22), and 6.4% binder content

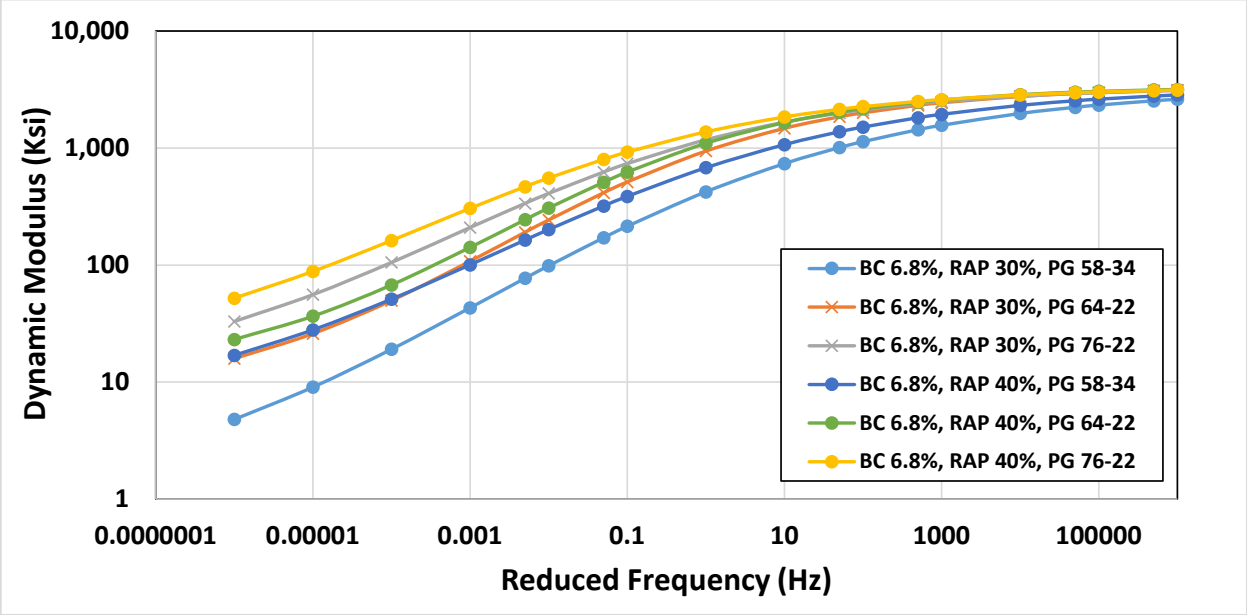

Figure 3.24. Master curves of dynamic modulus for the mixtures with different RAP contents (30% and 40%), different binder grades (PG 58-34, PG 64-22, and PG 76-22), and 6.8% binder content

Based on AASHTO TP 79-13, the coefficient of variation (CV) of the dynamic modulus for each pair of tested samples should not be greater than 9.2%. Figure 3.25 to Figure 3.30 show the dynamic modulus of the mixtures at the frequencies of 10 Hz and 0.1 Hz, temperatures of 4 ^{o}C, 20 ^{o}C and 40 ^{o}C, as well as all the combinations of RAP contents, binder contents and binder grades. In these figures, B1 is PG 58-34, B2 is PG 64-22 and B3 is PG 76-22. Also, R30 is RAP 30%, R40 is RAP 40%, and BC refers to binder content. For all the mixtures shown, the CV values of the paired tested mixtures were less than 9.2% at 4 ^{o}C and 20 ^{o}C (except for the mixtures with 30% RAP, 6.8% binder content and PG 58-34 at 20 ^{o}C and 0.1 Hz). However, some of the paired mixtures had higher CV at 40 ^{o}C. Bonaquist (2011) reported in NCHRP Report 702 that the CV could be more than 10% for mixtures with low dynamic modulus. Therefore, observing higher CV for dynamic modulus at the test temperature of 40 °C is not unexpected. Moreover, it can be seen that the dynamic modulus decreases as the binder content increases for all the frequency levels and temperatures. It has an opposite trend as the RAP content increases.

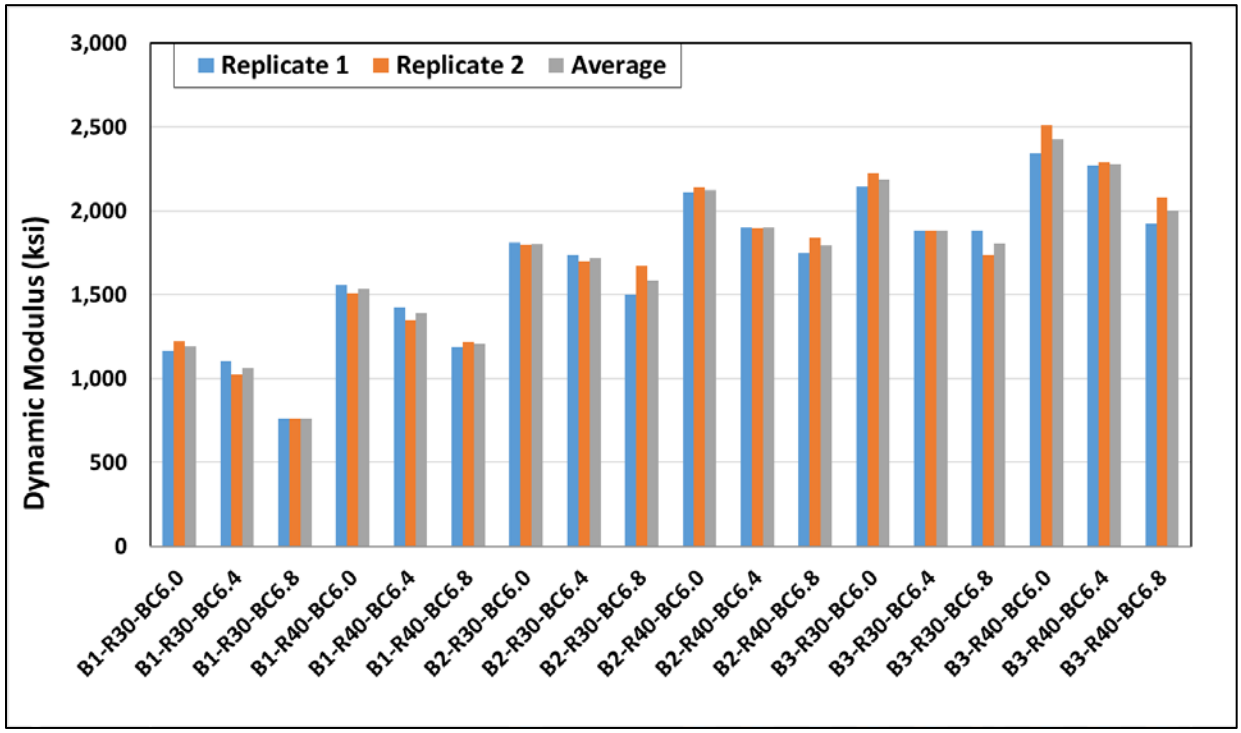

Figure 3.25. Dynamic modulus of the mixtures at 4 ^{o}C and 0.1 Hz and all the combinations of RAP contents, binder contents, and binder grades

Note: B1= PG 58-34, B2= PG 64-22, and B3 = PG 76-22.
R30 = 30% RAP, and R40 = 40% RAP.
BC6= 6% binder content, BC6.4 =6.4 % binder content, and BC6.8 = 6.8% binder content.

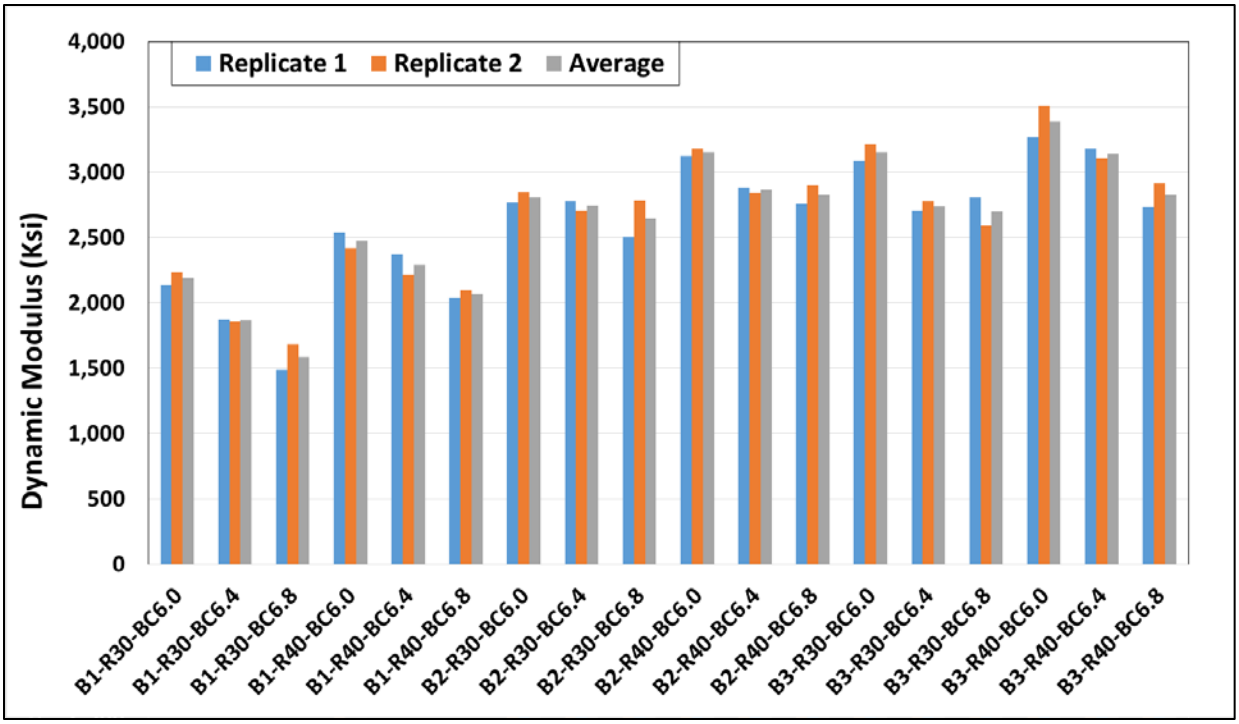

Figure 3.26. Dynamic modulus of the mixtures at 4 ^{o}C and 10 Hz and all the combinations of RAP contents, binder contents, and binder grades

Note: B1= PG 58-34, B2= PG 64-22, and B3 = PG 76-22.
R30 = 30% RAP, and R40 = 40% RAP.
BC6= 6% binder content, BC6.4 =6.4 % binder content, and BC6.8 = 6.8% binder content.

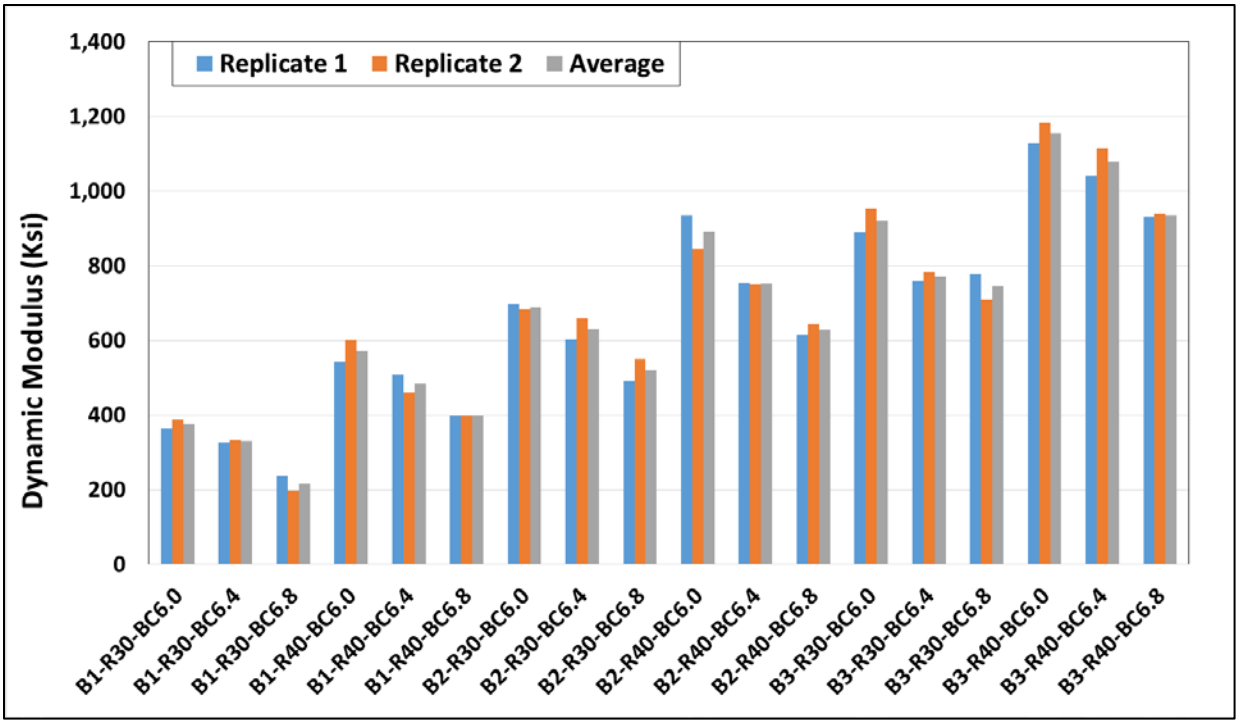

Figure 3.27. Dynamic modulus of the mixtures at 20 ^{o}C and 0.1 Hz and all the combinations of RAP contents, binder contents, and binder grades

Note: B1= PG 58-34, B2= PG 64-22, and B3 = PG 76-22.
R30 = 30% RAP, and R40 = 40% RAP.
BC6= 6% binder content, BC6.4 =6.4 % binder content, and BC6.8 = 6.8% binder content.

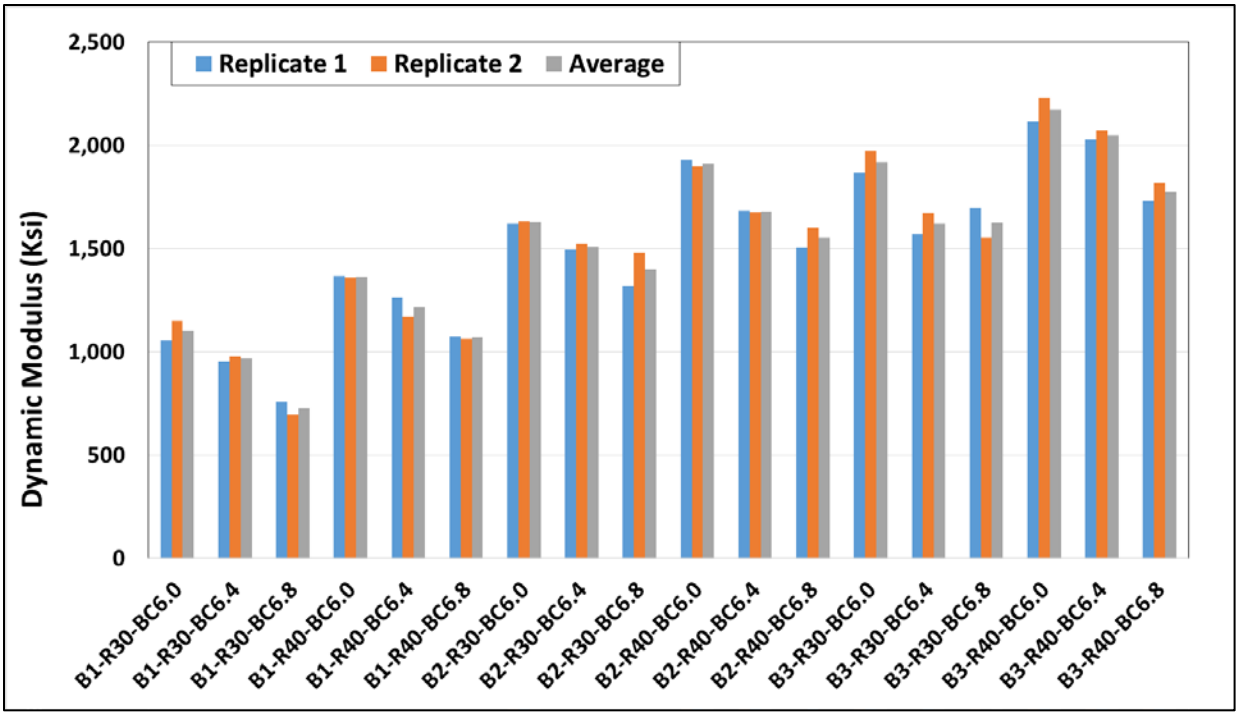

Figure 3.28. Dynamic modulus of the mixtures at 20 ^{o}C and 10 Hz and all the combinations of RAP contents, binder contents, and binder grades

Note: B1= PG 58-34, B2= PG 64-22, and B3 = PG 76-22.
R30 = 30% RAP, and R40 = 40% RAP.
BC6= 6% binder content, BC6.4 =6.4 % binder content, and BC6.8 = 6.8% binder content.

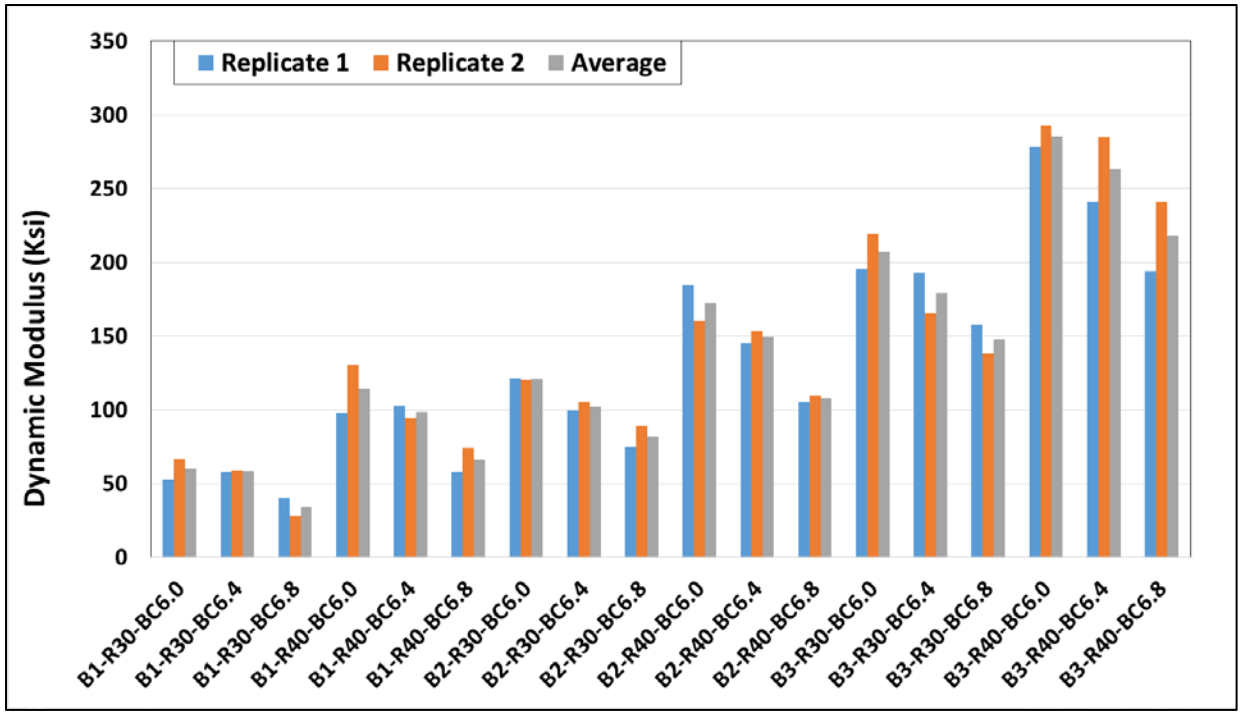

Figure 3.29. Dynamic modulus of the mixtures at 40 ^{o}C and 0.1 Hz and all the combinations of RAP contents, binder contents, and binder grades

Note: B1= PG 58-34, B2= PG 64-22, and B3 = PG 76-22.
R30 = 30% RAP, and R40 = 40% RAP.
BC6= 6% binder content, BC6.4 =6.4 % binder content, and BC6.8 = 6.8% binder content.

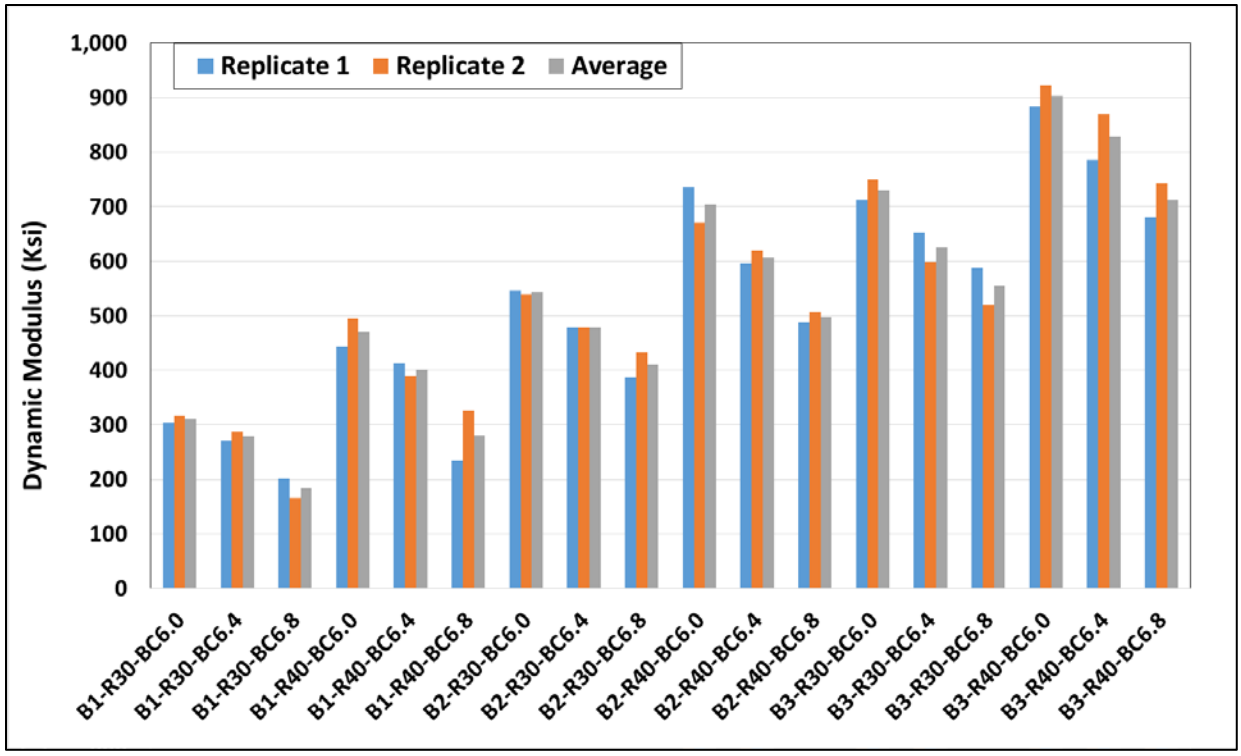

Figure 3.30. Dynamic modulus of the mixtures at 40 ^{o}C and 10 Hz and all the combinations of RAP contents, binder contents, and binder grades

Note: B1= PG 58-34, B2= PG 64-22, and B3 = PG 76-22.
R30 = 30% RAP, and R40 = 40% RAP.
BC6= 6% binder content, BC6.4 =6.4 % binder content, and BC6.8 = 6.8% binder content.

3.5.2.3.2 Master Curves for Phase Angle

The time delay between the time point at which peak stress is applied and the time point at which peak strain is observed is used to calculate phase angle. Phase angle shows energy absorption capacity of an asphalt mixture and represents viscoelastic characteristics of asphalt mixtures. A higher phase angle indicates that the asphalt mixture is more viscous, more susceptible to rutting and more resistant to cracking (Darnell Jr. and Bell 2015). Dynamic modulus and phase angle are inversely related to each other. A mixture with a comparatively high dynamic modulus (high stiffness) at a given frequency level has a low phase angle at the same frequency (Darnell Jr. and Bell 2015).

Phase angle master curves for all test results are plotted in Figure 3.31 to Figure 3.36. The same shift factor values, which were calculated and used for developing the master curves for DM tests, are used to develop the master curves for phase angles. Therefore, these master curves are not as smooth as the master curves of the dynamic modulus. Reference temperature for all master curves is 20 ^{o}C.

Figure 3.33 shows that stiff mixtures with a binder grade of PG 76-22 had lower phase angles at lower binder contents and higher RAP contents. For the same binder grade, asphalt mixtures with 40% RAP had smaller phase angles than the asphalt mixtures with 30% RAP for all the binder contents. Mixtures with softer binders (PG 64-22 and PG 58-34 [Figure 3.31 and Figure 3.32]) showed similar trends for the all the frequency levels, except for the lowest frequencies (low-speed condition). For 40% RAP-PG76-22, binder content effect on phase angle is minimal since high RAP content and stiff binder (PG 76-22) create a stiff mixture with low flexibility.

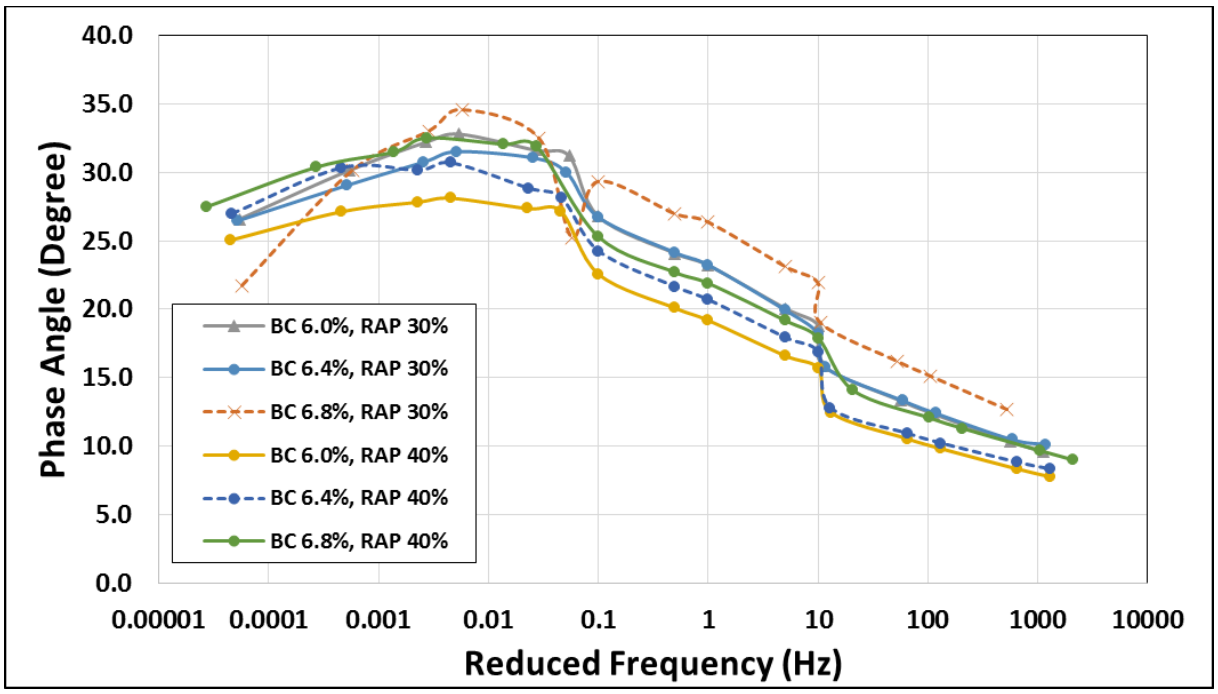

Figure 3.31. Master curves of phase angles for the mixtures with different RAP contents (30% and 40%), binder grade of PG 58-34, and different binder contents (6%, 6.4%, and 6.8%)

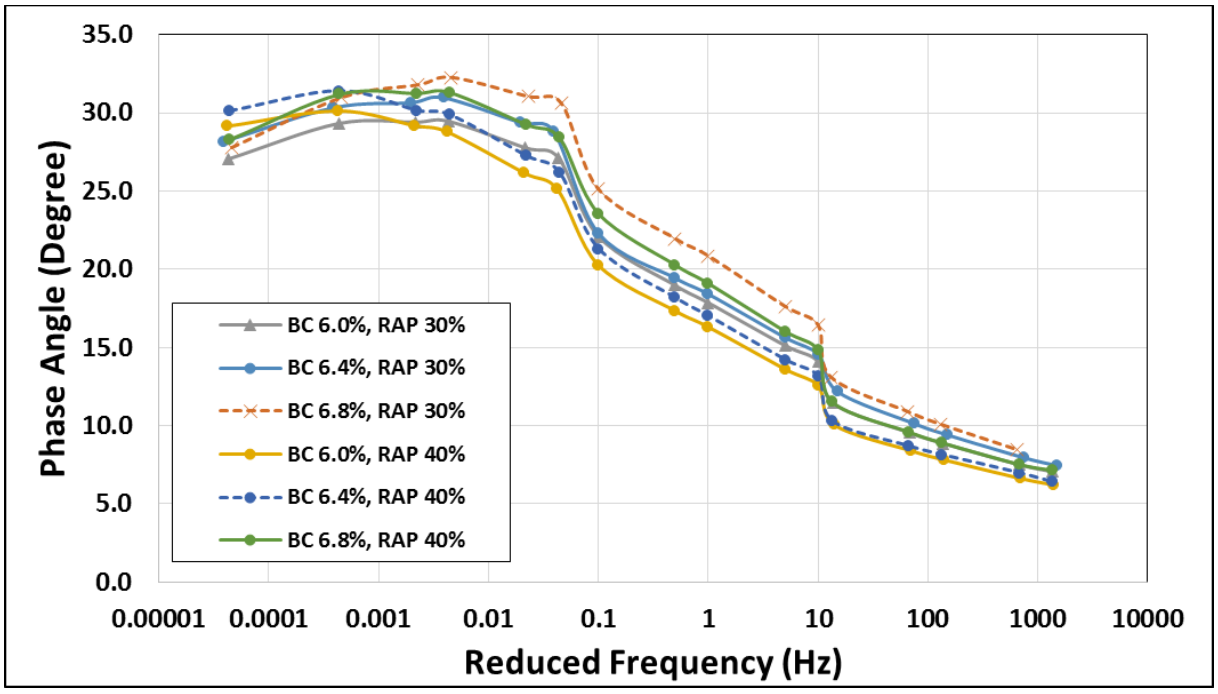

Figure 3.32. Master curves of phase angles for the mixtures with different RAP contents (30% and 40%), binder grade of PG 64-22, and different binder contents (6%, 6.4%, and 6.8%)

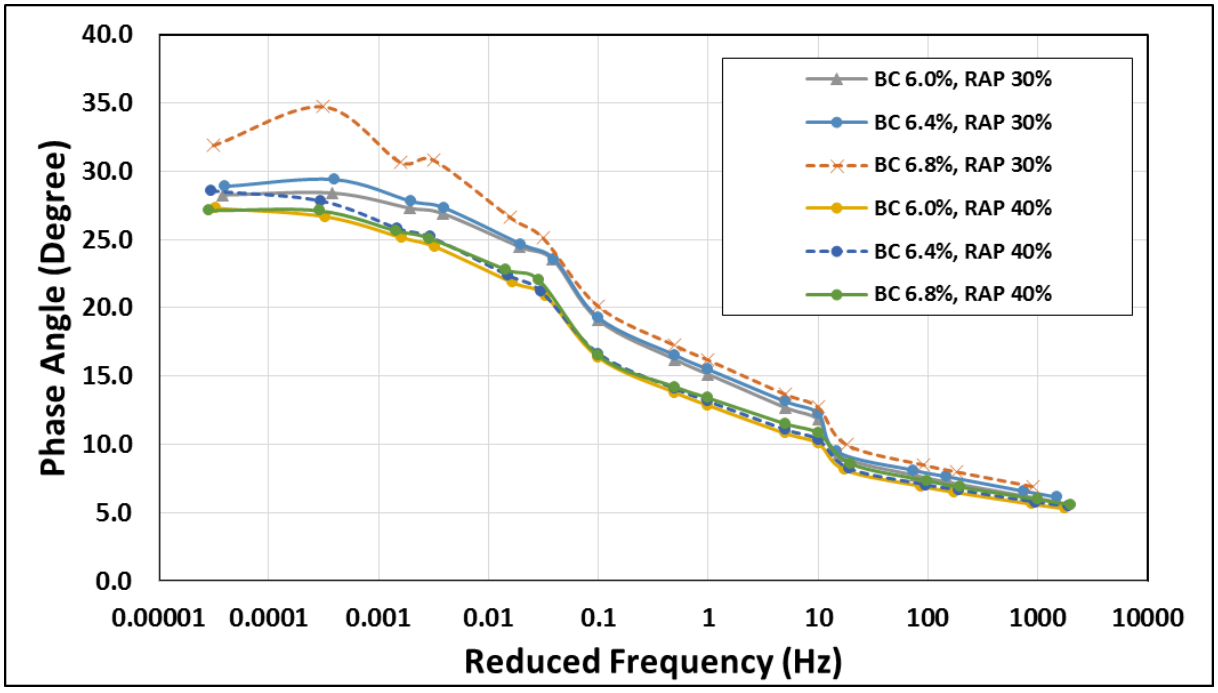

Figure 3.33. Master curves of phase angles for the mixtures with different RAP contents (30% and 40%), binder grade of PG 76-22, and different binder contents (6%, 6.4%, and 6.8%)

To compare the effect of binder grade on phase angle, Figure 3.34 to Figure 3.36 were developed. In general, mixtures with stiffer binder had smaller phase angles with respect to frequency. Also, it can be seen that the effect of RAP content was significant for the mixtures with PG 64-22 and PG 76-22 binders. Mixtures with 40% RAP had smaller phase angles than the mixtures with 30% RAP, regardless of their PG grades. On the contrary, mixtures with PG 58-34 binder had higher phase angles than the mixtures with PG 64-22 and PG 76-22 for the same binder content, regardless of their RAP contents. It can be concluded that RAP content has more significant effect on the phase angle than binder grade for the mixtures with PG 64-22 and PG 76-22 binders. However, the effect of binder grade on phase angle is more significant than RAP content for the mixtures with the softer binder (PG 58-34).

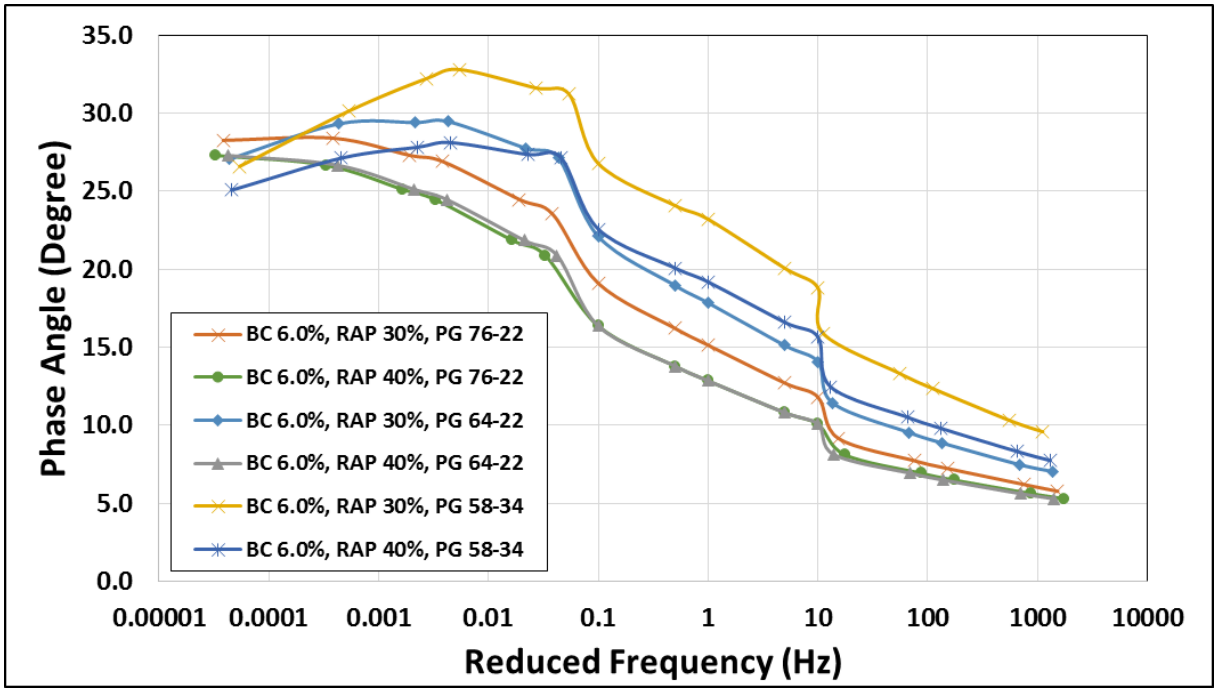

Figure 3.34. Master curves of phase angles for the mixtures with different RAP contents (30% and 40%), different binder grades of (PG 58-34, PG 64-22, and PG 76-22), and 6% binder content

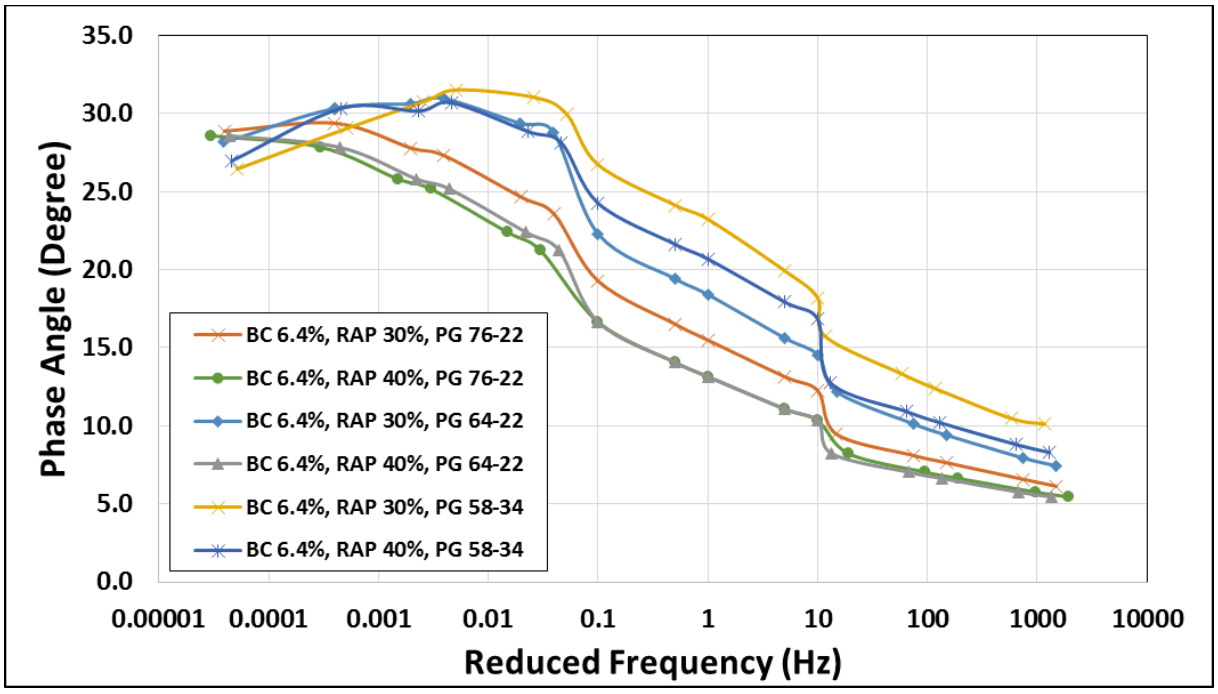

Figure 3.35. Master curves of phase angles for the mixtures with different RAP contents (30% and 40%), different binder grades of (PG 58-34, PG 64-22, and PG 76-22), and 6.4% binder content

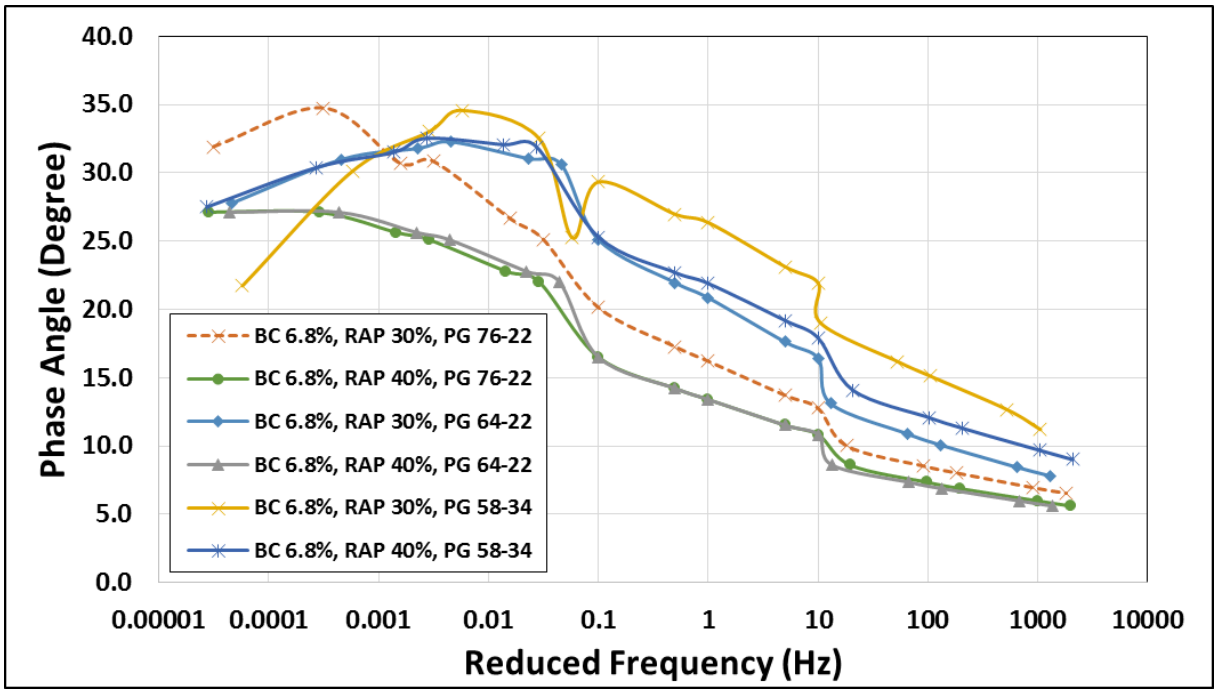

Figure 3.36. Master curves of phase angles for the mixtures with different RAP contents (30% and 40%), different binder grades of (PG 58-34, PG 64-22, and PG 76-22), and 6.8% binder content

3.5.2.4 Summary of Test Results

Results of SCB, DM and FN tests were presented in Sections 3.5.2.1 to 3.5.2.3 to evaluate the cracking and rutting performance of high RAP asphalt mixtures of this study. This section summarizes the general results of all conducted tests.

Although some of the asphalt mixtures show high cracking resistance (high FI), their rutting performance can be low due to high binder content and softer binders. Figure 3.37 shows the average FI (average of four replicate SCB tests) of the asphalt mixtures with all combinations of RAP contents, binder contents and binder grades. Average FN of the asphalt mixtures (average of two replicate FN tests) is also illustrated on top of each bar. The asphalt mixture with BC 6.8%, RAP 40% and PG 64-22 showed high rutting and cracking performance. It has a FN of 1230, which is higher than the recommended FN (FN=740) for a high traffic level (≥30 million ESALs). Also, its FI is within the acceptable range of cracking performance (FI=9-14) based on ODOT SPR785 project (Coleri 2017). Although some mixtures including 1) BC 6.8%, RAP 30%, PG 58-34, 2) BC 6.8%, RAP 30%, PG 64-22, 3) BC 6.8%, RAP 40%, PG 58-34, and 4) BC 6.4%, RAP 30%, PG 58-34 met the threshold for cracking performance, they did not meet the FN criteria required for high traffic levels (≥30 million ESALs). However, they still can be used for the traffic level of 10 to <30 million ESALs since their FNs are greater than 190. Since the mixtures with BC 6.8%, RAP 40% and PG 76-22 showed high rutting performance but low cracking performance, asphalt mixtures with 40% RAP, higher binder content (higher than 6.8%) and PG 76-22 binder may have acceptable cracking and rutting performance. Moreover, mixtures with higher RAP content (higher than 40%), 6.8% binder content and PG 58-34 may show high resistance to rutting and cracking. In the following section (Section 3.5.2.5), regression equations were developed and Monte Carlo simulations were performed using the developed equations to determine the required binder content, binder grade and RAP content of asphalt mixtures to meet rutting (FN>740) and cracking resistance (FI>10) requirements.

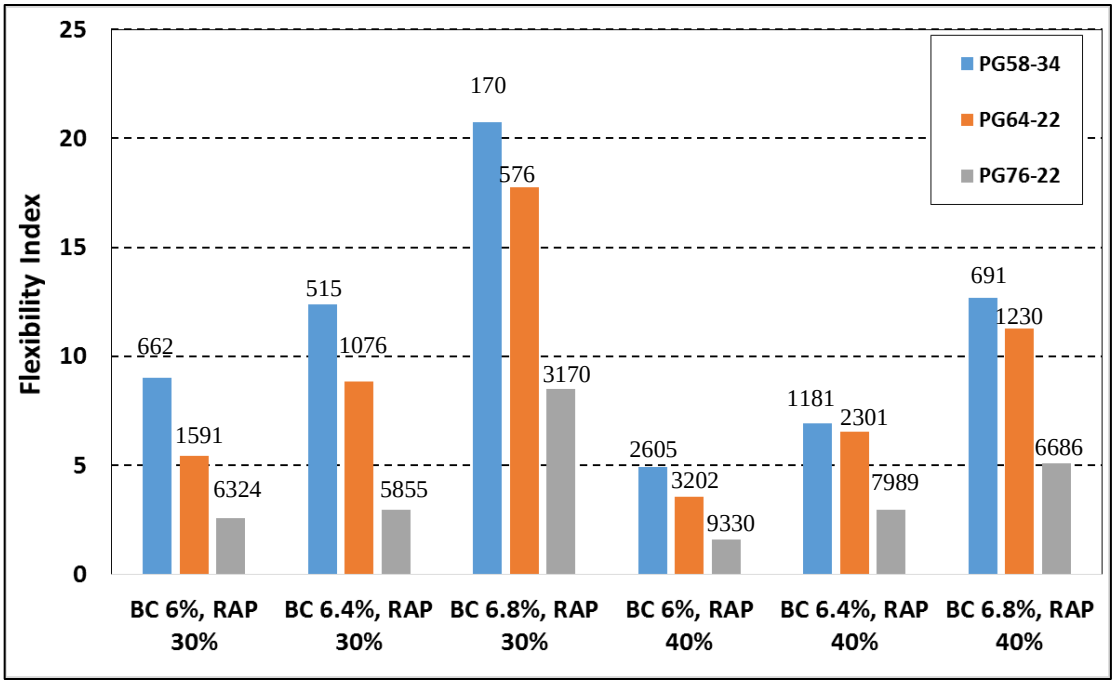

Figure 3.37. Flexibility index and flow number (numbers on each bar) of the mixtures with different RAP contents (30% and 40%), binder grades (PG 58-34, PG 64-22, and PG 76-22), and binder contents (6.0%, 6.4%, and 6.8%)

To evaluate possible correlations of dynamic modulus of mixtures at different temperatures and frequencies with FI and FN, Figure 3.38 to Figure 3.49 were created. It can be seen that dynamic modulus at 40 ^{o}C and 0.1 Hz has the highest correlation with FN. Therefore, dynamic modulus results at 40 ^{o}C and 0.1 Hz can be used to predict FN (rutting resistance of the asphalt mixtures). In general, there is not a strong correlation between dynamic modulus and FI, especially for PG 76-22. However, dynamic modulus has a strong correlation with FI at 20 ^{o}C and 4 ^{o}C for mixtures with PG 58-34 and can be used to predict FI. As the binder becomes stiffer, the correlations between FI and dynamic modulus become weaker.

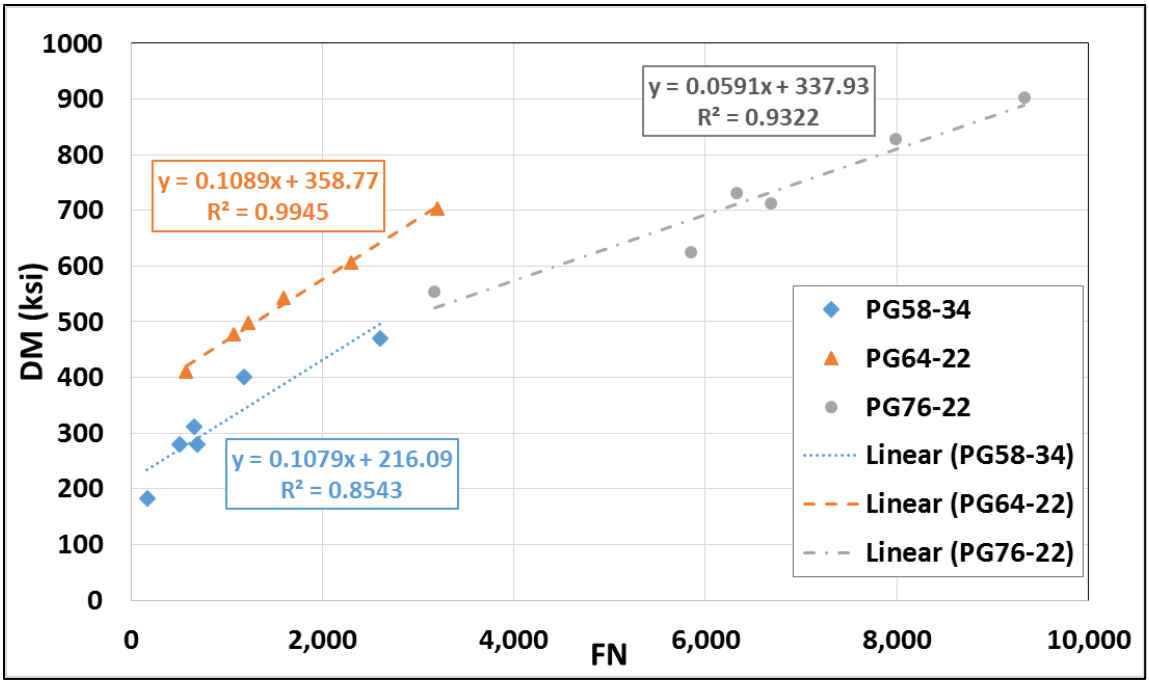

Figure 3.38. Dynamic modulus of mixtures at 40 °C and 10 Hz versus flow number for all the combinations of RAP content, binder content, and binder grades

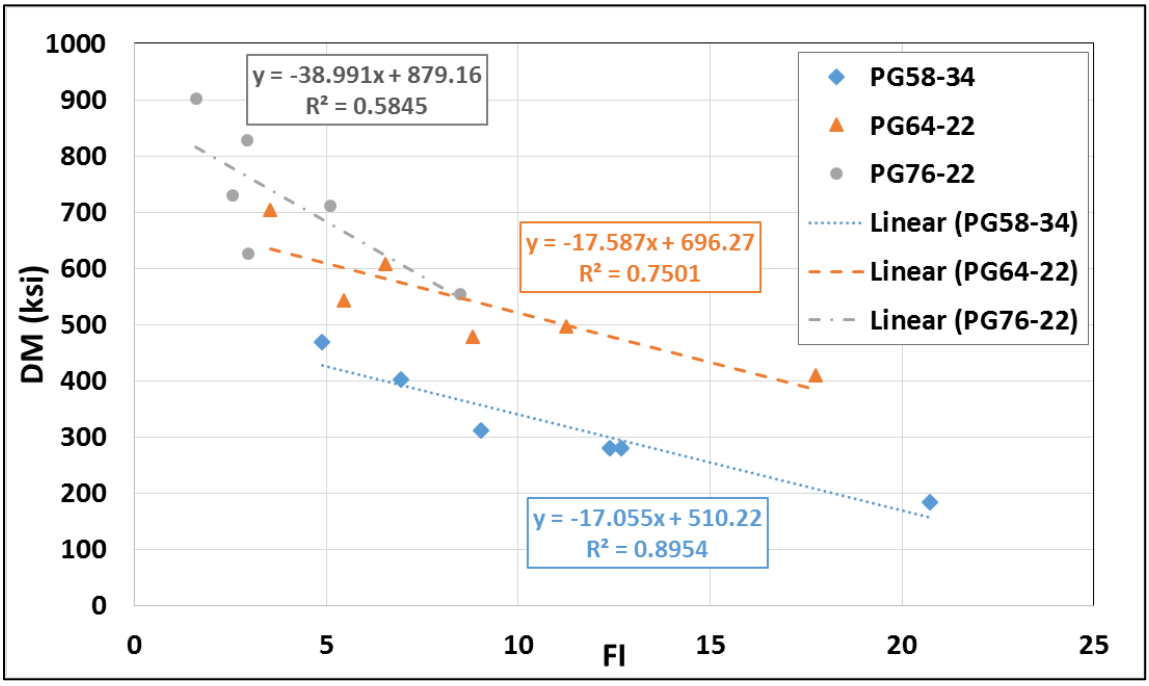

Figure 3.39. Dynamic modulus of mixtures at 40 °C and 10 Hz versus flexibility index for all the combinations of RAP content, binder content, and binder grades

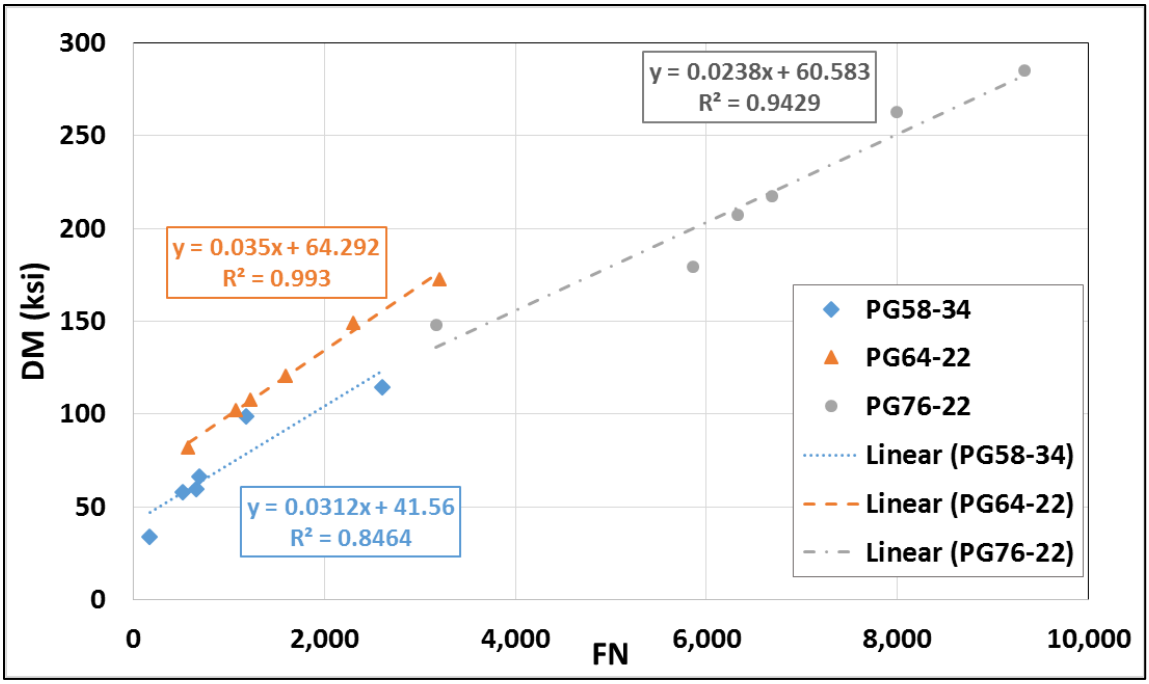

Figure 3.40. Dynamic modulus of mixtures at 40 °C and 0.1 Hz versus flow number for all the combinations of RAP content, binder content, and binder grades

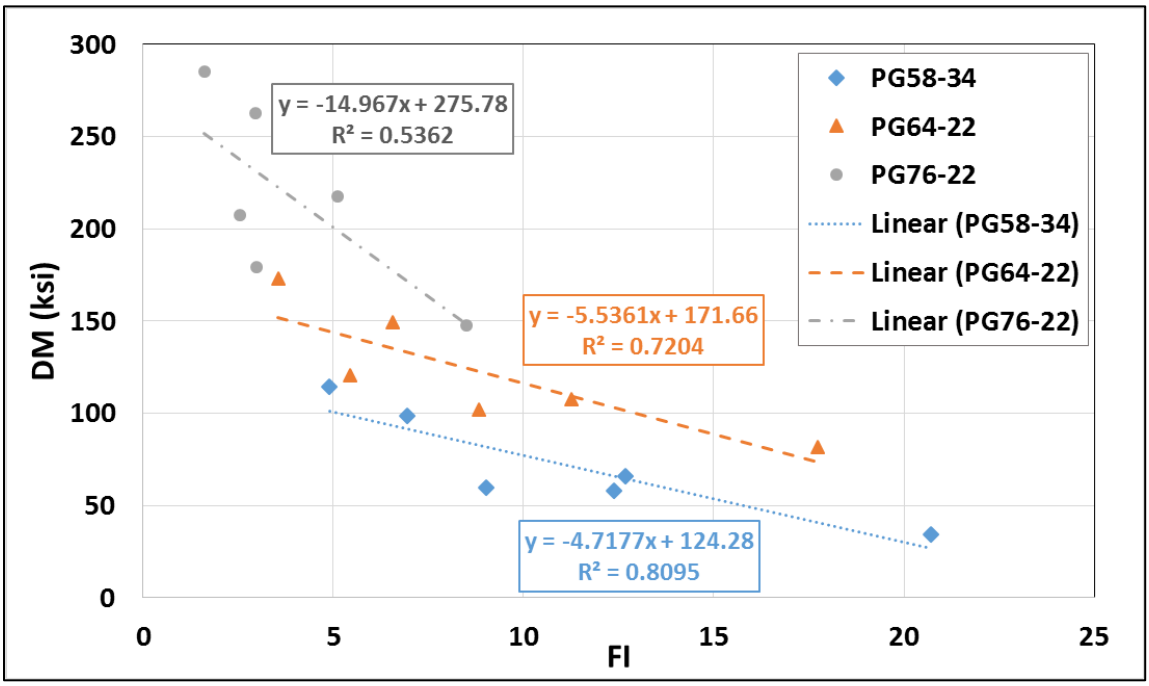

Figure 3.41. Dynamic modulus of mixtures at 40 °C and 0.1 Hz versus flexibility index for all the combinations of RAP content, binder content, and binder grades

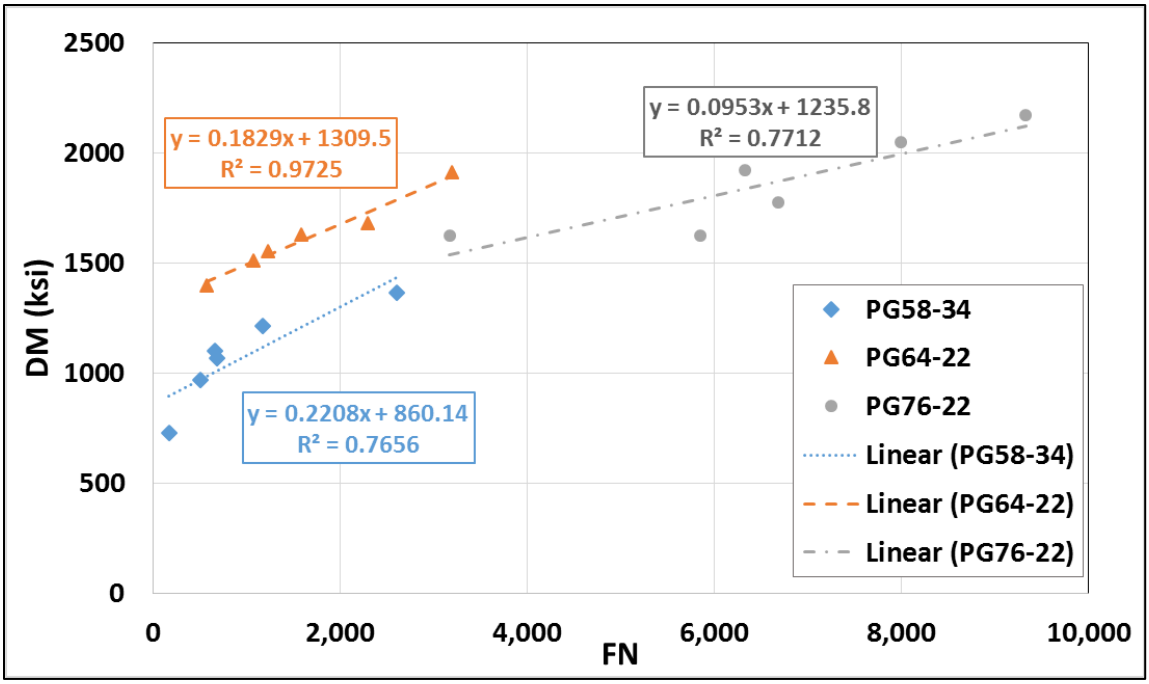

Figure 3.42. Dynamic modulus of mixtures at 20 °C and 10 Hz versus flow number for all the combinations of RAP content, binder content, and binder grades

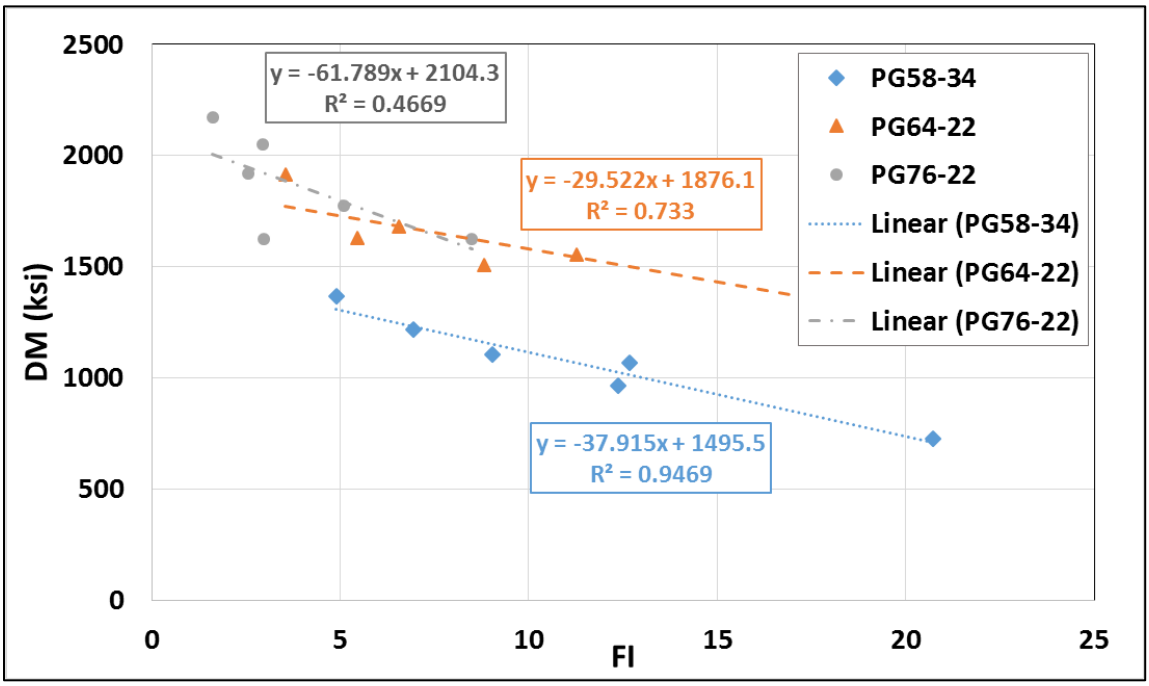

Figure 3.43. Dynamic modulus of mixtures at 20 °C and 10 Hz versus flexibility index for all the combinations of RAP content, binder content, and binder grades

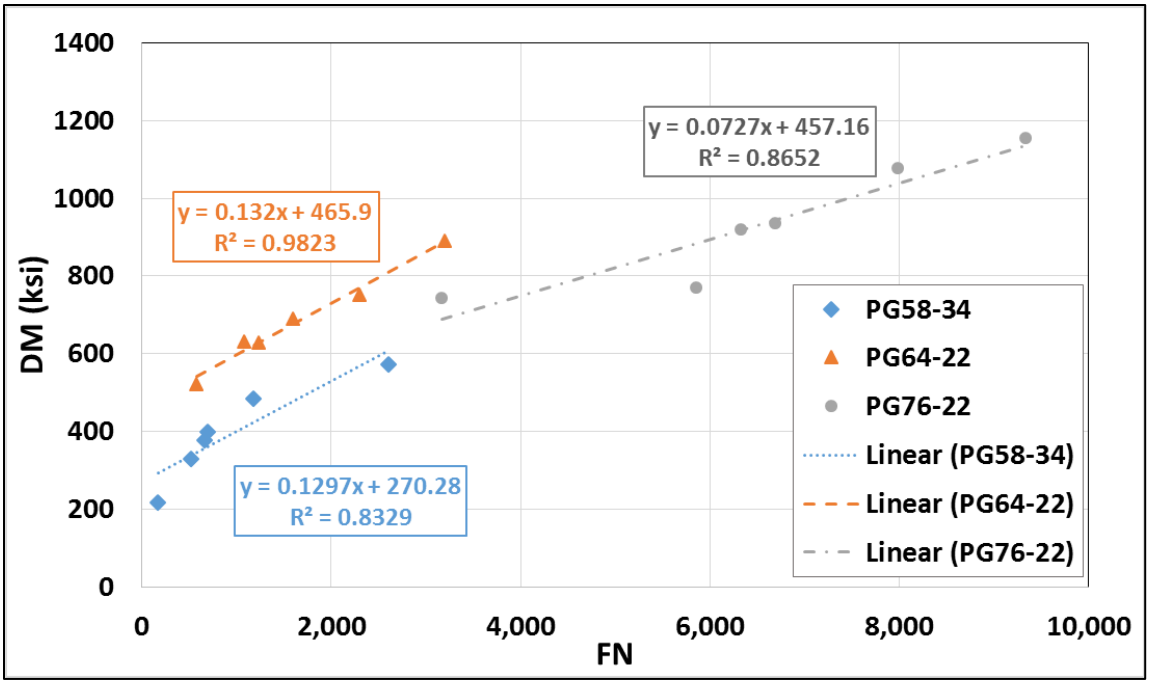

Figure 3.44. Dynamic modulus of mixtures at 20 °C and 0.1 Hz versus flow number for all the combinations of RAP content, binder content, and binder grades

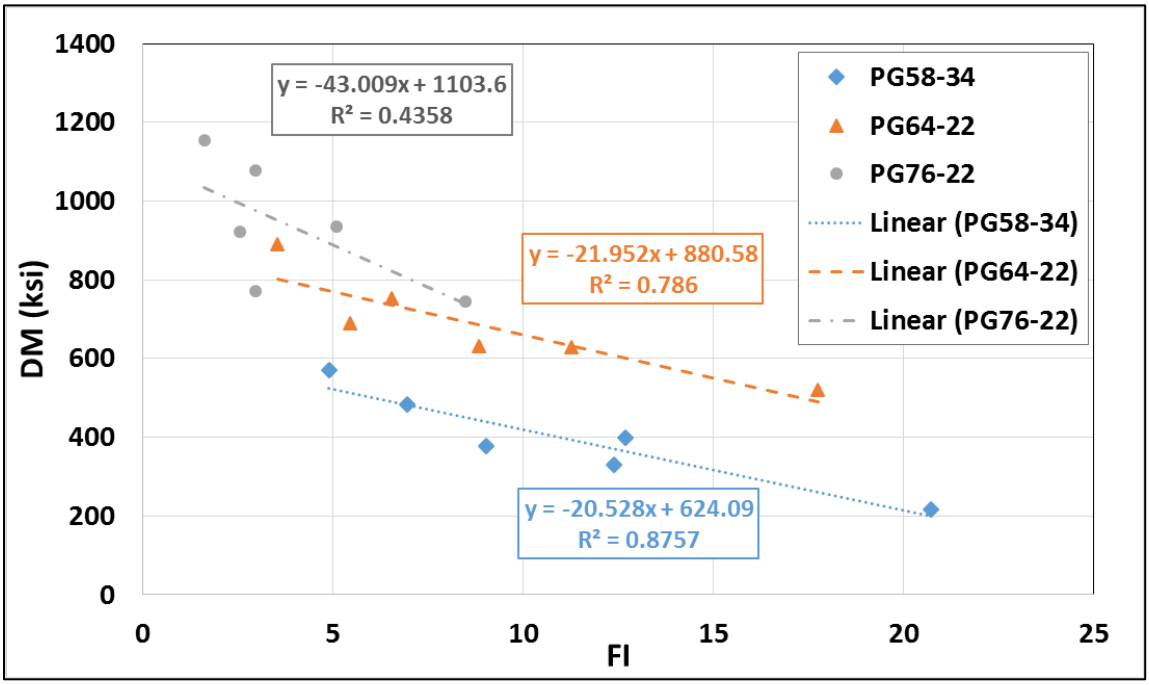

Figure 3.45. Dynamic modulus of mixtures at 20 °C and 0.1 Hz versus flexibility index for all the combinations of RAP content, binder content, and binder grades

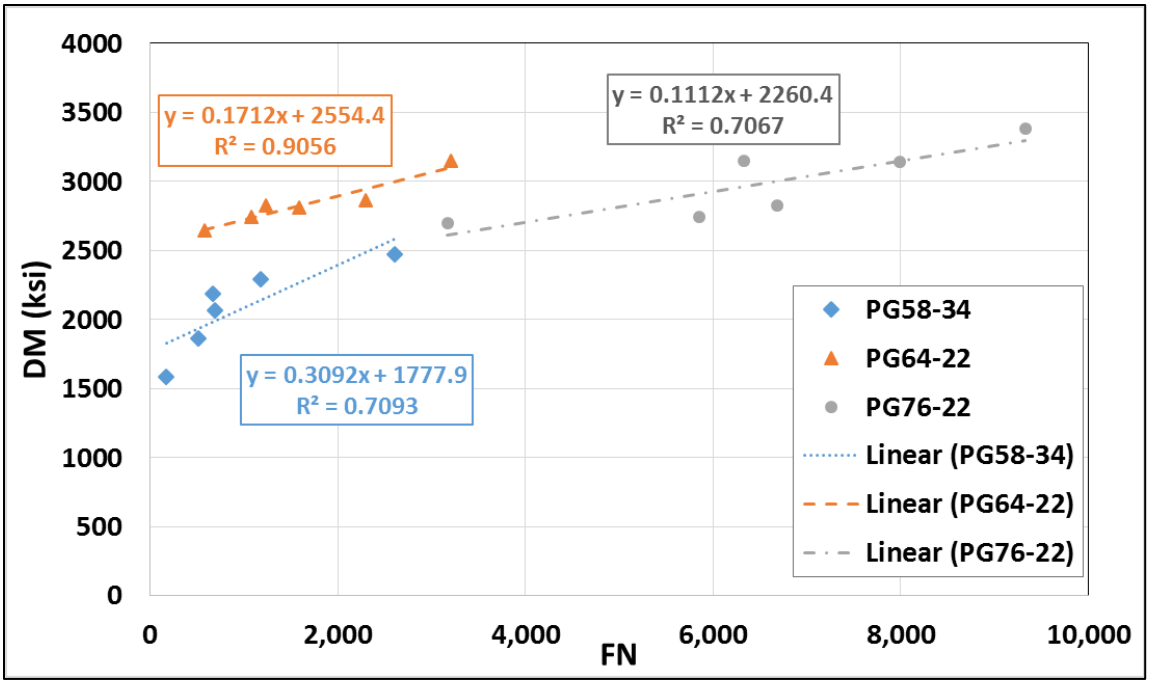

Figure 3.46. Dynamic modulus of mixtures at 4 °C and 10 Hz versus flow number for all the combinations of RAP content, binder content, and binder grades

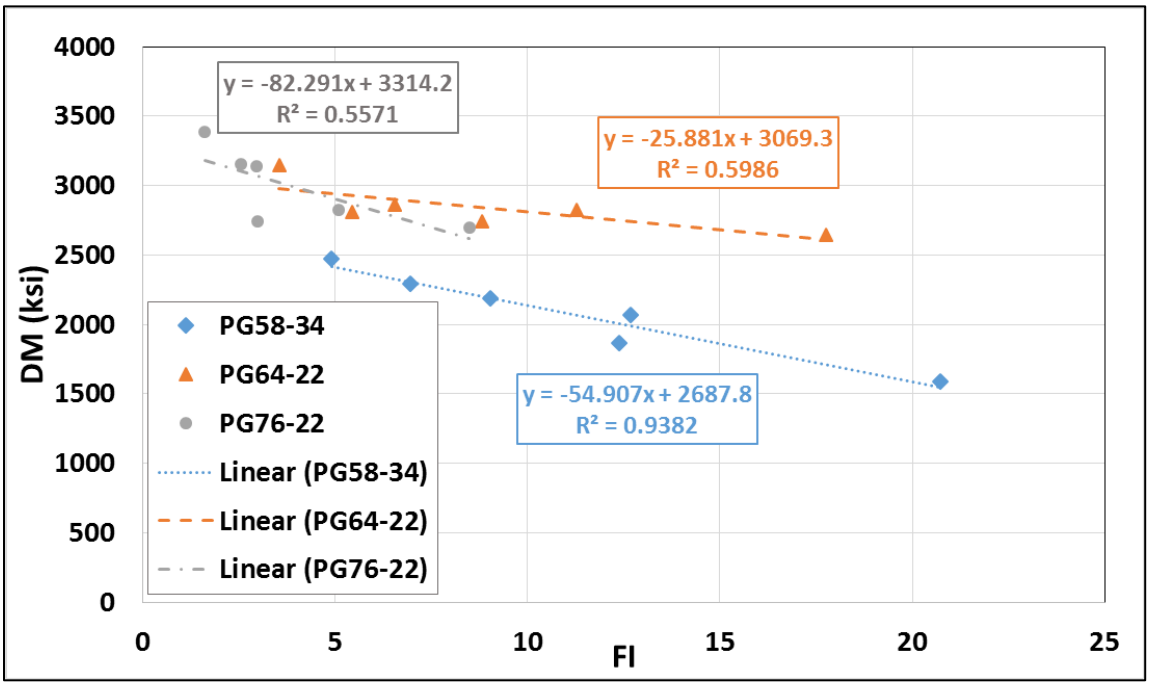

Figure 3.47. Dynamic modulus of mixtures at 4 °C and 10 Hz versus flexibility index for all the combinations of RAP content, binder content, and binder grades

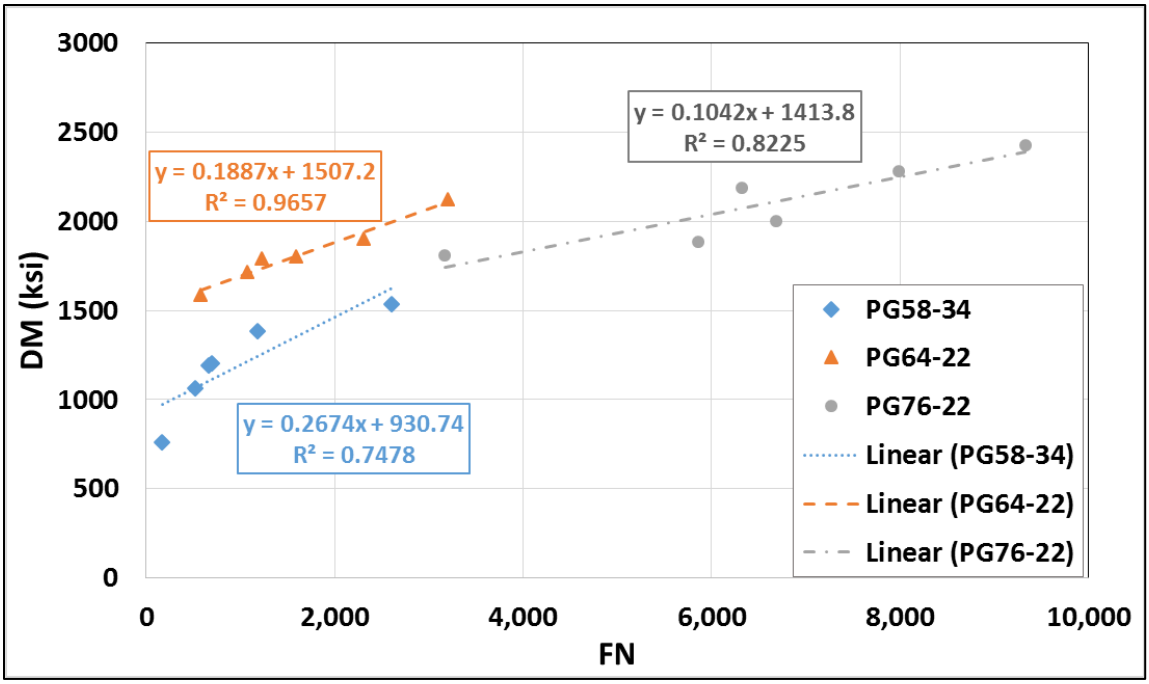

Figure 3.48. Dynamic modulus of mixtures at 4 °C and 0.1 Hz versus flow number for all the combinations of RAP content, binder content, and binder grades

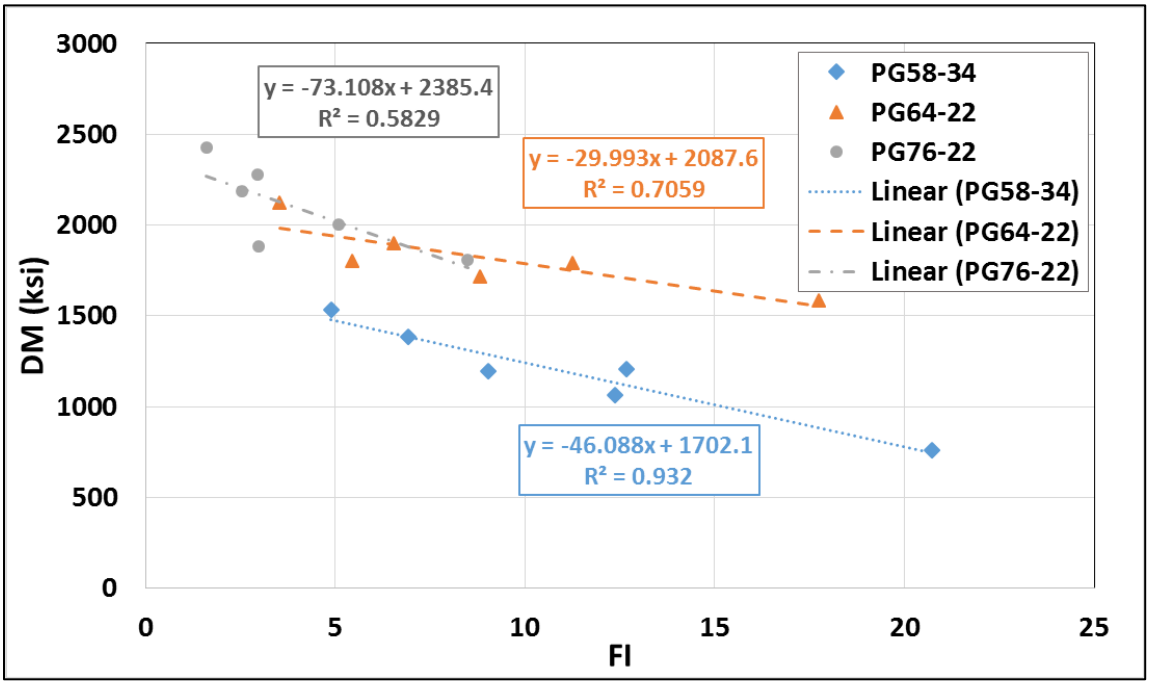

Figure 3.49. Dynamic modulus of mixtures at 4 °C and 0.1 Hz versus flexibility index for all the combinations of RAP content, binder content, and binder grades

Figure 3.50 shows the correlation between FI and FN results for all test results. Although there is a non-linear correlation between FN and FI, the correlation is not strong enough to be able to predict FI results using the FN results and vice versa. For this reason, both experiments need to be conducted separately to evaluate rutting and cracking resistance of asphalt mixtures.

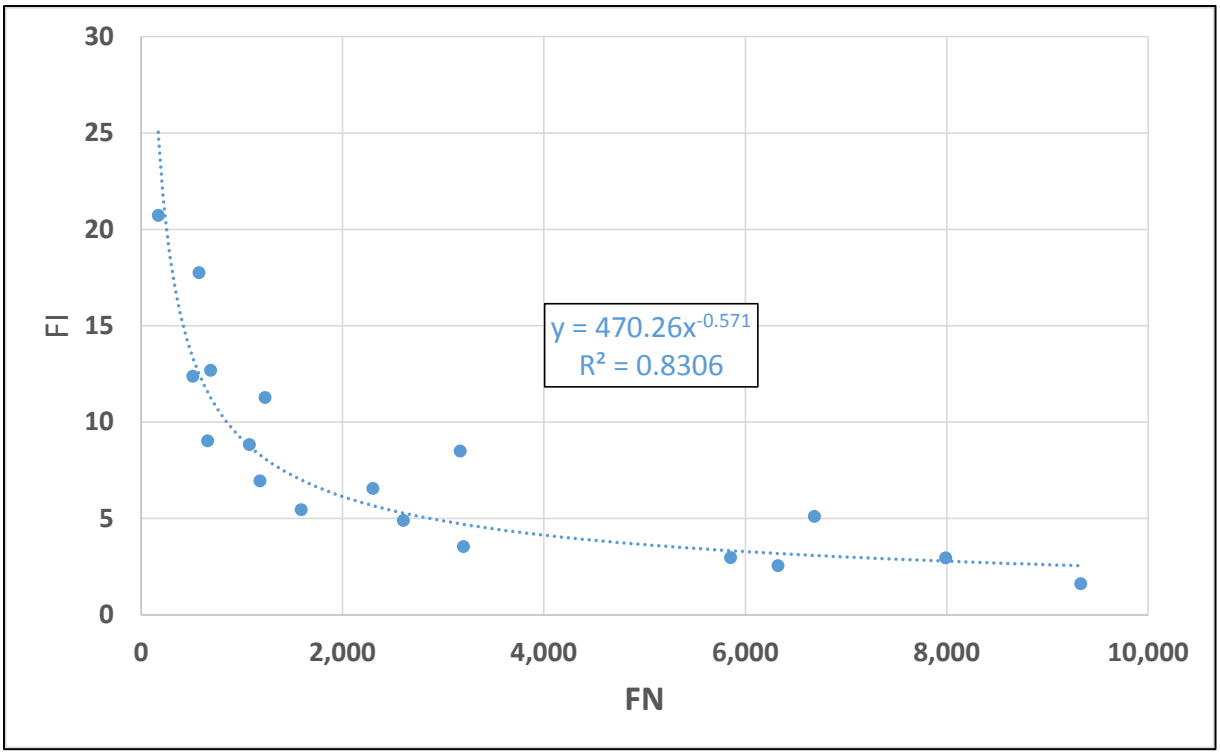

Figure 3.50. Correlation between FI and FN

3.5.2.5 Regression Modeling and Monte Carlo Simulations to Determine Asphalt Mixtures with High Rutting and Cracking Performance

Regression analysis is a statistical procedure describing the relationship between a dependent variable (response variable) and independent variables (predictors). In this section, regression analysis was performed to create linear models correlating FN and FI with RAP content, binder content and binder grade. Results of the SCB and FN tests (Sections 3.5.2.1 and 3.5.2.2) were used for FN and FI values, as dependent variables, in the regression model. Firstly, analysis of variance (ANOVA) was performed to determine which independent variables (RAP content, binder content and binder grade) were important. Then, regression models were developed. Finally, to find possible asphalt mixtures with acceptable cracking and rutting performance, FI and FN of asphalt mixtures with different RAP contents (25% to 45%), binder contents (5% to 8%), and binder grades (PG 58-34, PG 64-22 and PG 76-22) were predicted using the developed regression models (Monte Carlo simulations). All dependent and independent variables used for model development are shown in Table 3.6.

Table 3.6. Independent and Dependent Variables Used for Regression Models

Variable Type	Symbol	Description	Range
Dependent	FI	Flexibility Index	1.19 to 32.57
	FN	Flow Number	135 to 10000
Independent	RAP	RAP Content	30 and 40
	BC	Binder Content	6, 6.4, and 6.8
Category Independent	PG	Binder Grade	PG 58-34, PG 64-22, and PG 76-22

3.5.2.5.1 ANOVA Table

Analysis of Variance (ANOVA) was performed to estimate the effects of RAP content, binder content and binder grade on the dependent variables FI and FN. The F value in ANOVA analyses shows the statistical significance of each independent variable (Seber 1977). FN and FI were transformed logarithmically and linearly correlated with the dependent variables. As shown in Table 3.7, although all independent variables are important, binder content has the most significant effect on FI since it has the highest F value. Binder type and RAP content are the second and third most significant variables, respectively. Table 3.8 shows that all the independent variables have a significant effect on FN, with binder type being the first, RAP content being the second and binder content being the third of the significant variables. The effects of RAP content, binder content and binder grade on FI and FN were all significant based on ANOVA analysis. Therefore, all the independent variables were used for regression model development.

Table 3.7. ANOVA Table for the Regression Model Correlating FI Test Results with RAP Content, Binder Grade, and Binder Content

	Degrees of Freedom	Sum of Squares	Mean Square	F Value	Pr(F) Value
RAP	1	2.45	2.45	31.58	0.0000
BC	1	13.32	13.32	171.71	0.0000
Binder type	2	14.90	7.45	96.01	0.0000
Residuals	66	5.12	0.08		

Table 3.8. ANOVA Table for the Regression Model Correlating FN Test Results with RAP Content, Binder Grade, and Binder Content

	Degrees of Freedom	Sum of Squares	Mean Square	F value	Pr(F) Value
RAP	1	5.84	5.84	72.72	0.0000
BC	1	5.28	5.28	65.73	0.0000
Binder type	2	29.78	14.89	185.31	0.0000
Residuals	31	2.49	0.08		

3.5.2.5.2 Linear Regression Model for FI

FI values obtained from SBC tests were logarithmically transformed in order to allow the model to be estimated by linear regression. Figure 3.51 shows ln(FI) for each combination of RAP content, binder content, and binder grade. The model correlating ln(FI) with the independent variables was estimated as follows:

$$\ln(FI) = -4.831715 - 0.037713*RAP + 1.317014*BC - 0.239761*(PG64\text{-}22) \quad \textbf{(3.18)}$$

(0.0000) (0.0000) (0.0000) (0.0044)

$$-1.063465*(PG76\text{-}22)$$

(0.0000) $(R^2 = 0.85)$

In Equation (3.18), the P-values (standard error of regression coefficient) of the estimated regression coefficients are presented in parenthesis below each coefficient. The coefficient of determination (R^2) for the developed model is 0.85, indicating that 85 percent of the variance in the response is explained by the explanatory variables.

The residual plots for the regression model are shown in Figure 3.52. Figure 3.52a shows that the assumption of the constant variance in linear regression is met since the residuals are randomly scattered around the zero line. Figure 3.52b represents the observed data versus fitted values. Figure 3.52c shows that residuals follow a normal distribution. Finally, Figure 3.52d is developed to find the possible outliers (points with standardized residual values greater than 2 or less than -2). Most of the points fall between -2 and 2, so there are no outliers in the data.

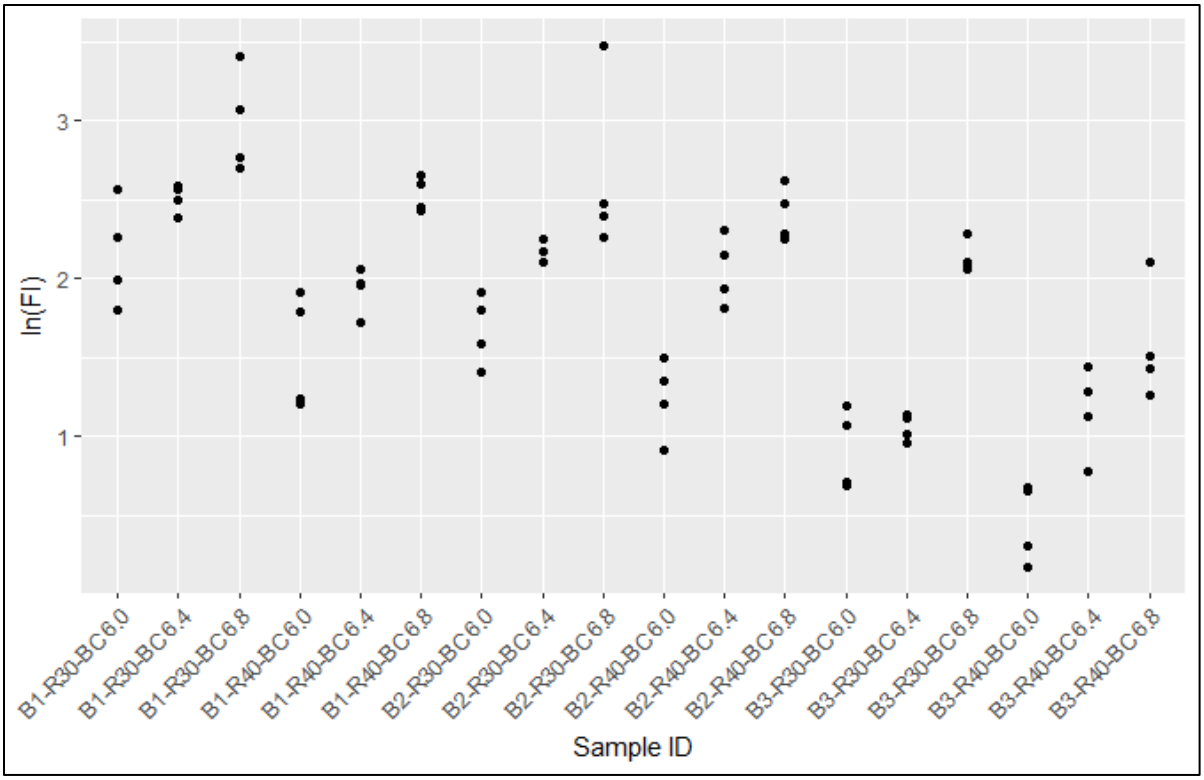

Figure 3.51. ln(FI) for each combination of RAP content, binder content, and binder grade

Note: B1= PG 58-34, B2= PG 64-22, and B3 = PG 76-22.
R30 = 30% RAP, and R40 = 40% RAP.
BC6= 6% binder content, BC6.4 =6.4 % binder content, and BC6.8 = 6.8% binder content.

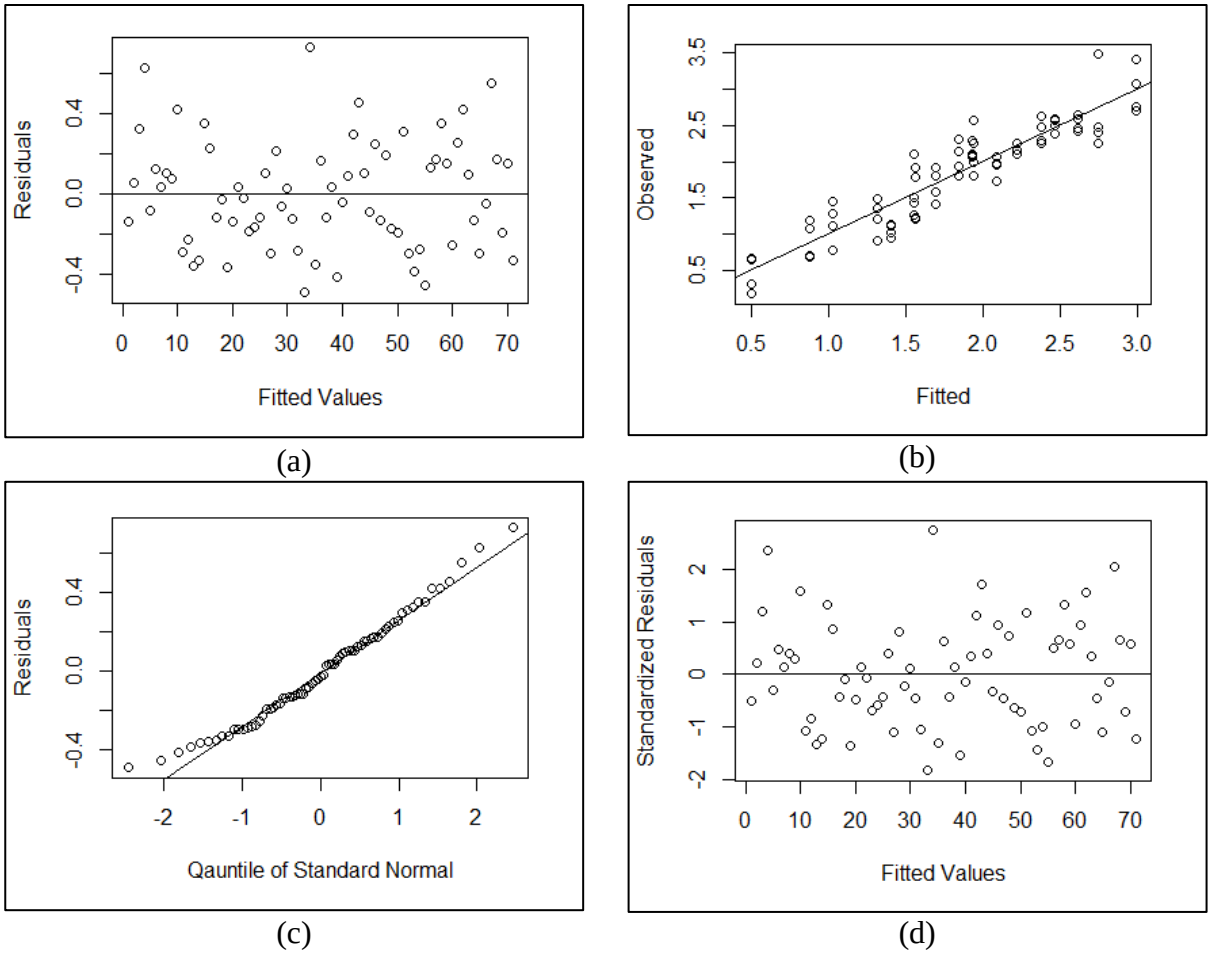

Figure 3.52. Residual plots for the regression model correlating ln(FI) with RAP content, binder content, and binder grade

3.5.2.5.3 Linear Regression Model for FN

The FN values obtained from FN tests were logarithmically transformed in order to allow the model to be estimated by linear regression. ln(FN) for all the tested mixtures in Section 3.5.2.2 are presented in Figure 3.53. The following Equation (3.19) shows the estimated model correlating ln(FN) with RAP content, binder content and binder grade. The P-values of each estimated coefficient is shown in parenthesis below them. The adjusted R^2 is 0.94, meaning that 94 percent of the variance in the response is explained by the explanatory variables.

$$\ln(FN) = \underset{}{11.230864} + \underset{(0.0000)}{0.080577}*RAP - \underset{(0.0000)}{1.172814}*BC + \underset{(0.0000)}{0.723180}*(PG64-22) \quad \textbf{(3.19)}$$

$$+\underset{(0.0000)}{2.186587}*(PG76-22) \qquad (R^2 = 0.94)$$

Residual plots of the developed regression model are presented in Figure 3.54. The residuals are scattered randomly around zero in Figure 3.54a, meaning that the assumption of the constant variance in the regression model is met. Figure 3.54b shows observed values versus predicted values. Figure 3.54c shows that the assumption of normality in linear regression is met as well. Finally, the outliers can be identified in Figure 3.54d, with the absolute value of standardized residuals greater than 2. One of the points seems to be an outlier since its standardized residual is around -3. To further investigate the effect of outliers, Figure 3.54e (Cook's distance plot) was developed. It can be seen that none of the observations had a Cook's distance greater than 0.5. Therefore, the outlier is not expected to create any bias in the developed linear regression model.

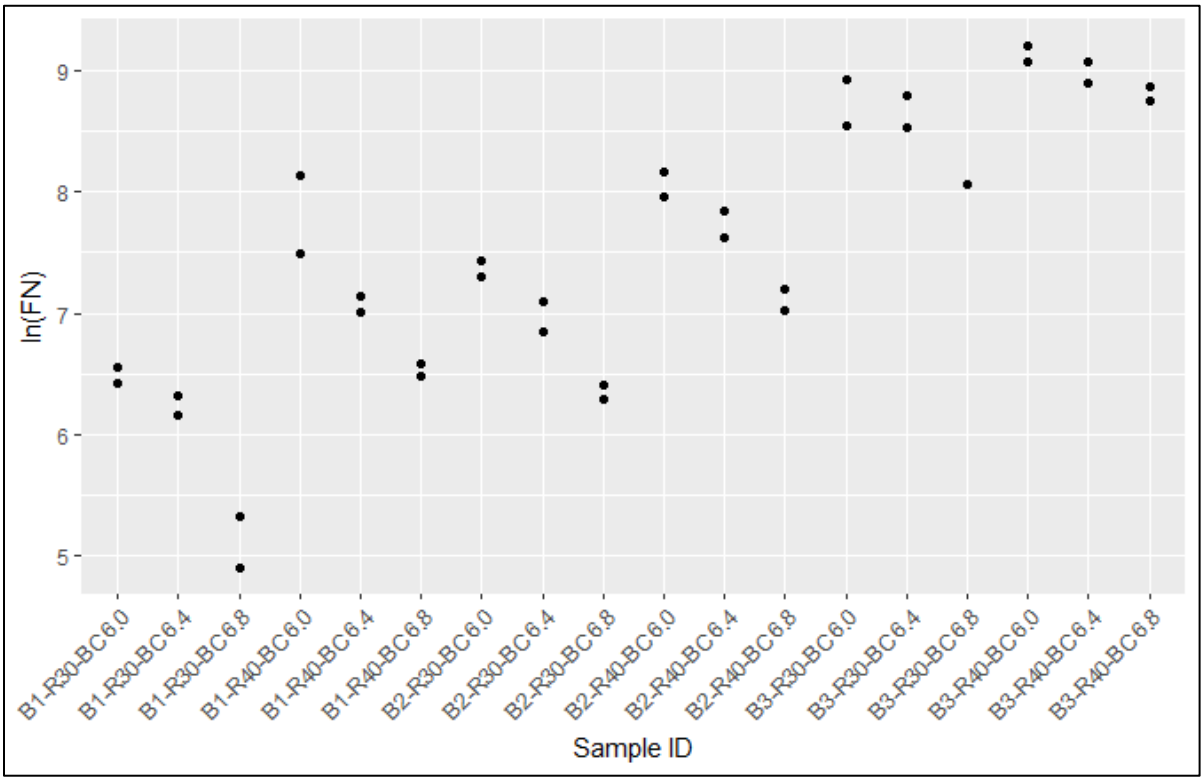

Figure 3.53. ln(FN) for each combination of RAP content, binder content, and binder grade

Note: B1= PG 58-34, B2= PG 64-22, and B3 = PG 76-22.
R30 = 30% RAP, and R40 = 40% RAP.
BC6= 6% binder content, BC6.4 =6.4 % binder content, and BC6.8 = 6.8% binder content.

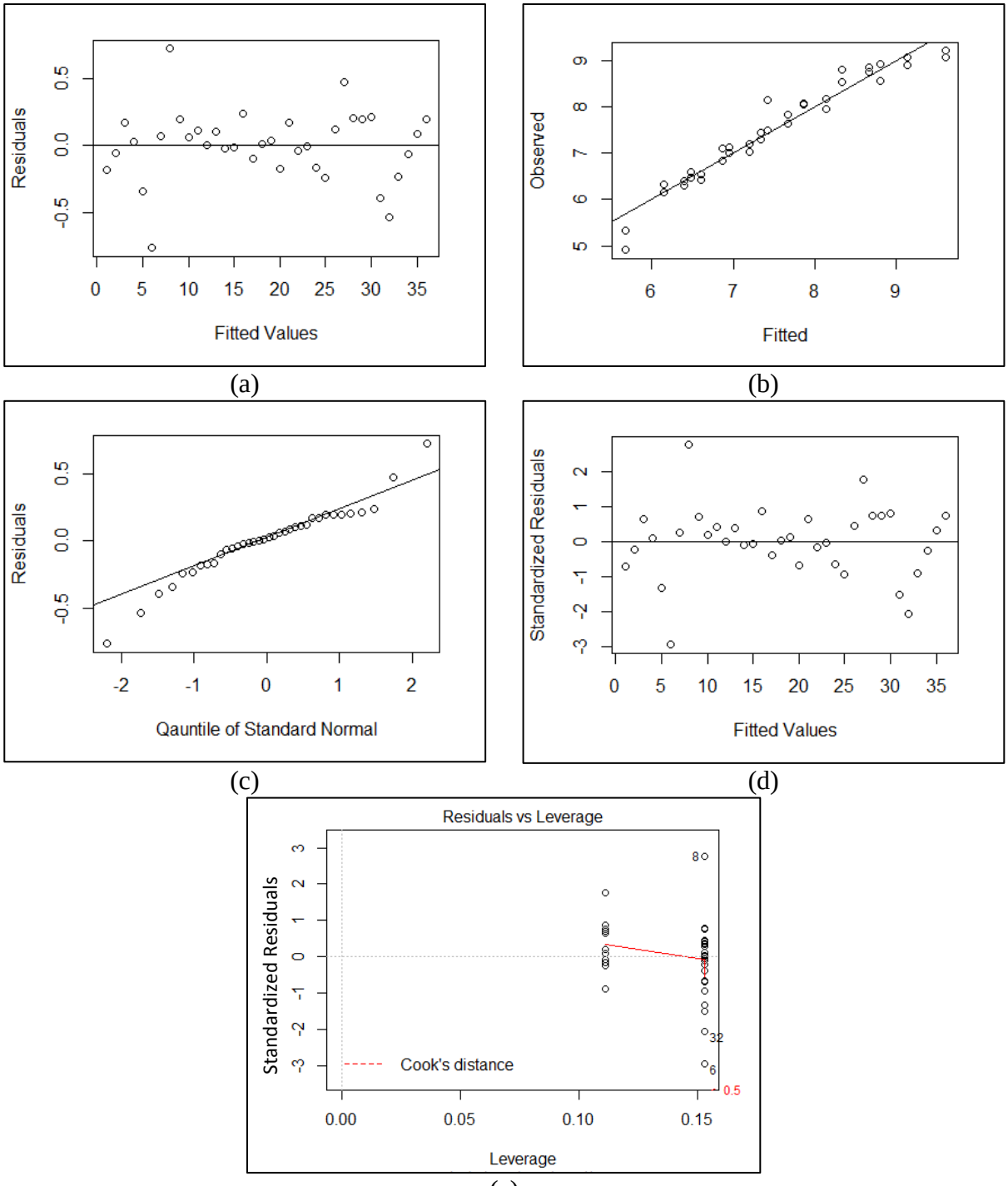

Figure 3.54. Residual plots for the regression model correlating ln(FN) with RAP content, binder content, and binder grade

3.5.2.5.4 Determination of Asphalt Mixtures with High Cracking and Rutting Performance – Suggested Strategies

To determine asphalt mixtures with high cracking and rutting performance, FI and FN of asphalt mixtures with different RAP contents (25% to 45%), binder contents (5% to 8%) and binder grades (PG 58-34, PG 64-22 and PG 76-22) were predicted using the regression models developed in Sections 3.5.2.5.2 and 3.5.2.5.3. All independent variables and their numerical ranges used for FI and FN predictions are presented in Table 3.9.

Predicted FI and FN for different RAP contents, binder contents and binder grades, along with the region of acceptance for cracking and rutting performance, are presented in Figure 3.55. Then, mixtures falling within the region of acceptance [FI greater than 10 and FN greater than 740 (AASHTO TP 79-13)] were found and presented in Table 3.10 as suggested mixtures. It is worthwhile to note that asphalt mixtures with RAP 40%, BC 6.6% and PG 58-34 showed acceptable predicted cracking (FI=10.51) and rutting performance (FN=823). Also, asphalt mixtures with RAP 45%, BC 6.8% and PG 58-34 fell within the region of acceptance although the same mixture with 40% RAP fails in rutting. Asphalt mixtures with 45% RAP and PG 64-22 required higher binder contents (6.9% to 7.6%) than mixtures with PG 58-34 to be resistant to cracking and rutting. For mixtures with RAP 40%, 35% and 30% and PG 64-22, binder content should be between 6.8%-7.3%, 6.7%-6.9% and 6.5%-6.6%, respectively. For the lowest RAP content (25%), only mixtures with PG 76-22 and BC 7%-7.5% had acceptable predicted FI and FN values. For mixtures with RAP 45%, 40%, 35%, and 30% and PG 76-22 binder, mixtures with binder contents of 7.6%-8%, 7.4%-8%, 7.3%-8% and 7.1%-8.5%, respectively, fell within the region of acceptance. Material costs for constructing a 1-mile roadway section (12 ft lane width) with a 3 inch layer thickness are also given in Table 3.10. The procedure followed to calculate the costs is described in Section 5.4.

Table 3.9. Independent Variables and their Ranges for FI and FN Predictions

Variable Type	Symbol	Description	Range
Independent	RAP	RAP Content	25 to 45 with 5 increments
	BC	Binder Content	5 to 8 with 0.1 increments
Category Independent	PG	Binder Grade	PG 58-34, PG 64-22, and PG 76-22

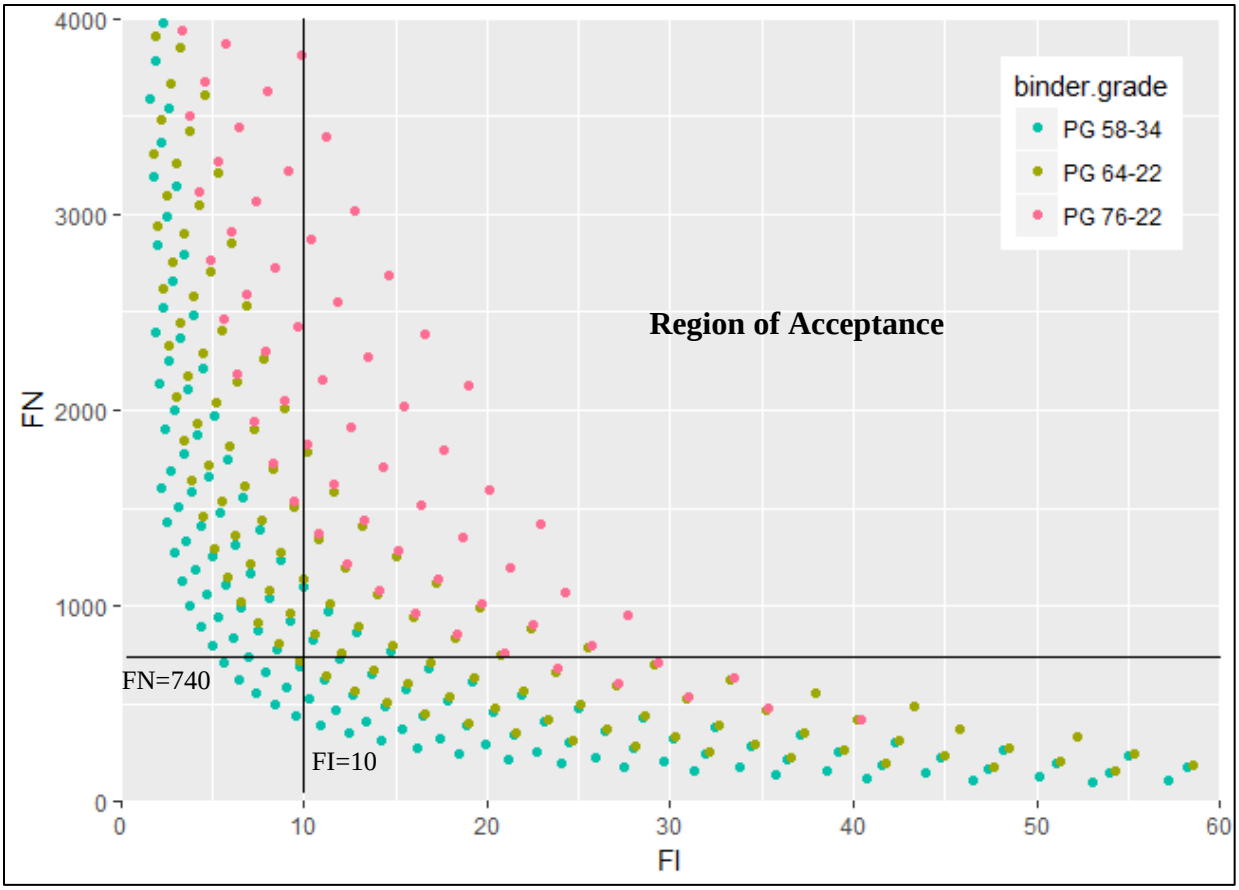

Figure 3.55. Predicted FI and FN for different RAP contents, binder contents, and binder grades

Table 3.10. Suggested Strategies - Mixes with FN Greater than 740 and FI Greater than 10

#Sample	RAP Content (%)	Binder Content (%)	ABR[1] (%)	Active BC[2] (%)	Binder Grade	FN	FI	Cost ($)
1	45	6.8	41.2	5.6	PG 58-34	974	11.3	38,337
2	45	6.9	40.6	5.7	PG 58-34	866	12.9	38,827
3	45	7.0	40.0	5.8	PG 58-34	771	14.7	39,316
4	45	6.9	40.6	5.7	PG 64-22	1786	10.2	36,391
5	45	7.0	40.0	5.8	PG 64-22	1588	11.6	36,821
6	45	7.1	39.4	5.9	PG 64-22	1412	13.2	37,251
7	45	7.2	38.9	6.0	PG 64-22	1256	15.1	37,681
8	45	7.3	38.3	6.1	PG 64-22	1117	17.2	38,111
9	45	7.4	37.8	6.2	PG 64-22	993	19.6	38,541
10	45	7.5	37.3	6.3	PG 64-22	883	22.4	38,971
11	45	7.6	36.8	6.4	PG 64-22	786	25.6	39,401
12	45	7.6	36.8	6.4	PG 76-22	3395	11.2	43,679
13	45	7.7	36.4	6.5	PG 76-22	3019	12.8	44,198
14	45	7.8	35.9	6.6	PG 76-22	2685	14.6	44,717
15	45	7.9	35.4	6.7	PG 76-22	2388	16.7	45,236
16	45	8.0	35.0	6.8	PG 76-22	2124	19.0	45,755
17	40	6.6	37.7	5.5	PG 58-34	823	10.5	38,513
18	40	6.8	36.6	5.7	PG 64-22	1342	10.8	36,930
19	40	6.9	36.1	5.8	PG 64-22	1194	12.3	37,360
20	40	7.0	35.5	5.9	PG 64-22	1061	14.0	37,790
21	40	7.1	35.0	6.0	PG 64-22	944	16.0	38,220
22	40	7.2	34.6	6.1	PG 64-22	840	18.2	38,650
23	40	7.3	34.1	6.2	PG 64-22	747	20.8	39,080
24	40	7.4	33.6	6.3	PG 76-22	2869	10.4	43,887
25	40	7.5	33.2	6.4	PG 76-22	2551	11.9	44,406
26	40	7.6	32.7	6.5	PG 76-22	2269	13.5	44,925
27	40	7.7	32.3	6.6	PG 76-22	2018	15.5	45,445
28	40	7.8	31.9	6.7	PG 76-22	1795	17.6	45,964
29	40	7.9	31.5	6.8	PG 76-22	1596	20.1	46,483
30	40	8.0	31.1	6.9	PG 76-22	1419	22.9	47,002
31	35	6.7	32.5	5.8	PG 64-22	1009	11.4	37,470
32	35	6.8	32.0	5.9	PG 64-22	897	13.0	37,900
33	35	6.9	31.6	6.0	PG 64-22	798	14.8	38,330
34	35	7.3	29.8	6.4	PG 76-22	2156	11.0	44,615
35	35	7.4	29.4	6.5	PG 76-22	1918	12.6	45,134

Table 3.10. Suggested Strategies - Mixtures with FN Greater than 740 and FI Greater than 10 (Continued)

#Sample	RAP Content (%)	Binder Content (%)	ABR[1] (%)	Active BC[2] (%)	Binder Grade	FN	FI	Cost ($)
36	35	7.5	29.0	6.6	PG 76-22	1705	14.3	45,653
37	35	7.6	28.6	6.7	PG 76-22	1517	16.4	46,172
38	35	7.7	28.3	6.8	PG 76-22	1349	18.7	46,691
39	35	7.8	27.9	6.9	PG 76-22	1200	21.3	47,211
40	35	7.9	27.6	7.0	PG 76-22	1067	24.3	47,730
41	35	8.0	27.2	7.1	PG 76-22	949	27.7	48,249
42	30	6.5	28.7	5.7	PG 64-22	852	10.6	37,579
43	30	6.6	28.3	5.8	PG 64-22	758	12.1	38,009
44	30	7.1	26.3	6.3	PG 76-22	1822	10.2	44,823
45	30	7.2	25.9	6.4	PG 76-22	1620	11.7	45,342
46	30	7.3	25.6	6.5	PG 76-22	1441	13.3	45,862
47	30	7.4	25.2	6.6	PG 76-22	1282	15.2	46,381
48	30	7.5	24.9	6.7	PG 76-22	1140	17.3	46,900
49	30	7.6	24.6	6.8	PG 76-22	1014	19.7	47,419
50	30	7.7	24.2	6.9	PG 76-22	902	22.5	47,938
51	30	7.8	23.9	7.0	PG 76-22	802	25.7	48,457
52	25	7.0	22.2	6.3	PG 76-22	1369	10.8	45,551
53	25	7.1	21.9	6.4	PG 76-22	1218	12.3	46,070
54	25	7.2	21.6	6.5	PG 76-22	1083	14.1	46,589
55	25	7.3	21.3	6.6	PG 76-22	963	16.1	47,108
56	25	7.4	21.0	6.7	PG 76-22	857	18.3	47,628
57	25	7.5	20.7	6.8	PG 76-22	762	20.9	48,147

Note: [1] Asphalt binder replacement (percentage of binder replaced by RAP)
[2] Active BC: Virgin binder + RAP binder blended into the mix. Calculated using measured blending percentage. The blending measurement process is described in Chapter 4.

3.6 ASPHALT MIXTURES WITH LOWER RAP CONTENTS AND RAP/RAS – PHASE II

This section presents the results of SCB tests to evaluate cracking performance of asphalt mixtures with lower RAP contents (0% and 15%) and RAP&RAS [asphalt binder replacement matching the 30% RAP mixture from Section 3.5 (Phase I)]. FN tests were used to quantify the rutting performance of asphalt mixtures. DM test results were used to quantify the viscous and elastic behavior of all mixes. Using the SCB and FN test results for low RAP and RAP&RAS mixtures, regression equations were developed. Monte Carlo simulations were performed using the developed equations to determine the required binder content, binder grade and RAP content of asphalt mixtures to meet rutting and cracking resistance requirements.

3.6.1 Experimental Plan

This section summarizes the experimental plan followed for asphalt mixtures with lower RAP contents (0% and 15%) and RAP&RAS [asphalt binder replacement (ABR) matching the ABR of 30% RAP mixture from Section 3.5 (Phase I)]. The goal was to find the effects of changing binder content, RAP content and binder grade on cracking and rutting performance of asphalt mixtures. Therefore, samples with different binder content, binder grade and RAP content were prepared while other variables including air-void content, gradation and sample dimensions were kept the same for all the samples. Mix properties and experimental plan are given as follows:

The SCB, DM and FN tests were conducted on samples with two RAP contents (0% and 15%) and a RAP&RAS mixture with 19% RAP and 3% RAS [asphalt binder replacement (ABR) matching the ABR of 30% RAP mixture from Section 3.5 (Phase I)], two binder contents (6% and 6.8%), and two binder grades (PG64-22 and PG76-22). Since only four buckets of PG58-34 binder were available during initial sampling and all of them were used in Phase 1, this binder type could not be used for Phase 2 mixture preparation. However, it should be noted that according to the results of this study, soft PG58-34 binder can improve the cracking resistance of RAP&RAS mixtures and should be evaluated as an option to improve RAP&RAS mixture performance in a future study. Table 3.5 shows the experimental plan followed in this study.

Table 3.11. Experimental Plan

Test type	Binder content	RAP content	Binder grade	Temp.[2]	Air-void content	Repl.[3]	Total tests
SCB	6.0% 6.8%	0% 15% RAP&RAS[4]	PG 64-22 PG 76-22	25 ^{o}C	7%	4	48
Dynamic Modulus	6.0% 6.8%	0% 15% RAP&RAS	PG 64-22 PG 76-22	1 run[1]	7%	2	24
Flow Number	6.0% 6.8%	0% 15% RAP&RAS	PG 64-22 PG 76-22	54.7 ^{o}C	7%	2	24

Note: [1]Samples were tested at temperatures of 4 ^{o}C, 20 ^{o}C, and 40 ^{o}C and the loading frequencies of 0.1, 0.5, 1, 5, and 10 Hz. A loading frequency of 0.01 Hz was also used for 40 ^{o}C tests

[2]Temp. = Temperature

[3]Repl. = Replicate

[4]RAP&RAS = 19% RAP and 3% RAS [asphalt binder replacement (ABR) matching the ABR of 30% RAP mixture from Section 3.5 (Phase I)]

3.6.2 Results and Discussion

3.6.2.1 Semi-Circular Bend Test

SCB tests were conducted at 25 ^{o}C in this study to evaluate cracking performance of asphalt mixtures. A full factorial experimental plan with two RAP contents (0% and 15%) and a RAP&RAS mixture, two different binder contents (6% and 6.8%) and two binder grades (PG 64-22 and PG 76-22) is followed in this study (see Table 3.11). Four replicates were tested for each combination. In total, 48 SCB tests were conducted. Fracture energy (G_f), fracture toughness (K_{IC}), secant stiffness (S) and flexibility index (FI) are the testing parameters obtained from the test results. The results of SCB tests are presented in Figure 3.56 to Figure 3.61. Figure 3.56 shows the FI for the mixtures tested in Phase II (0% RAP, 15% RAP and RAP&RAS).

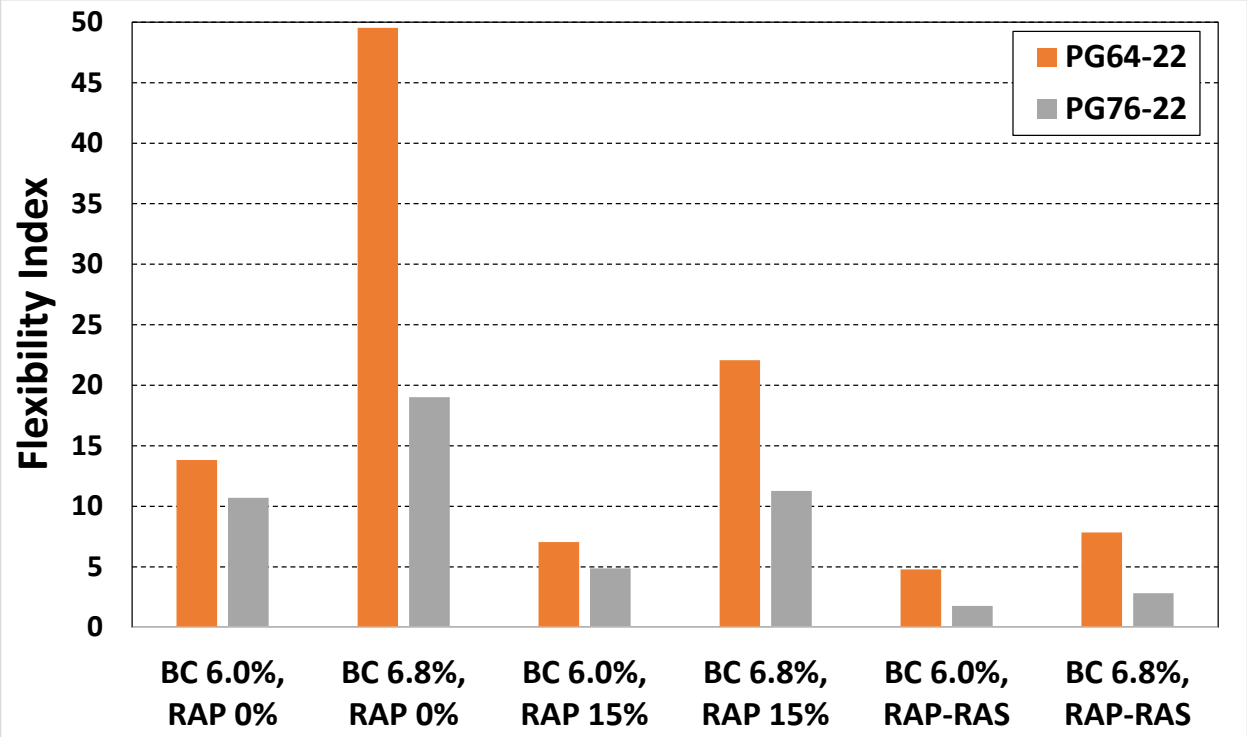

Figure 3.56. **Flexibility index for mixtures with different RAP contents (0% and 15%) and RAP&RAS, binder grades (PG 64-22 and PG 76-22) and binder contents** (6% and 6.8%)

Figure 3.57 shows the FI for all the mixtures tested in Phases I and II (0%, 15%, 30% and 40% RAP and RAP&RAS). As is shown in Figure 3.56 and Figure 3.57, FI increases as the binder content increases for mixtures with the same RAP contents. Asphalt mixtures with lower binder contents are more brittle and more susceptible to cracking. Results also show that increasing RAP content results in more brittle mixtures and reduces the cracking resistance. Moreover, using softer binder increases FI. As was expected, the

mixture with PG 76-22 binder grade, 6% binder content and 40% RAP content shows the lowest FI value. Using the FI of 10 as the threshold for acceptable cracking resistance (Coleri 2017), it can be observed from Figure 3.56 that all the asphalt mixtures with 0% and 15% RAP have average FIs larger than 10 except the ones with 15% RAP and 6% binder contents.

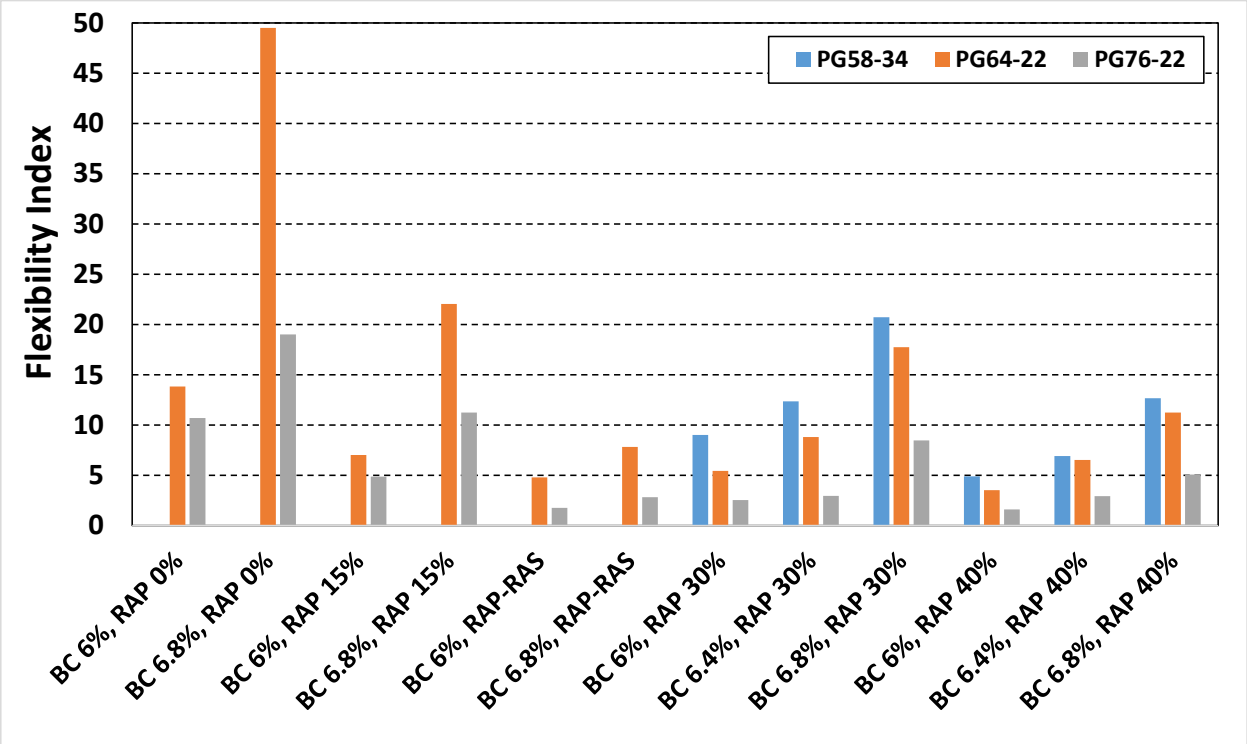

Figure 3.57. Flexibility index for all asphalt mixtures - RAP&RAS, high (30% and 40%) and low RAP (0% and 15%) (Phases I and II).

Figure 3.58 is developed by using the FIs for 30% RAP, 40%RAP and RAP&RAS [asphalt binder replacement (ABR) matching the ABR of the 30% RAP mixture]. It can be observed that since RAP&RAS mixtures are very stiff, increasing binder content from 6% to 6.8% is not creating any significant impact on the performance of RAP&RAS mixtures. On the other hand, increasing binder content is an effective strategy to improve the cracking resistance of 30% and 40% RAP mixtures. None of the mixtures with RAP&RAS fulfill the criteria for FI (all samples less than 10). However, all possible combinations of binder content and binder grade to achieve acceptable cracking and rutting performance for RAP&RAS mixtures are determined using regression equations and provided in Section 3.6.2.5.

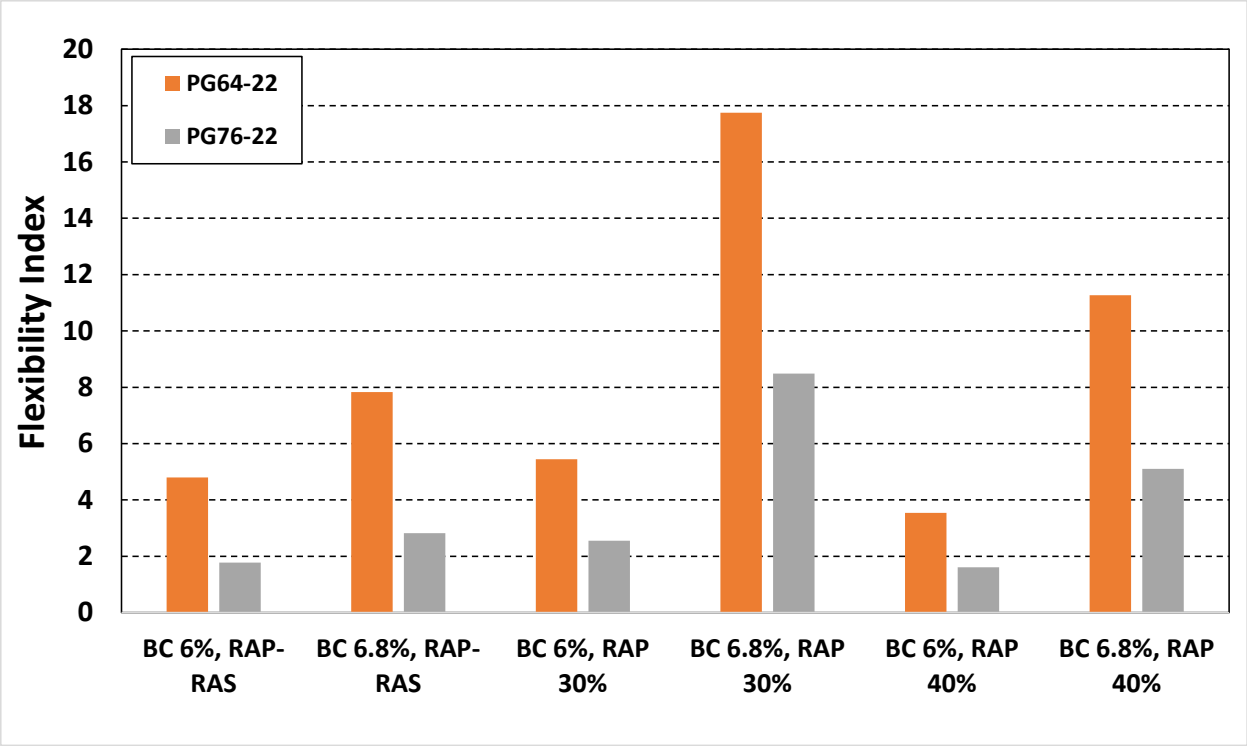

Figure 3.58. Flexibility index for asphalt mixtures with RAP&RAS and high RAP (30% and 40%).

Fracture energy for the RAP&RAS, 0% RAP and 15% RAP mixtures at binder contents of 6.0% and 6.8% are shown in Figure 3.59. As is seen in the plot, as fracture energy (G_f) increases, the work required for crack formation and propagation increases. Therefore, asphalt mixtures with higher G_f values are expected to show higher resistance to cracking (Ozer et al. 2016). Results of this study show that for mixtures with low RAP (0 and 15%) and RAP&RAS, the G_f parameter can capture the effect of binder content on cracking resistance (increasing binder content increases G_f). However, there is not a strong correlation between the effect of asphalt binder replaced and G_f. In addition, G_f cannot separate mixtures with soft and stiff binders. These results suggest that G_f, the most common parameter that has been used to characterize cracking resistance of asphalt mixtures in several research studies, is not an effective parameter to use for cracking performance evaluation.

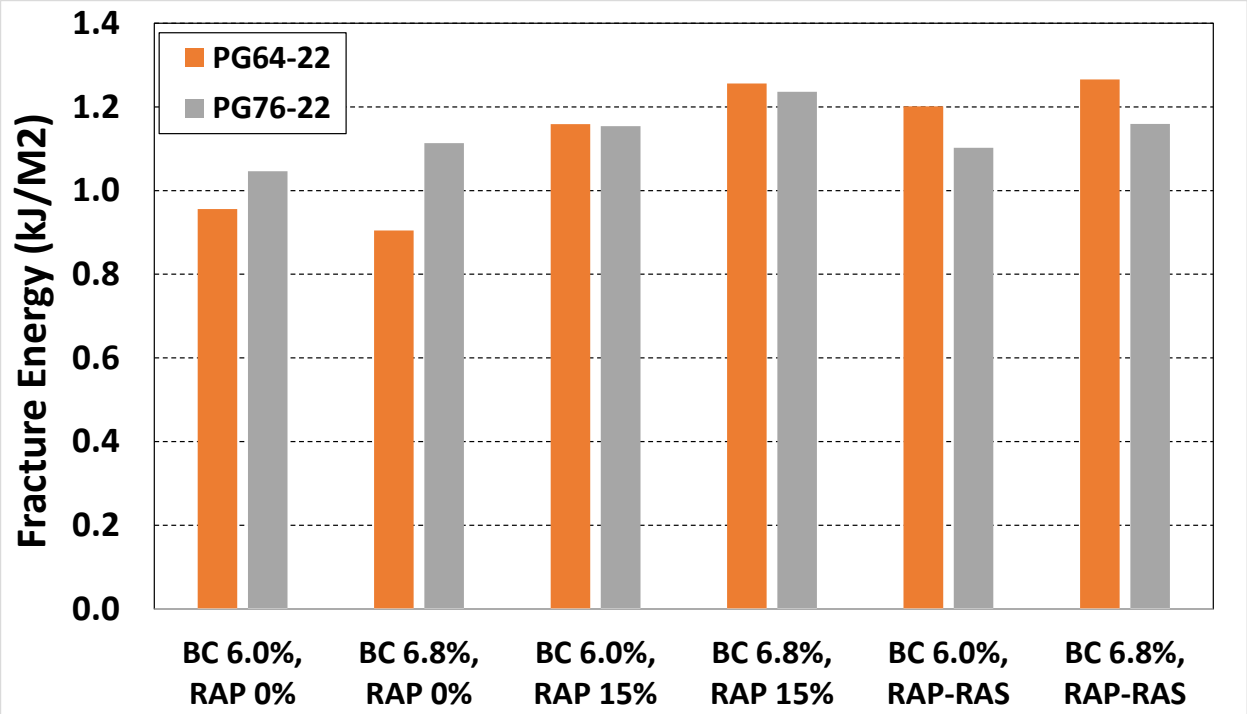

Figure 3.59. Fracture energy for mixtures with different RAP contents (0% and 15%) and RAP&RAS, binder grades (PG 64-22 and PG 76-22), and binder contents (6% and 6.8%)

Test results for low RAP and RAP&RAS mixtures showed that fracture toughness (K_{IC}) and secant stiffness (S) correlate well with cracking resistance and brittleness. Higher values for these two variables indicates higher resistance to crack formation and higher brittleness. Figure 3.60 and Figure 3.61 show that for low RAP and RAP&RAS mixtures, mixtures with BC 6.8%, RAP 0%, PG 64-22 and BC 6%, RAP&RAS, PG 76-22 have the lowest and the highest S and K_{IC}, respectively. Asphalt mixtures with lower K_{IC} and S values and higher FI require less energy for crack initiation, but since they are more ductile, they have higher crack propagation resistance. In this study, although the mixture with RAP&RAS, 6% binder content and PG 76-22 had the highest K_{IC} and S values, it had the lowest FI value. This means that it requires higher energy for crack initiation, but once the crack starts, it propagates rapidly. In other words, overall cracking resistance will be low.

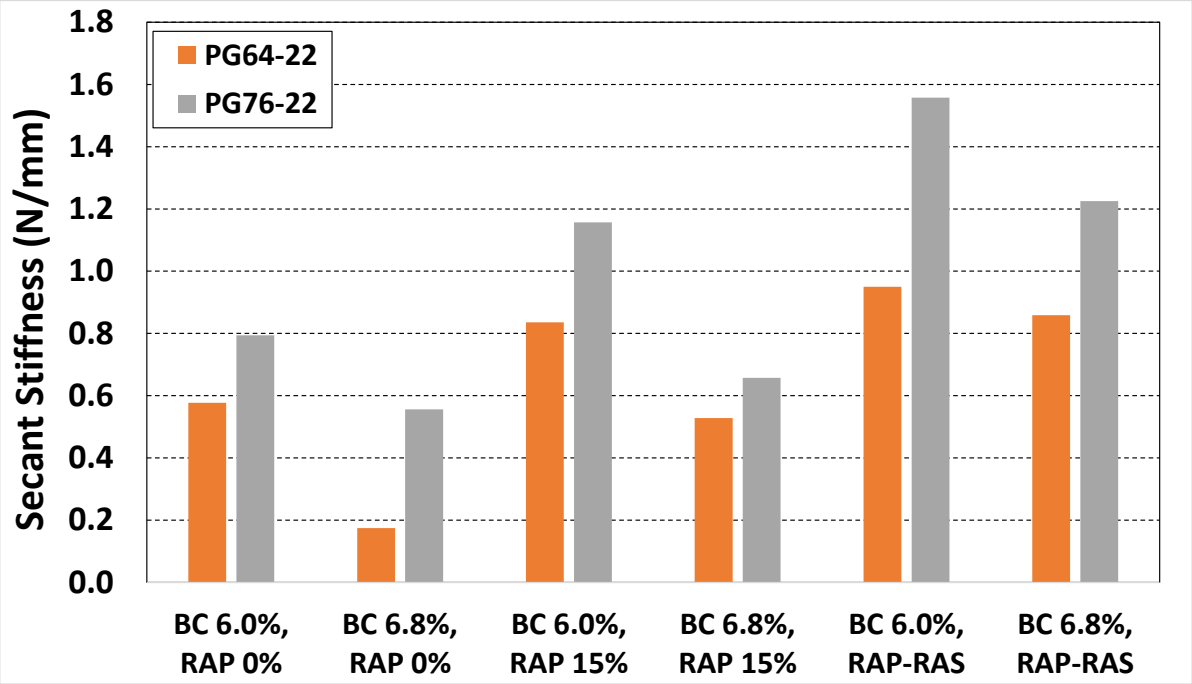

Figure 3.60. Secant stiffness for mixtures with different RAP contents (0% and 15%) and RAP&RAS, binder grades (PG 64-22 and PG 76-22), and binder contents (6% and 6.8%)

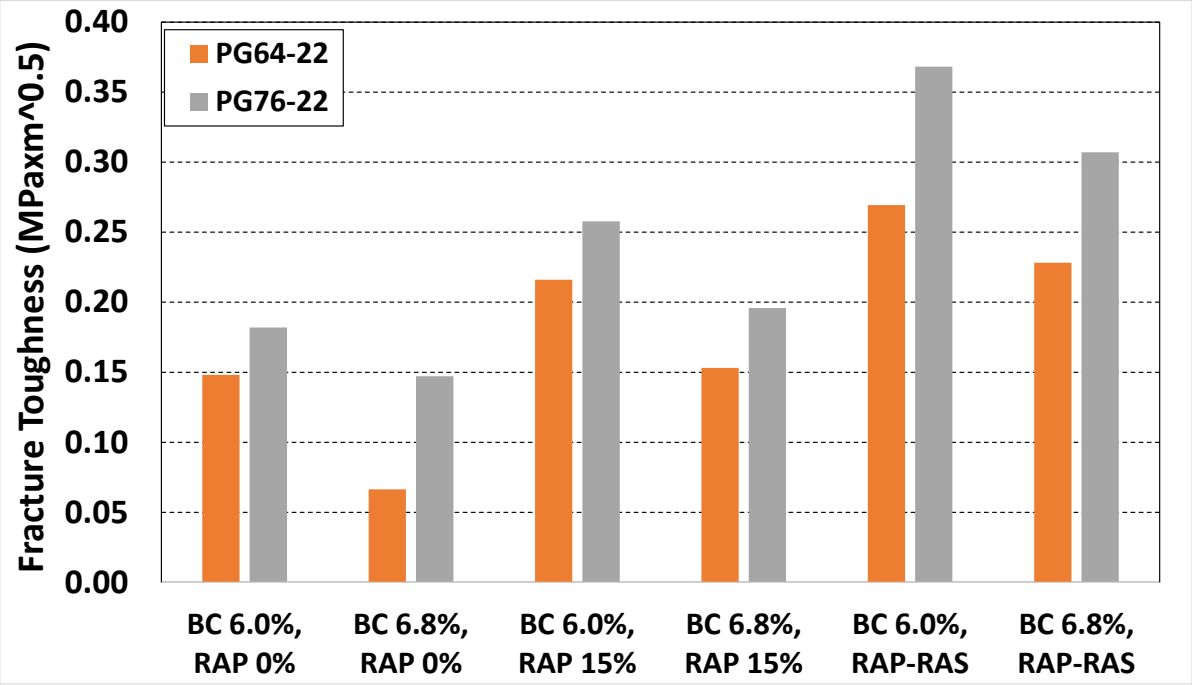

Figure 3.61. Fracture toughness for mixtures with different RAP contents (0% and 15%) and RAP&RAS, binder grades (PG 64-22 and PG 76-22), and binder contents (6% and 6.8%)

3.6.2.2 Flow Number Test

The flow number (FN) test is a simple performance test for evaluating rutting performance of asphalt concrete mixtures (Bonaquist et al. 2003). High FN values indicate that asphalt mixtures have high rutting resistance. Figure 3.62 and Figure 3.63 summarize the FN values for all tested asphalt mixtures for Phase II. Figure 3.64 shows the FN values for all asphalt mixtures with low RAP content, high RAP content and RAP&RAS (Phases I and II).

Minimum required FNs suggested by AASHTO TP 79-13 for different traffic levels are presented in Table 3.4. Suggested FN for the traffic level of 10 million to 30 million ESALs is specified as 190 while the FN limit for roadways with ESALs more than 30 million were specified as 740. In Figure 3.62 to Figure 3.64, the dashed and solid red lines show the recommended FN for the traffic levels of 10 to <30 and ≥30 million ESALs, respectively. FN values for all the asphalt mixtures were greater than 50, which is the recommended FN for the traffic level of 3 million to 10 million ESALs. None of the low RAP asphalt mixtures with PG 64-22 binder had FN values higher than 740, except for the mixture with BC 6% and RAP 15%. All RAP&RAS mixtures meet the FN criteria for highest traffic (FN>740). All of the low RAP asphalt mixtures with PG 76-22 binder has FN values higher than 740, except for the mixture with BC 6.8% and RAP 0%. These results suggest that mixtures with PG76-22 binder are not expected to have any rutting failures in the field.

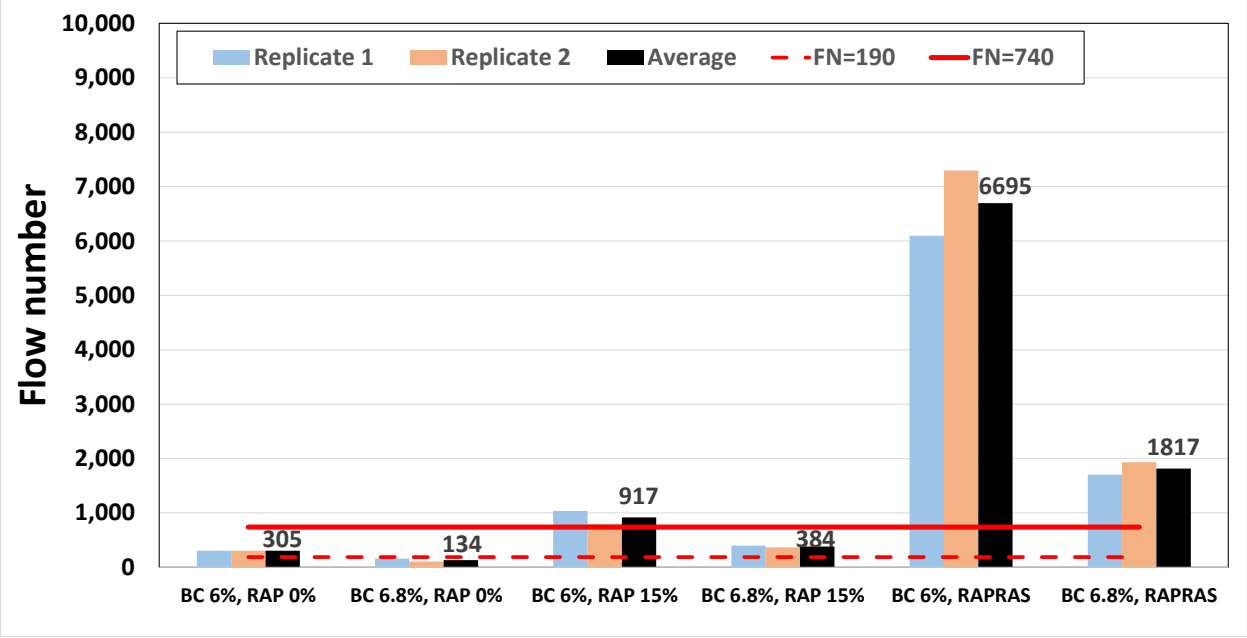

Figure 3.62. Flow number of the mixtures with different RAP contents (0% and 15%) and RAP&RAS, binder grade of PG 64-22, and binder contents (6% and 6.8%)

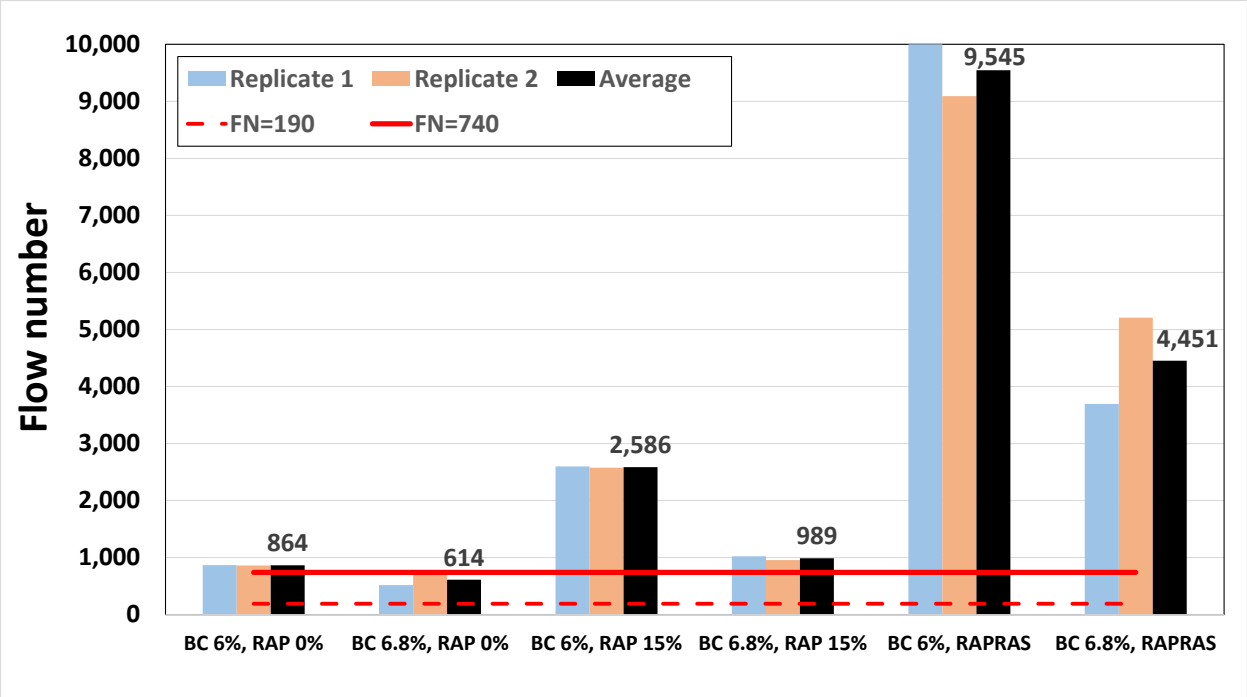

Figure 3.63. Flow number of the mixtures with different RAP contents (0% and 15%) and RAP&RAS, binder grade of PG 76-22, and binder contents (6% and 6.8%)

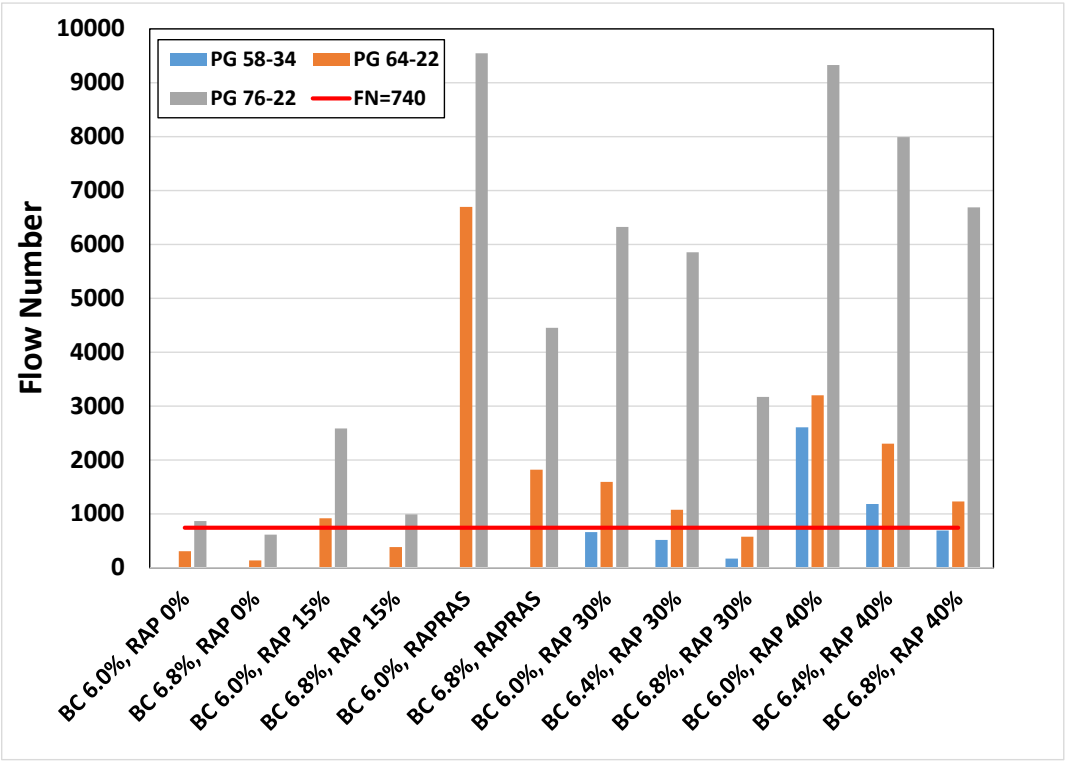

Figure 3.64. Average flow number of all asphalt mixtures - RAP&RAS, high (30% and 40%) and low RAP (0% and 15%) (Phases I and II).

3.6.2.3 Dynamic Modulus Test

The DM tests for Phase II were conducted on asphalt mixtures with different RAP contents (0% and 15%) and RAP&RAS, binder contents (6% and 6.8%) and binder grades (PG 64-22 and PG 76-22). Two replicate experiments were conducted for each combination of the variables of interest. Therefore, 24 samples in total were tested at the testing frequencies and temperatures given in Section 3.4.2. The testing procedure without any confining pressure described in AASHTO TP 79-13 was followed. Dynamic modulus and phase angle master curves are presented and discussed in the following sections.

3.6.2.3.1 Master Curves for Dynamic Modulus

This section presents the dynamic modulus master curves for asphalt mixtures. Average of test results for two replicate mixtures were used to develop each master curve as recommended by AASHTO TP 79-13.

Master curves of dynamic modulus for Phase II asphalt mixtures with PG 64-22 and PG 76-22 binders are presented in Figure 3.65 and Figure 3.66, respectively. The reference temperature for all the master curves is 20^{o}C. In general, higher RAP content and lower binder content resulted in higher dynamic moduli while the stiffnesses for asphalt mixtures with PG 76-22 binder were significantly higher than the mixtures with PG 64-22 binder. For mixtures with PG 64-22 binder, master curves for mixtures with 6% binder content and 0% RAP were determined to be close to mixtures with 6.8% binder content and 15% RAP. Significantly lower stiffness for the mixture with 6.8% binder content, 0% RAP and PG 64-22 binder indicated that this mixture is likely to fail from rutting in the field. The average measured flow number of 134 (Figure 3.62) for this mixture also validates this conclusion. For mixtures with PG 76-22 binder, master curves for mixtures with 6% binder content and 15% RAP were determined to be close to mixtures with 6.8% binder content and RAP&RAS. These master curves were used in Chapter 5 to perform mechanistic-empirical pavement design simulations.

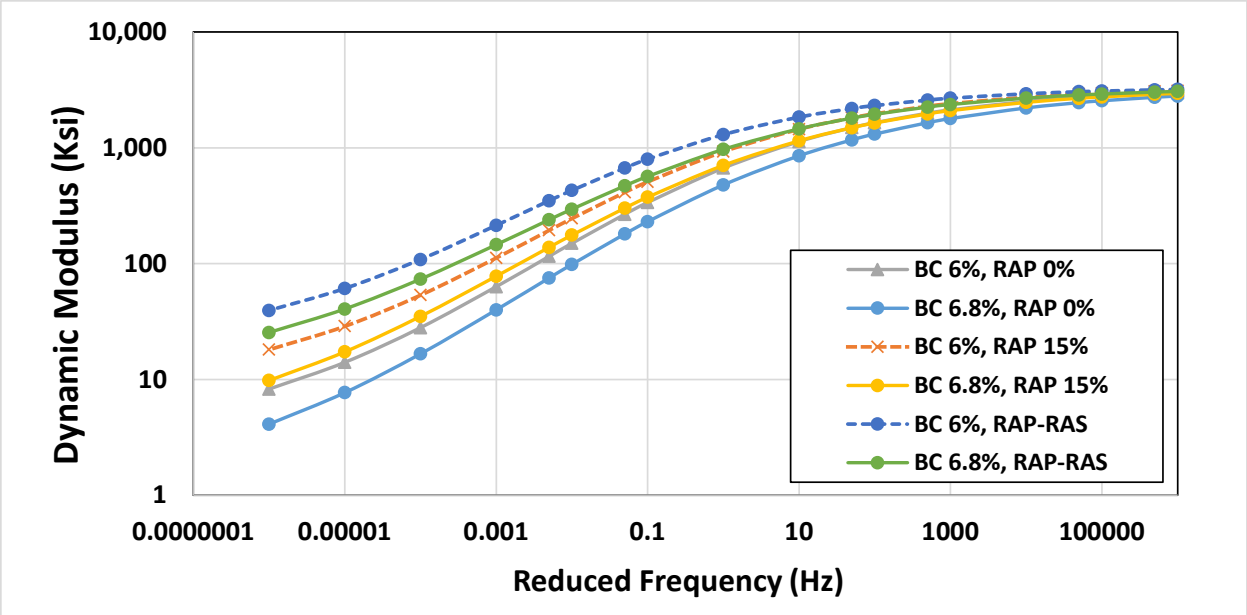

Figure 3.65. Master curves of dynamic modulus for the mixtures with different RAP contents (0% and 15%) and RAP&RAS, binder grade of PG 64-22, and different binder contents (6% and 6.8%)

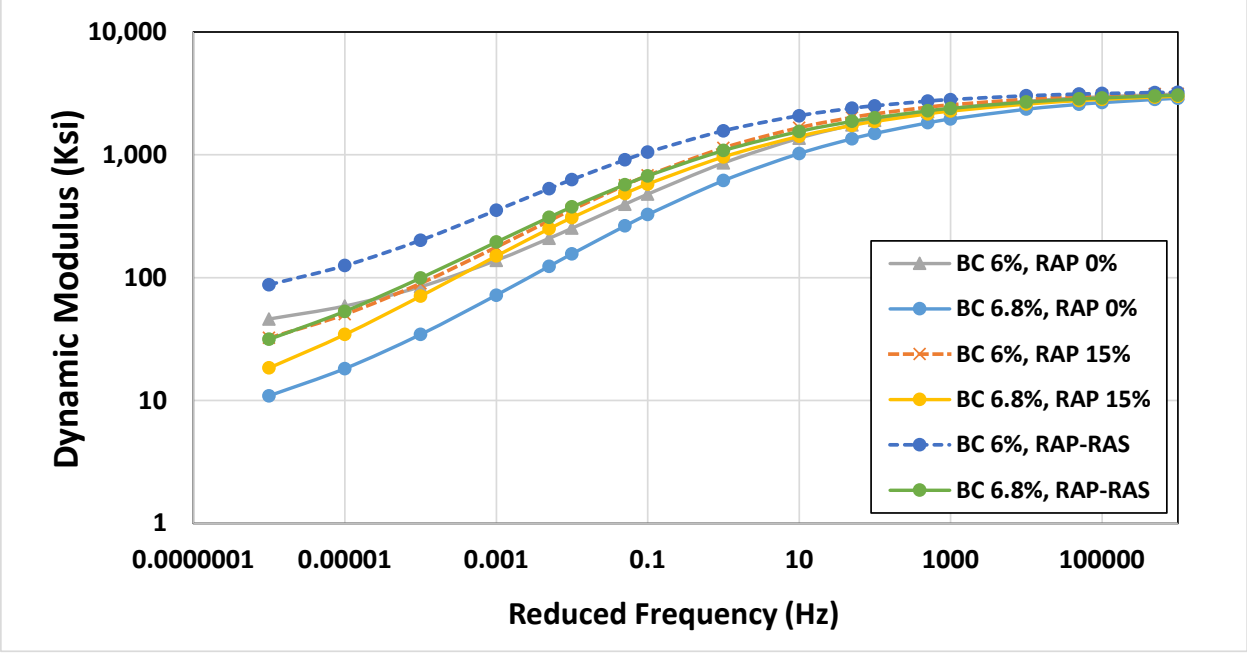

Figure 3.66. Master curves of dynamic modulus for the mixtures with different RAP contents (0% and 15%) and RAP&RAS, binder grade of PG 76-22, and different binder contents (6% and 6.8%)

Based on AASHTO TP 79-13, the coefficient of variation (CV) of the dynamic modulus for each pair of tested samples should not be greater than 9.2%. Figure 3.67 to Figure 3.72 show the dynamic moduli of Phase II mixtures (low RAP and RAP&RAS) at frequencies of 0.1 Hz and 10 Hz and temperatures of 4 ^{o}C, 20 ^{o}C and 40 ^{o}C. In these figures, B2 is PG 64-22 and B3 is PG 76-22. Also, R15 is RAP 15% and BC refers to binder content. For all the mixtures shown, the CV of the paired tested mixtures were less than 9.2% at 4 ^{o}C, and 20 ^{o}C (except for the mixtures with 15% RAP, 6.8% binder content, and PG 76-22 and 0% RAP, 6.8% binder content, and PG 64-22 at 20 ^{o}C and 0.1 Hz). However, some of the replicate mixtures had higher CV values at 40 ^{o}C. Bonaquist (2011) reported in NCHRP Report 702 that the CV could be more than 10% for mixtures with low dynamic moduli. Therefore, observing a higher CV for dynamic modulus at the test temperature of 40°C is not unexpected. Moreover, it can be seen that the dynamic modulus decreases as the binder content increases for all the frequency levels and temperatures. It has an opposite trend as the RAP content increases.

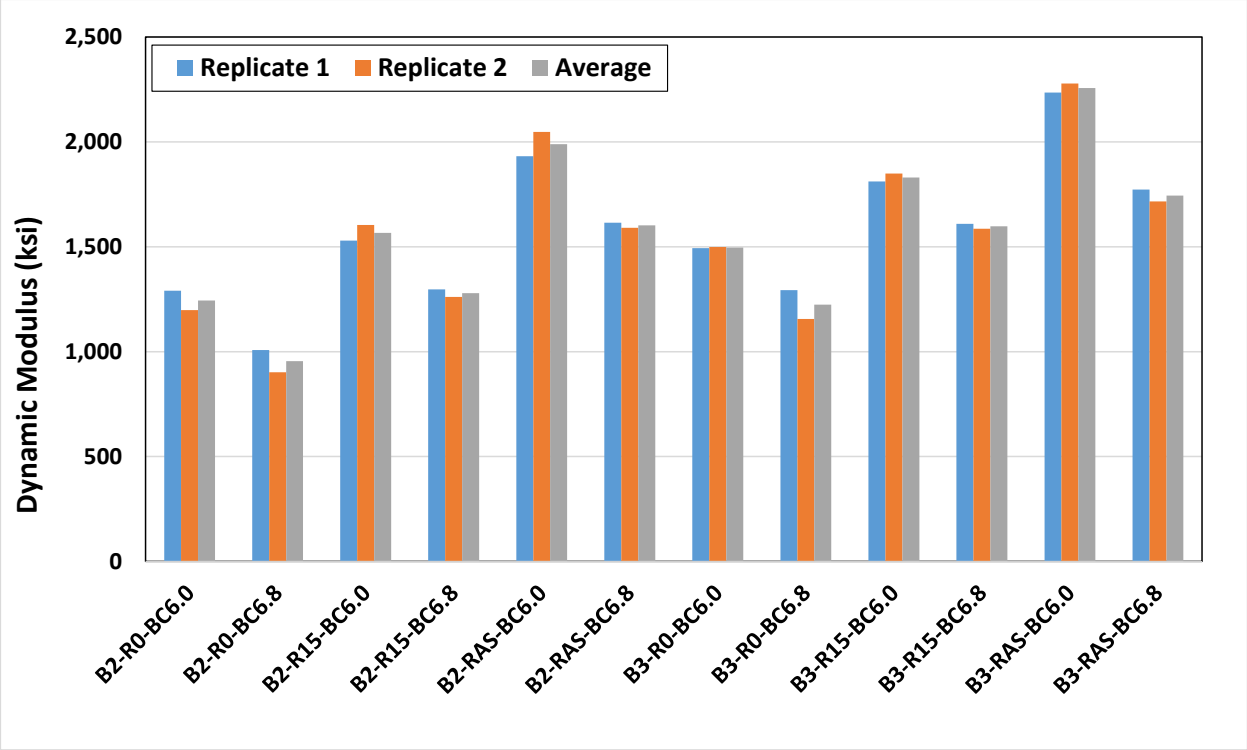

Figure 3.67. Dynamic modulus of the mixtures at 4 ^{o}C and 0.1 Hz and all the combinations of RAP contents, RAP&RAS, binder contents, and binder grades

Note: B2= PG 64-22 and B3 = PG 76-22.
R0 = 0% RAP and R15 = 15% RAP.
BC6.0= 6% binder content and BC6.8 = 6.8% binder content.
RAS=Mix with 19 %RAP and 3% RAS.

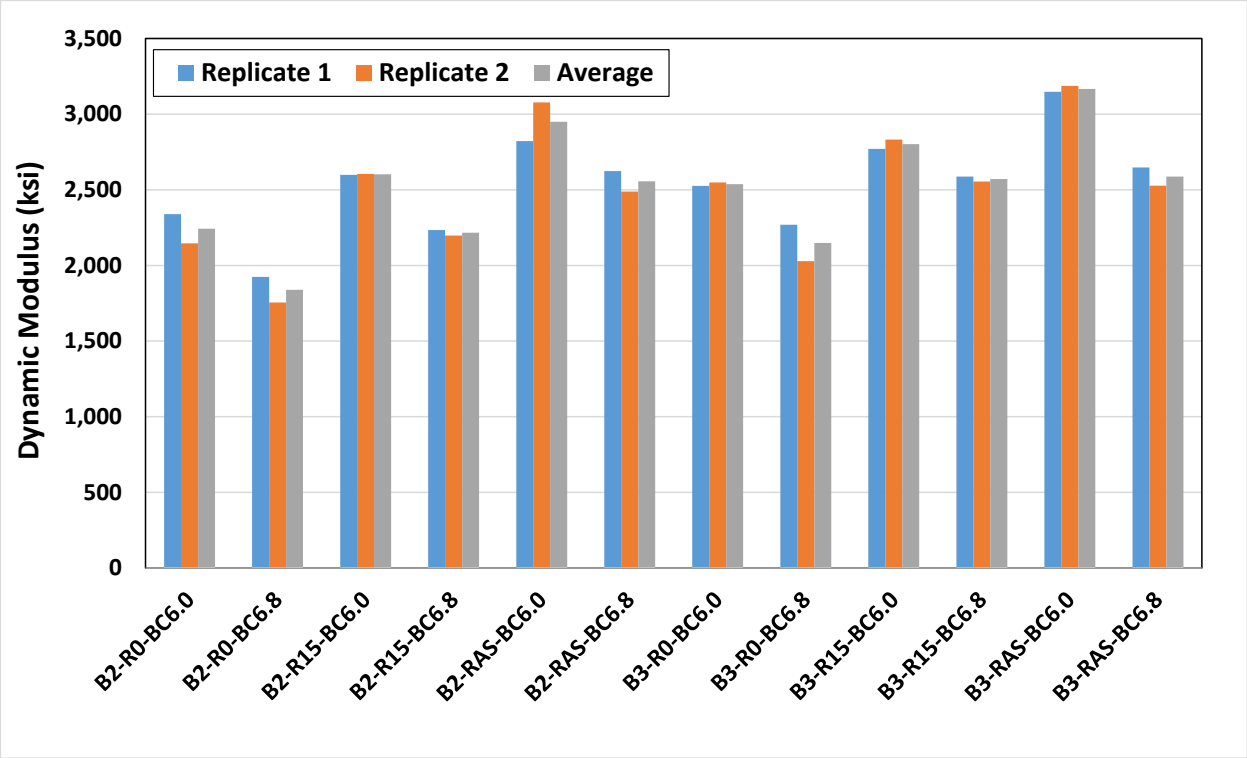

Figure 3.68. Dynamic modulus of the mixtures at 4 ^{o}C and 10 Hz and all the combinations of RAP contents, RAP&RAS, binder contents, and binder grades

Note: B2= PG 64-22 and B3 = PG 76-22.
R0 = 0% RAP and R15 = 15% RAP.
BC6.0= 6% binder content and BC6.8 = 6.8% binder content.
RAS=Mix with 19 %RAP and 3% RAS.

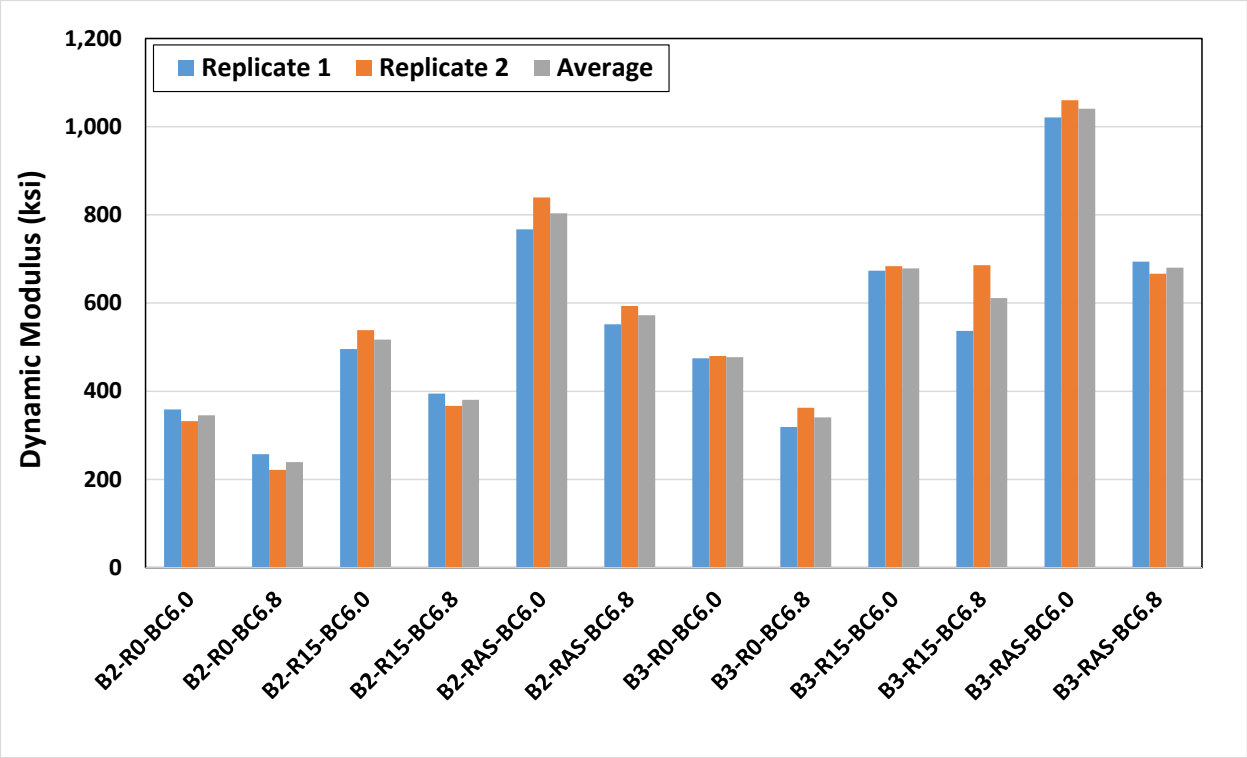

Figure 3.69. Dynamic modulus of the mixtures at 20 ^{o}C and 0.1 Hz and all the combinations of RAP contents, RAP&RAS, binder contents, and binder grades

Note: B2= PG 64-22 and B3 = PG 76-22.
R0 = 0% RAP and R15 = 15% RAP.
BC6.0= 6% binder content and BC6.8 = 6.8% binder content.
RAS=Mix with 19 %RAP and 3% RAS.

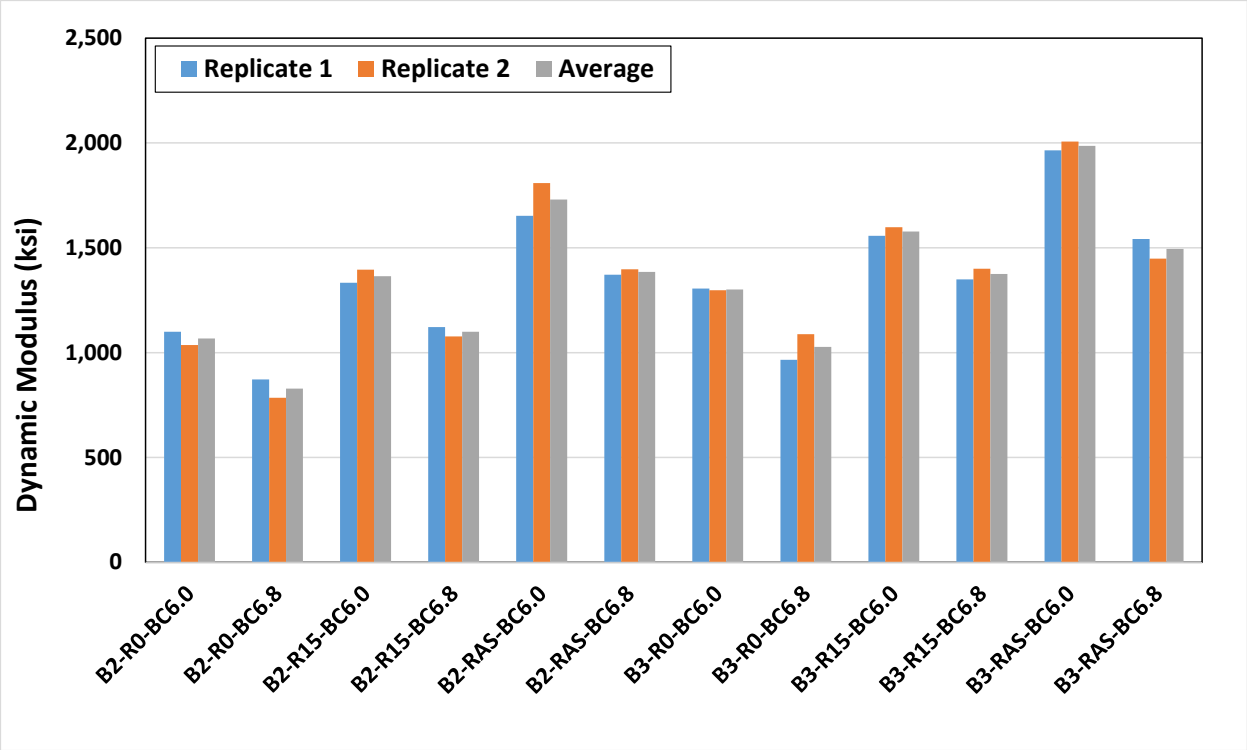

Figure 3.70. Dynamic modulus of the mixtures at 20 ^{o}C and 10 Hz and all the combinations of RAP contents, RAP&RAS, binder contents, and binder grades

Note: B2= PG 64-22 and B3 = PG 76-22.
R0 = 0% RAP and R15 = 15% RAP.
BC6.0= 6% binder content and BC6.8 = 6.8% binder content.
RAS=Mix with 19 %RAP and 3% RAS.

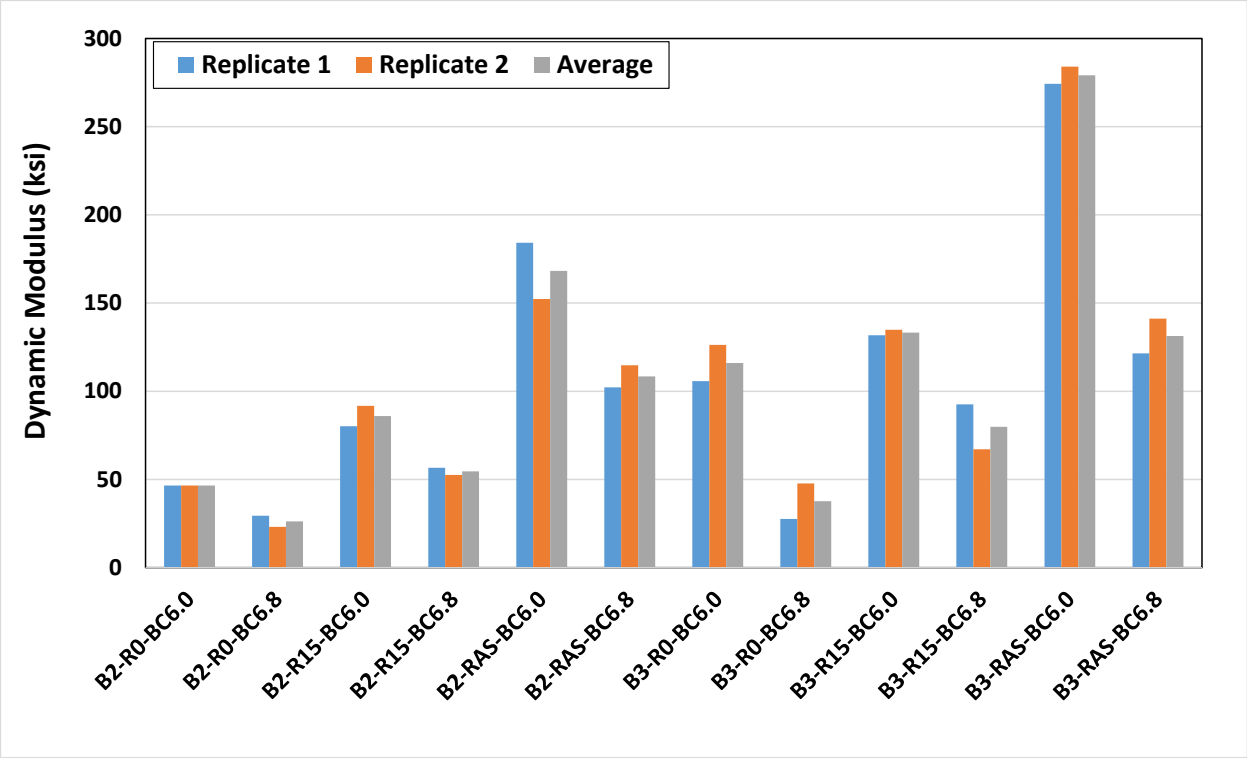

Figure 3.71. Dynamic modulus of the mixtures at 40 ^{o}C and 0.1 Hz and all the combinations of RAP contents, RAP&RAS, binder contents, and binder grades

Note: B2= PG 64-22 and B3 = PG 76-22.
R0 = 0% RAP and R15 = 15% RAP.
BC6.0= 6% binder content and BC6.8 = 6.8% binder content.
RAS=Mix with 19 %RAP and 3% RAS.

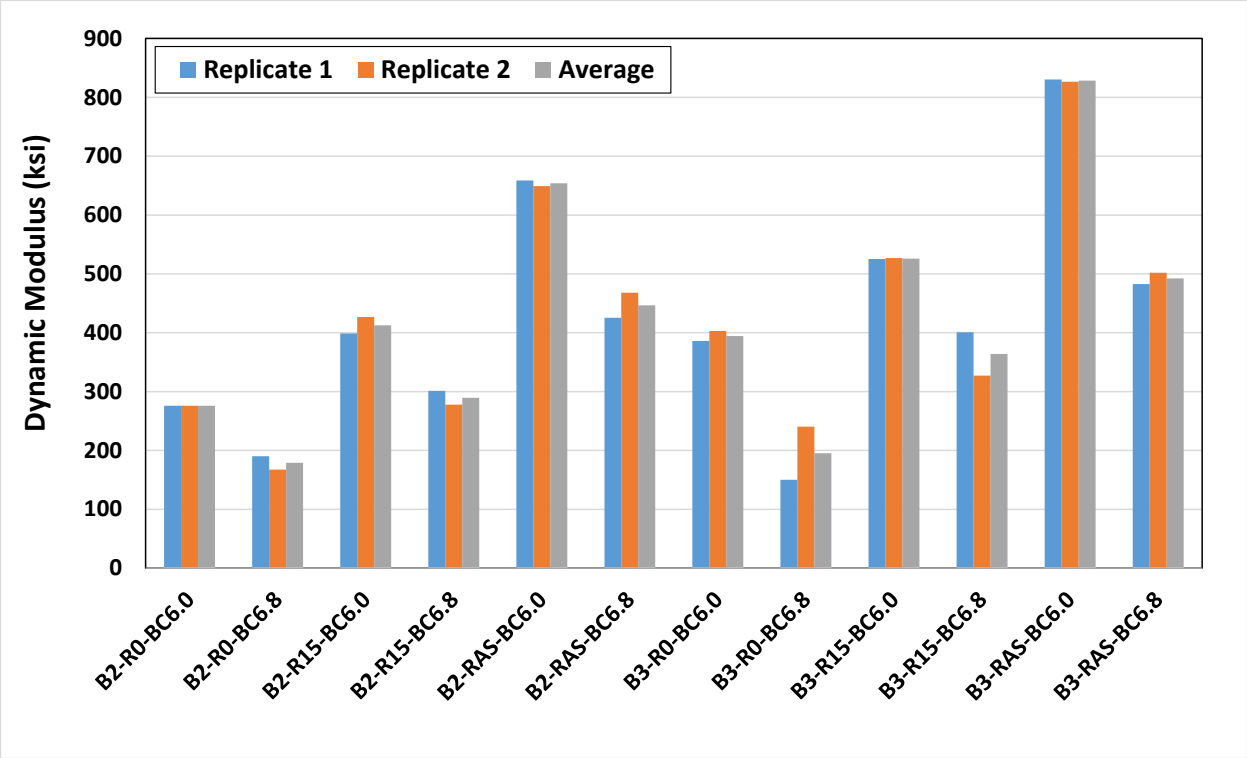

Figure 3.72. Dynamic modulus of the mixtures at 40 ^{o}C and 10 Hz and all the combinations of RAP contents, RAP&RAS, binder contents, and binder grades

Note: B2= PG 64-22 and B3 = PG 76-22.
R0 = 0% RAP and R15 = 15% RAP.
BC6.0= 6% binder content and BC6.8 = 6.8% binder content.
RAS=Mix with 19 %RAP and 3% RAS.

3.6.2.3.2 Master Curves for Phase Angle

Phase angle master curves for all Phase II test results are plotted in Figure 3.73 and Figure 3.74. The same shift factor values, which were calculated and used for developing the master curves for DM tests, are used to develop the master curves for phase angles. Therefore, these master curves are not as smooth as the master curves of the dynamic modulus. The reference temperature for all master curves is 20 ^{o}C.

Figure 3.73 and Figure 3.74 show that mixtures with RAP&RAS have the lowest phase angles indicating that their cracking resistance when compared to the mixtures with 0% and 15% RAP will be lower. In general, mixtures with the stiff PG 76-22 binder have the lowest phase angles.

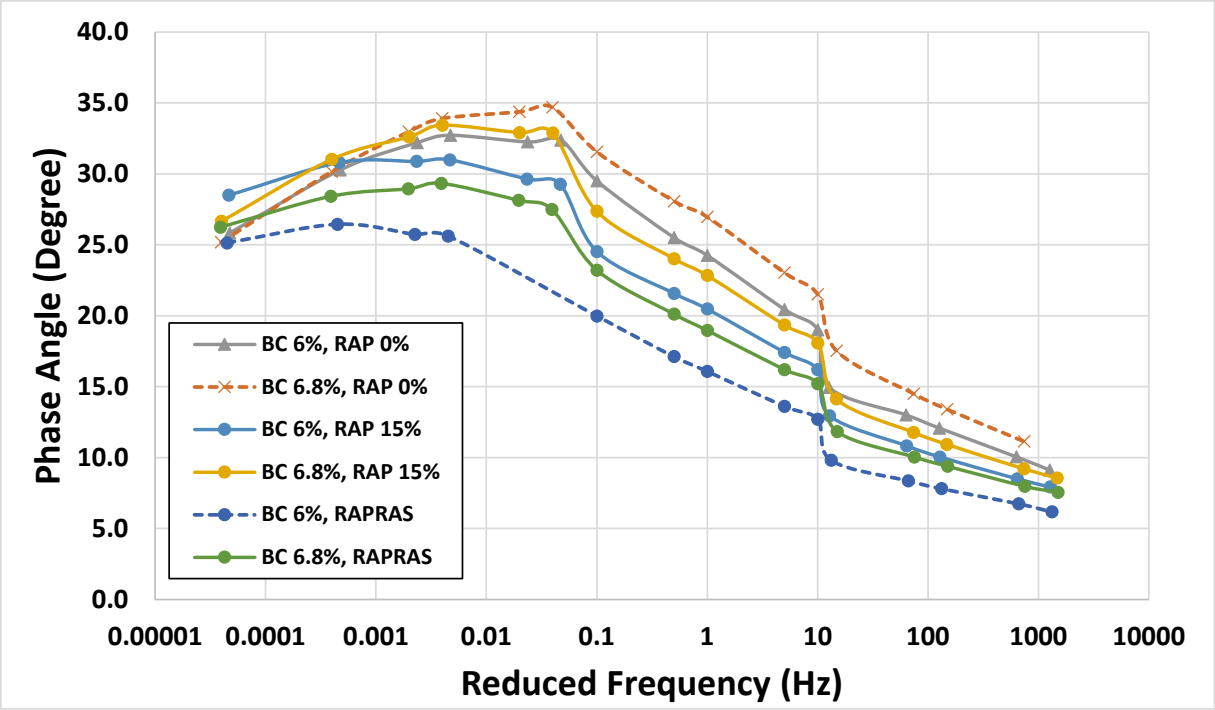

Figure 3.73. Master curves of phase angles for the mixtures with different RAP contents (0% and 15%) and RAP&RAS, binder grade of PG 64-22, and different binder contents (6% and 6.8%)

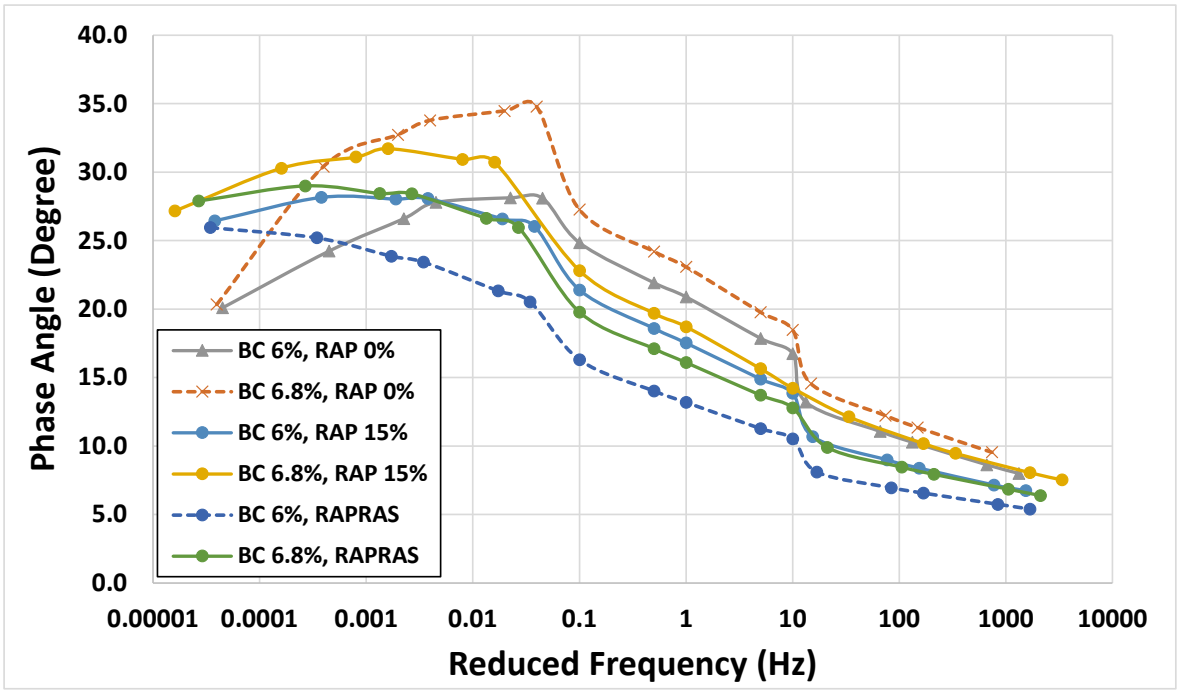

Figure 3.74. Master curves of phase angles for the mixtures with different RAP contents (0% and 15%) and RAP&RAS, binder grade of PG 76-22, and different binder contents (6% and 6.8%)

3.6.2.4 Summary of Test Results

Results of the SCB, DM and FN tests were presented in Sections 3.6.2.1 to 3.6.2.3 to evaluate the cracking and rutting performance of low RAP (0% and 15%) and RAP&RAS [asphalt binder replacement (ABR) matching the ABR of 30% RAP mixture from Section 3.5 (Phase I)] asphalt mixtures of this study. This section summarizes the general results of all conducted tests.

Although some of the asphalt mixtures showed high cracking resistance (high FI), their rutting performance can be low due to high binder content and softer binders. Figure 3.75 shows the average FI (average of four replicate SCB tests) of the asphalt mixtures with all combinations of RAP contents and RAP&RAS, binder contents and binder grades. The average FN of the asphalt mixtures (average of two replicate FN tests) is also shown on top of each bar. It can be observed that mixtures with no RAP do not require high percentages of asphalt binder to achieve required cracking resistance. However, since all of the binder in the mixture will be virgin binder, the cost of asphalt mixtures with no RAP may be higher than other mixtures. Mixtures with 0% RAP, 6% binder content, and PG 76-22 binder and 15% RAP, 6.8% binder content, and PG 76-22 binder were observed to be passing the cracking and rutting requirements (FI>10 and FN>740).

Results show that RAP&RAS asphalt mixtures with binder contents ranging from 7.29% to 7.59% and binder grade of PG 64-22 had acceptable cracking and rutting performance (See Section 3.6.2.5). Using a binder grade of PG 76-22 and RAP&RAS make asphalt mixtures brittle. Therefore, there are no combinations of binder content, PG 76-22 and RAP&RAS identified to provide high cracking and rutting performance.

Analyses for the low RAP mixtures (See Section 3.6.2.6) showed that there is no combination of binder content and RAP content for mixtures with PG 64-22 that will provide high cracking and rutting performance. For mixtures with 20% RAP content and PG 76-22, binder content should be between 7% and 7.6%. As RAP content decreases, required binder content decreases. For mixtures with 15% RAP, 10% RAP, 5% RAP and 0% RAP, suggested binder content ranges are 6.8%-7.2%, 6.6%-6.9%, 6.4%-6.6% and 6.2%, respectively.

In the following sections (Sections 3.6.2.5 and 3.6.2.6), regression equations were developed and Monte Carlo simulations were performed using the developed equations to determine the required binder content, binder grade and RAP content of asphalt mixtures to meet rutting (FN>740) and cracking resistance (FI>10) requirements.

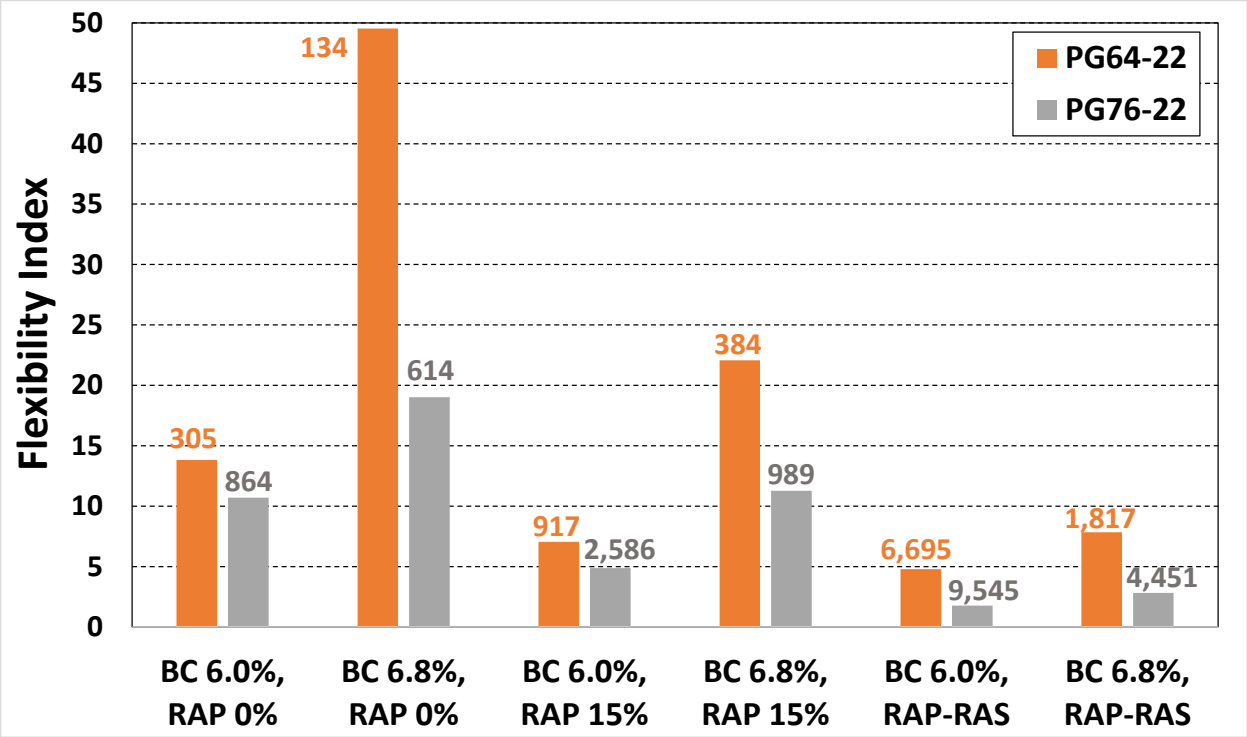

Figure 3.75. Flexibility index and flow number (numbers on each bar) of the mixtures with different RAP contents (0% and 15%) and RAP&RAS, binder grades (PG 64-22 and PG 76-22), and binder contents (6.0% and 6.8%)

3.6.2.5 Determination of RAP/RAS Asphalt Mixtures with High Cracking and Rutting Performance – Suggested Strategies

The results of SCB and FN tests were used to develop linear regression models correlating FN and FI (dependent variables) with binder content and binder grade (independent variables) for the mixtures with RAP&RAS. First, analysis of variance (ANOVA) was conducted to evaluate which independent variables are important. Then, regression models were developed. Dependent and independent variables for the developed regression models are presented in Table 3.12.

Table 3.12. Independent and Dependent Variables Used for Regression Models

Variable Type	Symbol	Description	Range
Dependent	FI	Flexibility Index	1.31 to 8.99
	FN	Flow Number	1,702 to 10,000
Independent	BC	Binder Content	6 and 6.8
Category Independent	PG	Binder Grade	PG 64-22 and PG 76-22

3.6.2.5.1 ANOVA Table

The effects of binder content and binder grade on FN and FI were evaluated for the mixtures with RAP&RAS by performing analysis of variance (ANOVA). FN and FI were logarithmically transformed and linearly correlated with binder content (BC) and binder grade (PG). As shown in Table 3.13 and Table 3.14, independent variables (binder content and binder grade) have a significant effect on FN and FI. Therefore, all the independent variables were used for regression model development.

Table 3.13. ANOVA Table for the Regression Model Correlating FI Test Results with Binder Grade and Binder Content

	Degrees of Freedom	Sum of Squares	Mean Square	F Value	Pr(F) Value
BC	1	0.89	0.89	11.08	0.0054
PG	1	4.09	4.09	51.03	0.0000
Residuals	13	1.04	0.08		

Table 3.14. ANOVA Table for the Regression Model Correlating FN Test Results with Binder Grade and Binder Content

	Degrees of Freedom	Sum of Squares	Mean Square	F Value	Pr(F) Value
BC	1	2.16	2.16	47.85	0.0010
PG	1	0.77	0.77	17.05	0.0091
Residuals	5	0.23	0.05		

3.6.2.5.2 Linear Regression Model for FI

To develop the linear regression model, FI values obtained from SCB tests were logarithmically transformed. Then, they were linearly correlated with binder content and binder grade. Figure 3.76 shows ln(FI) for each combination of binder content and binder grade. The developed model is as follows:

$$\ln(FI) = \underset{}{-1.9905} + \underset{(0.1034)}{0.5887}*BC - \underset{(0.0054)}{1.0108}*PG\ \underset{(0.0000)}{76\text{-}22} \qquad R^2 = 0.80 \qquad \textbf{(3.20)}$$

The P-values of the estimated regression coefficients are presented in parenthesis below each coefficient. The coefficient of determination (R^2) for the developed model is 0.80, indicating that 80 percent of the variance in the response is explained by the explanatory variables.

Residual plots of the developed regression model are presented in Figure 3.77. Since residuals are randomly scattered around the zero line in Figure 3.77a, the assumption of the constant variance is met. Figure 3.77b shows the observed data versus fitted values. The assumption of normality in linear regression models is also met (Figure 3.77c). Figure 3.77d shows that the standardized residuals are between -2 and 2. Therefore, there are no outliers in the data.

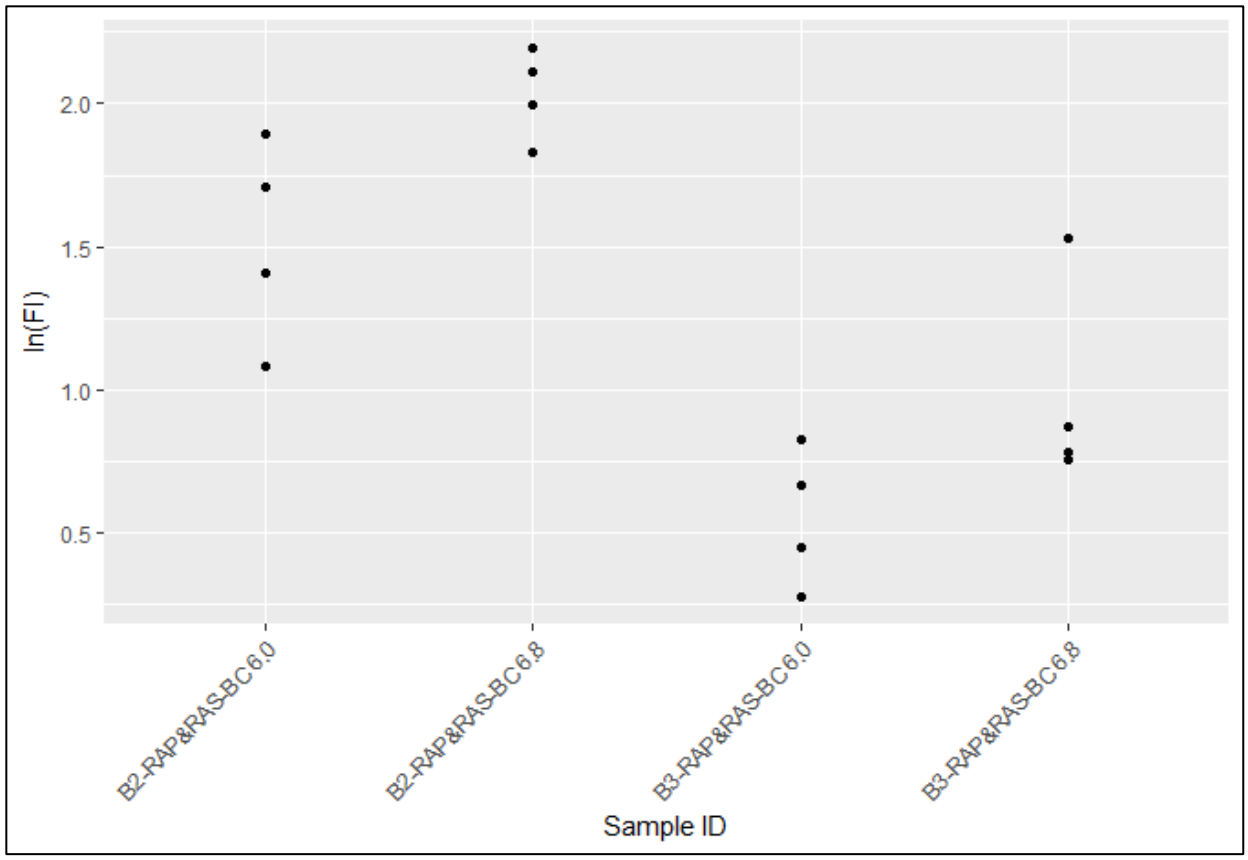

Figure 3.76. ln(FI) for each combination of binder content and binder grade

Note: B2= PG 64-22, and B3 = PG 76-22.
BC6= 6% binder content and BC6.8 = 6.8% binder content.

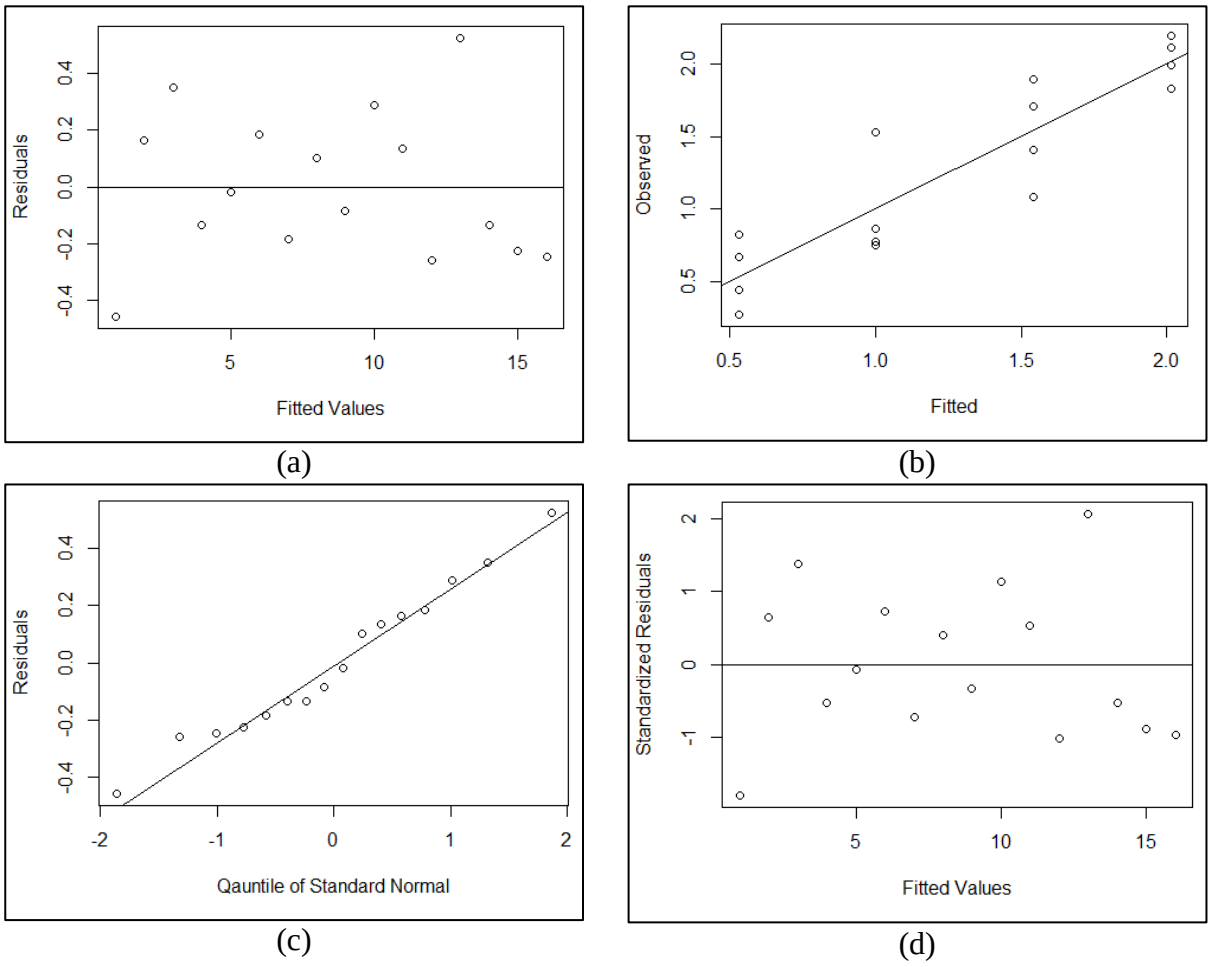

Figure 3.77. Residual plots for the regression model correlating ln(FI) binder content and binder grade

3.6.2.5.3 Linear Regression Model for FN

Firstly, FN values obtained from FN tests were logarithmically transformed. Then, the linear regression models were developed correlating ln(FN) with binder content and binder grade. Figure 3.78 shows the ln(FN) for all the combinations of binder contents and binder grade. The developed model is as follows:

$$\ln(FN) = \underset{(0.0000)}{16.4682} - \underset{(0.0009)}{1.2991}*BC + \underset{(0.0091)}{0.6204}*PG\ 76\text{-}22 \qquad R^2 = 0.90 \qquad \textbf{(3.21)}$$

In the equation above, the P-values of each regression coefficient are presented in the parenthesis below them. The coefficient of determination (R^2) for the developed model is 0.89, indicating that 89 percent of the variance in the response is explained by the explanatory variables.

Residual plots of the developed model are shown in Figure 3.79. Figure 3.79a shows that residuals have constant variance since they are randomly scattered around the zero line. Figure 3.79b illustrates the observed data versus fitted values. Also, Figure 3.79c shows that the assumption of normality of linear regression is met. Since the standardized residuals are between -2 and 2 (Figure 3.79d), there are no outliers in the data.

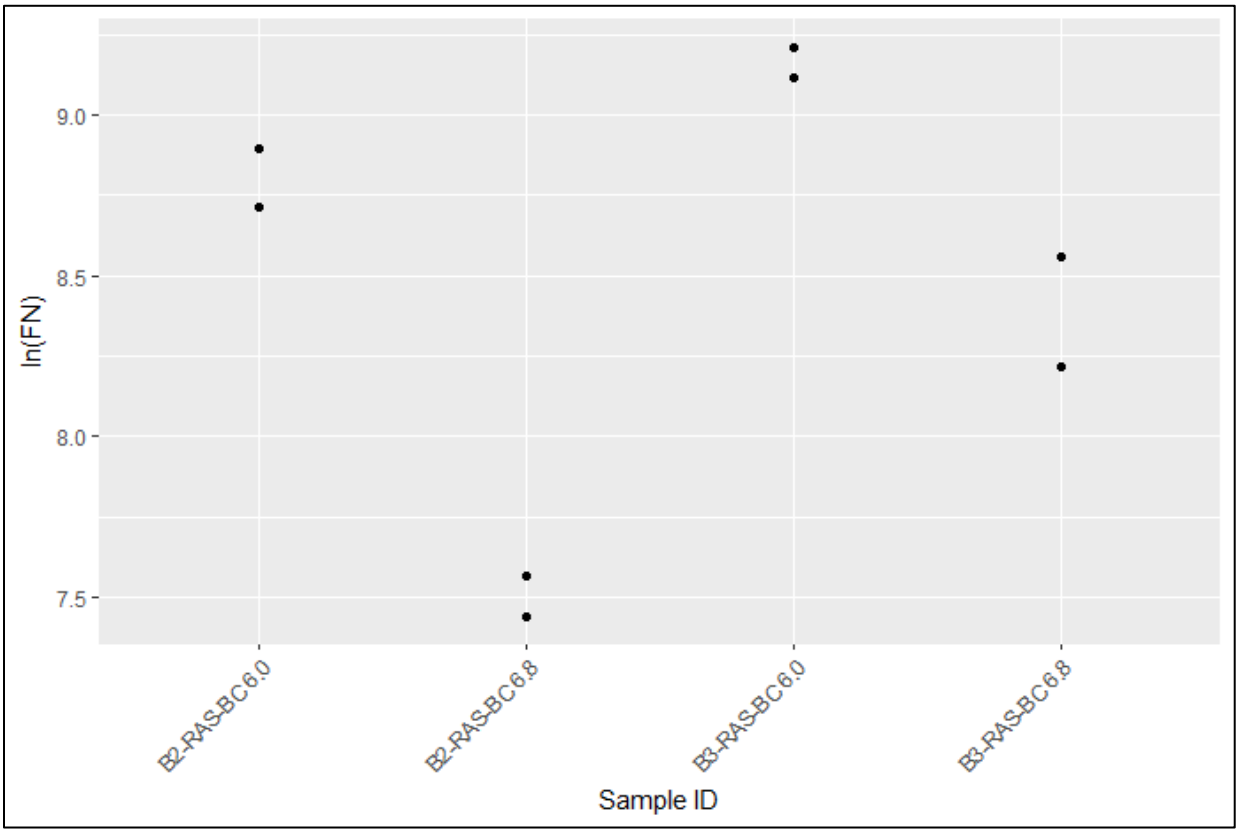

Figure 3.78. ln(FN) for each combination of binder content and binder grade

Note: B2= PG 64-22, and B3 = PG 76-22.
BC6= 6% binder content and BC6.8 = 6.8% binder content.

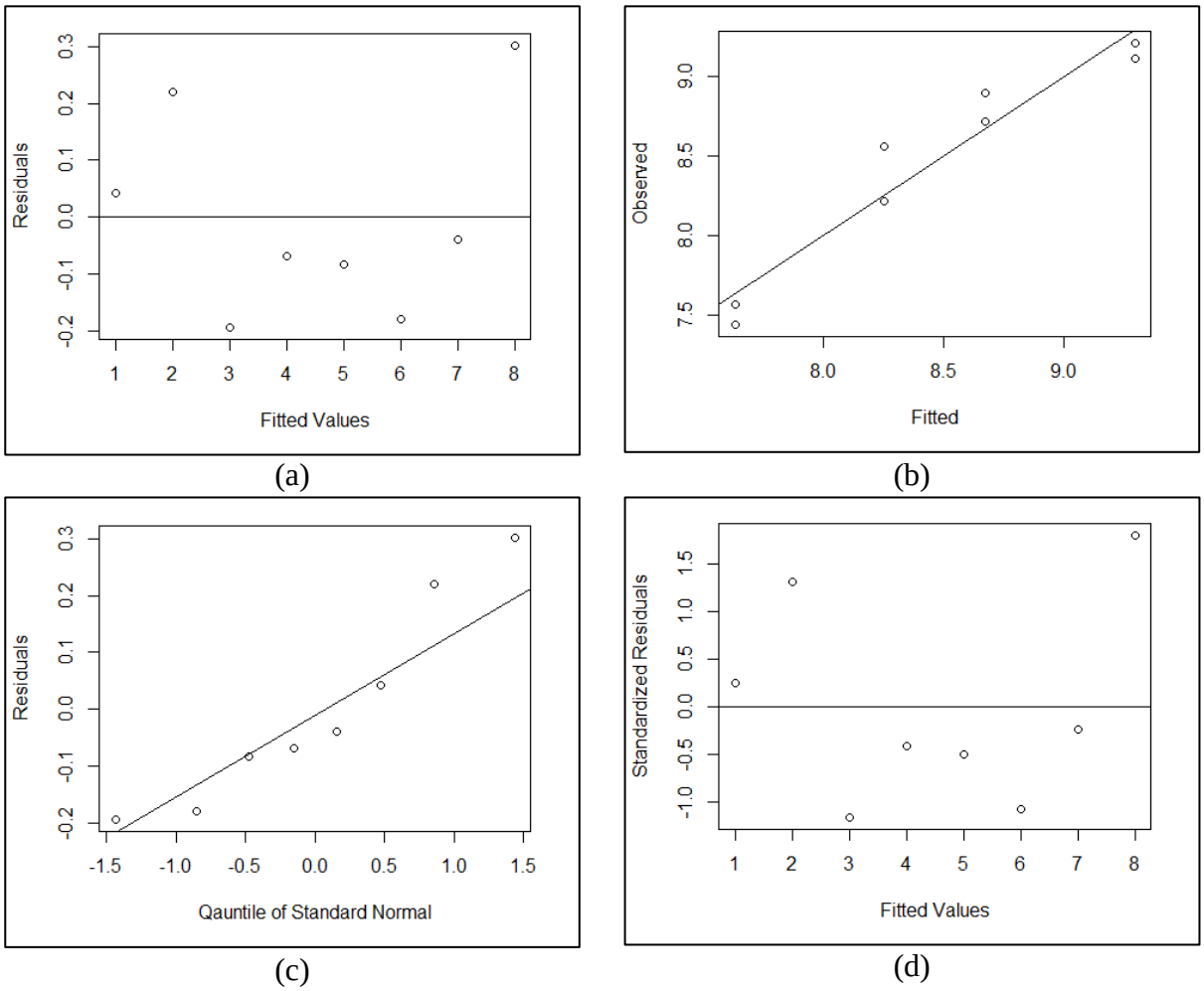

Figure 3.79**. Residual plots for the regression model correlating ln(FN) binder content and binder grade**

3.6.2.5.4 Finding Asphalt Mixtures with Acceptable Cracking and Rutting Performance

Linear regression models developed for asphalt mixtures with RAP&RAS were used to predict asphalt mixtures with acceptable cracking and rutting performance (FI>10 and FN>740). Required binder contents for asphalt mixtures with FI values greater than 10 and FN values greater than 740 were predicted (see Table 3.15). Results show that asphalt mixtures with binder contents ranging from 7.29% to 7.59% and binder grade of PG 64-22 have acceptable cracking and rutting performance. Using a binder grade of PG 76-22 and RAP&RAS makes asphalt mixtures brittle. In order to enhance the cracking performance, the binder content should be increased up to 9.26%. However, to achieve acceptable rutting performance, binder content should be less than 8.07%. Therefore, it seems that there are no combinations of binder content, PG 76-22 and RAP&RAS identified to provide acceptable cracking and rutting performance.

Table 3.15. Asphalt Mixtures with RAP&RAS and High Cracking and Rutting Performance

Binder Content for Mixtures with FN>740	Binder Content for Mixtures with FI>10	Binder Grade
<7.59	> 7.29	PG 64-22
<8.07	> 9.01	PG 76-22

3.6.2.6 Determination of Low RAP Asphalt Mixtures with High Cracking and Rutting Performance – Suggested Strategies

Results of the DM and FN tests were used to develop linear regression models correlating DM and FN with RAP content, binder content and binder grade for the mixtures with low RAP contents. Table 3.16 shows independent and dependent variables used in developing the regression models. After conducting the analysis of variance (ANOVA), it was found that all the independent variables are important and have a significant effect on FI and FN. Therefore, all the independent variables were used for regression model development.

Table 3.16. Independent and Dependent Variables Used for Regression Models

Variable Type	Symbol	Description	Range
Dependent	FI	Flexibility Index	2.8 to 82.11
	FN	Flow Number	106 to 2597
Independent	BC	Binder Content	6 and 6.8
Category Independent	PG	Binder Grade	PG 64-22 and PG 76-22

3.6.2.6.1 Linear Regression Model for FI

To develop a linear regression model correlating FI with the independent variables, the FI values obtained from SCB tests were logarithmically transformed. Figure 3.80 shows ln(FI) for all the combinations of RAP contents, binder contents and binder grades. The developed model is shown in Equation(3.22). The P-value of each estimated regression coefficient is shown in the parentheses below them.

$$\ln(FI) = -4.232886 - 0.046291*RAP + 1.162876*BC - 0.568286*PG\ 76\text{-}22 \quad R2 = 0.8073$$
$$(0.0000) \qquad (0.0000) \qquad (0.0000) \qquad (0.0000)$$

(3.22)

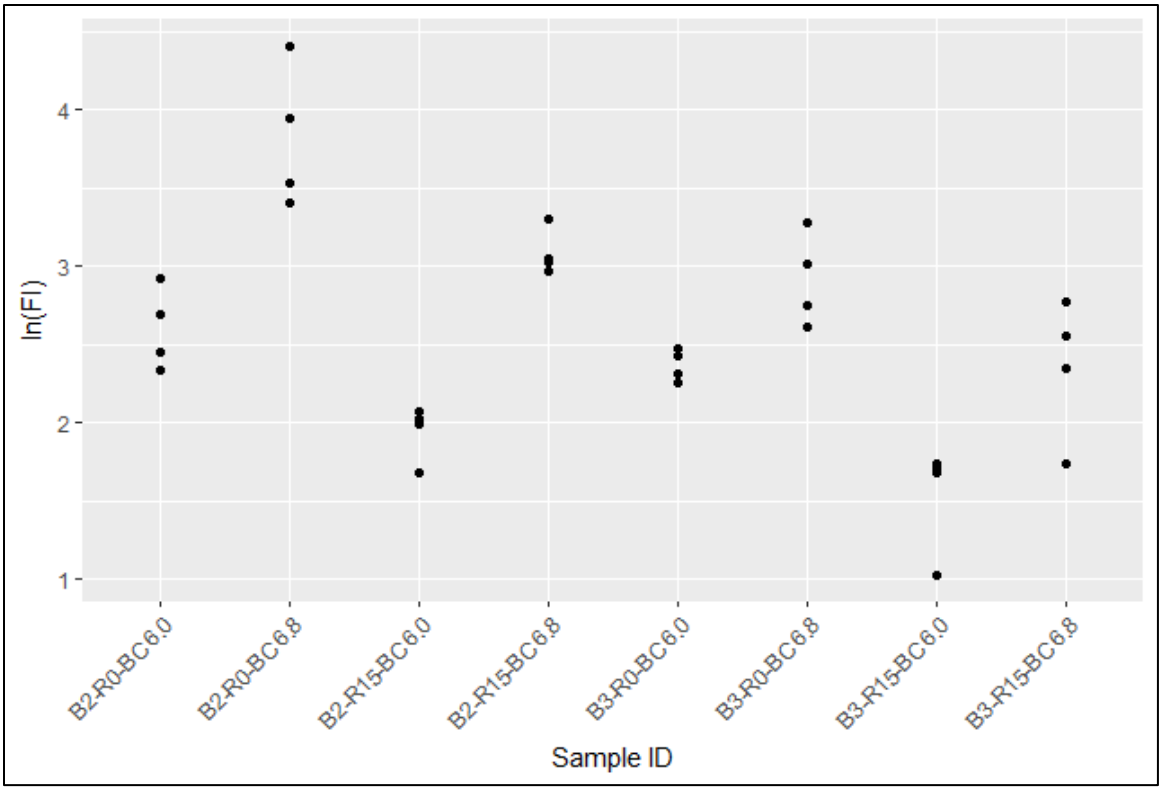

Figure 3.80. ln(FI) for each combination of RAP content, binder content, and binder grade

Note: R0= 0% RAP and R15= 15% RAP.
B2= PG 64-22, and B3 = PG 76-22.
BC6= 6% binder content and BC6.8 = 6.8% binder content.

3.6.2.6.2 Linear Regression Model for FN

To develop regression models, FN values obtained from FN tests were logarithmically transformed and linearly correlated with RAP content, binder content and binder grade. ln(FN) for all the combinations of the independent variables are shown in Figure 3.81. The developed linear model is as follows in (3.23, with the P-value of each estimated regression coefficient shown in the parentheses below them:

$$\ln(FN) = 11.422432 + 0.062581*RAP - 0.945819*BC + 1.141669*PG\ 76\text{-}22 \quad R^2 = 0.947$$

(0.0000) (0.0000) (0.0000) (0.0000)

(3.23)

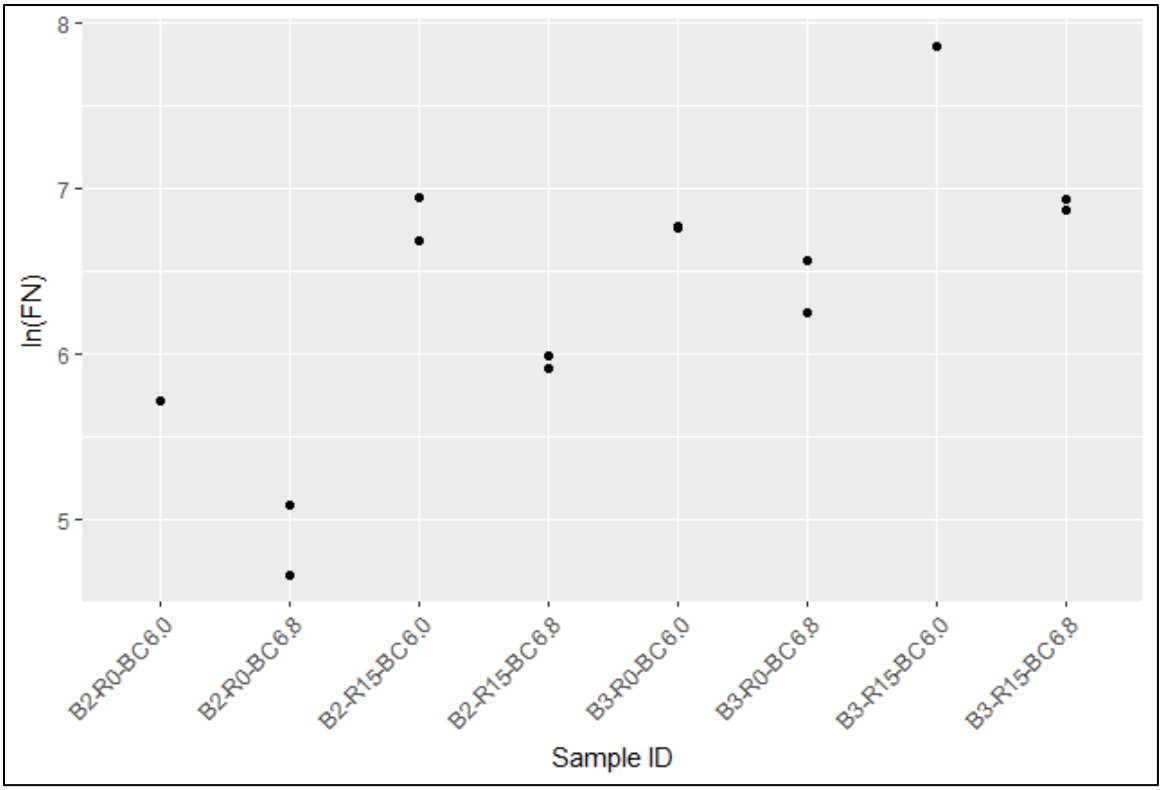

Figure 3.81. ln(FN) for each combination of RAP content, binder content, and binder grade

Note: R0= 0% RAP and R15= 15% RAP.
B2= PG 64-22, and B3 = PG 76-22.
BC6= 6% binder content and BC6.8 = 6.8% binder content

3.6.2.6.3 Finding Asphalt Mixtures with Acceptable Cracking and Rutting Performance

To predict the asphalt mixtures with acceptable cracking and rutting performance, regression models developed in Sections 3.6.2.6.1 and 3.6.2.6.2 were used. FI and FN were predicted for the mixtures with different RAP contents (0% to 20%), binder contents (5% to 8%) and binder grades (PG 64-22 and PG 76-22). All independent variables and their numerical ranges used for FI and FN predictions are presented in Table 3.17.

Predicted FI and FN for mixtures with different RAP contents, binder contents and binder grades are presented in Figure 3.82. Mixtures with FI values greater than 10 and FN values greater than 740 have acceptable cracking and rutting performance (see

Table 3.18). Analyses for the low RAP mixtures showed that there is no combination of binder content and RAP content for mixtures with PG 64-22 that will provide high cracking and rutting performance. However, it should be noted that the limits for FN and FI used as cracking and rutting performance thresholds in this study (FN>740 and FI>10) maybe too conservative. Field verification of these thresholds needs to be sought. For mixtures with 20% RAP content and PG 76-22, binder content should be between 7% and 7.6%. As RAP content decreases, required binder content decreases. For mixtures with 15% RAP, 10% RAP, 5% RAP and 0% RAP, suggested binder content ranges are 6.8%-7.2%, 6.6%-6.9%, 6.4%-6.6% and 6.2%, respectively.

Table 3.17. Independent Variables and Their Ranges for FI and FN Predictions

Variable Type	Symbol	Description	Range
Independent	RAP	RAP Content	0 to 20 with 5 increments
	BC	Binder Content	5 to 8 with 0.1 increments
Category Independent	PG	Binder Grade	PG 64-22 and PG 76-22

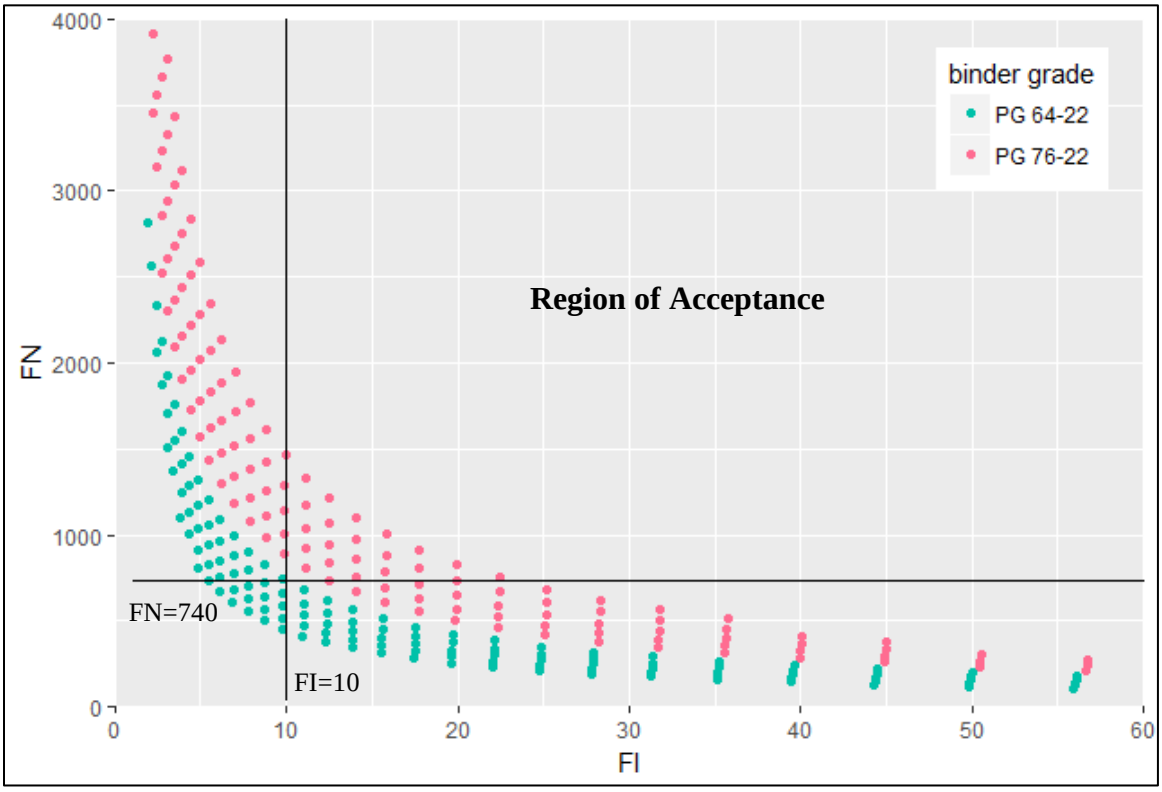

Figure 3.82. Predicted FI and FN for different RAP contents, binder contents, and binder grades

Table 3.18. Suggested Strategies - Mixtures with FN Greater than 740 and FI Greater than 10

#Sample	RAP Content (%)	Binder Content (%)	ABR[1] (%)	Active BC[2] (%)	Binder Grade	FN	FI
1	20	7.0	17.8	6.4	PG 76-22	1333	11.2
2	20	7.1	17.5	6.5	PG 76-22	1212	12.5
3	20	7.2	17.3	6.6	PG 76-22	1103	14.1
4	20	7.3	17.0	6.7	PG 76-22	1004	15.8
5	20	7.4	16.8	6.8	PG 76-22	913	17.8
6	20	7.5	16.6	6.9	PG 76-22	831	20.0
7	20	7.6	16.4	7.0	PG 76-22	756	22.4
8	15	6.8	13.7	6.4	PG 76-22	1178	11.2
9	15	6.9	13.5	6.5	PG 76-22	1071	12.5
10	15	7.0	13.3	6.6	PG 76-22	975	14.1
11	15	7.1	13.1	6.6	PG 76-22	887	15.8
12	15	7.2	13.0	6.7	PG 76-22	807	17.8
13	10	6.6	9.4	6.3	PG 76-22	1041	11.1
14	10	6.7	9.3	6.4	PG 76-22	947	12.5
15	10	6.8	9.1	6.5	PG 76-22	861	14.1
16	10	6.9	9.0	6.6	PG 76-22	783	15.8
17	5	6.4	4.9	6.3	PG 76-22	919	11.1
18	5	6.5	4.8	6.4	PG 76-22	836	12.5
19	5	6.6	4.7	6.5	PG 76-22	761	14.0
20	0	6.2	0.0	6.2	PG 76-22	812	11.1

Note: [1] Asphalt binder replacement (percentage of binder replaced by RAP)
[2] Active BC: Virgin binder + RAP binder blended into the mix. Calculated using measured blending percentage. Blending measurement process is described in Chapter 4.

4 QUANTIFICATION OF RAP BINDER BLENDING TO PROVIDE RECOMMENDATIONS FOR ASPHALT MIX DESIGN

4.1 INTRODUCTION

In order to fully evaluate the effects of RAP in HMA mixes, the level of blending between the RAP and virgin binders needs to be determined. Asphalt mixtures are designed with the assumption that full blending between RAP and virgin binders is attained. However, the actual percentage of binder blending is unknown. It is critical to quantify the level of blending between virgin and RAP binders to be able to develop strategies to improve the performance of high RAP mixtures. Since the binder of asphalt mixtures with RAP is a combination of both the virgin binder and the binder from the RAP material, increasing the total RAP percentage of the asphalt mixture will increase the amount of the aged RAP binder in the final mixture and reduce the ductility of the final product. However, in addition to the increased stiffness effect, lower blending percentages can also reduce the total binder content of the asphalt mixture and reduce cracking resistance. For instance, if the total design binder content of the asphalt mixture is 6% and 40% of the binder is coming from the RAP material, for a blending level of 50%, the actual active binder content of the mix will be 4.8% (6%*0.40*0.50+6%*0.60). By looking at the SCB test results for mixtures with different binder contents presented in Chapter 3, it can be observed that a 1.2% reduction in binder content (due to limited blending) can create significant reductions in cracking resistance. For this reason, virgin binder content of the asphalt mixture needs to be increased to account for the RAP binder that is not blended into the mixture.

In this study, blending of RAP and virgin asphalt binders is quantified using binder extraction and recovery and SCB testing. First, the asphalt binder around RAP aggregates was extracted using a chemical extraction process. Then, the extracted binder was recovered using a rotary evaporator. Recovered binder was blended with the virgin binder at different percentages (0%, 50%, and 100%) using a mixer to simulate different levels of blending and the prepared binders were used to prepare asphalt mixtures with different blending levels. SCB tests were conducted for the mixtures with 0%, 50%, and 100% blending levels to determine the average FI for each set. Specimens were also prepared to simulate the actual blending case. Using the measured FI for the three different blending levels, blending percentage versus FI curves were developed. By entering the developed curve using the FI for the mixture with actual blending, the blending percentage of the RAP and virgin binders was quantified. To determine the impact of mixing temperature on blending, additional mixtures were also prepared by using aggregates 96^{o}C (at 250 ^{o}C) warmer than the actual blending case (actual blending case aggregate mixing temperature: 154 ^{o}C). Blending percentages for two RAP sources and two gradations were determined to evaluate the impact of gradation and RAP source on blending levels.

4.2 OBJECTIVES

The main objectives of this portion of the study are to:

1. Quantify the percentage of binder around RAP materials blending into asphalt mixtures and the effect of blending on mixture performance;
2. Determine the impact of mixing temperatures on blending;
3. Determine the impact of RAP source and gradation on blending; and
4. Calculate and present the actual active binder content of high RAP asphalt mixture strategies suggested in Chapter 3.

4.3 MATERIALS AND METHODS

4.3.1 Material properties and experimental plan

In this study, asphalt specimens with 40% RAP were prepared to simulate four different cases: i) 0% blending; ii) 50% blending; iii) 100% blending; iv) actual; and v) high temperature blending (only for RAP source#2). In addition, three gradation and RAP source combinations were used to determine the impact of RAP source and gradation on blending and cracking resistance. A total of 56 SCB experiments (Section 3.4.1) were conducted. The experimental plan for the blending evaluation is given in Table 4.1.

Table 4.1. Experimental Plan

Blending (%)	Binder type	RAP (%)	Binder content (%)	Target air void (%)	Replicates	RAP source and gradation
0 50 100 Actual HT[1]	PG 64-22	40	6.4	7	4	RS#1[2]- C RS#2- F RS#2- C

Note: [1] HT: High temperature mixing (to determine the impact of mixing temperature on blending)-Only for RS#2

[2] RS#1-C: RAP source#1 with coarse gradation

[3] RS#2-F: RAP source#2 with fine gradation

For all cases, PG 64-22 binder used to prepare asphalt mixtures in Chapter 3 was used to prepare specimens for the blending evaluation. For RS#1-Coarse mixtures, gradations given in Table 3.3 were used for mixture preparation. Gradations given in Table 4.2 were used to prepare specimens for RS#2 mixtures. RAP gradations in Table 4.2 were determined with the RAP material after removing the binder using an ignition oven (AASHTO T 308-10). All RAP gradations were determined for five replicate samples and average is presented in Table 4.2 and used for batching. Gradations of RAP aggregates from chemical extraction and ignition oven methods are compared in Figure 4.1. It can be observed that although ignition oven gradations are close to the gradations for chemical extraction, gradations of the RAP aggregates processed by the ignition oven are slightly finer than the gradations for the RAP material processed by chemical extraction. This might be a result of the breakdown of aggregates due to extreme heat created

during ignition oven extraction. It might also be a result of the removal of some fine aggregate particles (dust particles passing the centrifuge filter) from the centrifuge during chemical extraction. However, since the binder-solvent mixture from the centrifuge was further filtered after extraction, particles coming out of the centrifuge are not expected to affect extracted binder properties. By following AASHTO T 308-10, the quantity of binder in RAP materials for RS#1-C, RS#2-F and RS#2-C were determined to be 6.22%, 5.26%, and 5.1%, respectively.

Table 4.2. Extracted RAP (Ignition Oven), Stockpiled Aggregate, and Target Gradations

Stockpile	RS#2-F Aggregate	RS#2-F RAP	RS#2-F Target	RS#2-C Aggregate	RS#2-C RAP	RS#2-C Target
3/4"	100.0	100.0	100.0	100.0	100.0	100
1/2"	100.0	100.0	100.0	94.0	97.6	96
3/8"	100.0	96.8	99.4	81.1	88.3	85
1/4"	85.8	78.4	84.3	61.7	69.9	63
#4	64.7	66.4	65.1	50.4	59.6	50
#8	39.9	45.1	40.4	32.1	42.0	32
#16	28.1	31.5	28.1	22.3	31.0	22
#30	21.4	23.8	21.4	16.5	24.0	17
#50	14.5	17.4	14.8	11.5	17.5	11
#100	10.1	12.9	10.2	8.5	12.8	9
#200	8.0	8.4	7.7	6.4	8.6	6.6

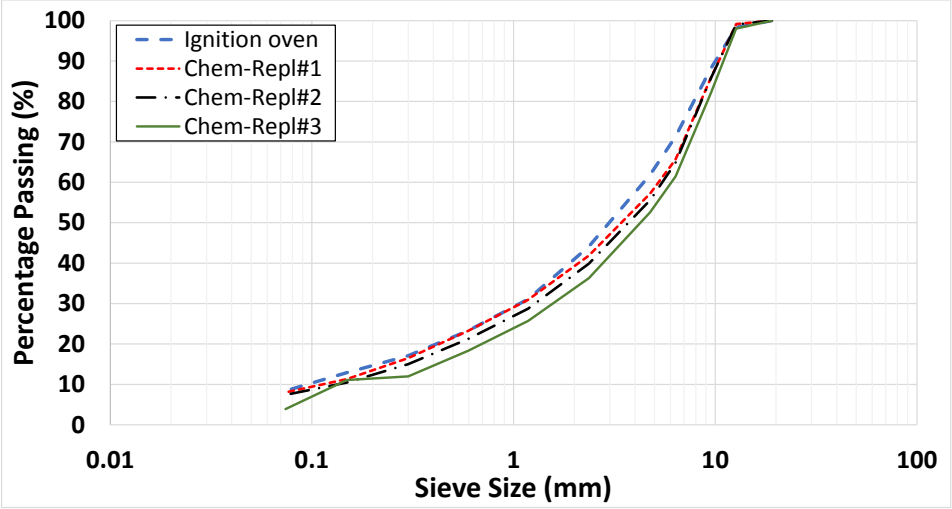

(a)

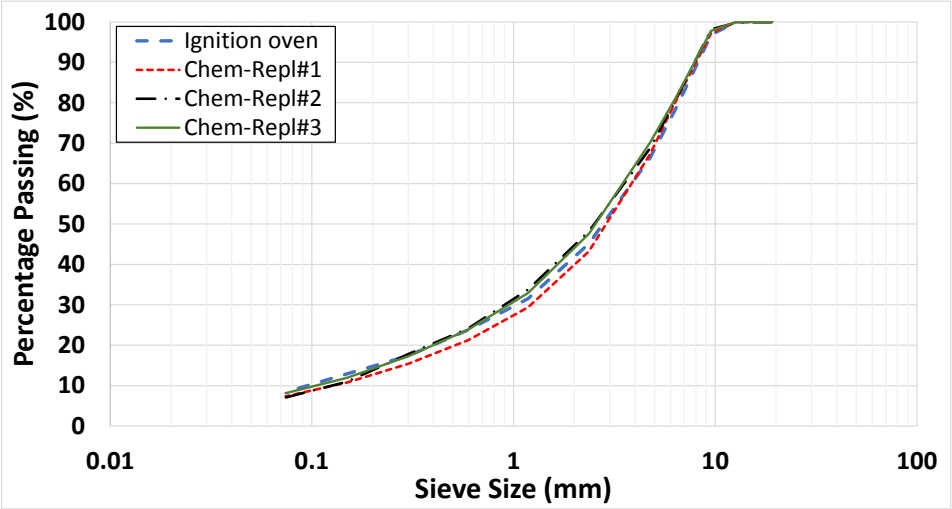

(b)

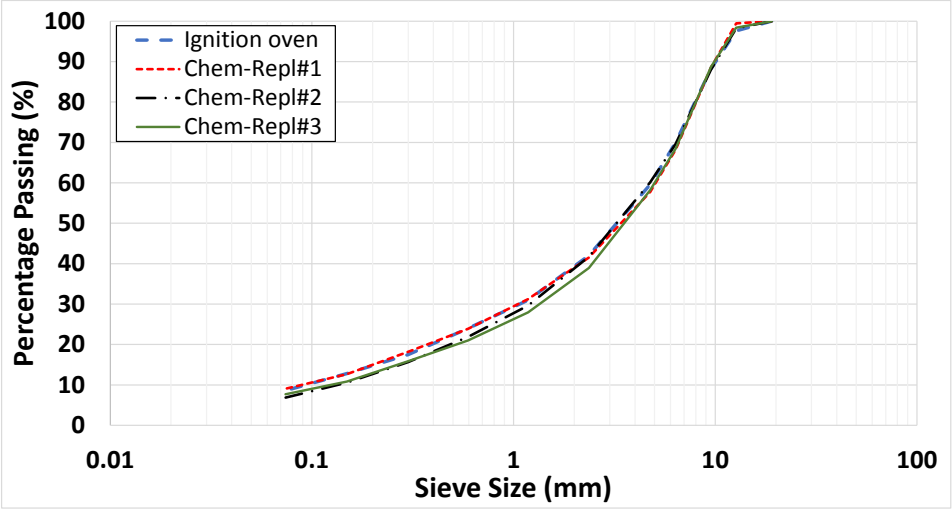

(c)

Figure 4.1. Gradation of RAP aggregates after chemical and ignition oven extraction

4.3.2 Procedure for blending quantification

The procedure followed for the extraction and recovery of RAP binder is outlined below (Figure 4.2):

1. Each RAP source was fan-dried before samples of about 500 g were individually weighed and added to the extraction bowl (Figure 4.2a).
2. The bowl was inserted into the centrifuge extractor (Figure 4.2b), the lid was secured and 450 mL of n-propyl bromide solvent was added to the top of the extractor. After 25 minutes (conditioning time), the centrifuge extractor was allowed to run and a mixture of solvent and binder was extracted (Figure 4.2c). Three additional washes with 250 mL aliquots and finally one wash with 200 mL, were conducted.
3. The extracted RAP aggregates were collected in a pan and left in a drying oven at about 120 ˚C for 3 hours to evaporate remaining solvent from the aggregates (Figure 4.2d). Sieve analyses were performed on each of the RAP sources to evaluate the performance of the extractions (Figure 4.1). RAP and virgin aggregates were then batched according to theoretical specific gravity (G_{mm}) results for mixing and compaction (Table 4.2).
4. The extracted solvent/binder mixture was filtered via vacuum filtration to remove fine particles that were suspended in the solution (Figure 4.2e).
5. The filtered solvent/binder solution was isolated by rotary evaporation (Figure 4.2f). Prior to the complete distillation of solvent from the binder, the solvent/binder solution was transferred to a centrifuge and allowed to spin for 25 minutes at 900 rpm. This allowed for enhanced separation of solvent and binder. The solution was then transferred back to the recovery flask and placed onto the rotary evaporator until the solvent was fully distilled. Nitrogen gas was then introduced at a rate of 1000 mL/min for 30 minutes.
6. The recovered binder was poured into tin cans to be used for blending and mixing (Figure 4.2g).
7. Both recovered binder and virgin binder (PG 64-22), along with the extracted RAP aggregate and virgin aggregate, were heated in the oven for 2 hours in preparation for mixing (Figure 4.2h).
8. Virgin and recovered binder were mixed in a metal container and blended using a stand mixer and hot plate to achieve uniform blending between the binder types (Figure 4.2i).
9. The blended binder was weighed, added to the combined dry aggregates and mixed (Figure 4.2j).
10. The mixed asphalt was laid out in pans and placed in the oven to reach the compaction temperature (141^{o}C).
11. The asphalt with the predetermined weight was poured into molds and compacted in a gyratory compactor to reach a compaction height of 130 mm to achieve the G_{mb} for 7% air-void content.
12. The compacted asphalt core was extruded from the gyratory mold and allowed to cool before air-void content measurements (Figure 4.2k).
13. Compacted samples were cut and notched to produce SCB test samples for testing (Section 3.4.1.1). Two samples with the thicknesses of 57 ± 2 mm were cut from each gyratory compacted sample using a high-accuracy saw (Figure 3.5a). Then the circular

samples (cores) were cut into two identical halves (Figure 3.5b) using a special jig designed and developed at Oregon State University (OSU). A notch along the axis of symmetry of each half was created with the table saw using another special cutting jig developed at OSU (Figure 3.5c). Notches were 15 ± 0.5- mm in length and 3 mm wide.

14. SCB tests were conducted with the mixtures with 0%, 50% and 100% blending levels by following AASHTO TP 105-13 to determine the average FI for each set. Specimens were also prepared to simulate actual blending and high temperature aggregate blending cases. Using the measured FI for the three different blending levels, blending percentage versus FI curves were developed. By entering the developed curve using the average FI for the mixture with actual blending and high temperature aggregate blending, percentage blending of the RAP and virgin binders was quantified.

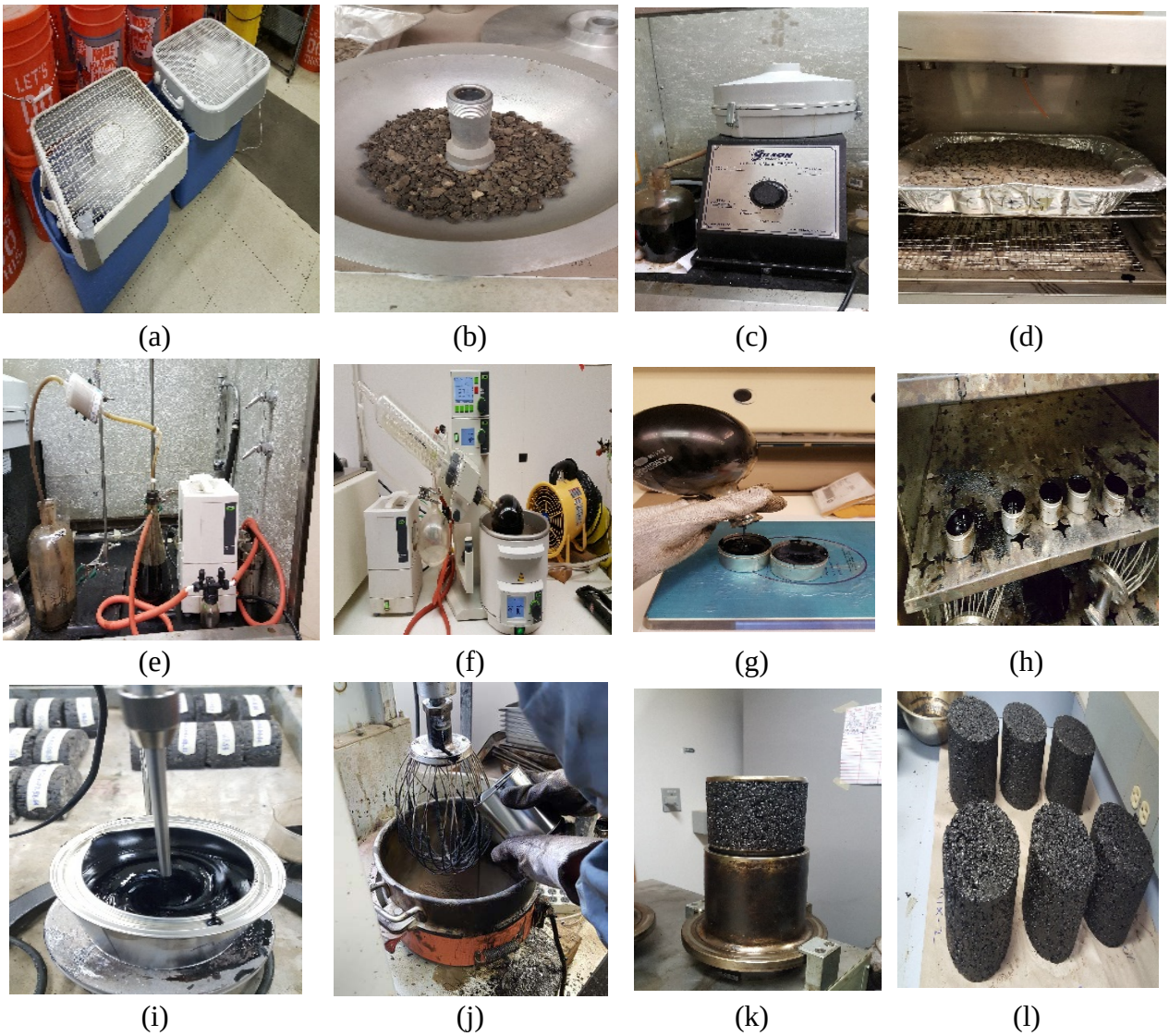

Figure 4.2. General procedure followed for extraction, recovery, blending, mixing, and compaction of RAP

4.4 RESULTS AND DISCUSSION

4.4.1 SCB test results and blending calculations

The average FIs for 0%, 50% and 100% blending cases are shown in Figure 4.3. The blue bars represent the average FI from four replicate experiments while the length of the error bar on each bar represents the variability of the measured FI for each set (error bar length = two standard deviations). It can be observed that FI increases with increasing blending. Average FI values from Figure 4.3 are used to develop the blending versus FI curves given in Figure 4.4. Polynomial curves (shown on each plot in Figure 4.4) were fitted to the average FI values to characterize the relationship between blending and FI for all three mixtures used in this study (RS#1-C, RS#2-F and RS#2-C). By entering the developed curves using the average FI for the mixture with actual (indicated as "Normal") blending and high temperature aggregate blending (indicated as "HT"), percentage blending of the RAP and virgin binders was quantified. Percentage blending for normal mixing case ("Normal") for RS#1-C, RS#2-F and RS#2-C mixtures were determined to be 57.42%, 55.04% and 57.18%, respectively. Percentage blending for high temperature (HT) mixing case for RS#2-F and RS#2-C mixtures were determined to be 42.51% and 59.16%, respectively. These results suggest that a significant percentage of the binder around the RAP aggregates (about 40% to 55%) is not blending into the mixture. Since all asphalt mixtures were designed with the assumption that there will be 100% blending between RAP and virgin binders, the final mixture has a significantly lower binder content than the design binder content. In other words, the active binder content (design binder content minus the percentage of the RAP binder not blending into the mixture) in the final mixture is less than it should be to be able resist thermal and traffic loads as designed.

The following calculations were performed to calculate the active binder content for all the mixture strategies suggested in Chapter 3 (Table 3.10) by using the measured blending percentage for RAP source #1 (57.42%) which had a RAP binder content of 6.22% measured by ignition oven extraction:

For the 45% RAP mixture with 6.8% design binder content (first row in Table 3.10), the percentage of virgin binder that is added to the mixture will be 4% of the total mixture weight (6.8% - 6.22%*45%). The remaining 2.8% of binder is expected to come from the RAP material with the assumption that 100% of RAP binder will be blending with the virgin binder. Using the measured percentage of blending for RAP source #1 (57.42%), the percentage of binder coming from the RAP aggregates will only be 1.6%. By adding 1.6% RAP binder to 4% added virgin binder, the total active binder content of the mixture will be 5.6%. In other words, the actual active binder content will be 1.2% lower than the design binder content. *For this reason, although the binder contents of the suggested high RAP strategies in Table 3.10 are significantly higher than general asphalt mixture binder contents used in Oregon, active binder contents for high RAP mixtures will mostly be within the 5.5%-6.5% range. The low performance of high RAP mixtures is likely to be a result of the lower binder content which is a result of limited blending. By considering the blending percentages in mix design and increasing virgin binder contents accordingly, performance of asphalt mixtures with high RAP contents can be improved.*

Results from Figure 4.4 also suggested that using aggregates with higher temperatures (about 96°C higher) during mixing did not have any significant effect on blending. It can also be observed from Figure 4.3 and Figure 4.4 that FIs for the RS#2-F mixture are significantly lower than the FIs for the RS#2-C mixture. The same quantity of binder used to prepare both mixtures (6.4%) is expected to create a better coating for the coarser gradation with less surface area, which resulted in higher FIs.

Results also suggested that RS#1-C mixture (Figure 4.4a) had a significantly lower FI than the RS#2-C mixture (Figure 4.4a), although both mixtures were designed to have similar gradations and the same design binder content (6.4%). The observed difference in cracking resistance for the two mixtures was expected to be a result of the higher binder content of the RAP source #1 aggregates (RS#1-C – 6.22%). By following the steps outlined above, the active binder contents for RS#1-C and RS#2-C mixtures were calculated to be:

RS#1-C: Active bind. cont. = [6.4% - (6.4%-6.22%*40%)]*0.5742+(6.4%-6.22%*40%) = **5.3%**

RS#2-C: Active bind. cont. = [6.4% - (6.4%-5.1%*40%)]*0.5742+(6.4%-5.1%*40%) = **5.5 %**

This 0.2% difference in active binder content for RS#1-C and RS#2-C mixtures is a result of assuming 100% blending in mixture design. For this reason, RAP aggregates with higher binder contents are expected to provide mixtures with less active binder content and lower cracking resistance. For this reason, RAP and virgin binder blending should be considered during mixture design. Other reasons for higher FI for RS#2-C mixtures might be softer RAP binder and/or better RAP aggregate quality.

Since blending percentages for all three mixtures are close, an average blending percentage of 56.5% is suggested to be used for mixture design and performance evaluation. However, specimens with different RAP materials and gradations should be prepared and tested to validate the results of this study.

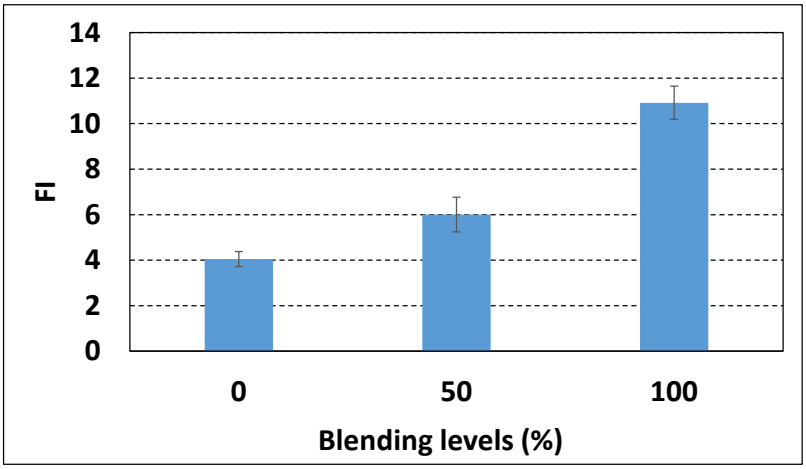

(a)

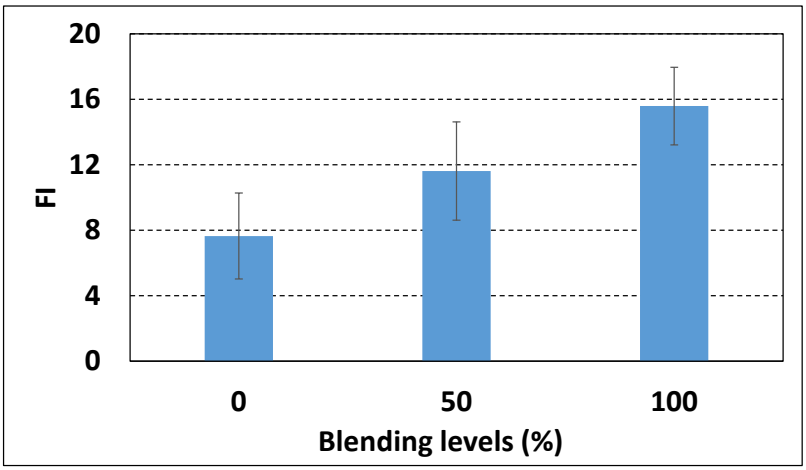

(b)

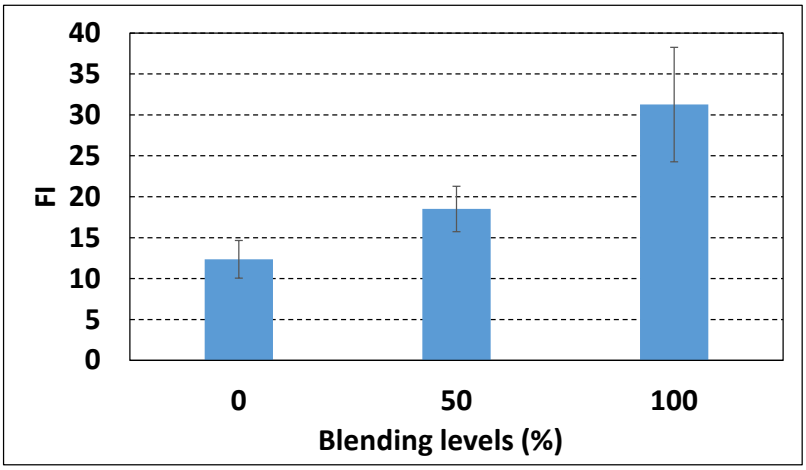

(c)

Figure 4.3. Average FIs for 0%, 50%, and 100% blending cases (a) RAP source#1- Coarse (b) RAP source#2- Fine (c) RAP source#2- Coarse

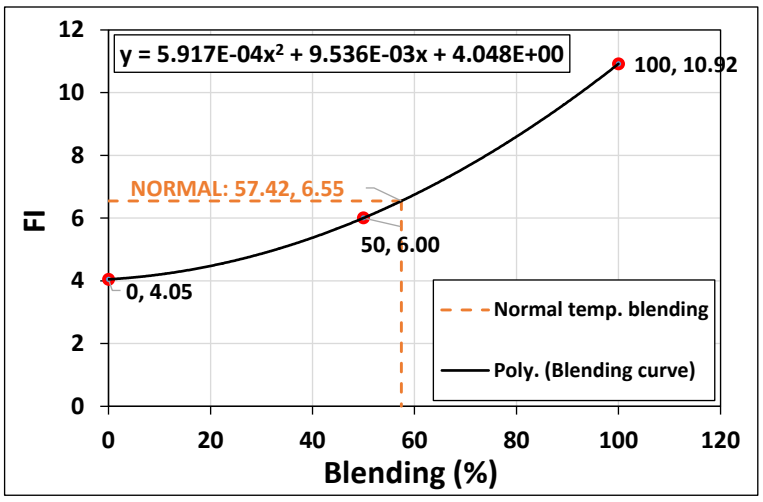

(a)

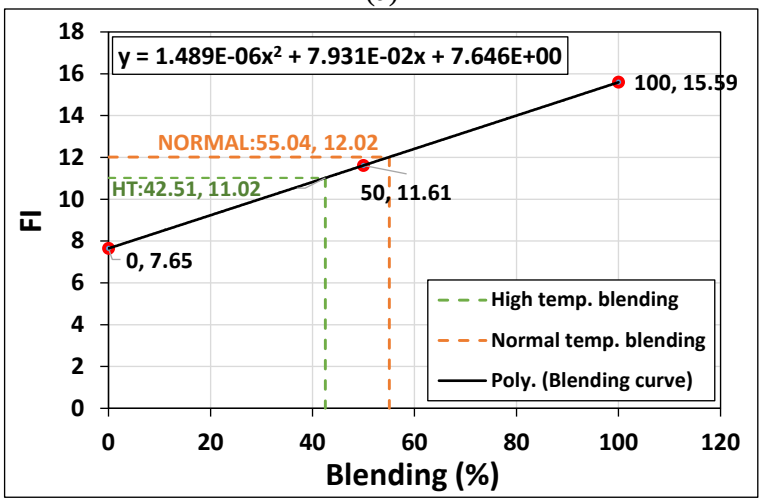

(b)

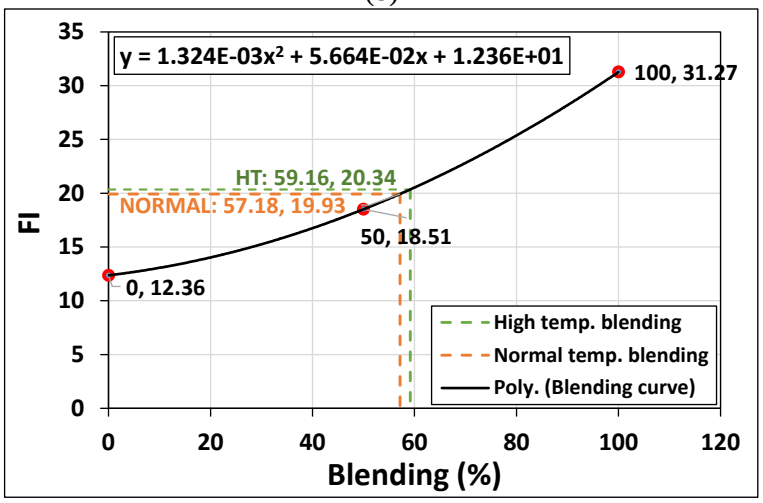

(c)

Figure 4.4. Blending curves and quantified percent blending (a) RAP source #1- Coarse (b) RAP source #2- Fine (c) RAP source #2- Coarse

4.5 SUMMARY AND CONCLUSIONS

This portion of the study focused on quantifying the blending of RAP and virgin asphalt binders using binder extraction and recovery and SCB testing. The impact of RAP source, mixing temperature and gradation on blending was also investigated.

The analyses presented in this Chapter have yielded the following conclusions:

1. FI increases with increasing blending.
2. A significant percentage of the binder around the RAP aggregates (about 40% to 55%) is not blending into the mixture. Since all asphalt mixtures were designed with the assumption that there will be 100% blending between RAP and virgin binders, the final mixture has asignificantly lower binder content than the design binder content. In other words, the active binder content (design binder content minus the percentage of the RAP binder not blending into the mixture) in the final mixture is less than it should be to be able resist thermal and traffic loads as designed.
3. Although the binder contents of the suggested high RAP strategies in Table 3.10 are significantly higher than general asphalt mixture binder contents used in Oregon, active binder contents for high RAP mixtures will mostly be within the 5.5%-6.5% range. The low performance of high RAP mixtures is likely to be a result of the lower binder content which is a consequence of limited blending. By considering the blending percentages in mix design and increasing virgin binder contents accordingly, performance of asphalt mixtures with high RAP contents can be improved.
4. Using aggregates with higher temperatures (about 96 $^{\circ}$C higher) during mixing did not have any significant effect on blending.
5. FIs for RS#2-F mixture are significantly lower than the FIs for the RS#2-C mixture. The same quantity of binder used to prepare both mixtures (6.4%) is expected to create a better coating for the coarser gradation with less surface area.
6. The 0.2% difference in active binder content for RS#1-C and RS#2-C mixtures can be considered to be one of the reasons for lower FI for the RS#1-C mix. This difference in binder content is a result of assuming 100% blending in mixture design. For this reason, RAP aggregates with higher binder contents are expected to provide mixtures with less active binder content and lower cracking resistance. For this reason, RAP and virgin binder blending should be considered during mixture design. Other reasons for higher FI for RS#2-C mixtures might be softer RAP binder and/or better RAP aggregate quality.
7. Since blending percentages for all three mixtures are close, an average blending percentage of 56.5% is suggested to be used for mixture design and performance evaluation.

5 MECHANISTIC-EMPIRICAL PAVEMENT DESIGN GUIDE (MEPDG) SIMULATIONS AND LIFE CYCLE COST ANALYSIS TO DETERMINE THE COST AND PERFORMANCE EFFECTIVENESS OF HIGH AND LOW RAP AND RAP&RAS STRATEGIES

5.1 INTRODUCTION

This portion of the study focused on development of MEPDG models (AASHTOWare 1.0™ 2008) to quantify the impact of RAP content and RAP&RAS, binder content and binder type on in-situ rutting and alligator cracking (bottom-up cracking) performance. For this purpose, Level 1 MEPDG simulations (the level with highest accuracy) were conducted by using the dynamic modulus and binder dynamic shear rheometer test results. Measured asphalt mixture properties (effective binder content) for all tested asphalt mixtures were also used to improve model predictions. In this study, MEPDG longitudinal (top-down cracking) cracking models were not used for simulations since the accuracy of these models were determined to be low (Williams and Shaidur 2013). Findings of the NCHRP 9-30 (Von Quintus et al. 2009) also suggested not including current longitudinal cracking models in the local calibration guide (NCHRP 1-40B).

In this study, a material cost-calculation tool was also developed to calculate the asphalt mixture costs for different binder contents, binder types, and RAP and RAS contents. Using the predicted performance curves and calculated material and agency costs, life-cycle cost analyses (LCCAs) were performed to determine the most cost effective strategies.

5.2 MEPDG RUTTING AND FATIGUE CRACKING MODELS

5.2.1 Fatigue Cracking Models

Miner's law is one of the most basic recursive-incremental damage accumulation methods used in fatigue cracking prediction (Miner 1945). It is based on the cumulative damage theory and defined as the ratio of number of cycles applied at each stress level to the number of cycles to failure, as shown in Equation(5.1). For fatigue cracking, the number of cycles to failure in Miner's law is defined as the number of repetitions to fatigue cracking or the allowable number of repetitions. In mechanistic-empirical (ME) pavement design, the number of repetitions to fatigue cracking are calculated for all trucks on a highway section with different loads, speeds and temperatures via transfer functions developed by using laboratory fatigue cracking test results. Then, damage created by a specific axle for a specific time interval (using load, speed and temperature for the corresponding time interval) is calculated by dividing 1 by the calculated number of repetitions to fatigue cracking. By summing up calculated damage created by all truck axles for a specific design period while considering variable traffic, climate and changing

material properties, total accumulated damage for the design period can be calculated. Fatigue cracking is assumed to occur when the accumulated damage value reaches a value of '1'.

$$DI = \sum(\Delta DI)_{j,m,l,p,T} = \sum\left(\frac{n}{N_{f-HMA}}\right)_{j,m,l,p,T} \quad \textbf{(5.1)}$$

Where:

n = Actual number of axle load applications within a specific time period

N_{f-HMA} = Allowable number of axle load applications for a flexible pavement and HMA overlays to fatigue cracking

j = Axle-load interval

m = Axle-load type (single, tandem, tridem, quad or special axle configuration)

l = Truck type using the truck classification groups included in the MEPDG

p = Month

T = Median temperature for the five temperature intervals used to subdivide each month

The most common type of model used to predict the number of load repetitions required for initiation of fatigue cracking is a function of the tensile strain and stiffness of the mix. The general form of the number of load repetitions equation (transfer function) used in MEPDG is shown in Equation (5.2) (Witczak et al. 2004).

$$N_f = Ck_1\left(\frac{1}{\varepsilon_t}\right)^{k_2}\left(\frac{1}{E}\right)^{k_3} \quad \textbf{(5.2)}$$

Where:

N_f = Number of repetitions to fatigue cracking.

ε_t = Tensile strain at the critical location.

E = Stiffness of the material.

k_1, k_2, k_3 = Laboratory regression coefficients.

C = Laboratory to field adjustment factor.

The damage transfer function for the alligator (bottom-up) cracking calculation is given in Equation (5.3).

$$FC_{Bottom} = \left(\frac{6000}{1+e^{\left(C_1 * C_1^{\delta} + C_2 * C_2^{\delta} * Log(DI_{Bottom})\right)}}\right) * \left(\frac{1}{60}\right) \quad \textbf{(5.3)}$$

Where:

FC_{Bottom} = Alligator cracking, percent of total area

C_1 = Calibration coefficient

C_2 = Calibration coefficient

C_1^{δ} $= -2 * C_2^{\delta}$

C_2^{δ} $= -2.40874 - 39.748(1 + H_{HMA})^{-2.856}$

H_{HMA} = Total HMAC thickness, inches

DI_{Bottom} = Bottom incremental damage, percent

5.2.2 Rutting Models

Rutting in the asphalt and unbound layers are separately predicted in MEPDG. Total surface rutting is calculated by summing the predicted rutting in all layers. Asphalt layer rutting is calculated by using the field-calibrated equation given below:

$$\Delta_{p(HMA)} = \varepsilon_{p(HMA)} h_{HMA} = \beta_{r_1} k_z \varepsilon_{r(HMA)} 10^{k_1} n^{k_2 \beta r 2} T^{k_2 \beta r 2} \quad \textbf{(5.4)}$$

Where:

$\Delta_{p(HMA)}$ = Accumulated permanent or plastic vertical deformation in the HMA layer/sublayer, inches

$\varepsilon_{p(HMA)}$ = Accumulated permanent or plastic axial strain in the HMA layer/sublayer, inches/inches

h_{HMA} = Thickness of the HMA layer/sublayer, inches

n = Number of axle load repetitions

T = Mix or pavement temperature, °F

k_z = Depth confinement factor, inches

$k_{1,2,3}$ = Global field calibration parameters (from the NCHRP 1-40D recalibration; k_1=-3.35412, k_2=1.5606, k_3=0.4791)

$\beta r_{1,2,3}$ = Local or mixture field calibration constants; for the global calibration, these constants were all set to 1.0

$$k_z = (C_1 + C_2 D) * 0.328196^D \quad (5.5)$$

$$C_1 = -0.1039 * (H_{HMA})^2 + 2.4868 * H_{HMA} - 17.324 \quad (5.6)$$

$$C_2 = 0.0172 * (H_{HMA})^2 - 1.7331 * H_{HMA} + 27.428 \quad (5.7)$$

Where:

D = Depth below the surface, inches

H_{HMA} = Total HMA thickness, inches

The field-calibrated equation used to calculate unbound layers' vertical deformation is given in Equation (5.8) below:

$$\delta_a(N) = \beta_{s1} k_1 \varepsilon_v h_{soil} \left(\frac{\varepsilon_0}{\varepsilon_r}\right) e^{-\left(\frac{\rho}{n}\right)^{\beta}} \quad (5.8)$$

Where:

$\delta_a(N)$ = Permanent or plastic deformation for the layer/sublayer, inches

n = Number of axle load repetitions

ε_0 = Intercept determined from laboratory repeated load permanent deformation tests, inches/inches

ε_r = resilient strain imposed in laboratory test to obtain material properties ε_0, β and ρ, inches/inches

ε_v = Average vertical resilient or elastic strain in the layer/sublayer and calculated by the structural response model, inches/inches

h_{soil} = Thickness of the unbound layer/sublayer, inches

k_1 = Global calibration coefficients; k_1 = 2.03 for granular materials and 1.35 for fine-grained materials

β_{s1} = Local calibration constant for the rutting in the unbound layers (base or subgrade); the local calibration constant was set to 1.0 for the global calibration effort. Note that β_{s1} represents base layer.

$$log\beta = -0.61119 - 0.017638(W_e) \quad (5.9)$$

$$\rho = 10^9 \left(\frac{C_0}{\left(1-(10^9)^{\beta}\right)} \right)^{\frac{1}{\beta}} \quad (5.10)$$

$$C_0 = Ln\left(\frac{a_1 {M_r}^{b_1}}{a_9 {M_r}^{b_9}}\right) = 0.0075 \quad (5.11)$$

Where:

W_e = Water content, percent

M_r = Resilient modulus of the unbound layer or sublayer, psi

$a_{1,9}$ = Regression constants; a_1=0.15 and a_9= 20.0

$b_{1,9}$ = Regression constants; b_1=0.0 and b_9= 0.0

Since rutting in aggregate base and subgrade layers is not expected to be significant in Oregon (Williams and Shaidur 2013), calibration factors for aggregate base and subgrade layers are set to 0 in this study.

5.3 LEVEL 1 MEPDG SIMULATIONS USING EXPERIMENTAL RESULTS

Three hierarchical levels of inputs are available in MEPDG (AASHTOWare 1.0™ 2008). Level 1 input represents the highest level of accuracy and requires laboratory or field test results to characterize material properties. Level 2 analysis requires binder, aggregate and general mixture properties and uses these input variables to estimate HMA stiffnesses by using correlation functions embedded in MEPDG. Level 3 analysis will provide the lowest level of accuracy. Average values for material properties for the U.S. are selected by the user as input parameters. Experiments are not conducted to measure any material properties to use as input variables for modeling.

In this study, MEPDG models were developed to quantify the impact of RAP content and RAP&RAS, binder content, and binder type on in-situ rutting and alligator cracking (bottom-up cracking) performance. For this purpose, Level 1 MEPDG simulations (the level with highest accuracy) were conducted by using the dynamic modulus (presented in Chapter 3) and binder dynamic shear rheometer test results and field calibration constants. Measured asphalt mixture properties (effective binder content) for all tested asphalt mixtures were also used to improve model predictions (APPENDIX B:). Table 5.1 shows all the cases modeled with MEPDG to

determine the impact of climate, RAP content and RAP&RAS, binder content and binder type on in-situ rutting and alligator cracking (bottom-up cracking) performance.

Table 5.1. Cases Modeled with MEPDG

Category	Binder content	RAP content	Binder grade	Climate	Traffic (AADTT)	Number of models
High RAP	6.0% 6.4% 6.8%	30% 40%	PG 58-34 PG 64-22 PG 76-22	Ontario Portland	6,000	36
RAP&RAS	6.0% 6.8%	ABR equal to 30% RAP	PG 64-22 PG 76-22	Ontario Portland	6,000	8
Low RAP	6.0% 6.8%	0% 15%	PG 64-22 PG 76-22	Ontario Portland	6,000	16

Note: [1] AADTT: Average annual daily truck traffic.

Mastersolver V2.2, a spreadsheet developed by Dr. Ramon Bonaquist of Advanced Asphalt Technologies, is used to develop master curves and develop the parameters required to perform Level 1 MEPDG analysis. APPENDIX D: shows an example of the data generated by the test equipment for the DM test, along with the procedure for developing the master curves. Calculated parameters under the MEPDGINPUT tab (Figure D-7) are used as input parameters to conduct Level 1 MEPDG analysis.

Williams and Shaidur (2013) performed a local calibration by using the pavement management system data of Oregon Department of Transportation (ODOT). In this study, alligator cracking (bottom-up) and rutting model calibration factors from Williams and Shaidur (2013) (Table 5.2) were used to perform Level 1 MEPDG simulations. Calibration coefficients from local calibration and Level 1 inputs are expected to provide realistic performance predictions for the cases analyzed in this study. However, it should be noted that MEPDG longitudinal (top-down cracking) cracking models were not used for simulations since the accuracy of these models were determined to be low (Williams and Shaidur 2013). Findings of NCHRP 9-30 (Von Quintus et al. 2009) also suggested excluding current longitudinal cracking models in the local calibration guide (NCHRP 1-40B)

Table 5.2. Summary of Calibration Factors for Oregon (Williams and Shaidur 2013).

Calibration factor	MEPDG default value	Calibrated value
Alligator cracking		

C1	1	0.560
C2	1	0.225
C3	6,000	6,000
AC rutting		
βr1	1	1.48
βr2	1	1.00
βr3	1	0.90
Base rutting		
βs1	1	0
Subgrade rutting		
βs1	1	0

MEPDG models were developed for identical structures for all cases while the material properties for new asphalt overlays used the dynamic modulus test results obtained for different mixture types. The typical structure used for model development for the initial rehabilitation is shown in Figure 5.1a. A full friction interface is assumed for all layers. MEPDG rehabilitation analysis was conducted. The top 1 inch of the existing 3-inch layer was milled for the analysis (a 2 inch thick layer was left for modeling). After milling, a 3-inch-thick asphalt overlay was constructed as the new layer. Level 1 parameters were entered for the top 3 inch overlay while the existing asphalt layer was assumed to in "Fair" condition with a PG64-22 binder. After running the initial rehabilitation model and finding the service life, the top layer from the model was milled and a 2nd 3-inch overlay was constructed (Figure 5.1b). These simulations were continued until the total service life of modeled structures exceed 50 years, which is the analysis period for LCCA. If a structure did not fail within a 50-year period, a 50 year design life was assumed and used for the LCCA. In this study, alligator cracking is considered to be the only distress for LCCA since almost none of the sections were failing from rutting.

Analyses were conducted with an initial traffic level of 6,000 average annual daily truck traffic (AADTT) and an annual traffic growth rate of 3%. For the 2nd and 3rd rehabilitation models, the previous year's traffic from the last rehabilitation was used as the starting traffic level for the following rehabilitation to maintain the continuous traffic growth for the section. Climate stations from Portland and Ontario were used for simulations. Typical air temperature distributions for both cities are given in Figure 5.2. Since Ontario is colder in winter and warmer in summer when compared to Portland, cracking and rutting accumulation rates are expected to be higher.

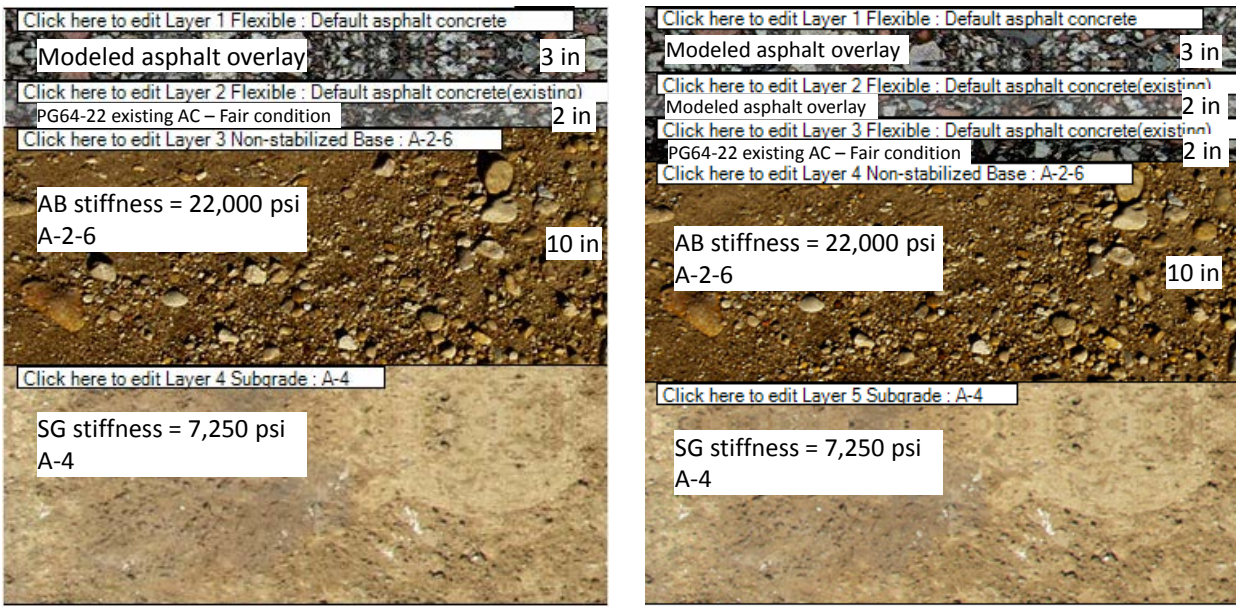

Figure 5.1. Cross sections of structures used for MEPDG modeling (a) initial rehabilitation (overlay) b) Structure after the 2nd rehabilitation.

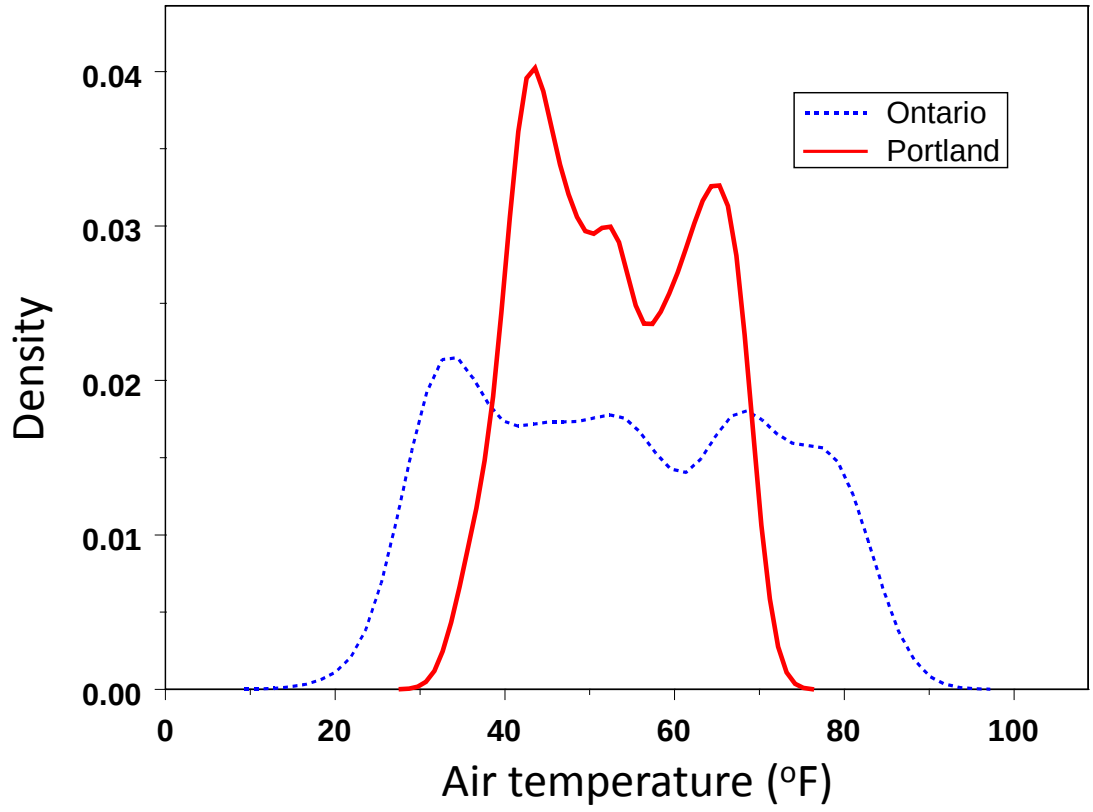

Figure 5.2. Air temperature distributions for Portland and Ontario.

5.4 COST CALCULATION TOOL

The use of RAP and RAS in Hot Mix Asphalt (HMA) paving is often considered a cost-saving measure. Although it can make the pavement more susceptible to cracking failure, it is considered a sustainable alternative to asphalt mixtures with all-virgin materials, both in terms of cost and environmental impacts. However, contractors and agencies who are not able to accurately quantify savings brought on by using RAP or RAS in HMA mixes may be discouraged from using these materials due to their reduction in HMA cracking resistance. Cost analysis becomes even more difficult when different binder types are incorporated to the mix, which is a practice discussed in this study for combatting cracking susceptibility. The culmination of these factors yields a necessity for a simple way to analyze different mix design options.

In this study, a tool was created that allows the users to compare mix design strategies against one another in order to calculate the potential savings they can realize by choosing mix designs with different RAP and RAS contents, as well as different binder types and binder contents. This simple tool, created using a Microsoft Excel spreadsheet, is meant to increase incentive for users

to use recycled materials in their HMA mixes, thereby increasing the sustainability and cost-effectiveness of asphalt pavement construction. Given the geometry of a pavement section and pertinent material cost data, the contractor and/or agency can evaluate the total estimated cost of implementing a particular mix design strategy for their project.

A screenshot of the developed tool's input and output tabs are given in Figure 5.3 and Figure 5.4, respectively. In order to use the tool, the user must input data about their HMA mix design, such as target density, binder content and recycled materials content. Input data about the geometry of the pavement section, such as length, lane width, number of lanes and compacted layer thickness, should also be entered. The tool will automatically calculate the volume and weight of HMA material that is anticipated for the target density and pavement section geometry. The user must also input cost data for the materials. The user can input their unit costs for binder, aggregate and recycled materials (RAP and RAS). Input fields are shown in orange with blue text and calculated fields are shown in gray with orange text. The total mix design cost for the pavement section is shown at the bottom of each mix design spreadsheet in dark gray text.

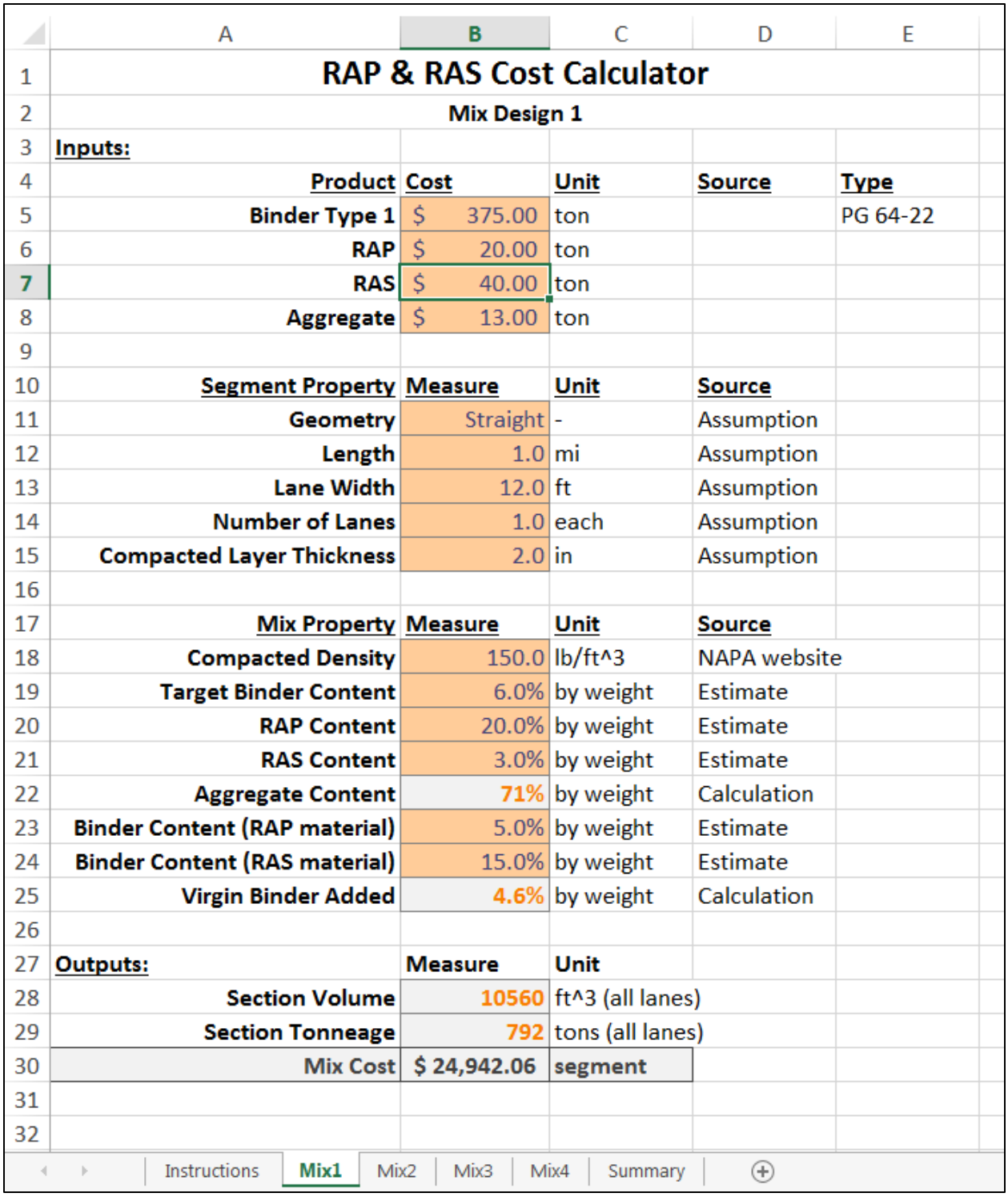

	A	B	C	D	E
1	**RAP & RAS Cost Calculator**				
2	**Mix Design 1**				
3	**Inputs:**				
4	**Product**	**Cost**	**Unit**	**Source**	**Type**
5	**Binder Type 1**	$ 375.00	ton		PG 64-22
6	**RAP**	$ 20.00	ton		
7	**RAS**	$ 40.00	ton		
8	**Aggregate**	$ 13.00	ton		
9					
10	**Segment Property**	**Measure**	**Unit**	**Source**	
11	**Geometry**	Straight	-	Assumption	
12	**Length**	1.0	mi	Assumption	
13	**Lane Width**	12.0	ft	Assumption	
14	**Number of Lanes**	1.0	each	Assumption	
15	**Compacted Layer Thickness**	2.0	in	Assumption	
16					
17	**Mix Property**	**Measure**	**Unit**	**Source**	
18	**Compacted Density**	150.0	lb/ft^3	NAPA website	
19	**Target Binder Content**	6.0%	by weight	Estimate	
20	**RAP Content**	20.0%	by weight	Estimate	
21	**RAS Content**	3.0%	by weight	Estimate	
22	**Aggregate Content**	71%	by weight	Calculation	
23	**Binder Content (RAP material)**	5.0%	by weight	Estimate	
24	**Binder Content (RAS material)**	15.0%	by weight	Estimate	
25	**Virgin Binder Added**	4.6%	by weight	Calculation	
26					
27	**Outputs:**	**Measure**	**Unit**		
28	**Section Volume**	10560	ft^3 (all lanes)		
29	**Section Tonneage**	792	tons (all lanes)		
30	**Mix Cost**	**$ 24,942.06**	**segment**		
31					
32					

Instructions | Mix1 | Mix2 | Mix3 | Mix4 | Summary

Figure 5.3. Cost calculation tool input tab

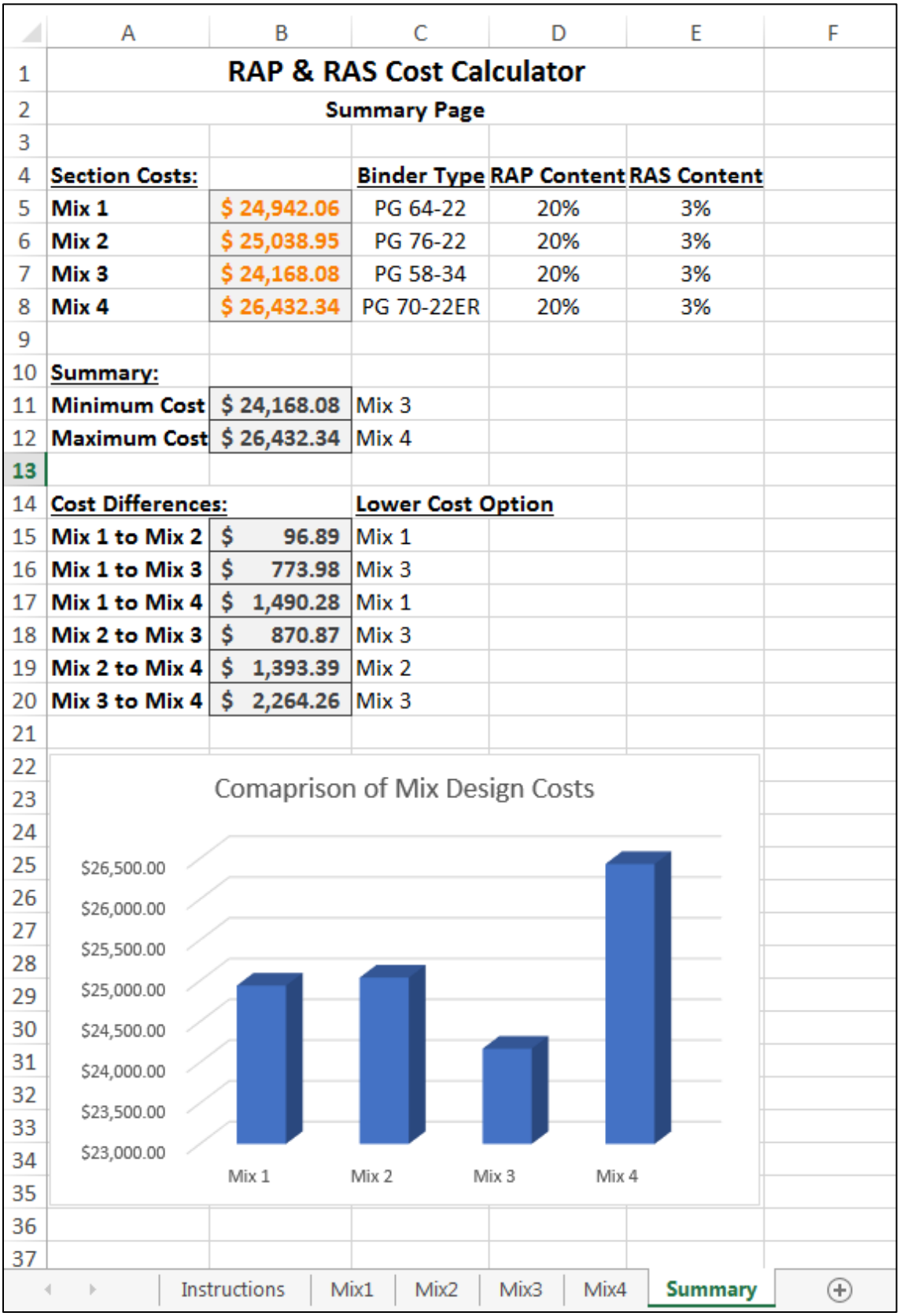

Figure 5.4. Cost calculation tool output tab

The tool can compare up to four different mix strategies. This means the user can evaluate differences in total cost for up to four different binder types and/or RAP/RAS contents. A summary spreadsheet compares the various mix design options (Figure 5.4). This sheet shows the cost differences between each individual mix design, as well as maximum and minimum cost options. The lowest and highest cost options are indicated. A simple bar chart shows a side-by-side comparison of each mix design strategy in order to visualize the costs of each option.

In this study, the following costs were used to calculate the total material cost of asphalt mixtures:

- RAP: $20/ton
- RAS: $40/ton
- Aggregate: $13/ton
- PG58-34 binder: $425/ton
- PG64-22 binder: $375/ton
- PG76-22 binder: $450/ton

This tool is meant to allow for contactors and agencies to make preliminary comparisons of mix design strategies as an aid for decision making. The tool is limited by the fact that it assumes a straight section geometry for the pavement section. Its accuracy may decrease if a curved pavement section is used as an input. It also does not account for variability in compacted density. It assumes a completely homogeneous pavement structure throughout the section of interest. This tool is not intended to be used for project bidding and the costs for each mix design option should be checked before using this information for such a purpose.

5.5 LIFE-CYCLE COST ANALYSIS

In this study, life-cycle cost analyses (LCCAs) were performed by using the service lives for pavement structures obtained from MEPDG simulations described in Section 5.3. Material cost of each strategy (for the cases outlined in Table 5.1) were calculated by using the cost calculation tool described in Section 5.4. Material production costs, plant operation costs and profit were not considered in the analysis. First, analyses were performed by only considering material costs to be able to compare the impact of RAP content and RAP&RAS, binder content, binder grade and climate on life cycle costs. Then, analyses were performed by considering agency costs that were comprised of material, equipment, labor, traffic handling and lane closure costs.

In this study, each section was assumed to be a single-lane having a width of 12 ft (3.7 m) and a length of 1 mile and material costs were calculated for all the sections based on the thicknesses. The cost calculation tool described in Section 5.4 was used to estimate material costs.

Costs corresponding to lane closure and traffic handling were considered to be 1,000 dollars per day per lane (Herbsman and Glagola 1998). North Carolina Department of Transportation (NCDOT) (2014) has reported the rate of application of asphalt pavement to be around 200 to 500 tons/day. In order to estimate operation days, lane closure and traffic handling costs, a rate of application of 500 tons/day was assumed for overlays. Since each 1-mile section requires about 1,200 tons of asphalt, lane closure and traffic handling costs for a 1-mile 1-lane section was assumed to be 2,400 dollars ([1,200tons/500ton/day]*$1,000/day).

Based on the data obtained from Berkeley Lab (Berkeley Lab 2017), equipment and total labor costs for an asphalt overlay were estimated using the following relationship:

Equipment and total labor costs for asphalt overlay = 0.19*(total construction costs including material costs).

Total agency costs were calculated by summing up the equipment, total labor, material, traffic handling and lane closure costs. After finding the service lives for each strategy, agency costs were estimated for each year at which the treatment was applied. Net present value (NPV) of agency costs were determined afterwards using a 4 percent interest rate for a 50 year analysis period by using Equation (5.12). Analyses were also performed with a 5 percent interest rate to determine the impact of interest rates on cost effectiveness of each strategy. At the end of the analysis period, the NPV of the salvage value of the pavements were computed as the agency benefits and added to NPV of agency costs.

$$NPV = \sum_{t=0}^{T} \frac{C_t}{(1+r)^t} \quad \textbf{(5.12)}$$

Where:

C_t = estimated agency costs at year t,

r = interest rate, and

T = number of time periods.

Example Calculation

For the cases with PG64-22 binder, 0% RAP, the Portland climate, and 6% and 6.8% binder content, MEPDG simulations were performed by using the laboratory test results as the input parameters. Service lives for the sections with 6% and 6.8% binder contents were determined to be 17.67 and 30.67 years, respectively. Using the cost calculation tool, material costs were calculated to be $41,247 and $44,688 for a 3 inch overlay construction for the 1-mile 1-lane section for sections with 6% and 6.8% binder contents, respectively. After the pavement failed, 1-inch of asphalt was milled and another 3 inch overlay was constructed. For this reason, material costs for the overlays following the initial construction are equal to the cost for the initial construction. Milling costs were not used for the analysis. Figure 5.5 shows example diagrams used for LCCA. Using Equation (5.13)and (5.14), NPV for both cases were calculated as follows:

$$\mathrm{NPV}_{6\%\mathrm{BC}} = \frac{\$41{,}247}{(1+0.04)^{0}} + \frac{\$41{,}247}{(1+0.04)^{17.67}} - \frac{17.67}{50} \cdot \frac{\$41{,}247}{(1+0.04)^{50}} = \$59{,}822 \quad \textbf{(5.13)}$$

$$\mathrm{NPV}_{6.8\%\mathrm{BC}} = \frac{\$44{,}688}{(1+0.04)^{0}} + \frac{\$44{,}688}{(1+0.04)^{30.67}} - \frac{30.67}{50} \cdot \frac{\$44{,}688}{(1+0.04)^{50}} = \$54{,}251 \quad \textbf{(5.14)}$$

It can be observed that although material cost for the asphalt mixture with 6.8% binder content is higher than the mixture with 6% binder content, the life-cycle cost for the mixture with 6% binder is higher due to the significantly lower service life. In other words, increasing binder content from 6% to 6.8% created a high-performance mixture that will cost less when the 50-year analysis period is considered.

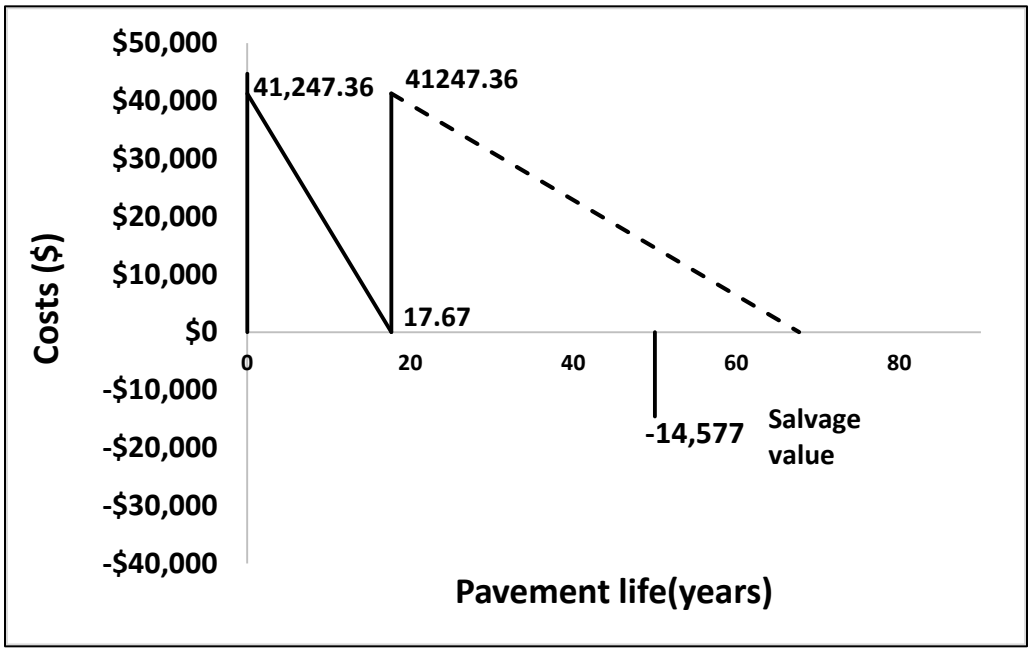

(a)

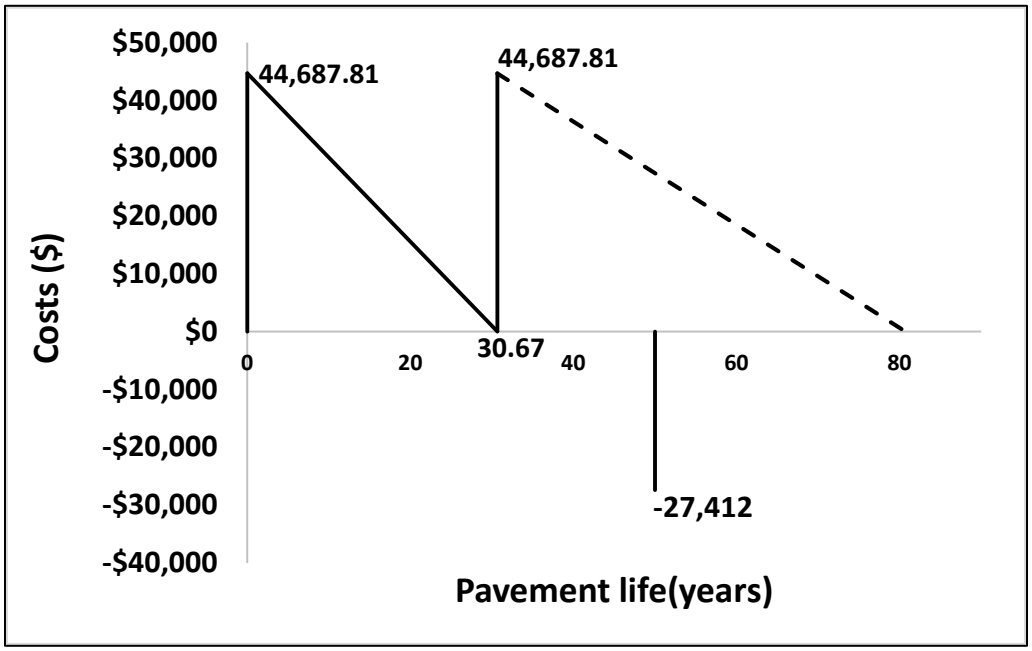

(b)

Figure 5.5. Diagrams used for LCCA (a) PG64-22, 0% RAP, and Portland climate, and 6% binder content (b) PG64-22, 0% RAP, and Portland climate, and 6.8% binder content.

5.6 RESULTS AND DISCUSSION

In this section, results of the MEPDG simulations are presented. MEPDG predictions, material costs and LCCA are used to evaluate the cost effectiveness of asphalt mixtures with different RAP content and RAP&RAS, binder content and binder type. LCCAs were performed by only considering material costs (just raw material costs, production costs are not considered) and by considering total agency costs including material, equipment, labor, traffic handling and lane closure costs.

5.6.1 MEPDG Performance Predictions

Level 1 MEPDG simulations were performed using the input parameters given in Section 5.3. Predicted asphalt concrete rutting for all the 30% and 40% RAP cases (Table 5.1) for Portland and Ontario climates are shown in Figure 5.6. Asphalt concrete rutting for all sections for Portland and Ontario climates are given in Figure 5.7 and Figure 5.8, respectively. It can be observed that the rutting accumulation rate for Ontario is significantly higher than the Portland climate due to higher summer temperatures for Ontario (Figure 5.2). Binder type was observed to be the most significant factor controlling asphalt concrete rutting. This result agrees with the flow number test results given in Chapter 3 (see Table 3.8). It was also observed that increasing binder content and decreasing RAP content would increase rutting. Results also show that none of the sections fail from rutting within the first 15 years for failure criteria of 0.5 inch rut depth while majority of the sections do not fail within the first 25 years. Since asphalt aging is going to significantly increase asphalt stiffness during this long time period, it is highly likely that none of the sections will fail from rutting. For this reason, alligator cracking was used as the only failure criteria for the LCCA.

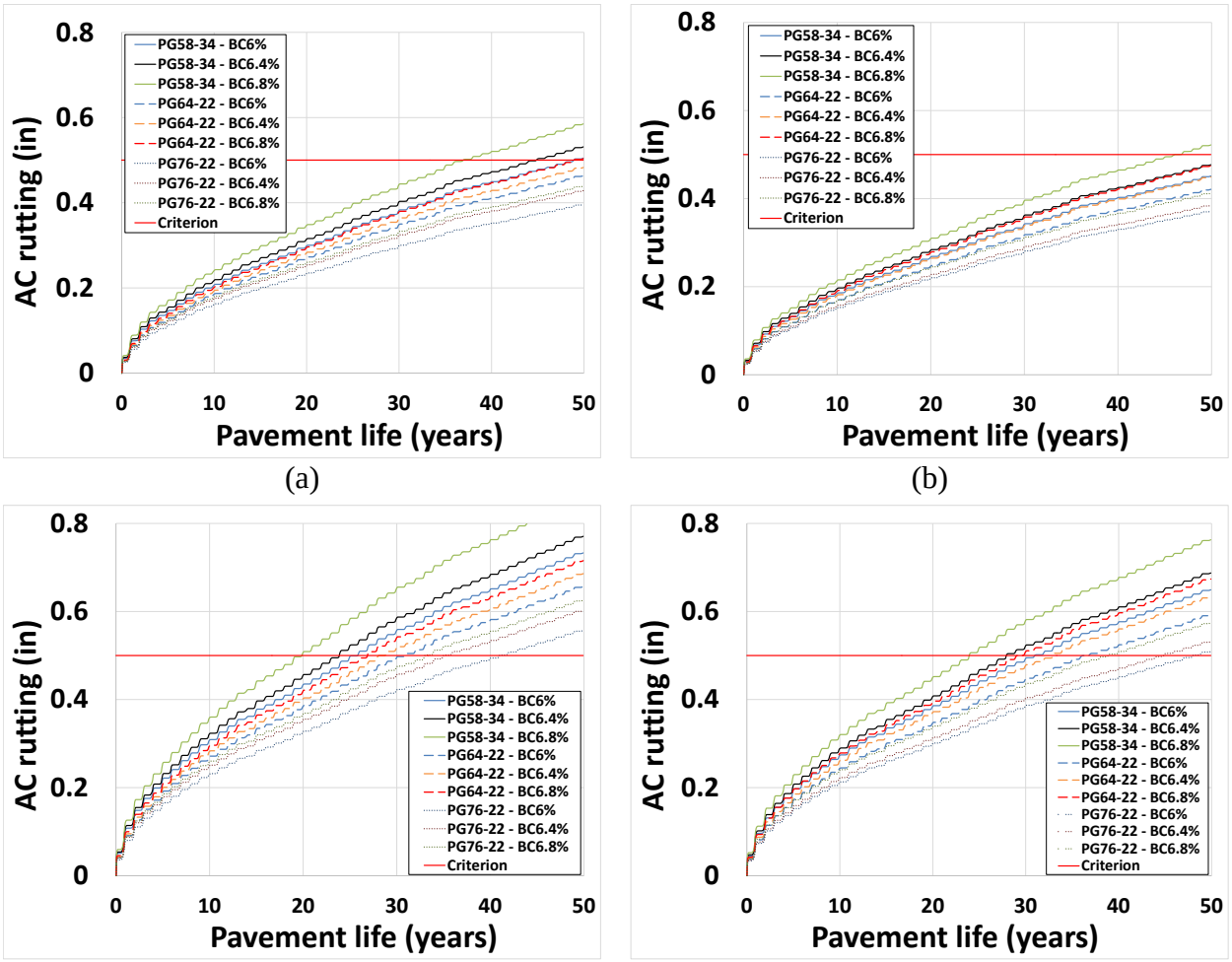

Figure 5.6. Predicted asphalt concrete (AC) rutting for mixes with 30% and 40% RAP (a) Portland – 30% RAP (b) Portland – 40% RAP (c) Ontario – 30% RAP (d) Ontario – 40% RAP.

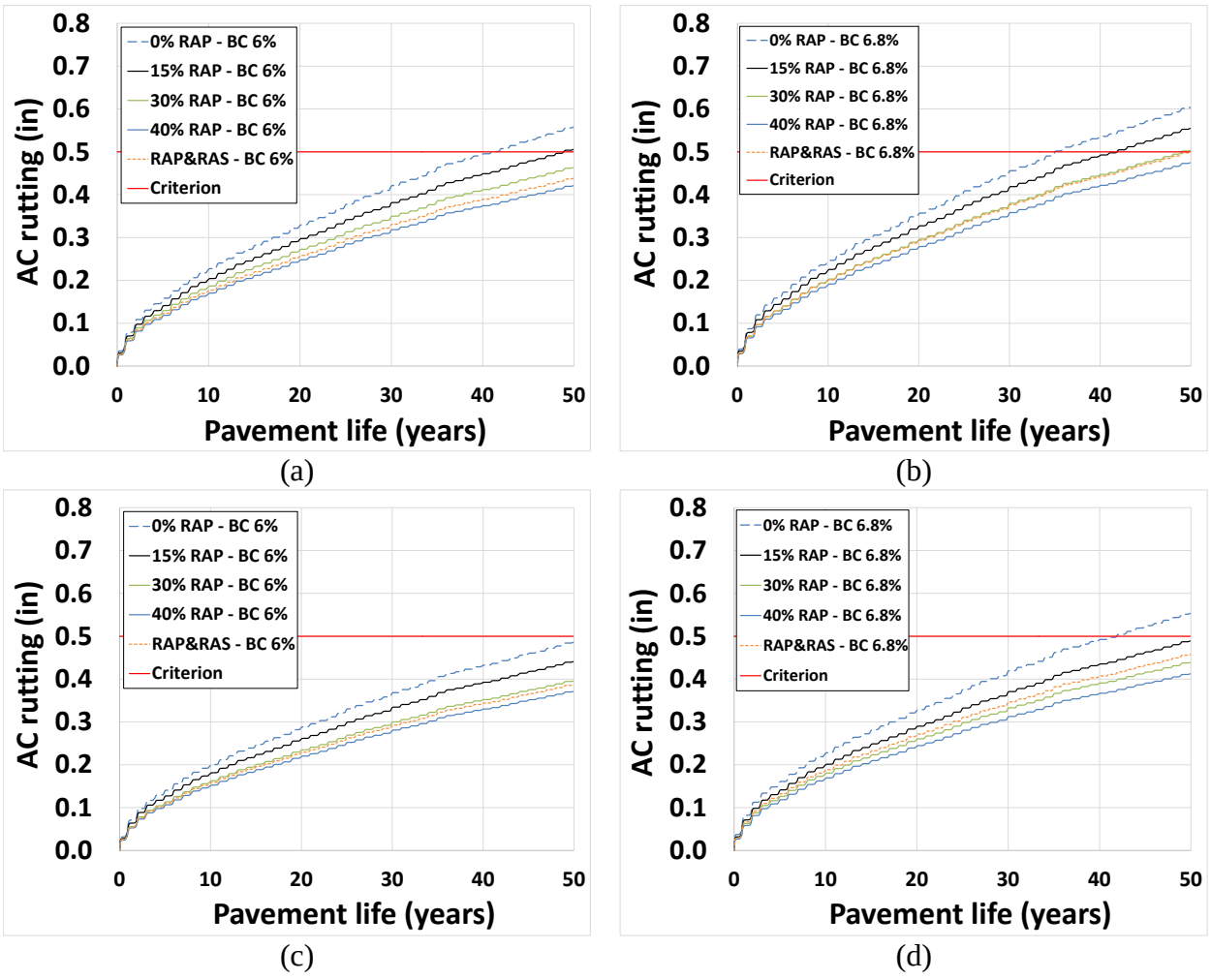

Figure 5.7. Predicted asphalt concrete (AC) rutting for Portland for mixes with PG64-22 and PG76-22 binders (a) PG64-22 – 6% binder content (b) PG64-22 – 6.8% binder content (c) PG76-22 – 6% binder content (d) PG76-22 – 6.8% binder content.

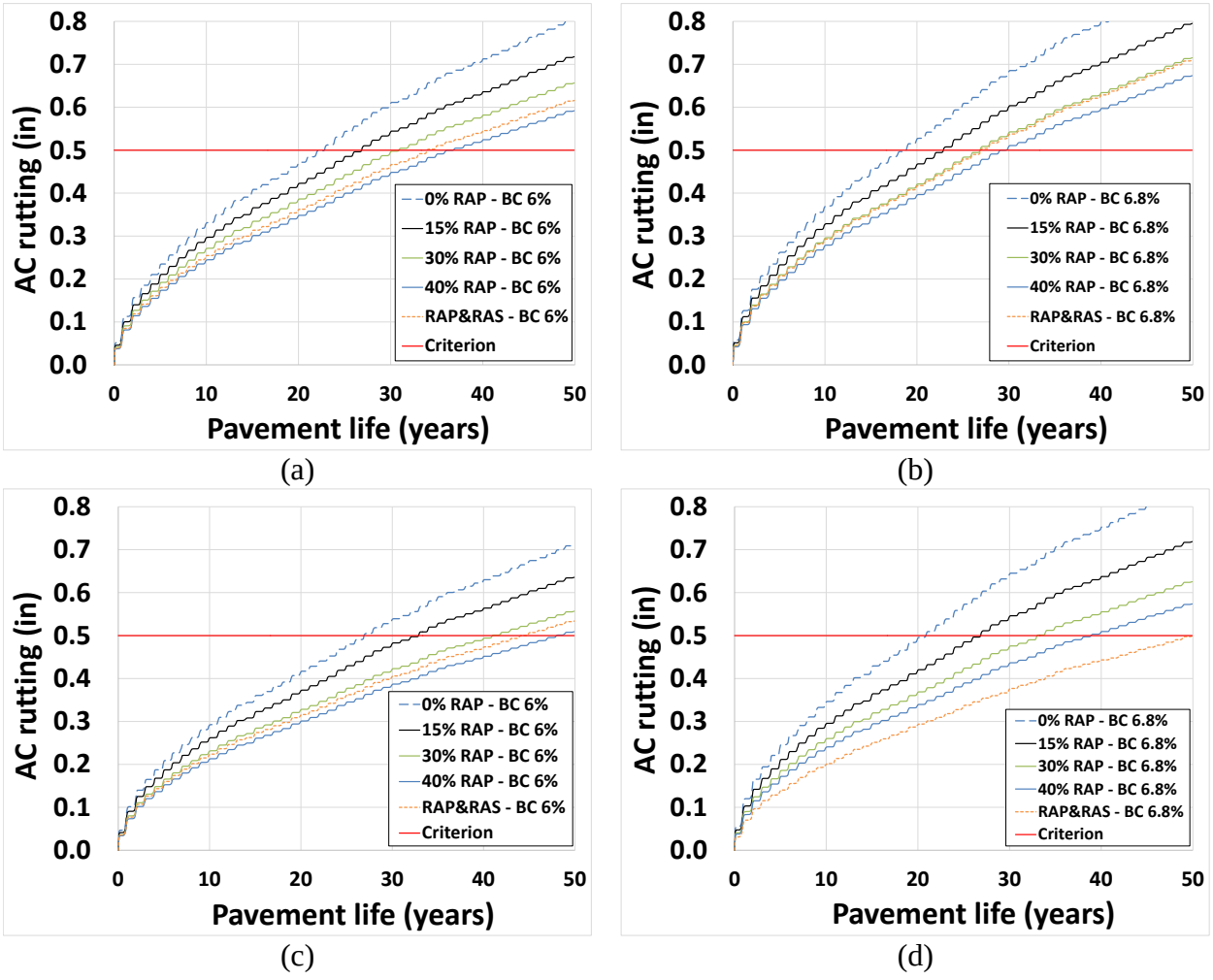

Figure 5.8. Predicted asphalt concrete (AC) rutting for Ontario for mixes with PG64-22 and PG76-22 binders (a) PG64-22 – 6% binder content (b) PG64-22 – 6.8% binder content (c) PG76-22 – 6% binder content (d) PG76-22 – 6.8% binder content.

Predicted bottom-up cracking for all the 30% and 40% RAP cases (Table 5.1) for Portland and Ontario climates are shown in Figure 5.9. Bottom-up cracking for all sections for Portland and Ontario climates are given in Figure 5.10 and Figure 5.11, respectively. It can be observed that the cracking accumulation rate for Ontario is higher than the Portland climate due to lower winter temperatures for Ontario (Figure 5.2). Binder content was observed to be most significant factor controlling bottom-up cracking. This result agrees with the SCB test results given in Chapter 3 (see Table 3.7). Increasing binder content and decreasing RAP content was also observed to decrease cracking accumulation. For the sections with PG76-22 binder, cracking performance was observed to be significantly lower. Increasing binder content and decreasing RAP content for this binder type did not appear to create significant changes in performance. However, it should be noted that none of the cases simulated in this report are for the asphalt mixture strategies suggested in Chapter 3. Asphalt mixtures with PG76-22 binder and higher binder contents (7.2% to 7.8%) can create mixtures highly resistant to both rutting and cracking.

Dynamic modulus tests should be conducted with the suggested mixtures to be able to develop MEPDG models and simulate their rutting and cracking performances.

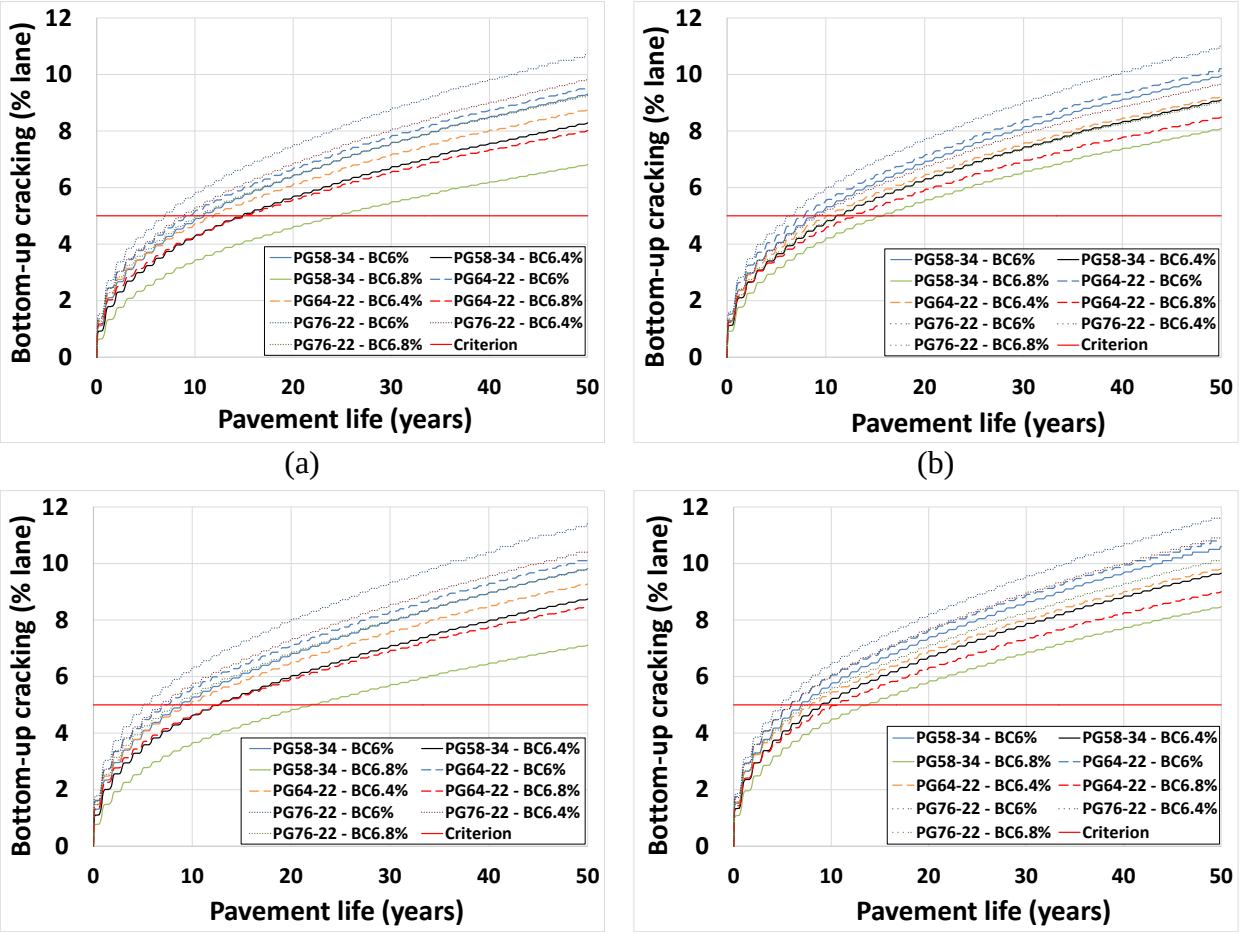

Figure 5.9. Predicted bottom-up cracking (alligator) for mixes with 30% and 40% RAP (a) Portland – 30% RAP (b) Portland – 40% RAP (c) Ontario – 30% RAP (d) Ontario – 40% RAP.

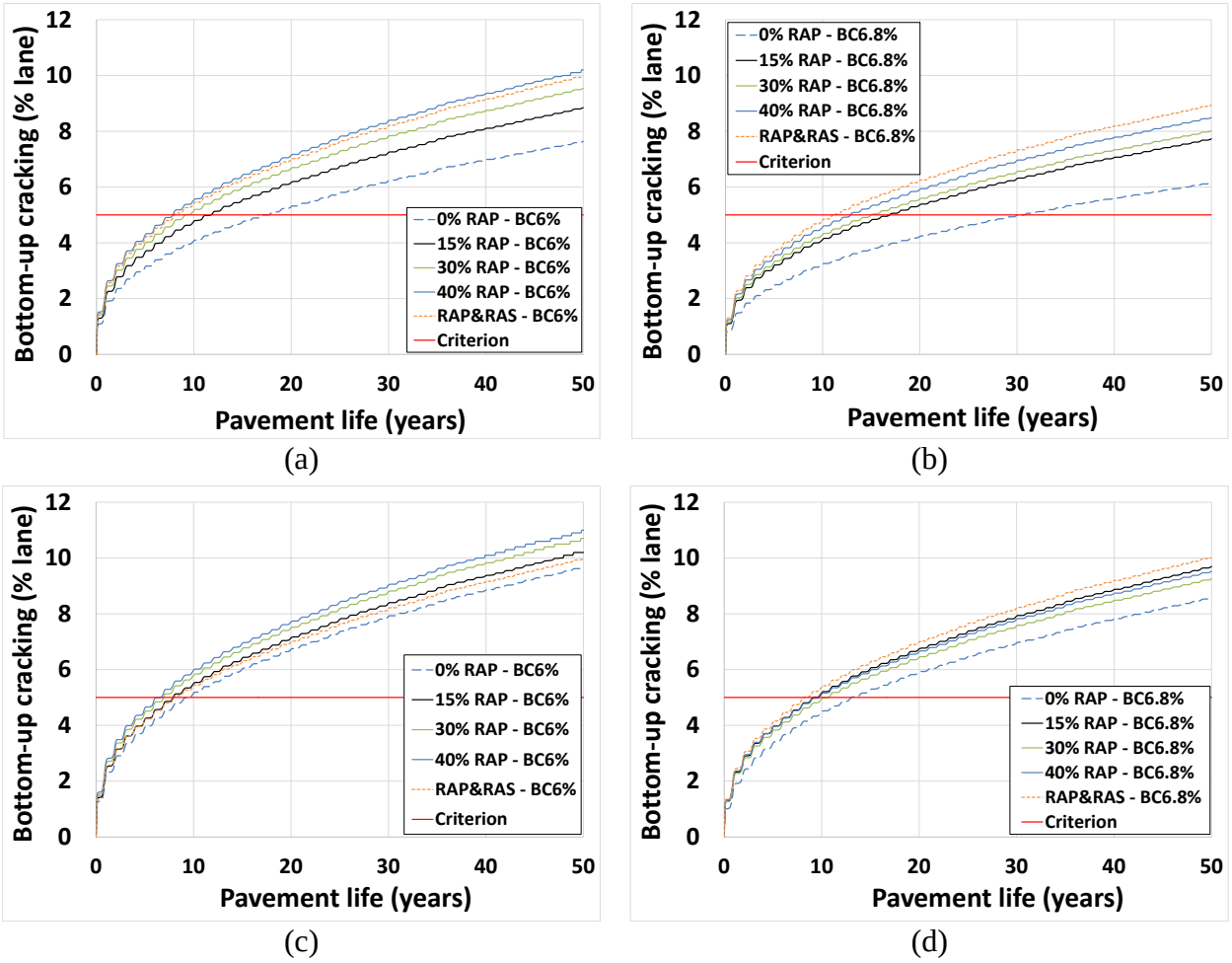

Figure 5.10. Predicted bottom-up cracking (alligator) for Portland for mixes with PG64-22 and PG76-22 binders (a) PG64-22 – 6% binder content (b) PG64-22 – 6.8% binder content (c) PG76-22 – 6% binder content (d) PG76-22 – 6.8% binder content.

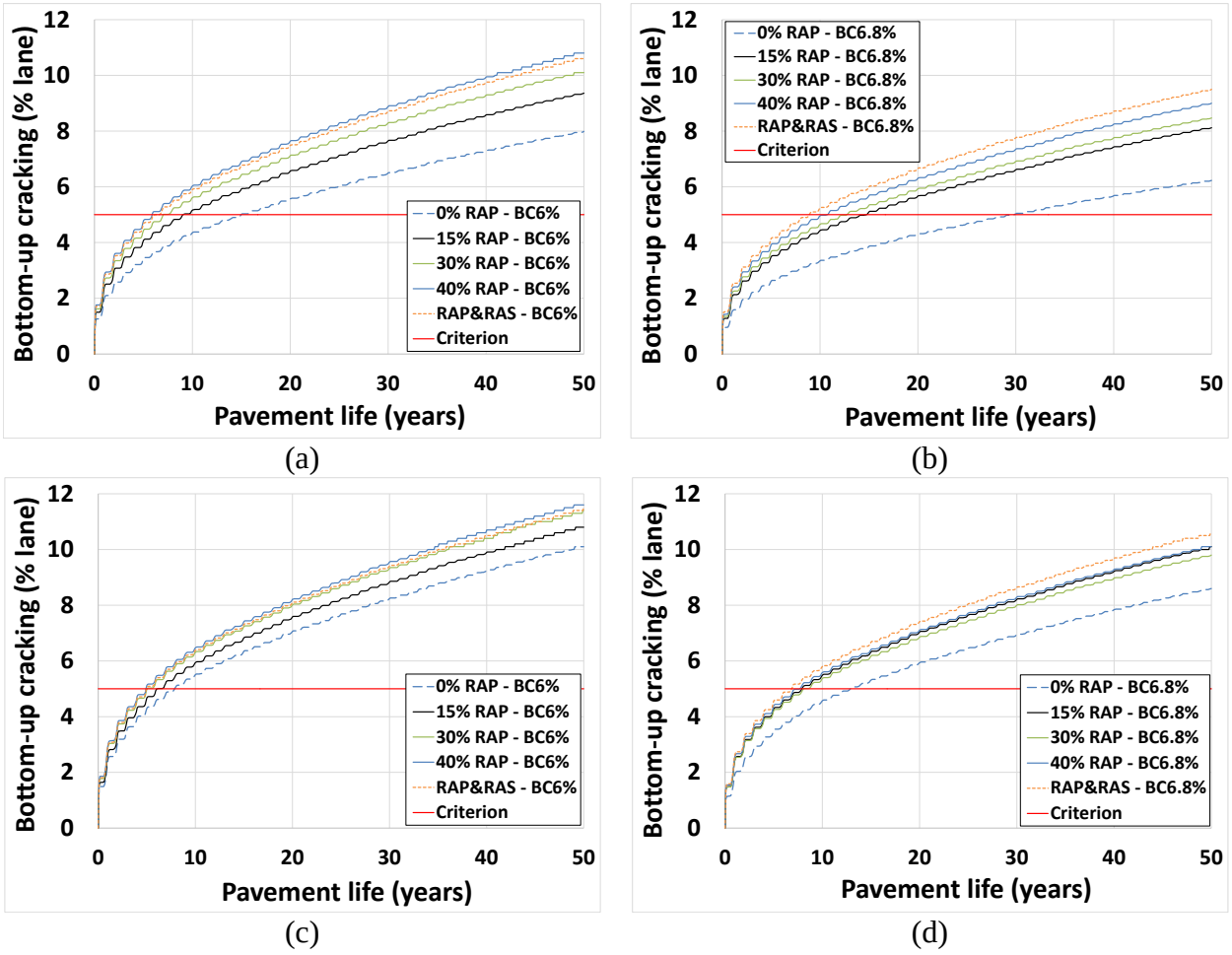

Figure 5.11. Predicted bottom-up cracking (alligator) for Ontario for mixes with PG64-22 and PG76-22 binders (a) PG64-22 – 6% binder content (b) PG64-22 – 6.8% binder content (c) PG76-22 – 6% binder content (d) PG76-22 – 6.8% binder content.

All rutting and cracking curves presented in this section are for the structure shown in Figure 5.1a (a 3 inch asphalt overlay on a 2 inch milled existing asphalt layer). To be able to determine service lives after initial failure, simulations were also performed after the first failure (pavement structure shown in Figure 5.1b) by milling 1 inch from the existing overlay surface and placing a new 3 inch asphalt overlay. Traffic levels were also adjusted for all simulations to have a continuous increase in AADTT of 3% throughout the analysis period. This process was repeated until the total life of all constructed pavements reached or exceeded the 50-year analysis period. Figure 5.12 shows the bottom-up cracking performance curves for the section with PG76-22 binder, RAP&RAS, 6% binder content and the Portland climate. In this study, the asphalt overlay was constructed when the bottom-up cracking reached 5% of the lane area (rehabilitation trigger value or failure criteria). Since total service life did not reach 50 years (analysis period) after two rehabilitations, the structure in Figure 5.1b was milled 1 inch and a 3 inch thick asphalt overlay was constructed for a third time. Since the section is getting 2 inches thicker with every asphalt overlay construction, service life is increasing. Using the service lives for each

construction (6.83, 30 and 48.33 years for the case in Figure 5.12) and calculated costs, LCCA was performed in the next section.

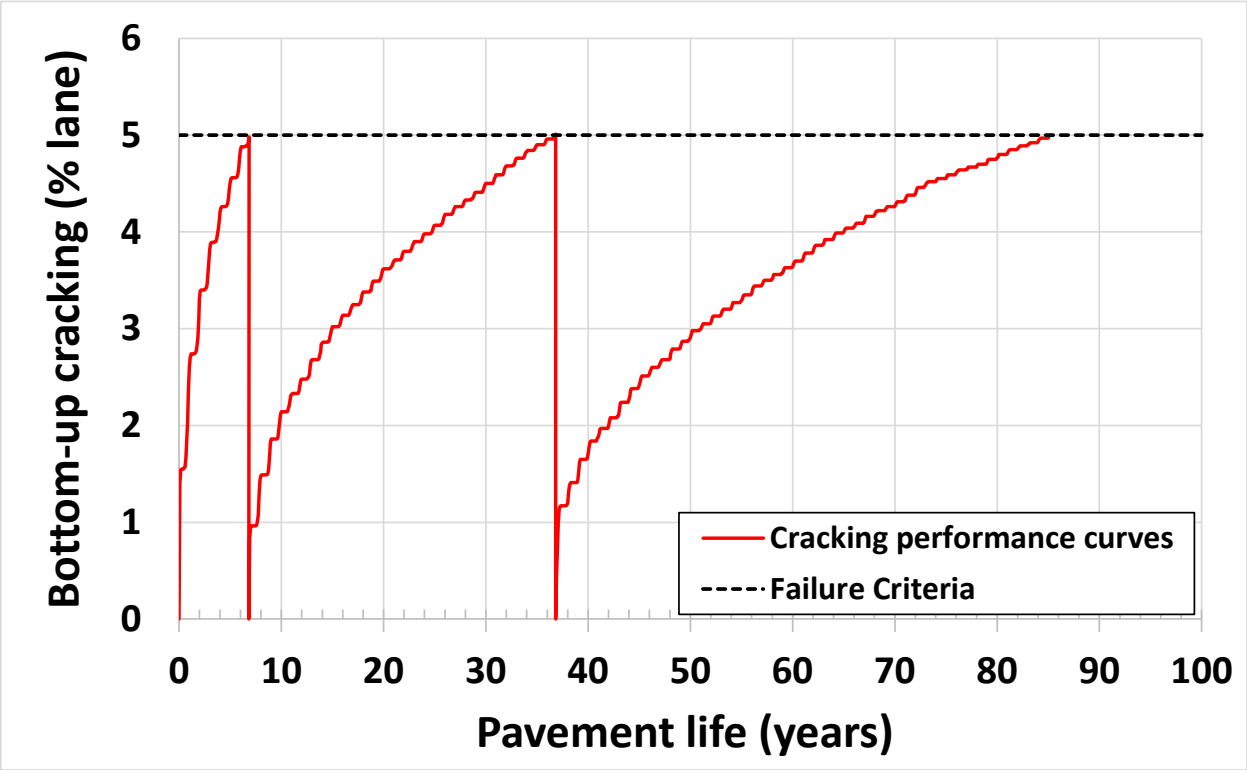

Figure 5.12. Cracking performance curves for the section with PG76-22 binder, RAP&RAS, 6% binder content, and Portland climate.

5.6.2 Life-Cycle Cost Analysis

5.6.2.1 Results of LCCA by Only Considering Material Costs

LCCA was performed by following the process described in Section 5.5. Material costs of each strategy (for the cases outlined in Table 5.1) were calculated by using the cost calculation tool described in Section 5.4. Material production costs, plant operation costs and profit were not considered in the analysis. In this section, analyses were performed by only considering material costs to be able to compare the impact of RAP content and RAP&RAS, binder content, binder grade and climate on life cycle costs. Table 5.3 shows the service lives and material costs for all cases. Calculated salvage values and NPVs for all cases are also given in Table 5.3. Figure 5.13 compares the NPVs for all cases. An interest rate of 4% was used for NPV calculations.

It can be observed from Figure 5.13 and Table 5.3 that although increasing binder content increases the mixture costs, increased performance generally results in higher cracking resistance and lower life-cycle costs. This result suggests that increasing the binder content of asphalt mixture is an effective strategy to improve the condition of highway network and reduce long-term costs. In addition, higher RAP contents generally result in lower life-cycle costs. However,

the case with PG64-22 binder, 0% RAP and 6.8% binder content has a significantly higher performance which results in lower life-cycle costs for both climates. Since the cost of PG64-22 binder ($375/ton) is lower than PG58-34 ($425/ton) and PG76-22 ($450/ton) binders, life-cycle costs for the sections constructed with PG64-22 were also determined to be lower. Due to lower binder cost for PG64-22, changes in binder content and RAP content were observed to have a less significant effect on life-cycle costs of sections constructed with PG64-22 binder. Due to colder temperatures, simulations with the Ontario climate resulted in lower cracking resistance. Lower cracking resistance increased the life-cycle costs for these sections.

For the sections with PG76-22 binder, cracking performance was observed to be significantly lower. Calculated life-cycle costs were also higher for the section with PG76-22 binder. However, it should be noted that none of the cases simulated in this report are for the asphalt mixture strategies suggested in Chapter 3. Asphalt mixtures with PG76-22 binder and higher binder contents (7.2% to 7.8%) can create mixtures highly resistant to both rutting and cracking. Dynamic modulus tests should be conducted with the suggested mixtures to be able to develop MEPDG models and simulate rutting and cracking performance of sections with PG76-22 binders and higher binder contents.

Table 5.3. Results of Life Cycle Costs Analysis – Only Material Costs

Mix	Cost T#1 ($)	Service life#1	Cost T#2	Service life#2	Cost T#3	Service life#3	Salvage value ($)	NPV ($)
B2-R0-BC6.0-ON	41,247	14.92	41,247	50.00	-	-	12,308	62,491
B2-R0-BC6.8-ON	44,688	29.83	44,688	50.00	-	-	26,661	54,807
B2-R0-BC6.0-PO	41,247	17.67	41,247	50.00	-	-	14,577	59,822
B2-R0-BC6.8-PO	44,688	30.67	44,688	50.00	-	-	27,412	54,251
B3-R0-BC6.0-ON	46,593	7.83	46,593	37.00	46,593	45.18	41,262	83,090
B3-R0-BC6.8-ON	50,747	12.83	50,747	50.00	-	-	13,022	79,595
B3-R0-BC6.0-PO	46,593	9.58	46,593	50.00	-	-	8,927	77,337
B3-R0-BC6.8-PO	50,747	13.00	50,747	50.00	-	-	13,194	79,367
B2-R15-BC6.0-ON	38,338	9.00	38,338	50.00	-	-	6,901	64,303
B2-R15-BC6.8-ON	41,779	14.75	41,779	50.00	-	-	12,325	63,471
B2-R15-BC6.0-PO	38,338	11.75	38,338	50.00	-	-	9,009	61,252
B2-R15-BC6.8-PO	41,779	16.83	41,779	50.00	-	-	21,592	61,391
B3-R15-BC6.0-ON	42,853	6.08	42,853	32.92	42,853	50	33,425	81,194
B3-R15-BC6.8-ON	47,006	7.83	47,006	38.08	47,006	50	6,073	87,977
B3-R15-BC6.0-PO	42,853	7.83	42,853	42.17	-	-	0	74,375
B3-R15-BC6.8-PO	47,006	9.08	47,006	50.00	-	-	8,536	78,727
B2-RAS-BC6.0-ON	35,913	6.58	35,913	50.00	-	-	4,726	62,993
B2-RAS-BC6.8-ON	39,354	8.83	39,354	50.00	-	-	6,950	66,210
B2-RAS-BC6.0-PO	35,913	7.92	35,913	50.00	-	-	5,689	61,437
B2-RAS-BC6.8-PO	39,354	11.00	39,354	50.00	-	-	8,658	63,699
B3-RAS-BC6.0-ON	39,684	4.92	39,684	19.08	39,684	30	5,291	87,141
B3-RAS-BC6.8-ON	43,837	6.83	43,837	31.00	43,837	42	31,135	82,934
B3-RAS-BC6.0-PO	39,684	6.83	39,684	30.00	39,684	48.33	28,870	75,340
B3-RAS-BC6.8-PO	43,837	8.08	43,837	47.08	-	-	4,805	75,092
B1-R30-BC6.0-ON	37,885	8.83	37,885	20.08	37,885	50	21,905	73,789
B1-R30-BC6.4-ON	39,843	12.67	39,843	25.17	39,843	50	30,153	68,872
B1-R30-BC6.8-ON	41,800	21.92	41,800	39.08	-	-	11,766	61,659
B1-R30-BC6.0-PO	37,885	10.83	37,885	35.33	37,885	45	34,652	63,980
B1-R30-BC6.4-PO	39,843	14.83	39,843	48.17	-	-	10,753	63,968
B1-R30-BC6.8-PO	41,800	24.67	41,800	50.00	-	-	20,624	57,018
B2-R30-BC6.0-ON	35,429	7.00	35,429	50.00	-	-	4,960	61,654
B2-R30-BC6.4-ON	37,149	9.75	37,149	50.00	-	-	7,244	61,474
B2-R30-BC6.8-ON	38,870	12.75	38,870	50.00	-	-	9,912	61,049
B2-R30-BC6.0-PO	35,429	9.08	35,429	50.00	-	-	6,434	59,338
B2-R30-BC6.4-PO	37,149	11.92	37,149	50.00	-	-	8,856	59,179
B2-R30-BC6.8-PO	38,870	14.92	38,870	50.00	-	-	11,599	58,888

(Continued)

Mix	Cost T#1 ($)	Service life#1	Cost T#2	Service life#2	Cost T#3	Service life#3	Salvage value ($)	NPV ($)
B3-R30-BC6.0-ON	39,113	5.00	39,113	21.83	39,113	31.17	10,039	83,503
B3-R30-BC6.4-ON	41,189	6.83	41,189	27.08	41,189	36.25	22,907	80,369
B3-R30-BC6.8-ON	43,266	8.08	43,266	29.92	43,266	38.00	29,603	80,362
B3-R30-BC6.0-PO	39,113	6.92	39,113	31.08	39,113	50.00	29,726	73,557
B3-R30-BC6.4-PO	41,189	8.83	41,189	43.25	-	-	2,081	73,574
B3-R30-BC6.8-PO	43,266	10.67	43,266	47.17	-	-	6,948	68,329
B3-R30-BC6.0-ON	39,113	5.00	39,113	21.83	39,113	31.17	10,039	83,503
B1-R40-BC6.0-ON	35,576	6.92	35,576	15.17	35,576	22.83	27,660	77,036
B1-R40-BC6.4-ON	37,534	8.92	37,534	19.17	37,534	24.92	4,534	75,822
B1-R40-BC6.8-ON	39,491	13.75	39,491	26.25	39,491	27.08	7,855	69,642
B1-R40-BC6.0-PO	35,576	8.83	35,576	26.17	35,576	37.08	21,184	66,773
B1-R40-BC6.4-PO	37,534	11.00	37,534	37.00	37,534	41.17	18,016	65,848
B1-R40-BC6.8-PO	39,491	15.67	39,491	45.25	39,491	-	9,530	59,510
B2-R40-BC6.0-ON	33,490	5.83	33,490	50.00	-	-	3,905	59,585
B2-R40-BC6.4-ON	35,210	7.92	35,210	50.00	-	-	5,577	60,234
B2-R40-BC6.8-ON	36,930	10.75	36,930	50.00	-	-	7,940	60,038
B2-R40-BC6.0-PO	33,490	7.83	33,490	50.00	-	-	5,244	57,386
B2-R40-BC6.4-PO	35,210	10.00	35,210	50.00	-	-	7,042	58,006
B2-R40-BC6.8-PO	36,930	12.83	36,930	50.00	-	-	9,476	57,924
B3-R40-BC6.0-ON	36,619	4.83	36,619	21.08	36,619	26.17	2,910	79,764
B3-R40-BC6.4-ON	38,696	5.83	38,696	20.25	38,696	30.08	7,924	82,280
B3-R40-BC6.8-ON	40,772	7.67	40,772	25.25	40,772	34.17	20,392	79,293
B3-R40-BC6.0-PO	36,619	6.67	36,619	31.50	36,619	42.75	26,486	69,277
B3-R40-BC6.4-PO	38,696	7.75	38,696	31.25	38,696	49.00	18,323	73,053
B3-R40-BC6.8-PO	40,772	9.75	40,772	38.25	40,772	50.00	22,176	71,673

Note: B1= PG 58-34, B2= PG 64-22, and B3 = PG 76-22.
R0 = 0% RAP, and R15 = 15% RAP, R30 = 30% RAP, and R40 = 40% RAP.
BC6= 6% binder content, BC6.4 =6.4 % binder content, and BC6.8 = 6.8% binder content.

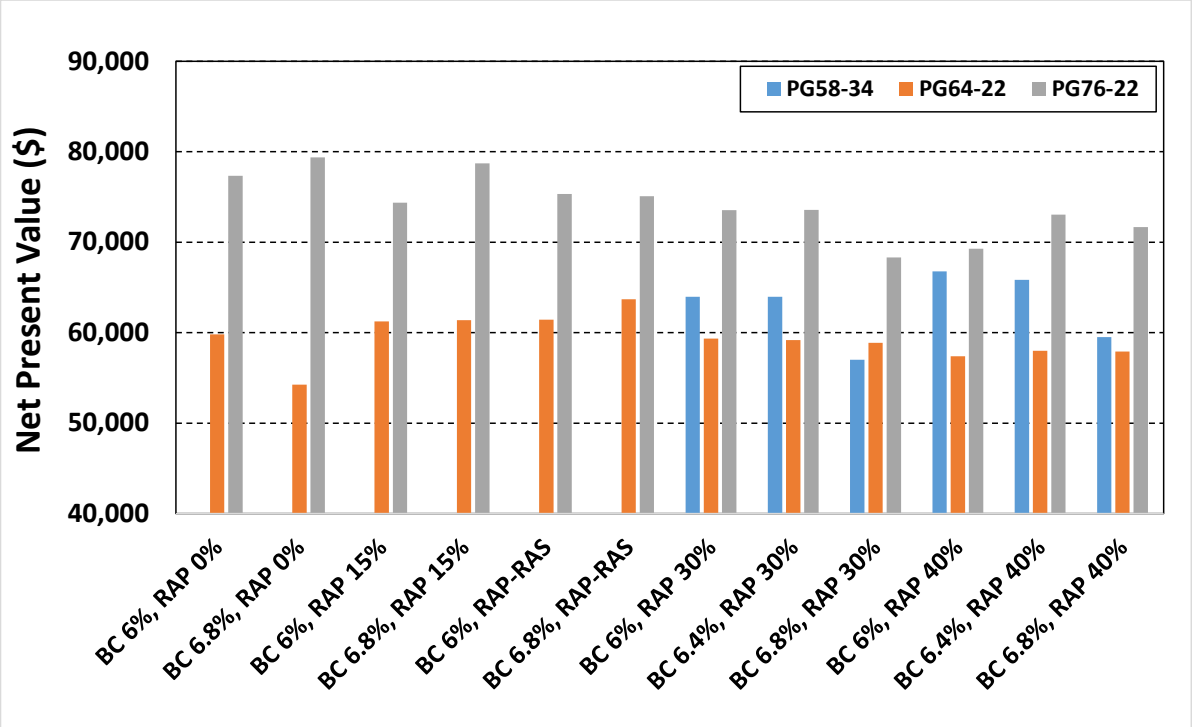

(a)

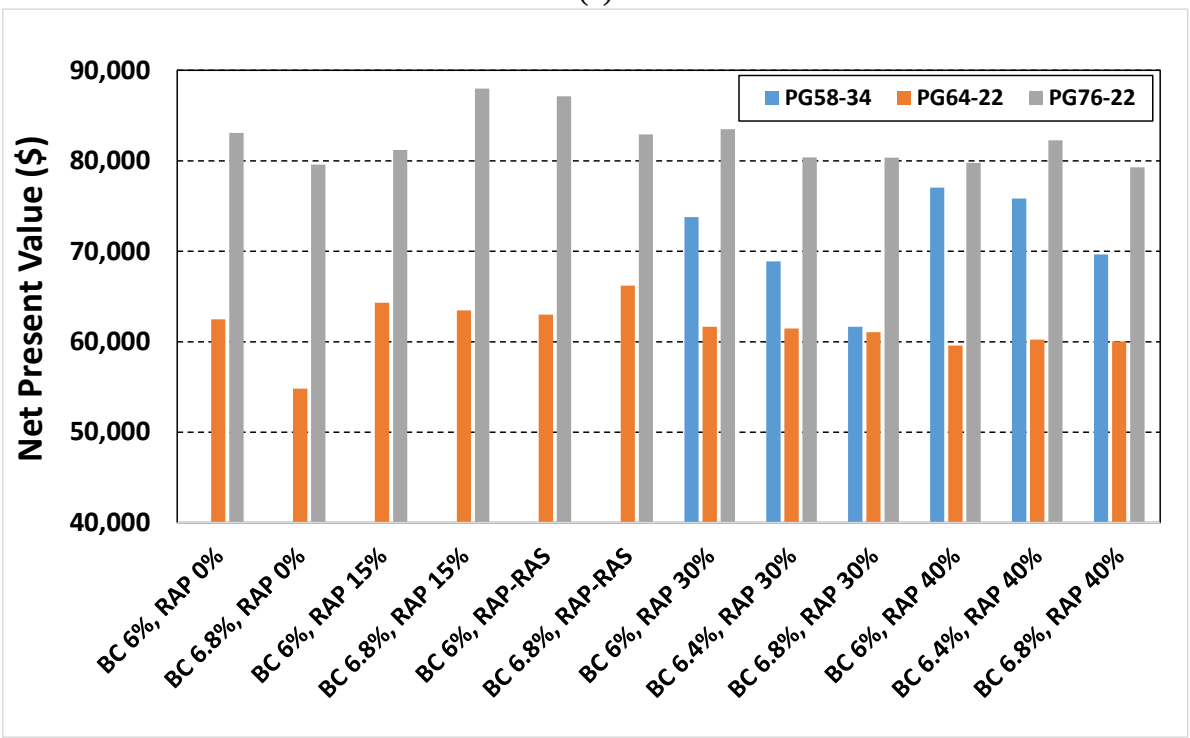

(b)

Figure 5.13. Calculated material cost NPVs for all cases (a) Portland (b) Ontario.

In order to determine the impact of interest rate on NPV ranking of the analyzed cases, NPVs for all cases were also calculated using a 5% interest rate (rather than the 4% initially used). Figure 5.14 shows the correlation between NPVs calculated by using 4% and 5% interest rates. Although using a 5% interest rate reduces the calculated NPVs (as expected), a strong linear correlation between NPVs for 4% and 5% interest rates suggests that increasing the interest rate does not change the rankings and conclusions.

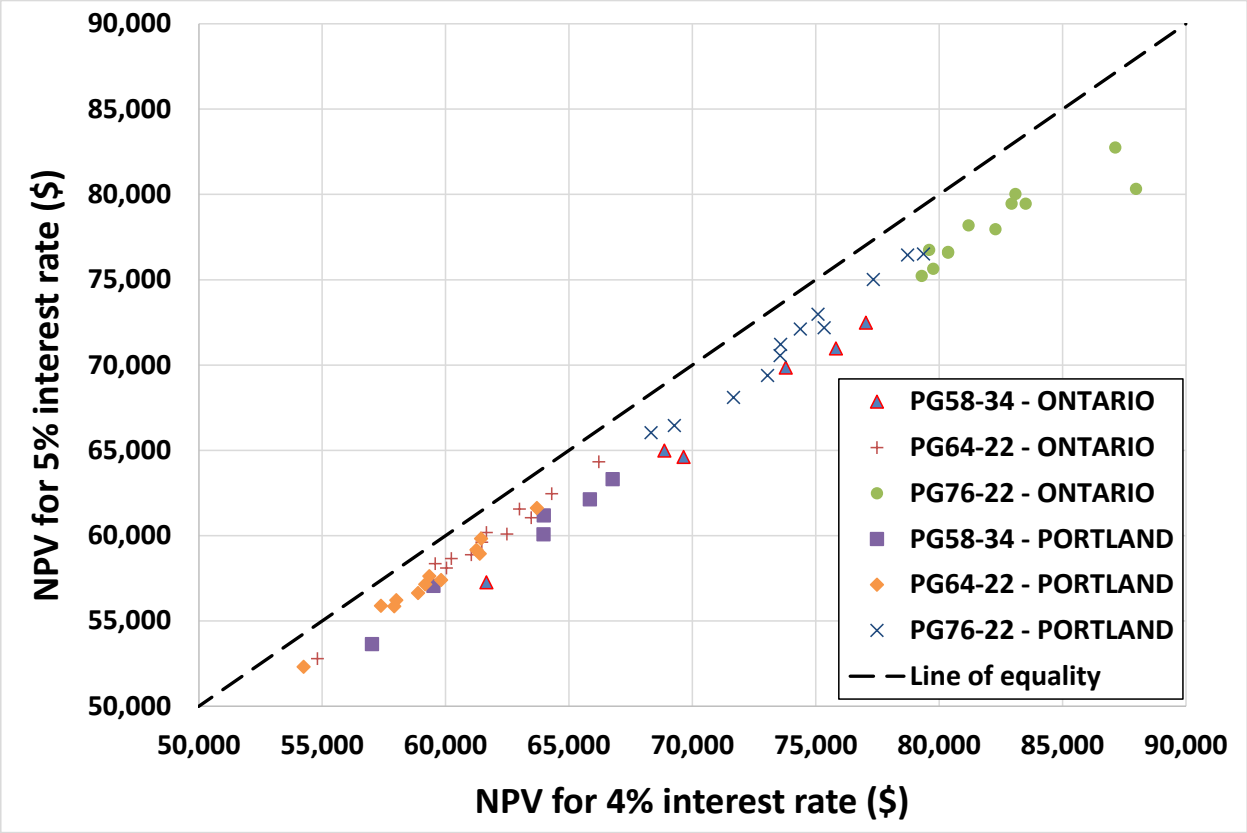

Figure 5.14. Correlation between NPVs calculated by using 4% and 5% interest rates

5.6.2.2 Results of LCCA by Considering Total Agency Costs

The procedure described in Section 5.5 was followed to calculate total agency costs. After finding the service lives for each strategy, agency costs were estimated for each year at which the treatment was applied. Net present value (NPV) of agency costs for each strategy was determined afterwards using a 4% interest rate for a 50-year analysis period by using Equation (5.12). Figure 5.15 compares the NPVs for all cases. An interest rate of 4% was used for NPV calculations.

By comparing Figure 5.13 and Figure 5.15, it can be observed that using the total agency costs did not change the ranking of the life-cycle costs for mixtures with PG58-34 and PG64-22 binders. However, since mixtures with PG76-22 binder have shorter service lives and more than two rehabilitations are generally required within the 50-year analysis period, using total agency costs rather than only material costs changed the life-cycle cost rankings for very few cases. For

instance, when only material costs were used for LCCA, the asphalt mixture with 15% RAP and 6.8% binder content had the highest NPV while the NPV for the mixture with RAP&RAS and 6% binder content had the highest NPV when the total agency costs were used for LCCA. However, in general, using total agency costs rather than only material costs did not create any major changes in conclusions. Figure 5.16 shows the correlation between NPVs calculated by using material and total agency costs. Although using total agency costs increases the calculated NPVs (as expected), a strong linear correlation between NPVs for material and agency costs suggests that using agency costs rather than only material costs did not change the rankings and conclusions except for the three cases shown in Figure 5.16 (PG76-22-BC6.8%-RAP15%-Ontario, PG76-22-BC6.4%-RAP30%-Portland, PG76-22-BC6.8%-RAP30%-Portland).

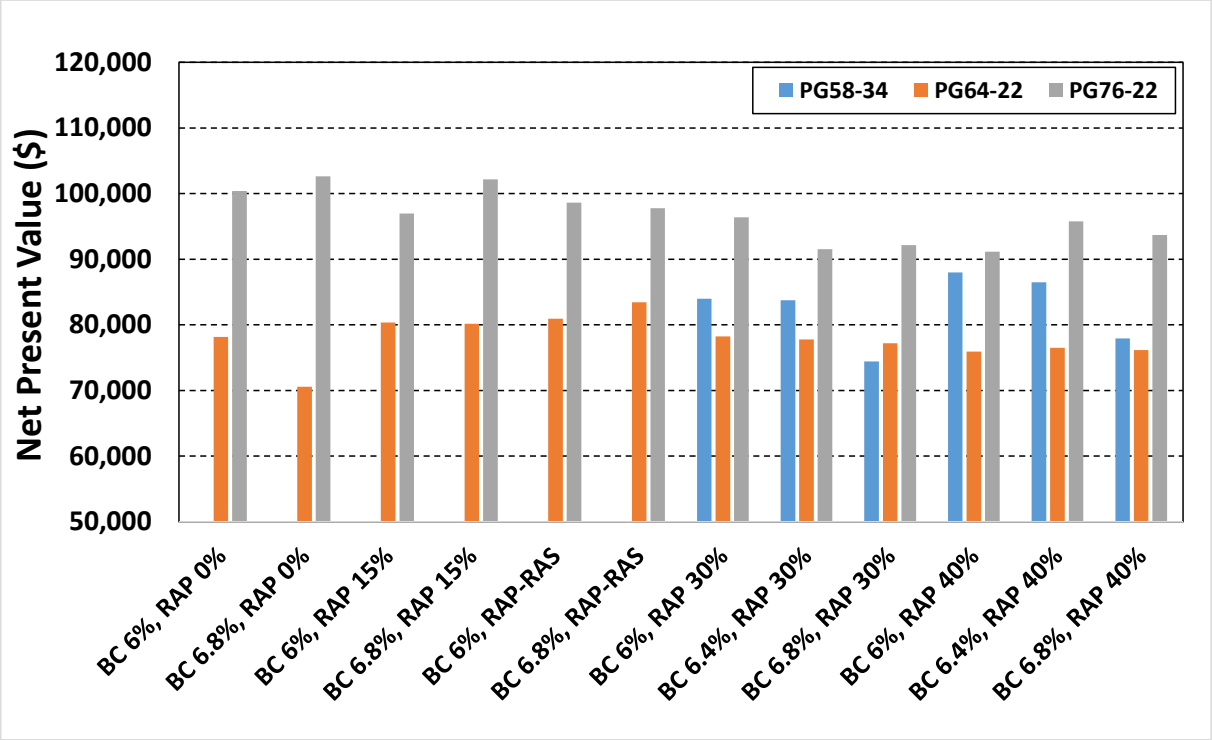

(a)

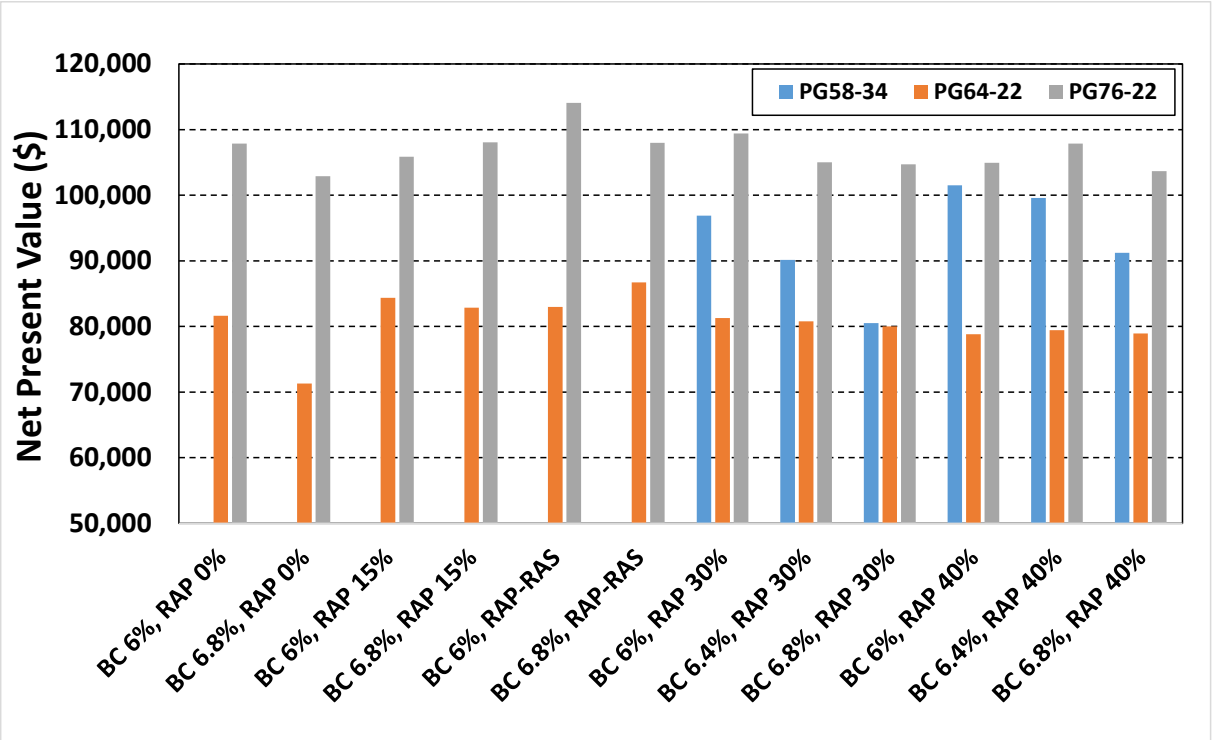

(b)

Figure 5.15. Calculated total agency cost NPVs for all cases (a) Portland (b) Ontario.

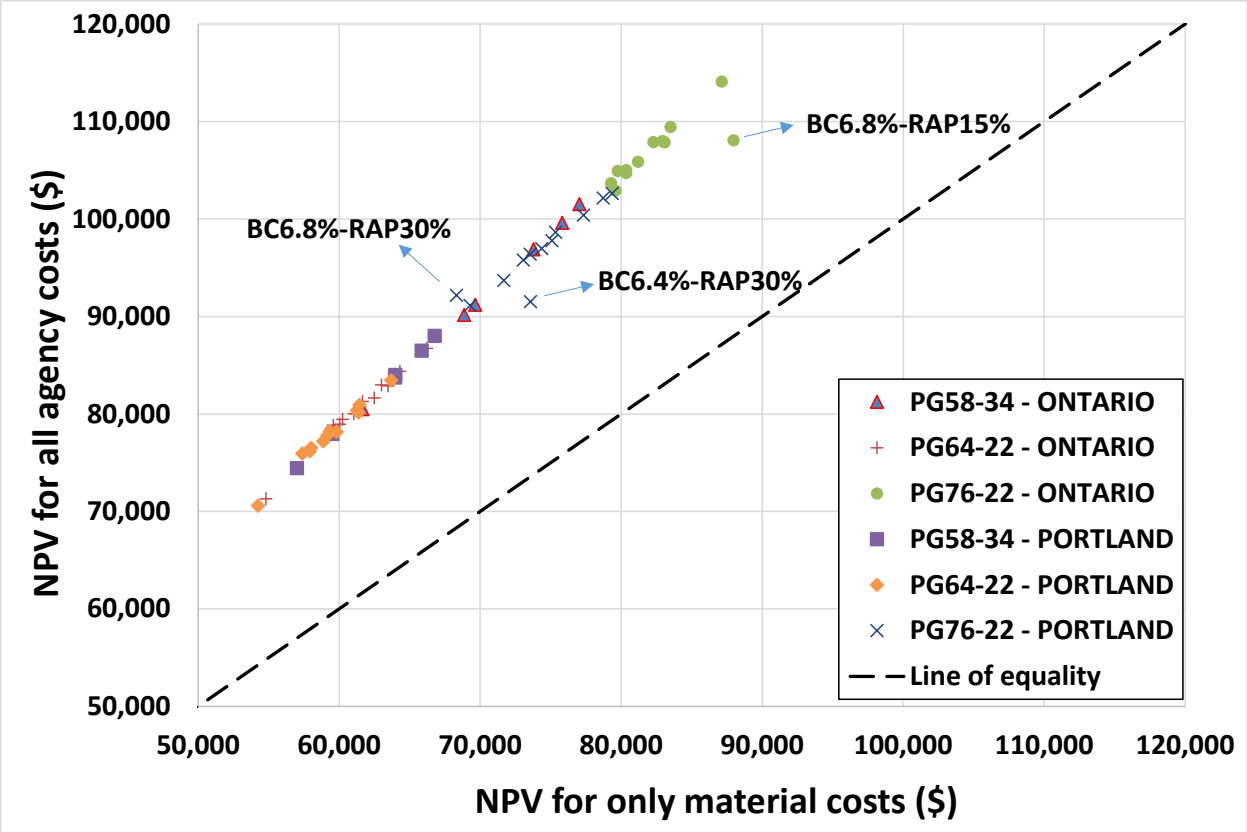

Figure 5.16. Correlation between NPVs calculated by using material and agency costs.

5.7 SUMMARY AND CONCLUSIONS

This portion of the study focused on development of MEPDG models to quantify the impact of RAP content and RAP&RAS, binder content and binder type on in-situ rutting and alligator cracking (bottom-up cracking) performance. A material cost-calculation tool was also developed to calculate the asphalt mixture costs for different binder contents, binder types, and RAP and RAS contents. Using the predicted performance curves and calculated material and agency costs, life-cycle costs analysis (LCCA) were performed to determine the most cost effective strategies.

The analyses presented in this chapter have yielded the following conclusions:

- The rutting accumulation rate for Ontario is significantly higher than for the Portland climate due to higher summer temperatures for Ontario.
- Binder type was observed to be most significant factor controlling asphalt concrete rutting. Increasing binder content and decreasing RAP content was also observed to increase rutting.

- None of the sections fail from rutting within the first 15 years for failure criteria of 0.5 inch rut depth while majority of the sections do not fail within the first 25 years. Since asphalt aging is going to significantly increase asphalt stiffness during this long time period, it is highly likely that none of the sections will fail from rutting. For this reason, alligator cracking was used as the only failure criteria for LCCA.

- Cracking accumulation rate for Ontario is higher than for the Portland climate due to lower winter temperatures for Ontario,

- Binder content was observed to be most significant factor controlling bottom-up cracking. Increasing binder content and decreasing RAP content was observed to decrease cracking accumulation.

- For the sections with PG76-22 binder, cracking performance was observed to be significantly lower. Increasing binder content and decreasing RAP content did not appear to create significant changes in performance. However, it should be noted that none of the cases simulated in this report are for the asphalt mixture strategies suggested in Chapter 3. Asphalt mixtures with PG76-22 binder and higher binder contents (7.2% to 7.8%) can create mixtures highly resistant to both rutting and cracking. Dynamic modulus tests should be conducted with the suggested mixtures to be able to develop MEPDG models and simulate their rutting and cracking performance.

- Increasing the binder content of an asphalt mixture is an effective strategy to improve the condition of the highway network and reduce long-term costs.

- Higher RAP contents generally result in lower life-cycle costs.

- Due to colder temperatures, simulations with the Ontario climate resulted in lower cracking resistance. Lower cracking resistance increased the life-cycle costs for these sections.

- Although using a 5% interest rate reduces the calculated NPVs (as expected), a strong linear correlation between NPVs for 4% and 5% interest rates suggests that increasing interest rate does not change the rankings and conclusions.

- Although using total agency costs increased the calculated NPVs (as expected), a strong linear correlation between NPVs for material and agency costs suggests that using agency costs rather than only material costs did not change the rankings and conclusions except for three cases shown in Figure 5.16 (PG76-22-BC6.8%-RAP15%-Ontario, PG76-22-BC6.4%-RAP30%-Portland, PG76-22-BC6.8%-RAP30%-Portland).

6 SUMMARY AND CONCLUSIONS

This research study presents a comprehensive investigation consisting of laboratory testing, mechanistic-empirical pavement modeling, life-cycle cost analysis, field coring and production sampling of asphalt mixtures used in Oregon. The performance and cost-benefit comparisons of using binder-grade bumping and increased binder content strategies in RAP/RAS mixture production in Oregon were quantified. To be able to provide recommendations for asphalt mixture design procedures, blending of binder around RAP with virgin binder was also quantified by using an innovative procedure developed in this study. While the use of binder-grade bumping and high virgin binder content strategies generally increase the initial cost of virgin binder used in the asphalt mixture, increased RAP/RAS content and improved RAP/RAS performance may reduce the overall life-cycle cost of recycled asphalt concrete material used in construction. In this study, laboratory test results were used to develop mechanistic-empirical (ME) pavement models for different RAP/RAS mixtures. Using the predicted performance from ME models and cost calculations for different combinations of RAP content, binder content and binder type, life-cycle cost analyses (LCCAs) were conducted to investigate the performance and cost-benefit of using binder-grade bumping and high binder content in Oregon RAP/RAS mixes. Binder-grade bumping and high binder content strategies recommended in this study are expected to increase the RAP/RAS content in asphalt mixtures, reduce the life-cycle cost, improve the cracking performance and encourage the widespread use of high RAP/RAS asphalt mixtures in Oregon.

Conclusions based on the experimental and analytical findings, products developed, recommendations and additional research are discussed in the following sections.

6.1 CONCLUSIONS

The major conclusions drawn from the results of this study are as follows:

Development of Strategies to Improve Performance of RAP/RAS Mixtures:

1. FI is a good performance indicator since it can differentiate between the cracking performance of asphalt mixtures with different RAP contents, binder contents and binder grades.
2. Fracture energy, the most common parameter used to characterize the cracking resistance of asphalt mixtures in several research studies, is not an effective parameter to use for cracking performance evaluation.
3. Fracture toughness and secant stiffness correlate well with cracking resistance and brittleness.

4. Dynamic modulus tests at 40 ^{o}C and 0.1 Hz have the highest correlation with FN. Therefore, dynamic modulus results at 40 ^{o}C and 0.1 Hz can be used to predict FN (rutting resistance of the asphalt mixtures).
5. In general, there is not a strong correlation between dynamic modulus and FI, especially for PG 76-22. However, dynamic modulus had a strong correlation with FI at 20 ^{o}C and 4 ^{o}C for mixtures with PG 58-34 and can be used to predict FI in these cases. As the binder becomes stiffer, the correlations between FI and dynamic modulus become weaker.
6. Although there is a non-linear correlation between FN and FI, the correlation is not strong enough to be able to predict FI results using the FN results and vice versa. For this reason, both experiments need to be conducted separately to evaluate rutting and cracking resistance of asphalt mixtures.
7. Binder content is the most significant variable controlling FI. Binder type and RAP content are the second and third most significant variables, respectively.
8. All the independent variables have a significant effect on FN, with binder type being the first, RAP content being the second and binder content being the third most significant variables.
9. Increasing binder content from 6% to 6.8% does not create any significant impact on the cracking performance of RAP&RAS mixtures. On the other hand, increasing binder content is an effective strategy to improve the cracking resistance of 30% and 40% RAP mixtures.
10. Asphalt mixtures with RAP&RAS with binder contents ranging from 7.29% to 7.59% and a binder grade of PG 64-22 have acceptable cracking and rutting performance.
11. Using a binder grade of PG 76-22 and RAP&RAS makes asphalt mixtures very brittle. In order to enhance the cracking performance, the binder content should be increased up to 9.26%. However, to reach acceptable rutting performance, the binder content should be less than 8.07%. Therefore, it seems that there are no combinations of binder content, PG 76-22 and RAP&RAS identified to provide acceptable cracking and rutting performance.
12. For low RAP mixtures (0% to 25% RAP), there is no combination of binder content and RAP content for mixtures with PG 64-22 that will provide high cracking and rutting performance. However, it should be noted that the limits for FN and FI used as cracking and rutting performance thresholds in this study (FN>740 and FI>10) maybe too conservative. Field verification of these thresholds needs to be sought.
13. For mixtures with 20% RAP content and PG 76-22, the binder content should be between 7% and 7.6%. As RAP content decreases, the required binder content decreases. For mixtures with 15% RAP, 10% RAP, 5% RAP and 0% RAP, the suggested binder content ranges are 6.8%-7.2%, 6.6%-6.9%, 6.4%-6.6% and 6.2%, respectively.

Quantification of RAP Binder Blending to Provide Recommendations for Asphalt Mix Design

14. A significant percentage of the binder around the RAP aggregates (about 40% to 55%) is not blending into the mixture. Since all asphalt mixtures were designed with the assumption that there will be 100% blending between RAP and virgin binders, the final

mixture has a significantly lower binder content than the design binder content. In other words, the active binder content (design binder content minus the percentage of the RAP binder not blending into the mixture) in the final mixture is less than it should be to be able resist thermal and traffic loads as designed.

15. Although the binder contents of the suggested high RAP strategies in Table 3.10 are significantly higher than general asphalt mixture binder contents used in Oregon, active binder contents for high RAP mixtures will mostly be within the 5.5%-6.5% range. The low performance of high RAP mixtures is likely to be a result of the lower binder content, which is a consequence of limited blending. By considering the blending percentages during the mix design stage and increasing virgin binder contents accordingly, the performance of asphalt mixtures with high RAP contents can be improved.

16. Using aggregates with higher temperatures (about 96^{o}C higher than normal) during mixing did not have any significant effect on blending.

17. FIs for the RS#2-F mixture are significantly lower than the FIs for the RS#2-C mixture. The same quantity of binder used to prepare both mixtures (6.4%) is expected to create a better coating for the coarser gradation with less surface area.

18. RAP aggregates with higher binder contents are expected to provide mixtures with less active binder content and lower cracking resistance. For this reason, RAP and virgin binder blending should be considered during mixture design.

19. Since blending percentages for all three mixtures are close, an average blending percentage of 56.5% is suggested to be used for mixture design and performance evaluation.

Mechanistic-Empirical Pavement Design Guide (MEPDG) Simulations and Life Cycle Cost Analysis to Determine the Cost and Performance Effectiveness of High and Low RAP and RAP&RAS Strategies

20. Binder type is the most significant factor controlling asphalt concrete rutting. Increasing binder content and decreasing RAP content increase rutting.

21. None of the sections fail from rutting within the first 15 years for failure criteria of 0.5 inch rut depth and the majority of the sections do not fail within the first 25 years. Since asphalt aging significantly increases asphalt stiffness during this long time period, it is highly likely that none of the sections will fail from rutting.

22. Binder content is the most significant factor controlling bottom-up cracking. Increasing binder content and decreasing RAP content were also observed to decrease cracking accumulation.

23. For the sections with PG76-22 binder, cracking performance was observed to be significantly lower. Increasing binder content and decreasing RAP content did not appear to create significant changes in performance. However, it should be noted that none of the cases simulated in this report are for the asphalt mixture strategies suggested in Chapter 3 (Table 3.10). Asphalt mixtures with PG76-22 binder and higher binder contents (7.2% to 7.8%) can create mixtures highly resistant to both rutting and cracking.

24. Increasing the binder content of asphalt mixtures is an effective strategy to improve the condition of the highway network and reduce long-term costs.

25. Higher RAP contents generally result in lower life-cycle costs.

6.2 MAJOR RESEARCH PRODUCTS DEVELOPED IN THIS STUDY

The major research products developed in this study are given as follows:

- Recommended RAP and binder contents for mixtures with different binder types to meet rutting and cracking performance requirements;
- Recommended binder contents for RAP/RAS mixtures with different virgin binder types;
- Regression models to predict rutting and cracking performance of high (25% to 45% RAP) and low (0 to 25% RAP) RAP mixtures using binder content, RAP content and binder type as independent variables;
- An innovative process for RAP-to-virgin binder blending measurement;
- Blending percentages for different RAP sources and suggestions for mix design processes to account for reduced blending (active binder content concept);
- A cost calculation spreadsheet to compare unit cost of asphalt mixtures with different RAP/RAS contents, binder contents and binder types;
- A software to analyze the data produced by semi-circular bend (SCB) test; and
- A software to analyze the data produced by flow number (FN) test.

6.3 RECOMMENDATIONS AND FUTURE WORK

6.3.1 Development of Strategies to Improve Performance of RAP/RAS Mixtures

Field verification of the results presented in this study needs to be sought. Pilot sections should be constructed with strategies suggested for high RAP and RAP&RAS asphalt mixtures. Suggestions with higher FIs (>15) should be selected for pilot section construction to minimize the risk of cracking. Since rutting is going to be the expected failure distress for these highly flexible mixtures, rutting performance of the sections should be monitored for 2 to 4 years.

SCB and flow number test results conducted with RAP&RAS mixtures [asphalt binder replacement matching the 30% RAP mixture from Section 3.5 (Phase I)] with PG64-22 and PG76-22 binders showed that these binders are generally too stiff to be used with the RAP&RAS mixtures. In this study, due to the unavailability of soft PG58-34 binder for Phase II, RAP&RAS mixtures could not be prepared and tested with this soft binder. For this reason, the same

RAP&RAS mixture should be prepared using the soft PG58-34 binder to determine the effectiveness of binder grade bumping for RAP&RAS mixtures with a range of binder types.

This study constructs the beginnings of a performance-based balanced mix design method. It was determined that typical FI values for production mixtures (plant-produced) range from 9 to 14. However, more experiments need to be conducted to determine exact threshold for FI that will provide acceptable long-term pavement cracking performance. In a future study, flow number and SCB experiments should be conducted with several production mixtures from different sources to develop a distribution of FI and FN for Oregon mixtures. Cracking and rutting performance of the sections constructed with these mixtures should be monitored to determine the thresholds for FN and FI.

6.3.2 Quantification of RAP Binder Blending to Provide Recommendations for Asphalt Mix Design

Measured blending percentages for all three mixtures (with two RAP sources and two gradations) are similar and an average blending percentage of 56.5% is suggested to be used for mixture design and performance evaluation. However, specimens with different RAP materials and gradations should be prepared and tested to validate the results of this study. In addition, blending percentages for RAP should also be determined for these specimens. The impact of softening and rejuvenating agents on blending and cracking resistance should also be determined.

The active binder content concept developed in this study should be further investigated. The possibility of incorporating binder blending and the active binder concept into current mix design procedures should be evaluated.

6.3.3 Mechanistic-Empirical Pavement Design Guide (MEPDG) Simulations and Life Cycle Cost Analysis to Determine the Cost and Performance Effectiveness of High and Low RAP and RAP&RAS Strategies

In this study, MEPDG simulations were conducted to determine the rutting and bottom-up cracking performance of different asphalt mixtures. MEPDG longitudinal (top-down cracking) cracking models were not used for simulations since the accuracy of these models were determined to be low (Williams and Shaidur 2013; Von Quintus et al. 2009). Since top-down cracking is the major distress mode in Oregon, using top-down cracking models for performance prediction and LCCA will provide more realistic results. More effective models that can explain the mechanism behind top-down cracking are currently being developed in research project NCHRP 01-52. The analysis performed in this research study should also be performed with top-down fatigue cracking as the main failure mode to evaluate the cost and performance effectiveness of different high RAP strategies in Oregon.

For the sections with PG76-22 binder, cracking performance was observed to be significantly lower. Increasing binder content and decreasing RAP content did not appear to create significant changes in performance for these cases. However, it should be noted that none of the cases simulated in this report are for the asphalt mixture strategies suggested in Chapter 3. Asphalt

mixtures with PG76-22 binder and higher binder contents (7.2% to 7.8%) can create mixtures highly resistant to both rutting and cracking. Dynamic modulus tests should be conducted with the suggested mixtures to be able to develop MEPDG models and simulate their rutting and cracking performance. LCCA should also be performed using the performance curves to determine the cost effectiveness of suggested strategies.

7 REFERENCES

AASHTO. Standard Practice for Preparation of Cylindrical Performance Test Specimens Using the Superpave Gyratory Compactor. Washington, DC: *American Association of State and Highway Transportation Officials*, 2014, pp. 60-14.

AASHTO. Standard Practice for Developing Dynamic Modulus Master Curves for Hot Mix Asphalt (HMA) Using the Asphalt Mixture Performance Tester (AMPT). Washington, DC: *American Association of State and Highway Transportation Officials*, 2013, pp. 61-13.

AASHTO. Standard Practice for Mixture Conditioning of Hot Mix Asphalt (HMA). Washington, DC: *American Association of State and Highway Transportation Officials*, 2010. R. 30-10.

AASHTO. Standard Practice for Quantifying Roughness of Pavements. Washington, DC: *American Association of State and Highway Transportation Officials*, 2013, R. 43-07.

AASHTO. Bulk Specific Gravity (Gmb) of Compacted Hot Mix Asphalt (HMA) using Saturated Surface-Dry Specimens. Washington, DC: *American Association of State Highway and Transportation Officials*, 2012, T 166-12.

AASHTO T 209-12. Theoretical Maximum Specific Gravity (Gmm) and Density of Hot Mix Asphalt. Washington, DC: American Association of State Highway and Transportation Officials, 2012, T. 209-12.

AASHTO. Standard Method of Test for Sieve Analysis of Fine and Coarse Aggregates. Washington, DC: *American Association of State Highway and Transportation Officials*, 2011, T. 27-11.

AASHTO. Standard Method of Test for Mechanical Analysis of Extracted Aggregate. Washington, DC: *American Association of State Highway and Transportation Officials*, 2010, T. 30-10.

AASHTO. Determining the Asphalt Binder Content of Hot Mix Asphalt (HMA) by the Ignition Method. Washington, DC: *American Association of State and Highway Transportation Officials*, 2010, T. 308-10.

AASHTO. Preparing and Determining the Density of Hot Mix Asphalt (HMA) Specimens by Means of the Superpave Gyratory Compactor. Washington, DC: *American Association of State Highway and Transportation Officials*, 2012, T. 312-12.

AASHTO. Viscosity Determination of Asphalt Binder Using Rotational Viscometer. Washington, DC: *American Association of State and Highway Transportation Officials*, 2011, T. 316-11.

AASHTO. Standard Method of Test for Determining the Fatigue Life of Compacted Hot-Mix Asphalt (HMA) Subjected to Repeated Flexural Bending.Washington, DC: *American Association of State and Highway Transportation Officials*, 2007, T. 321-07.

AASHTO. Standard Method for Determining the Fracture Energy of Asphalt Mixtures Using the Semi Circular Bend Geometry (SCB). Washington, DC: *American Association of State Highway and Transportation Officials*, 2013, TP 105-13.

AASHTO. Standard Method for Determining the Dynamic Modulus and Flow Number for Hot Mix Asphalt (HMA) Using the Asphalt Mixture Performance Tester (AMPT). Washington, DC: *American Association of State and Highway Transportation Officials*, 2013, TP 79-13.

AASHTO. Ware-Pavement ME Design 1.0™. *American Association of State Highway and Transportation Officials*, 2008.

Aguiar-Moya, J., F. Hong, J. Prozzi. *RAP: Save Today, Pay Later?* Proceedings 90th Annual Meeting of the Transportation Research Board, Washington D.C, 2011.

Al-Qadi, I. L., and Ozer, H. *Impact of RAS and RAP on Asphalt Mixtures' Fracture: The Need for a Cracking Potential Index*. Illinois Center for Transportation University of Illinois at Urbana-Champaign, 2015.

Al-Qadi, I.L., Ozer, H., Lambros, J., El Khatib, A., Singhvi, P., Khan, T., Rivera-Perez, J. and Doll, B.Testing *Protocols to Ensure Performance of High Asphalt Binder Replacement Mixes Using RAP and RAS*. Publication FHWA-ICT-15-017. Illinois Center for Transportation/Illinois Department of Transportation, 2015.

Andreen, B., H. Rocheville, K. Ksaibati. *A Method of Cost-Benefit Analysis of RAP in Various Highway Applications*. Proceedings 91st Annual Meeting of the Transportation Research Board, Washington D.C., 2012.

Asphalt Institute Technical Advisory Committee Version 1.1. *Determining Laboratory Mixing and Compaction Temperatures*, 2014.

Aurangzeb, Q., I. Al-Qadi, I. Abuawad, W. Pine, and J. Trepanier. Achieving Desired Volumetrics and Performance for Mixtures with High Percentage of Reclaimed Asphalt Pavement. Transportation Research Record: *Journal of the Transportation Research Board*, No. 2294, 2012, pp.34-42.

Aurangzeb, Q., I. L. Al-Qadi, H. Ozer, R. Yang. Hybrid Life Cycle Assessment for Asphalt Mixtures with High RAP Content. *Journal of Resources, Conservation and Recycling*, 2013.

Bennert, T., J. Daniel, and W. Mogawer. Strategies for Incorporating Higher Recycled Asphalt Pavement Percentages: Review of Implementation Trials in Northeast States. Transportation Research Record: *Journal of the Transportation Research Board*, No. 2445, 2014, pp. 83-93.

Berkeley Lab, *Energy End-Use Forecasting Group*, Retrieved form: http://enduse.lbl.gov/http://enduse.lbl.gov/, enduse.lbl.gov/Info/pavements_LCCA_web.xls. Accessed February 14, 2017.

Biligiri, K., Kaloush, K., Mamlouk, M. and Witczak, M. Rational Modeling of Tertiary Flow for Asphalt Mixtures. Transportation Research Record: *Journal of the Transportation Research Board*, 2001, 2007, pp.63-72.

Bonaquist, R. *Can I Run More RAP? HMAT: Hot Mix Asphalt Technology*, 12(5), 2007, pp.11-13.

Bonaquist, R.F. Precision of the Dynamic Modulus and Flow Number Tests Conducted with the Asphalt Mixture Performance Tester. NCHRP Report, No. 702, National Cooperative Highway Research Program, Washington D.C., 2011.

Bonaquist, R.F., Christensen, D.W. and Stump, W. Simple Performance Tester for Superpave Mix Design: First-Article Development and Evaluation. *Transportation Research Board*, 2003, Vol. 513.

Carpenter, S.H. and J. R. Wolosick. Modifier Influence in the Characterization of Hot-Mix Recycled Material. *Transportation Research Record: Journal of the Transportation Research Board*, 1980, No. 777, pp.15-22.

Carvalho, R., H. Shirazi, M. Ayres Jr, and O. Selezneva. Performance of Recycled Hot-Mix Asphalt Overlays in Rehabilitation of Flexible Pavements. *Transportation Research Record: Journal of the Transportation Research Board*, 2010, No. 2155, pp.55-62.

Copeland, A. *Reclaimed Asphalt Pavement in Asphalt Mixtures: State of the Practice*. Federal Highway Administration, No. FHWA-HRT-11-021, 2011.

Darnell Jr, J. and Bell, C.A. *Performance Based Selection of RAP/RAS in Asphalt Mixtures*. Federal Highway Administration, No. FHWA-OR-RD-16-08, 2015.

Dongré, R., D'Angelo, J. and Copeland, A. Refinement of Flow Number as Determined by Asphalt Mixture Performance Tester: Use in Routine Quality Control—Quality Assurance Practice. *Transportation Research Record: Journal of the Transportation Research Board*, Vol. 2127, 2009, pp.127-136.

Coleri, E. *Adjusting Asphalt Mixes for Increased Durability and Implementation of a Performance Tester to Evaluate Fatigue Cracking of Asphalt Concrete*. ODOT Research Project Progress Presentation. 04/17/2017, Salem Oregon.

Francken, L. *Pavement Deformation Law of Bituminous Road Mixes in Repeated Load Triaxial Compression*. Presented at Fourth International Conference on the Structural Design of Asphalt Pavements, University of Michigan, Ann Arbor, 1977.

Hajj, E.Y., P. E. Sebaaly, and R. Shrestha. Laboratory Evaluation of Mixes Containing Recycled Asphalt Pavement (RAP). *Road Materials and Pavement Design*, 2009, 10(3), 495-517.

Hansen, K. R. and A. Copeland. *Asphalt Pavement Industry Survey on Recycled Materials and Warm Mix Asphalt Usage (5th ed)*. Lanham, MD: National Asphalt Pavement Association (NAPA), 2014.

Harvey, J., Liu, A., Zhou, J., Signore, M., Coleri, E. and HE, Y. *Superpave Implementation Phase II: Comparison of Performance-Related Test Results*. UCPRC Research Report No: UCPRC-RR-2015-01, 2015.

Herbsman, Z. J., and Glagola, C. R. Lane Rental- Innovative Way to Reduce Road Construction Time. *Journal of Construction Engineering and Management*, 124~5, 411–417, 1998.

Lee, N., C. Chou, K. Chen. *Benefits in Energy Savings and CO2 Reduction by Using RAP*. *Proceedings*. 91st Annual Meeting of the Transportation Research Board, Washington D.C., 2011.

Li, X., M. O. Marasteanu, R. C. Williams, and T. R. Clyne. Effect of Reclaimed Asphalt Pavement (Proportion and Type) and Binder Grade on Asphalt Mixtures. *Transportation Research Record: Journal of the Transportation Research Board*, 2008, No.2051, pp.90–97.

Mallick, R. B., P. S. Kandhal, and R. L. Bradbury. Using Warm-Mix Asphalt Technology to Incorporate High Percentage of Reclaimed Asphalt Pavement Material in Asphalt Mixtures. *Transportation Research Record: Journal of the Transportation Research Board*, No. 2051 2008, pp.71–79.

MATLAB R2016b: MATLAB and Statistics Toolbox. The MathWorks, Inc., Natick, Massachusetts, United States, 2016.

McDaniel, R., and R. M. Anderson. *NCHRP Web Document 30: Recommended Use of Reclaimed Asphalt Pavement in the Superpave Mix Design Method–Project 9-12*. Final Report, 2001.

Mohammad, L. N., B. Samuel, Cooper Jr, and A. E. Mostafa. Characterization of HMA Mixtures Containing High Reclaimed Asphalt Pavement Content with Crumb Rubber Additives. *Journal of Materials in Civil Engineering* 23, No. 11, 2011, pp.1560-1568.

Newcomb, D. E., E. R. Brown, and J. A. Epps. *Designing HMA Mixtures with High RAP Content: A Practical Guide.* National Asphalt Pavement Association (NAPA), 2007.

Newcomb, D.E. *Thin Asphalt Overlays for Pavement Preservation*. National Asphalt Pavement Association (NAPA). Information Series 135, 2009.

Newcomb, D.E. et al. *Short-term Laboratory Conditioning of Asphalt Mixtures*. Rep. No. 815, National Cooperative Highway Research Program (NCHRP), Transportation Research Board, Washington, DC, 2015.

Norouzi, A., Kim, D. and Kim, Y.R. Numerical Evaluation of Pavement Design Parameters for the Fatigue Cracking and Rutting Performance of Asphalt Pavements. *Materials and Structures*, 49(9), 2015, pp.3619-3634.

Nsengiyumva, G. *Development of Semi-Circular Bending (SCB) Fracture Test for Bituminous Mixtures*, 2015.

ODOT. *Preparation and Characterization of Recycled Asphalt Materials for Mix Design*, TM 319, Oregon Department of Transportation, undated.

Oliveira, J. R., H. M. Silva, C. M. Jesus, L. P. Abreu, and S. R. Fernandes. Pushing the Asphalt Recycling Technology to the Limit. International Journal of Pavement Research and Technology, 6(2), 2013, pp.109.

Ozer, H., Al-Qadi, I. L., Lambros, J., El-Khatib, A., Singhvi, P., & Doll, B. Development of the Fracture-Based Flexibility Index tor Asphalt Concrete Cracking Potential Using Modified Semi-Circle Bending Test Parameters. *Construction and Building Materials*, 115, 2016, pp. 390–401

Paul, H. R. Evaluation of Recycled Projects for Performance. *Asphalt Paving Technology*, No. 65 1996, pp.231-254.

Pavement Interactive. *Bulk Specific Gravity*. Retrieved from: http://www.pavementinteractive.org/bulk-specific-gravity. Accessed May 14, 2017.

Petersen, J. C. Chemical Composition of Asphalt as Related to Asphalt Durability: State of the Art. *Transportation Research Record: Journal of the Transportation Research Board*, No. 999, 1984.

Roberts, F. L., P. S. Kandhal, E. R. Brown, D. Y. Lee, and T. W. Kennedy. Hot Mix Asphalt Materials, Mixture Design and Construction. National Asphalt Pavement Association Research and Education Foundation, Lanham, MD., 1996.

Rodezno, M.C., West, R. and Taylor, A. Flow Number Test and Assessment of AASHTO TP 79-13 Rutting Criteria: Comparison of Rutting Performance of Hot-Mix and Warm-Mix Asphalt Mixtures. *Transportation Research Record: Journal of the Transportation Research Board*, (2507), 2015, pp.100-107.

Seber, G.A.F. *Linear Regression Analysis*, John Wiley & Sons, 1977.

Shen, J., S. Amirkhanian, and J. Aune Miller, J. Effects of Rejuvenating Agents on Superpave Mixtures Containing Reclaimed Asphalt Pavement. *Journal of Materials in Civil Engineering*, 19(5), 2007, pp.376–384.

Tao, M., and R. Mallick. Effects of Warm-Mix Asphalt Additives on Workability and Mechanical Properties of Reclaimed Asphalt Pavement Material. *Transportation Research Record: Journal of the Transportation Research Board*, No. 2126, 2009, pp.151-160.

Terrel, R. L., and J. A. Epps. *Using Additives and Modifiers in Hot Mix Asphalt*. National Asphalt Pavement Association (NAPA), Section A No. QIP-114A. 1989.

Tran, N., A. Taylor, and R. Willis. *Effect of Rejuvenator on Performance Properties of HMA Mixtures with High RAP and RAS Contents*. National Center for Asphalt Technology, NCAT Report 12–05, June 2012.

University of California (UC). International Symposium on Pavement LCA 2014, 2014. Retrieved from Summary Review Session (Day 3): http://www.ucprc.ucdavis.edu/p-lca2014/ProgramBreakouts.aspx

Von Quintus, H., J. Mallela, R. Bonaquist, C. Schwartz, and R.L. Carvalho. *Calibration of Rutting Models for HMA Structural and Mixture Design–Project 9-30*. Final Report, 2009.

West, R., A. Kvasnak, N. Tran, B. Powell, and P. Turner. Testing of Moderate and High Reclaimed Asphalt Pavement Content Mixes: Laboratory and Accelerated Field Performance Testing at the National Center for Asphalt Technology Test Track. *Transportation Research Record: Journal of the Transportation Research Board*, No. 2126, 2009, pp. 100-108.

West, R., J. Michael, R. Turochy, and S. Maghsoodloo. Use of Data from Specific Pavement Studies Experiment 5 in the Long-Term Pavement Performance Program to Compare Virgin and Recycled Asphalt Pavements. *Transportation Research Record: Journal of the Transportation Research Board*, No. 2208, 2011, pp.82-89.

West, R., Timm, D., Willis, R., Powell, B., Tran, N., Watson, D., Sakhaeifar, M., Brown, R., Robbins, M., Nordcbeck, A.V. and Villacorta, F.L. *Phase IV NCAT Pavement Test Track Findings*. Auburn, AL: National Center for Asphalt Technology, Report Number NCAT 12-10, 2012.

Williams, R. S., and R. Shaidur. *Mechanistic Design Guide Calibration for Pavement Rehabilitation*. Final Report. Oregon Department of Transportation, Salem, Oregon, 2013.

Williams, R. S., and R. Shaidur. SPR 734 *Premature Asphalt Concrete Pavement Cracking*. Final Report for Oregon Department of Transportation, Salem, Oregon, 2015.

Willis, J. R. *Effect of Recycled Materials on Pavement Life-cycle Assessment: A Case Study*. Proceedings 94th Annual Meeting of the Transportation Research Board, Washington D.C, 2015.

Willis, J. R., P. Turner, G. Julian, A. J. Taylor, N. Tran, and F. Padula. *Effects of Changing Virgin Binder Grade and Content on RAP Mixture Properties*. National Center for Asphalt Technology Report, (12-03), 2012.

World Highways. *Recycling Asphalt Provides Green Result*. 2013. http://www.worldhighways.com/categories/materials-production-supply/features/recycling-asphalt-provides-green-result. Accessed October 15, 2015.

Wu, Z., Mohammad, L.N., Wang, L.B. and Mull, M.A. Fracture Resistance Characterization of Superpave Mixtures Using the Semi-Circular Bending Test. *Journal of ASTM International*, 2(3), 2005, pp.1-15.

Xiao, F., S. Amirkhanian, and C. H. Juang. Rutting Resistance of Rubberized Asphalt Concrete Pavements Containing Reclaimed Asphalt Pavement Mixtures. *Journal of Materials in Civil Engineering*, 19(6), 2007, pp.475–483.

Xiao, F., S. N. Amirkhanian, J. Shen, and B. Putman. Influences of Crumb Rubber Size and Type on Reclaimed Asphalt Pavement (RAP) Mixtures. *Construction and Building Materials*, 23(2), 2009, pp.1028-1034.

Zaumanis, M., R. Mallick, and R. Frank. Evaluation of Rejuvenator's Effectiveness with Conventional Mix Testing for 100 % Reclaimed Asphalt Pavement Mixtures. *Transportation Research Record: Journal of the Transportation Research Board*, No. 2370, 2013, pp.17–25.

Zhao, S., B. Huang, X. Shu, X. Jia, and M. Woods. Laboratory Performance Evaluation of Warm-Mix Asphalt Containing High Percentages of Reclaimed Asphalt Pavement. *Transportation Research Record: Journal of the Transportation Research Board*, No. 2294, 2012, pp.98-105.

Zhou, F., S. Im, D. Morton, R. Lee, S. Hu, and T. Scullion. *Rejuvenator Characterization, Blend Characteristics, and Proposed Mix Design Method*. Association of Asphalt Paving Technologists, 2015.

APPENDIX A

A.0 GRADATION AND BINDER CONTENT OF RAP

This section represents the gradation, binder content and theoretical maximum specific gravity (G_{mm}) of RAP materials provided by ODOT. The RAP was provided by Old Castle for this study.

GRADATION OF RAP WORKSHEET

Project Name:
Mix Type:
Seperated Size:

Contract # :
Date : 10/28/15

Sample :	1	Sample :	2	Sample :	3
Mass Initial Dry:	1633.4	Mass Initial Dry:	1633.5	Mass Initial Dry:	1628.5
Mass Before Sieve:	1498.9	Mass Before Sieve:	1503.8	Mass Before Sieve:	1483.2

Sieve	Mass Ret.	% Ret.	%Pass
3/4	0	0	100
1/2	32	2.0	98.0
3/8	158.3	9.7	88.3
1/4	286.6	17.5	70.8
No. 4	155	9.5	61.3
No. 8	281.1	17.2	44.1
No. 16	213.2	13.1	31.1
No. 30	124.3	7.6	23.4
No. 50	104.1	6.4	17.1
No. 100	68.3	4.2	12.9
No. 200	54.5	3.3	9.6
Pan	21.1		
Mass After	1498.5	Sieve Dev.	0.0

Sieve	Mass Ret.	% Ret.	%Pass
3/4	0	0	100
1/2	38.7	2.4	97.6
3/8	165	10.1	87.5
1/4	302.7	18.5	69.0
No. 4	143.7	8.8	60.2
No. 8	288.7	17.7	42.5
No. 16	203.1	12.4	30.1
No. 30	128.3	7.9	22.2
No. 50	93.5	5.7	16.5
No. 100	66.5	4.1	12.4
No. 200	53.2	3.3	9.2
Pan	18.9		
Mass After	1502.3	Sieve Dev.	0.1

Sieve	Mass Ret.	% Ret.	%Pass
3/4	0	0	100
1/2	19.4	1.2	98.8
3/8	180.2	11.1	87.7
1/4	239.4	14.7	73.0
No. 4	149.3	9.2	63.9
No. 8	279.5	17.2	46.7
No. 16	213.5	13.1	33.6
No. 30	129.3	7.9	25.7
No. 50	113.1	6.9	18.7
No. 100	78	4.8	13.9
No. 200	60.6	3.7	10.2
Pan	20.5		
Mass After	1482.8	Sieve Dev.	0.0

Sample :	4	Sample :	5
Mass Initial Dry:	1627.5	Mass Initial Dry:	1637.8
Mass Before Sieve:	1496.4	Mass Before Sieve:	1515.5

Sieve	Mass Ret.	% Ret.	%Pass
3/4	0	0	100
1/2	24.4	1.5	98.5
3/8	125.8	7.7	90.8
1/4	253.7	15.6	75.2
No. 4	156.1	9.6	65.6
No. 8	298.1	18.3	47.3
No. 16	222.8	13.7	33.6
No. 30	144.8	8.9	24.7
No. 50	105.6	6.5	18.2
No. 100	77.2	4.7	13.5
No. 200	62.7	3.9	9.6
Pan	24.8		
Mass After	1496	Sieve Dev.	0.0

Sieve	Mass Ret.	% Ret.	%Pass
3/4	0	0	100
1/2	24.2	1.5	98.5
3/8	186.4	11.4	87.1
1/4	305	18.6	68.5
No. 4	165.8	10.1	58.4
No. 8	300.4	18.3	40.1
No. 16	209	12.8	27.3
No. 30	111	6.8	20.5
No. 50	87	5.3	15.2
No. 100	57.5	3.5	11.7
No. 200	51	3.1	8.6
Pan	17.5		
Mass After	1514.8	Sieve Dev.	0.0

~~DESIGN AVERAGE~~

Sieve	Percent Passing
3/4	100
1/2	98.3
3/8	88.3
1/4	71.3
No. 4	61.9
No. 8	44.1
No. 16	31.1
No. 30	23.3
No. 50	17.1
No. 100	12.9
No. 200	8.4

Figure A.1: RAP aggregate gradation

PROJECT	2016 RAP	MIX CLASS	
CONTRACT NO.		LEVEL (2,3,4)	
MIX PRODUCER		PROJECT MANAGER	
CMDT (print)		CMDT JMF MIX ID NO	

RAP WORKSHEET

Separated Size	1/2" - 0	G_b	1.026

AASHTO T-209: Theoretical Maximum Specific Gravity

Sample	1	2	3
Mass of Dry RAP (R_{hot})	1746.8	1794.2	1744.7
Mass of Added Binder ($Binder_{new}$)	52.4	53.8	52.3
$P_{b\text{-}new}$, %	2.912	2.911	2.910
Mass of Coated Sample (C)	1800.5	1849.3	1795.3
Actual Dry Mass Uncoated Sample (A)	1748.1	1795.5	1743.0
Actual Mass of Added Binder (C-A)	52.4	53.8	52.3
Mass @ SSD	1803.8	1853.6	1800.5
Pycnometer + Water	7391.5	7391.5	7391.5
Pycnometer + Water + Mix	8433.2	8462.0	8434.7
RAP G_{mm} SSD	2.459	2.457	2.468

Asphalt Content of RAP

Sample	1	2	3	4	5	
Basket Tare	3044.9	3046.2	3043.7	3045.7	3043.3	
Mass of Coated RAP + Basket	4794.4	4795.8	4793.1	4795.1	4793.7	
Mass of Agg and Basket	4678.3	4679.7	4672.2	4673.2	4681.1	
Mass Initial, M_i	1749.5	1749.6	1749.4	1749.4	1750.4	
Mass Final, M_f	1633.4	1633.5	1628.5	1627.5	1637.8	
$\%I = \{[M_i - M_f]/[M_i]\}x100$	6.64	6.64	6.91	6.97	6.43	Average
Corrected P_b, $C_f = 0.50$	6.14	6.14	6.41	6.47	5.93	6.22
					RAP Gse	2.713

AASHTO T-85: Specific Gravity and Absorption of Coarse Aggregate

Size	+ #4		Average
Source	Various		
A) Mass of Dry Sample	2013.7	2039.5	
B) Mass of SSD Sample	2055.4	2083.5	
C) Mass of Sample Immersed	1282.3	1295.7	
Bulk Specific Gravity (G_{sb})	2.605	2.589	2.597
Bulk Specific Gravity (SSD)	2.659	2.645	2.652
Apparent Specific Gravity (G_{sa})	2.753	2.742	2.748
Absorption (%)	2.07	2.16	2.11

Combined Specific Gravity
T-84 & T-85

Size	1/2"-0
Split Sieve	#4
Percent Retained Split Sieve	38.1
Burnt Bulk Specific Gravity (G_{sb})	2.611
Burnt Bulk Specific Gravity (SSD)	2.662
Burnt Apparent Specific Gravity	2.753
Absorption (%)	2.0

AASHTO T-84: Specific Gravity and Absorption of Fine Aggregate

Size	- #4		Average
Source	Various		
S) Mass of SSD Sample	500.0	500.0	
B) Mass of Pyc. + Water	658.9	654.2	
C) Mass of Pyc.+H2O+Sample	971.5	966.9	
Mass of Dry Sample + Pan			
Mass of Pan			
A) Mass of Dry Sample	490.8	490.6	
Bulk Specific Gravity (G_{sb})	2.619	2.619	2.619
Bulk Specific Gravity (SSD)	2.668	2.670	2.669
Apparent Specific Gravity (G_{sa})	2.754	2.758	2.756
Absorption (%)	1.87	1.92	1.9

Combined RAP Specific Gravity
ODOT TM-319

RAP G_{sb}	2.636
RAP G_{sa}	2.766

Certified Technician and Card Number:

Figure A.2: Binder content and theoretical maximum specific gravity (G_{mm}) of RAP

APPENDIX B

B.0 TEMPERATURE CURVES AND PROPERTIES OF VIRGIN BINDERS

The data below represents binder temperature curves used for this study. All temperature curves were provided by McCall Oil.

Table B.1: Mixing and Compaction Temperatures of PG 76-22 Binder

Binder	**PG 76-22**
Temp (F)	Viscosity (cp)
275	**768**
329	**250**

Mixing Temperature Range, F	345	-	359
Compaction Temperature Range, F	318	-	329

Specific Gravity@ 60F	**1.0377**

Table B.2: Mixing and Compaction Temperatures of PG 64-22 Binder

Binder	**PG 64-22**
Temp (F)	Viscosity (cp)
275	**363**
329	**113**

Mixing Temperature Range, F	303	-	314
Compaction Temperature Range, F	281	-	291

Specific Gravity@ 60F	**1.0306**

Table B.3. Mixing and Compaction Temperatures of PG 58-34 Binder

Binder	**PG 58-34**
Temp (F)	Viscosity (cp)
275	**250**
329	**113**

Mixing Temperature Range, F	292	-	308
Compaction Temperature Range, F	262	-	275

Specific Gravity@ 60F	**1.0291**

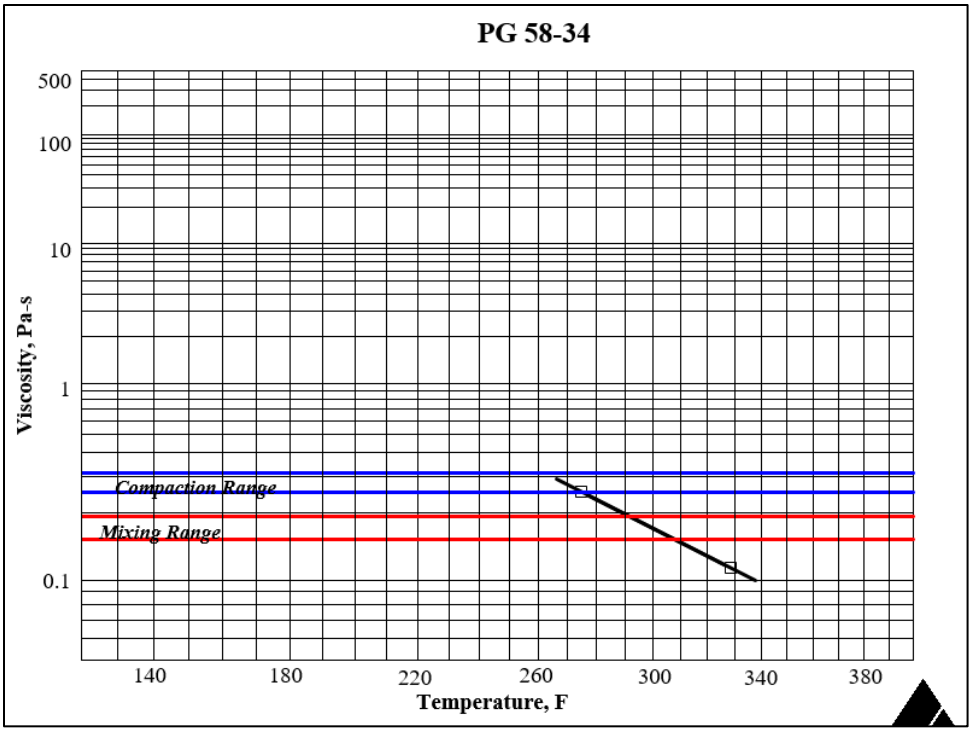

Figure B.1: Temperature curve of PG 58-34 binder

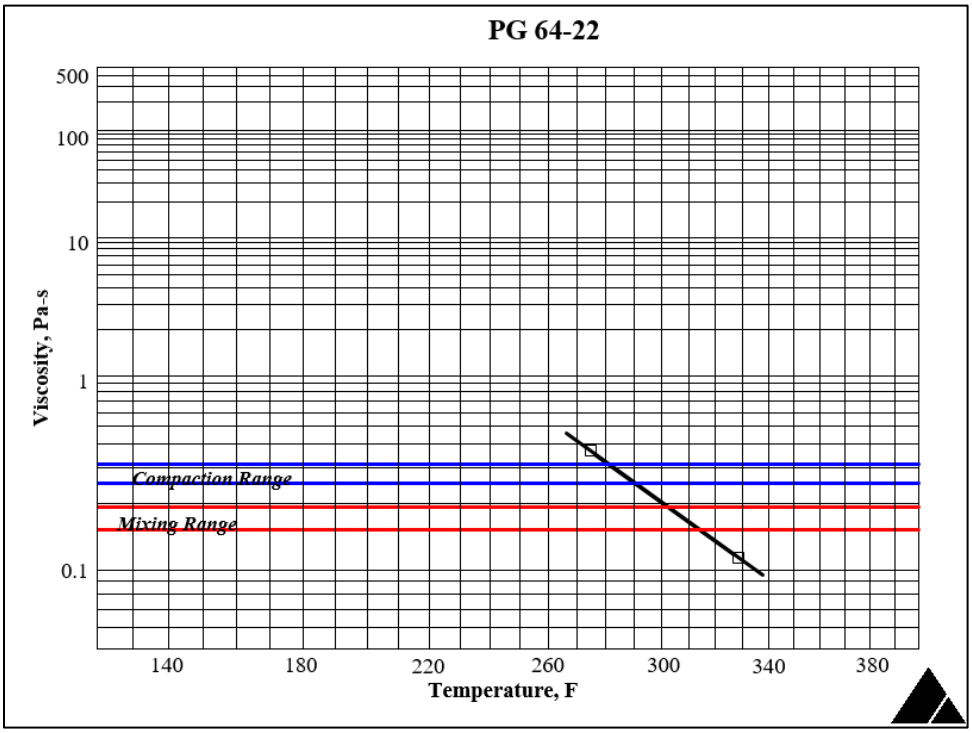

Figure B.2: Temperature curve of PG 64-22 binder

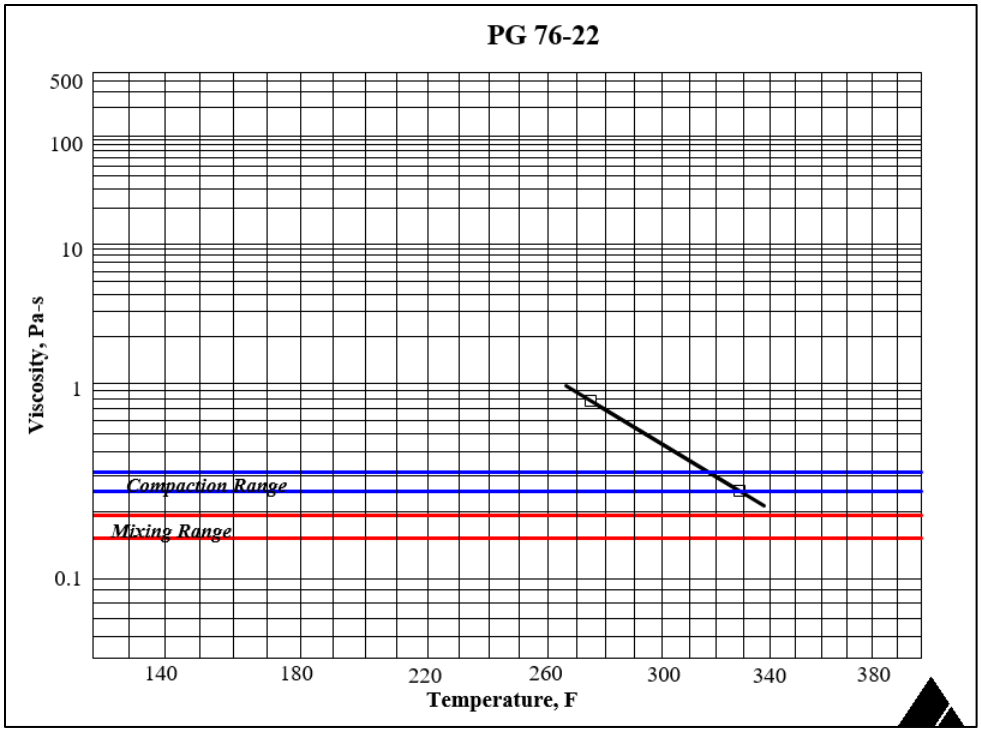

Figure B.3: Temperature curve of PG 76-22 binder

The following figures show the binder properties provided by McCall Oil.

PG 58-34

Certificate of Analysis

		Specification
Original Properties		
Specific Gravity @ 15.6 C (58 F)	1.0219	
Flashpoint, C	330	230+
Dynamic Shear, G*/sin δ, 58 C, kPa	1.38	1.0+
Fail Temp	60.7	
Rotational Viscosity, 135 C, Pas	0.288	3.00-
RTFO Residue Properties		
Loss on Heat, %	-0.514	1.00-
Dynamic Shear, G*/sin δ, 58 C, kPa	3.93	2.20+
Fail Temp	62.8	
PAV Residue Properties		
Dynamic Shear, G*sin δ, 16 C, kPa	3480	5000-
Fail Temp	8.0	
Creep Stiffness, -24 C, Mpa	250	300-
m-value, -24 C	0.303	0.300+
Fail Temp Creep Stiffness	-31.85	
Fail Temp M Value	-24.35	

True Grade PG 60.7-34.35

I certify that the asphaltic material identified above complies with current AASHTO M-320 (formerly MP-1) specifications, ASTM D6373, Washington State Department of Transportation Specifications for Asphalt Materials.

Figure B.4: PG 58-34 binder properties

PG64-22

Certificate of Analysis

Original Properties

	Result	Test Method AASHTO	SPEC.
Flashpoint, C	310	T48	230 +
Brookfield Viscosity, Pa sec	0.363	T316	3.000 -
Dynamic Shear @ 64 C, G*/sin delta, kPa	1.23	T315	1.0 +

Rolling Thin Film Oven Residue Properties

R.T.F.O. Loss on Heat, %	0.040	T240	1.000 -
Dynamic Shear @ 64 C, G*/sin delta, kPa	2.54	T315	2.2 +

Pressure Aging Vessel Residue

Dynamic Shear @ 25 C, G*sin delta, kPa	1890	T315	5000 -
Bending Beam @ -12 C			
Stiffness, Mpa	156	T313	300 -
m-value	0.330	T313	0.30 +

True Grade PG 64.5 – 26.03

I certify that the asphaltic material identified above complies with current AASHTO M-320 specifications, ASTM D6373, Washington State Department of Transportation, Oregon Department of Transportation, and Idaho Department of Transportation Standard Specifications for Asphalt Materials.

Figure B.5: PG 64-22 binder properties

PG76-22

Certificate of Analysis

		Specification
Original Properties		
Specific Gravity @ 15.6 C (60 F)	1.0408	
Flashpoint, C	250+	230+
Dynamic Shear, G*/sin δ, 76 C, kPa	1.27	1.0+
Rotation Viscosity, 135 C, Pas	0.788	3.00-
RTFO Residue Properties		
Loss on Heat, %	0.313	1.00-
Dynamic Shear, G*/sin δ, 76 C, kPa	4.64	2.20+
PAV Residue Properties		
Dynamic Shear, G*sin δ, 31 C, kPa	2020	5000-
Creep Stiffness, -12 C, Mpa	170	300-
m-value, -12 C	0.315	0.300+

I certify that the asphaltic material identified above complies with current AASHTO M-320 (formerly MP-1) specifications, ASTM D6373, Washington State Department of Transportation and Oregon Department of Transportation, Standard Specifications for Asphalt Materials.

Figure B.6: PG 76-22 binder properties

APPENDIX C

C.0 AN EXAMPLE FOR BATCHING SHEETS

The following example shows the procedure of calculating the quantity of materials for the mixture with 30% RAP, 6% binder content and binder grade of PG 58-34.

Table C.1: Quantity of Coarse, Medium, and Fine Aggregates and RAP Materials for the Mixture with 30% RAP, 6% Binder Content, and Binder Grade of PG 58-34

stockpile	coarse	medium	fine	RAP	Comparison: Combined vs. Target					
stockpile percentage, Psi	32	18	20	30						
total percentage	100				combined aggregate					
sieve size	percentage passing				%retained	cum. Retained	%passing	target %pass	Diff	Diff^2
3/4"	100.0	100.0	100.0	100.0	0.0	0.0	100.0	100	0.0	0.0
1/2"	95.8	100.0	100.0	98.3	1.9	1.9	98.1	98	-0.1	0.0
3/8"	53.1	98.2	100.0	88.3	16.8	18.7	81.3	83	1.7	2.9
1/4"	21.9	64.9	100.0	71.3	21.0	39.7	60.3	59	-1.3	1.7
#4	13.2	38.0	99.9	61.9	10.5	50.2	49.8	49	-0.8	0.7
#8	2.3	3.3	83.3	44.1	18.5	68.6	31.4	31	-0.4	0.1
#16	1.3	1.3	55.1	31.1	10.3	78.9	21.1	22	0.9	0.8
#30	1.2	1.2	35.8	23.3	6.3	85.2	14.8	16	1.2	1.5
#50	1.1	1.1	23.7	17.1	4.3	89.5	10.5	11	0.5	0.3
#100	1.1	1.1	15.6	12.9	2.9	92.5	7.5	8	0.5	0.2
#200	0.9	1.0	10.7	8.4	2.4	94.8	5.2	6.3	1.1	1.3
pan	0	0	0	0	5.2	100.0	0.0	0	0.0	0.0
binder conent	---	----	----	6.22	root mean square error					9.4

stockpile	coarse	medium	fine	RAP	coarse	medium	fine	RAP (agg)			
stockpile percentage, Psi	32	18	20	30	32	18	20	30			
total percentage	100										
sieve size	percentage retained				batch mass, grams				Virgin Agg (g)	RAP (total,g)	RAP + binder %remained
3/4"	0.0	0.0	0.0	0.0	0.0	0.0	0.0	0.0	0.0	0.0	0.0
1/2"	4.2	0.0	0.0	1.7	91.9	0.0	0.0	34.9	91.9	26.5	1.2
3/8"	42.7	1.8	0.0	10.0	923.5	22.8	0.0	205.1	946.2	429.5	19.6
1/4"	31.2	33.3	0.0	17.0	674.9	414.0	0.0	348.7	1088.9	596.6	27.3
#4	8.7	26.9	0.1	9.4	187.4	335.0	0.9	192.8	523.3	251.8	11.5
#8	10.9	34.7	16.6	17.8	236.5	432.1	228.7	365.2	897.3	366.8	16.8
#16	1.0	1.9	28.3	13.0	21.2	24.2	389.5	266.7	434.9	205.5	9.4
#30	0.1	0.1	19.3	7.8	2.9	1.8	266.3	160.0	271.0	125.3	5.7
#50	0.1	0.1	12.1	6.2	1.3	0.6	166.3	127.2	168.2	89.5	4.1
#100	0.1	0.0	8.1	4.2	1.3	0.5	112.1	86.2	114.0	43.0	2.0
#200	0.1	0.1	4.9	4.5	2.4	1.0	67.1	92.3	70.6	25.3	1.2
pan	0.9	1.0	10.7	8.4	20.5	12.6	147.4	172.3	180.5	27.6	1.3
					total weight						
					2163.63	1244.66	1378.40	2051.43	4786.7	2187.49	

Table C.2: Quantity of Binder, RAP Materials, and Total Aggregates for the Mixture with 30% RAP, 6% Binder Content, and Binder Grade of PG 58-34

target binder content %	6
aggregate mass, g	6838.107495
mixture mass, g	7274.582441
RAP binder (gr)	136.06
RAS binder (gr)	0
virgin binder (gr)	300.4127948
Gmm	2.487
Gmb	2.31291
airvoid content (%)	7
gyratory height	0.17
mass of sample in GC (g)	6928.173754

APPENDIX D

D.0 EXAMPLE OF DATA GENERATED BY UTM DEVICE FOR DYNAMIC MODULUS TEST AND DEVELOPING THE MASTER CURVES

The following tables show output data from the UTM device for dynamic modulus tests of the mixture with 30% RAP content, 6% binder content and PG 58-34 binder grade

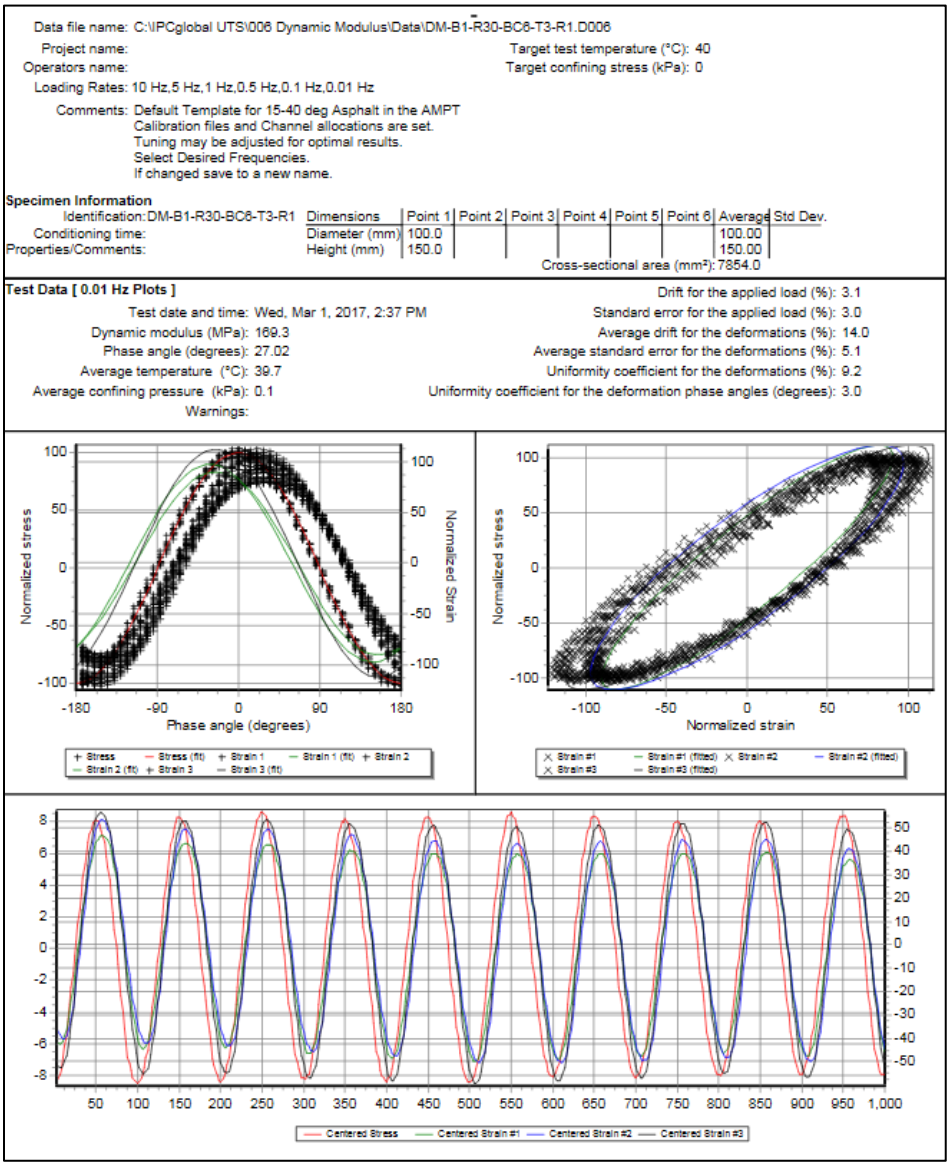

Figure D.1: An example of output dynamic modulus test of mixture with 30% RAP content, 6% binder content, and PG 58-34 binder grade

An example of the data used to make the dynamic modulus and phase angle master curves is shown in the tables below.

Table D.1: VMA and VFA of the Mixture with 30% RAP Content, 6% Binder Content and PG 58-34 Binder Grade

VMA	Volume, %	15.4
VFA	Volume, %	74.0
Reference Temp	20	

Table D.2: Dynamic Modulus and Phase Angles of Mixture with 30% RAP Content, 6% Binder Content and PG 58-34 Binder Grade at Different Temperatures and Frequencies

Conditions		Specimen 1		Specimen 2		Average	Modulus	Average	Std Dev
Temperature	Frequency	Modulus	Phase Angle	Modulus	Phase Angle	Modulus	CV	Phase	Phase
C	Hz	Ksi	Degree	Ksi	Degree	Ksi	%	Deg	Deg
4	0.1	1165.7	16.0	1222.4	15.7	1194.0	3.4	15.9	0.2
4	0.5	1482.6	13.4	1552.6	13.2	1517.6	3.3	13.3	0.1
4	1	1628.8	12.5	1706.5	12.3	1667.6	3.3	12.4	0.1
4	5	1977.6	10.4	2073.2	10.3	2025.4	3.3	10.3	0.1
4	10	2138.1	9.7	2231.8	9.5	2185.0	3.0	9.6	0.1
20	0.1	363.6	26.6	389.1	27.0	376.4	4.8	26.8	0.3
20	0.5	554.2	23.9	593.6	24.2	573.9	4.9	24.1	0.2
20	1	649.9	23.1	700.4	23.4	675.2	5.3	23.2	0.2
20	5	924.0	20.0	999.0	20.1	961.5	5.5	20.1	0.1
20	10	1055.4	18.8	1150.7	18.9	1103.1	6.1	18.8	0.1
40	0.01	24.6	27.0	33.7	26.2	29.1	22.2	26.6	0.6
40	0.1	53.0	30.6	66.6	29.7	59.8	16.1	30.2	0.6
40	0.5	99.6	31.3	116.5	33.1	108.0	11.0	32.2	1.3
40	1	130.6	31.7	148.2	34.0	139.4	9.0	32.8	1.6
40	5	241.3	30.8	256.3	32.5	248.8	4.2	31.6	1.2
40	10	304.6	31.0	316.8	31.4	310.7	2.8	31.2	0.3

Shift factors and best-fit curves are presented in the following tables and figures. Dynamic modulus data collected at various temperatures (See Figure D-2) can be shifted with respect to the loading frequencies so that the different curves can be aligned to form a single smooth master curve (See Figure D-4). The shift factor is the mechanism that allows horizontal shifting of the data on the master curve. Actual loading frequencies at different temperatures are shifted with respect to the reference temperature (20 ^{o}C in this report) using the shift factors to create the master curves. For example, in Figure D-2, loading frequencies at 4 ^{o}C are shifted to the right and frequencies at 40 ^{o}C are shifted to the left to create the master curve. Shift factors for different temperatures are presented in Figure D-5. The same shift factors created for the dynamic modulus were used to create the master curves for phase angles (See Figure D-6).

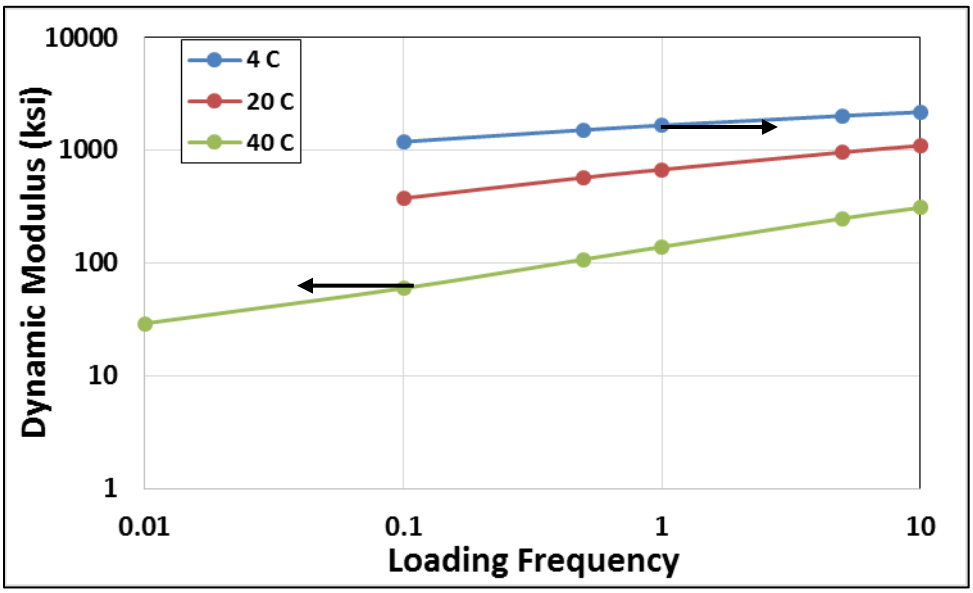

Figure D.2: Dynamic modulus of the mixture with 30% RAP content, 6% binder content, and PG 58-34 binder grade at different temperatures and frequencies

			Pc	E*, ksi	logE*													
Maximum Modulus			0.8769324	3340.413	3.52380015													
			Initial Values															
Log (Min)			0.485108	0.5	Copy Cells C4:C7 to													
Beta			-1.24166	-1	B4:B7 using													
Gamma			-0.46711	-0.5	Copy/Paste Values													
EA			199240.4	200000														
Reference Temp			20															
				Average	Average	Log Average												
Temperature		Frequency	Modulus		Phase Ang	Modulus		Predicted	Error	Error^2		loga(t)	log (wr)	wr		wr	log E*	E*, ksi
C		Hz	Ksi		Degree													
	4	0.1	1194.0	15.9	3.07701264			3.066767	0.010246	0.000105		2.048502	1.048502	11.18154		1000000	3.471475	2961.25
	4	0.5	1517.6	13.3	3.18115788			3.179657	0.001501	2.25E-06		2.048502	1.747472	55.90769		500000	3.463731	2908.916
	4	1	1667.6	12.4	3.22210321			3.220291	0.001812	3.28E-06		2.048502	2.048502	111.8154		100000	3.441169	2761.652
	4	5	2025.4	10.3	3.30650629			3.298568	0.007938	6.3E-05		2.048502	2.747472	559.0769		50000	3.429082	2685.851
	4	10	2185.0	9.6	3.33945004			3.326192	0.013258	0.000176		2.048502	3.048502	1118.154		10000	3.394072	2477.834
	20	0.1	376.4	26.8	2.57561827			2.565106	0.010512	0.000111		0	-1	0.1		1000	3.321965	2098.77
	20	0.5	573.9	24.1	2.75884695			2.765514	-0.00667	4.45E-05		0	-0.30103	0.5		500	3.293798	1966.971
	20	1	675.2	23.2	2.82940059			2.842687	-0.01329	0.000177		0	0	1		100	3.214046	1636.989
	20	5	961.5	20.1	2.98296168			2.99969	-0.01673	0.00028		0	0.69897	5		50	3.172682	1488.272
	20	10	1103.1	18.8	3.04260867			3.0579	-0.01529	0.000234		0	1	10		10	3.0579	1142.615
	40	0.01	29.1	26.6	1.46424461			1.459204	0.00504	2.54E-05		-2.2663	-4.2663	5.42E-05		1	2.842687	696.1253
	40	0.1	59.8	30.2	1.77690486			1.790095	-0.01319	0.000174		-2.2663	-3.2663	0.000542		0.1	2.565106	367.3722
	40	0.5	108.0	32.2	2.03354973			2.036682	-0.00313	9.81E-06		-2.2663	-2.56733	0.002708		0.05	2.470533	295.4831
	40	1	139.4	32.8	2.14424948			2.143122	0.001128	1.27E-06		-2.2663	-2.2663	0.005416		0.01	2.236184	172.2599
	40	5	248.8	31.6	2.39587163			2.383377	0.012495	0.000156		-2.2663	-1.56733	0.027081		0.005	2.130892	135.1737
	40	10	310.7	31.2	2.49230037			2.481668	0.010632	0.000113		-2.2663	-1.2663	0.054162		0.001	1.883411	76.45589
																0.0001	1.543301	34.93822
				Sy	0.57173048					0.001674	Use Solver on this Cell					0.00001	1.24747	17.67949
																0.000001	1.012326	10.28788

Figure D.3: An example of procedure of creating master curve

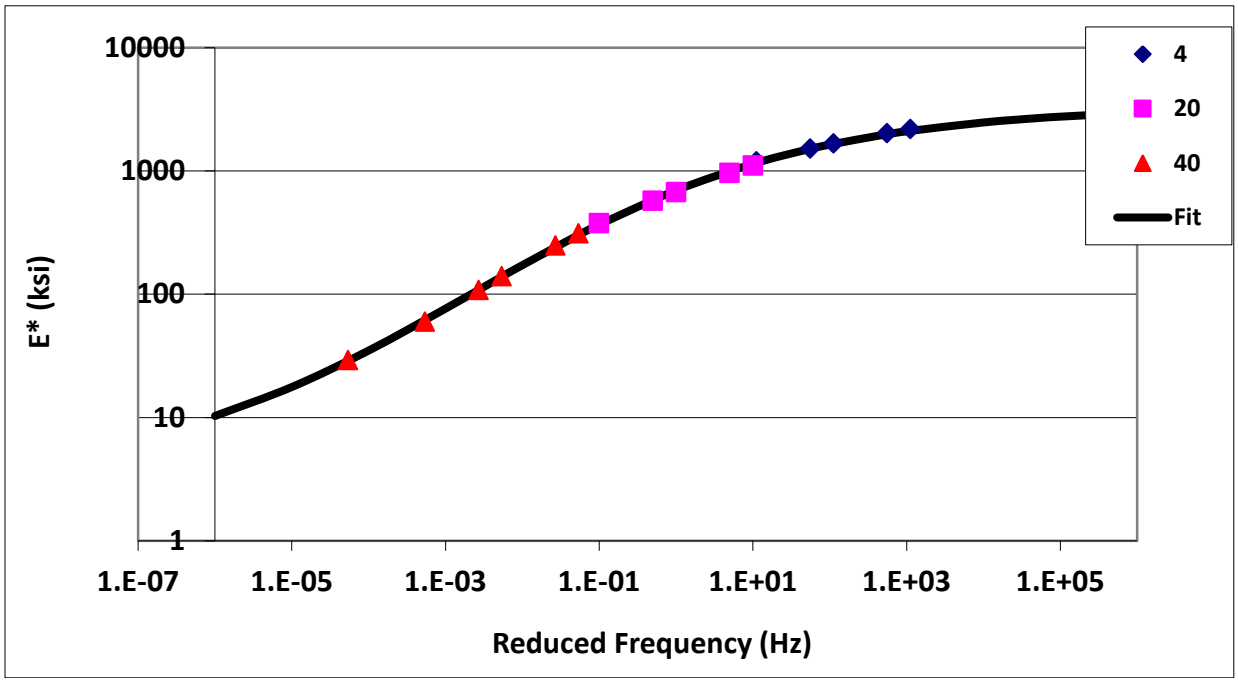

Figure D.4: An example of the master curve of dynamic modulus for the mixture with 30% RAP content, 6% binder content, and PG 58-34 binder grade

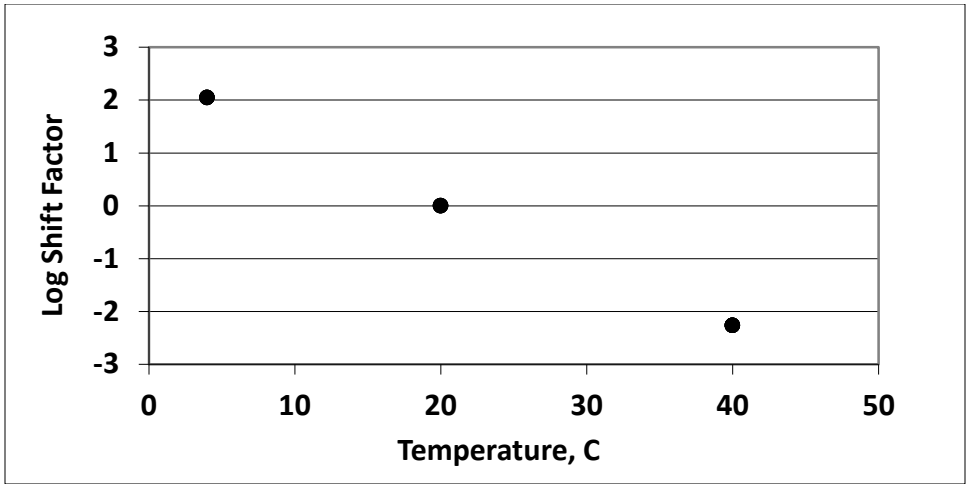

Figure D.5: Shift factor curve of the mixture with 30% RAP content, 6% binder content, and PG 58-34 binder grade

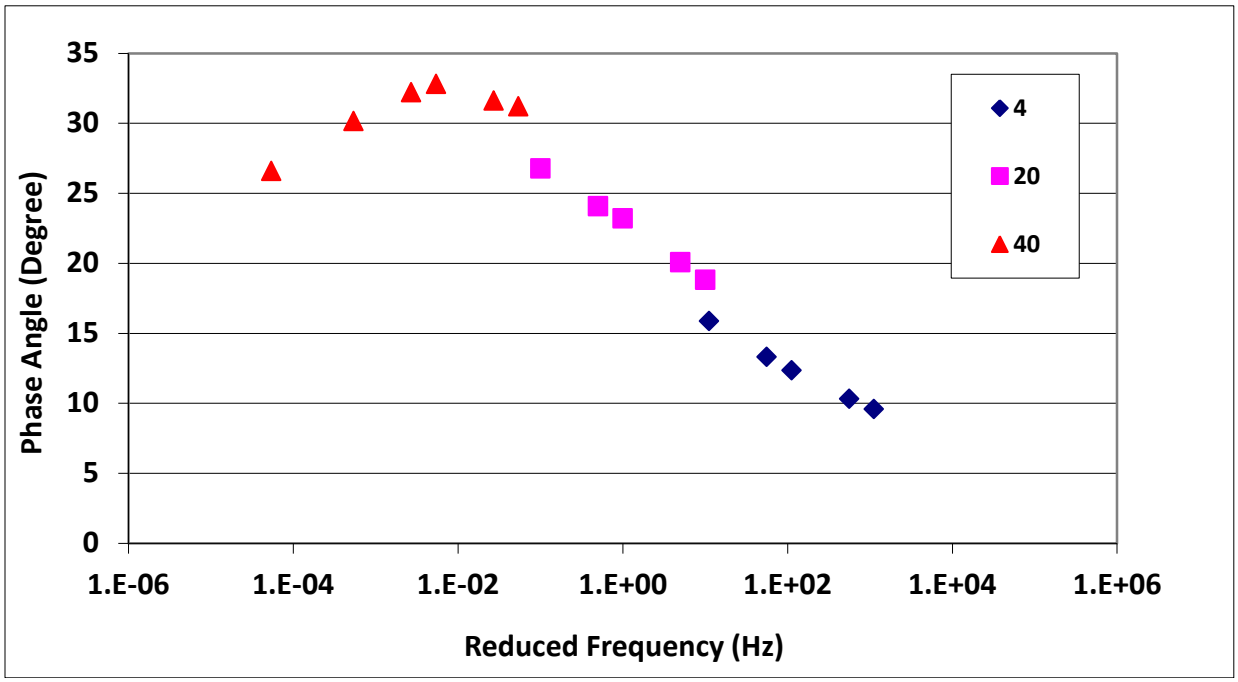

Figure D.6: An example of the master curve of phase angle for the mixture with 30% RAP content, 6% binder content, and PG 58-34 binder grade

Project:	OSU Recycle Increase	
Mix Identification:	9.5 mm with Air Blown Binder	
Date:	12/22/05	
Technician:	Sogol Sadat Haddadi	
Sample Description:		
Notes:		
Shift Factors:	Arrhenius log10 (a(T)) = EA/19.147143*(1/T - 1/Tr)	
Master Curve Model:	log(E*) = logMin) + (log(Max) - log(Min)) / (1+EXP (Beta + Gamma* log (wr)))	
Reference Temperature:	20	C

Temp C	Temp F	Frequency Hz	Shift Factor	Reduced Frequency	E* ksi	E* MPa
-10.0	14	25	4.045246	277450.7	2859.4	19721.4
-10.0	14	10	4.045246	110980.3	2772.4	19121.0
-10.0	14	5	4.045246	55490.13	2697.8	18606.4
-10.0	14	1	4.045246	11098.03	2492.7	17192.2
-10.0	14	0.5	4.045246	5549.013	2390.0	16483.8
-10.0	14	0.1	4.045246	1109.803	2117.9	14607.3
4.4	40	25	1.988411	2434.169	2256.4	15562.7
4.4	40	10	1.988411	973.6674	2093.8	14441.2
4.4	40	5	1.988411	486.8337	1961.8	13530.2
4.4	40	1	1.988411	97.36674	1631.3	11251.1
4.4	40	0.5	1.988411	48.68337	1482.5	10224.9
4.4	40	0.1	1.988411	9.736674	1137.0	7841.9
21.1	70	25	-0.13399	18.36343	1272.0	8773.0
21.1	70	10	-0.13399	7.345371	1078.1	7435.9
21.1	70	5	-0.13399	3.672685	937.5	6466.2
21.1	70	1	-0.13399	0.734537	644.2	4443.3
21.1	70	0.5	-0.13399	0.367269	536.2	3698.3
21.1	70	0.1	-0.13399	0.073454	333.9	2302.7
37.8	100	25	-2.02889	0.233913	472.6	3259.4
37.8	100	10	-2.02889	0.093565	359.9	2482.5
37.8	100	5	-2.02889	0.046783	289.2	1994.7
37.8	100	1	-2.02889	0.009357	168.3	1161.0
37.8	100	0.5	-2.02889	0.004678	132.0	910.7
37.8	100	0.1	-2.02889	0.000936	74.7	515.1
54.4	130	25	-3.73101	0.004644	131.7	908.4
54.4	130	10	-3.73101	0.001858	95.2	656.6
54.4	130	5	-3.73101	0.000929	74.5	513.8
54.4	130	1	-3.73101	0.000186	42.8	295.2
54.4	130	0.5	-3.73101	9.29E-05	34.1	235.3
54.4	130	0.1	-3.73101	1.86E-05	21.0	144.6

README | DATA | FIT | REPORT | **MEPDGINPUT** | Sheet1

Figure D.7: MEPDG inputs for the mixture with 30% RAP content, 6% binder content, and PG 58-34 binder grade.

APPENDIX E

E.0 FLOW NUMBER TEST RESULTS

An example of the data produced by UTM device Flow Number Test for the sample with 30% RAP content, 6% binder content and PG 58-34 binder grade is presented as follows. This data was used to estimate the flow numbers using Francken Model and compare the rutting resistance of asphalt mixtures with different binder grades, RAP contents and binder contents.

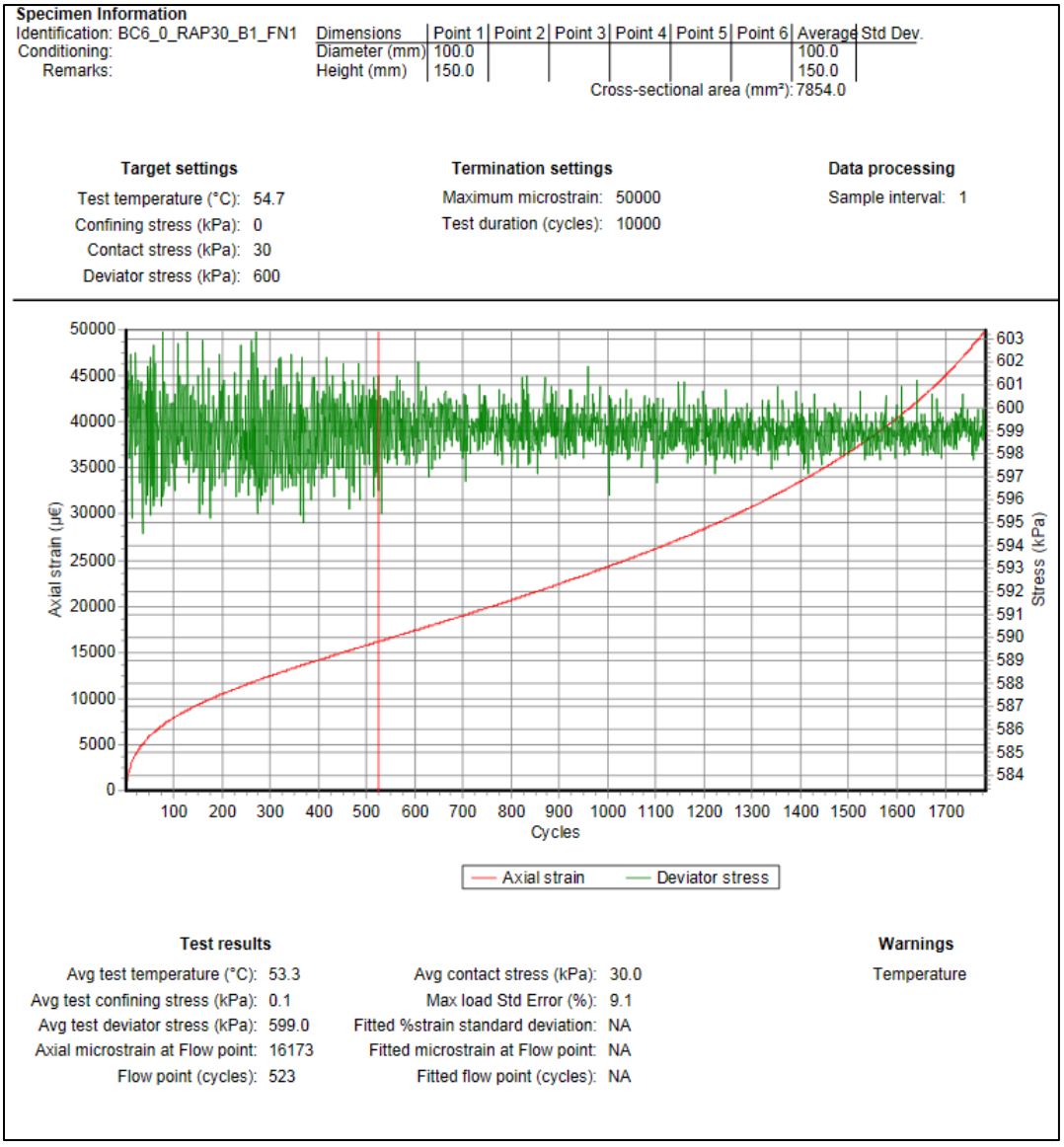

Figure E.1: An example of flow number test output data for the sample with 30% RAP content, 6% binder content, and PG 58-34 binder grade